UNIVERSITÉ DU LUXEMBOURG

PhD-FSTM, 2024-021
The Faculty of Sciences, Technology and Medicine

DISSERTATION

Defense held on 23/01/2025 in Esch-sur-Alzette

to obtain the degree of

DOCTEUR DE L'UNIVERSITÉ DU LUXEMBOURG

EN SCIENCES DE L'INGÉNIEUR

By

TARIK ČAMO
Born on 19 June 1989 in Novi Pazar, (Serbia)

STRUCTURAL HEALTH MONITORING: CONDITION ASSESSMENT OF BRIDGE STRUCTURES WITH THE DEFORMATION AREA DIFFERENCE (DAD) METHOD USING MOST MODERN MEASUREMENT TECHNIQUES SUCH AS PHOTOGRAMMETRY AND UAV

Dissertation defense committee

Prof. Dr. Danièle WALDMANN, dissertation supervisor
Professor, Technical University of Darmstadt

Prof. Dr. Andreas ZILIAN, Chairman
Professor, University of Luxembourg

Dr. Christoph CZADERSKI
EMPA - Swiss Federal Laboratories for Materials Science and Technology

Dr. Eftychia APOSTOLIDI
Donges SteelTec GmbH Darmstadt

Prof. Dr. Numa Joy BERTOLA, Vice Chairman
Professor, University of Luxembourg

"The life of a bridge, like that of a human, is determined not by its creation but by the *understanding* and *maintenance* that enable it to endure the forces that shape it."

I Acknowledgement

This thesis has been carried out within the framework of the PhD program in Engineering Sciences at the University of Luxembourg, supported by the Faculty of Science, Technology and Medicine (FSTM). The research was carried out as part of the ongoing efforts in the field of Structural Health Monitoring (SHM), with a particular focus on the further development of the Deformation Area Difference (DAD) method for the condition assessment of bridge structures. A crucial year of this work was spent at the Institute of Solid Structures of the Technical University of Darmstadt, where experimental investigations and collaborations enriched the scope and depth of this study. This dissertation combines state-of-the-art methods, collaborative contributions, and experimental validations to address some of the pressing challenges in SHM.

The successful completion of this dissertation would not have been possible without the support and contributions of many individuals and organizations. I am deeply grateful to everyone who has played a role in this journey, and I take this opportunity to express my heartfelt thanks.

First and foremost, I owe my deepest gratitude to my supervisor, Prof. Danièle Waldmann, who initially guided me at the University of Luxembourg and later continued her exceptional mentorship from the Technical University of Darmstadt. Her unwavering support, insightful feedback, and inspiring leadership have been instrumental in overcoming the challenges of this research. Prof. Waldmann's ability to foster an encouraging and stimulating research environment has allowed me to grow academically and professionally, and I will always be grateful for her confidence in my abilities.

I would like to sincerely thank the members of my Thesis Supervision Committee (CET): Prof. Andreas Zilian from the University of Luxembourg and Dr. Christoph Czaderski from the EMPA Zurich, whose constructive feedback and critical insights have significantly shaped the direction of my work. Their expertise and rigorous evaluation were invaluable throughout this process.

I would like to express my sincere gratitude to the members of my Ph.D. defense committee: Prof. Numa Joy Bertola of the University of Luxembourg and Dr. Eftychia Apostolidi of Donges Steeltech GmbH. Their thoughtful critiques, time, and interest in my work are greatly appreciated. I am especially grateful to Prof. Bertola for our engaging discussions that broadened my perspectives, and to Dr. Apostolidi for her collaboration, guidance, and warm friendship during our time in Darmstadt.

Special thanks are due to Prof. Jan Lagerwall from the Department of Physics and Material Science, whose leadership and generosity have profoundly influenced my work. His guidance and scientific contributions during the multidisciplinary collaboration on the ‘Revealing complex strain patterns and dangerous loads using cholesteric liquid crystal elastomers’ (REVEAL) project have been transformative. His kindness, dedication, and intellectual curiosity created a supportive and

enriching environment that greatly enhanced the collaboration. I also thank his team, especially Rijeesh Kizhakidathazhath, for their technical expertise and cooperation.

I appreciate the support of Prof. Ludger Wirtz, who kindly served as my manager during the last two years of my Ph.D., and Prof. Christoph Odenbreit for his guidance in supervising Master's students.

I am deeply grateful to my colleagues and friends at the University of Luxembourg, including Dr. Gelen Gaël Chewe Ngapeya, Vishojit Bahadur Thapa, Patrick Pereira Dias, Laddu Bhagya Jayasinghe, Lorenc Bogoviku, Hooman Eslami, Sinan Kaassamani, Anna Tokareva, and Suzanne Biwer. Their cooperation and support made this journey not only productive but also truly enjoyable.

During my year at the Technical University of Darmstadt, I was fortunate to work with Annika Becker, Lukas Bujotzek, Christian Herget, Truong Diep Hasenbank-Kriegbaum, Eftychia Apostolidi, Nicola Zeitler, Thomas Kloß, Ludwig Remmel, Ranwu Xu, Adrian Twardella, Luca Matschat, and Michaela Dahley-Müller. Their insights and technical support were invaluable, and I deeply appreciate the enriching experience of working with them.

The doctoral program team at the University of Luxembourg also deserves special recognition, especially Prof. Rebecca Teferle and Suzanne Biwer, for their commitment to fostering a supportive academic environment. Their efforts to ensure the success of graduate students have been invaluable. My sincere thanks go to all the staff at the University of Luxembourg who supported me during my Ph.D., including Dr. Silvia Venditti, Heidi Backstroem, Odile Marois, Adamantia Galani, Inmaculada Peral Alonso, Audrey Vari, Christine Isolano, Maria Huynh, Isabelle Majerus, Stéphanie Lucadello and Shayan Weber. I would also like to express my appreciation to the IT support team, especially Antoine Zoccolo and Samir Esber, for their continuous assistance in ensuring smooth technical operations throughout my Ph.D.

I am also deeply grateful to the laboratory teams in Luxembourg and Darmstadt. In Luxembourg, I would like to thank Marc Seil, Gilbert Klein, Mehdi Saeidi, Ed Weyer, Cyrille Inglebert, Cédric Bruyere, Vicente Reis Adonis, and Claude Colle for their technical support and expertise, especially for the bridge experiments. In Darmstadt, I deeply appreciate the support of Yves Kibnowski, Eric Rauschenbach, and Jörg Wiech, whose contributions were crucial to my experimental investigations.

I extend my heartfelt thanks to Yann Fux and Gilberto Fernandes at the Administration des Ponts et Chaussées for their close cooperation and discussions, financial support for equipment such as mobile inspection units and load testing, facilitating closures for bridge experiments, and for providing bridge structures for the application of this research.

Special thanks to Dr. Dolgion Erdenebat, whose foundational work this study builds upon, for his support, advice, and assistance with a bridge experiment. I would also like to thank Matteo Brunetti for his support related to the Grasshopper- SOFiSTiK interface, which was invaluable in advancing

my work. Additionally, I thank Prof. Ivan Duvnjak from the University of Zagreb for our valuable discussions on the method, which significantly enriched my understanding. I would also like to thank Dr. Jose Luis Sanchez Lopez and Prof. Miguel Angel Olivares Mendez for their discussions on drone technology, which helped me apply UAVs in my experiments. Further thanks go to Peter Seelig of Drohnenflugschule24 for the training and valuable discussions regarding UAV applications. Finally, I extend my gratitude to Dr.-Ing. Andrei Firus for his engaging and insightful discussions.

I would also like to thank Harald Krause for his assistance with the professional application of the photogrammetric software Elcovision 10. I would like to thank Aïcha Boutebal and Gauthier Pierlot from the Direction de l'Aviation Civile for their support in obtaining UAV authorization.

To the students who worked with me—Gabriel Ibosiola, Namo Sorani, Finn Wiegland, and Tarek El Rashidy—thank you for your dedication and enthusiasm. Your contributions were greatly appreciated.

I owe everything to my family. To my parents, Mirsad and Suada, your love, sacrifices, and belief in me have been my greatest source of strength. To my brother Alen, thank you for your support in life and our collaboration, which has always been a source of strength for me. To my sister Amina, our deep discussions have been invaluable, offering me a sense of clarity and perspective throughout this journey.

To my friends and extended family, your encouragement and support gave me strength throughout this process. I am deeply grateful to each of you.

To my beloved children Malik and Naïl, your joy and laughter have been my greatest motivation. Everything I do is for you.

Finally, to my partner Amela, your unwavering support, patience, and love have been my anchor throughout this journey. Your belief in me gave me strength, and this achievement is as much yours as it is mine. Without you by my side, this work would not have been possible, and I am endlessly grateful for everything you have done.

II Abstract

The implementation of Structural Health Monitoring (SHM) is of paramount importance for the assurance of the safety and durability of bridge infrastructure, particularly in light of the advancing age of existing structures and the concurrent increase in traffic loads. The Deformation Area Difference (DAD) method has emerged as a promising approach for detecting and assessing structural damage, offering a cost-effective alternative to traditional monitoring techniques. However, its real-world applicability has been limited by challenges such as sensitivity to noise, measurement point density, and performance under low-deflection scenarios. It is, therefore, essential to address these issues to advance the reliability and scalability of SHM solutions.

This doctoral thesis has the following objectives: firstly, to address the limitations of the DAD method; secondly, to enhance its precision and applicability through complementary techniques; and thirdly, to extend its functionality to support higher SHM levels. By systematically evaluating the method's performance and integrating innovative approaches, this work seeks to establish a comprehensive framework for accurate and practical SHM solutions.

The initial study examines the constraints of the DAD method through a comprehensive parametric numerical analysis, introducing the Damage Detection Range (DDR) to quantify its efficacy. The study reveals the impact of various factors, including deflection values, noise levels, and measurement point distances, on the performance of the DAD method. Additionally, it explores the influence of local cross-sectional damage for the first time. The second study addresses the method's noise sensitivity by introducing the Strain Area Difference (SAD) method, which leverages strain-based curvature analysis to enhance damage detection precision, particularly in low-deflection scenarios, and demonstrates resilience to noise through laboratory validation. The third study integrates low-complexity Model Updating (MU) techniques to enable damage level assessment.

The findings demonstrate that the limitations of the DAD method can be effectively mitigated through the implementation of innovative approaches. The DDR and local cross-sectional analysis provide new insights into the method's applicability across diverse scenarios. The SAD method significantly enhances damage detection precision and noise resilience, while MU techniques enable damage severity assessments. Collectively, these contributions expand the capabilities and applicability of the DAD method for SHM.

This dissertation addresses pivotal research questions pertaining to the constraints, improvements, and applications of the DAD method. By incorporating cutting-edge techniques such as the SAD method and model updating methodologies, it establishes a robust foundation for precise, scalable, and pragmatic SHM solutions for bridge structures, paving the way for future advancements in the field.

III List of Publications

1. T. Čamo, D. Waldmann, "Condition assessment of bridge structures with the DAD-Method using photogrammetry and drones" in Proceedings of the international conference on structural health monitoring of intelligent infrastructure, 2021, pp. 1523-1530, https://www.up.pt/arquivoweb/web.fe.up.pt/_shmii10/ficheiros/eBook_SHMII_2021.pdf
2. T. Čamo, D. Waldmann, "Potential and limits using the DAD method for condition assessment of bridge structures", Engineering Structures, vol. 308, 1 June 2024, 117972, doi: https://doi.org/10.1016/j.engstruct.2024.117972
3. T. Čamo, E. Apostolidi, D. Waldmann-Diederich, "Advancements in Structural Health Monitoring (SHM): Deformation Area Difference (DAD) method and model updating" in Bridge Maintenance, Safety, Management, Digitalization and Sustainability, 2024, pp. 3673-3680. doi: https://doi.org/10.1201/9781003483755
4. T. Čamo, E. Apostolidi, and D. Waldmann, "Enhancing SHM with the extension of the deformation area difference method into the strain area difference method," Structural Concrete, 2024, doi: https://doi.org/10.1002/suco.202400779
5. T. Čamo, R. Kizhakidathazhath, D. Waldmann-Diederich, and J. P. F. Lagerwall, "Optical crack detection and assessment using cholesteric liquid crystal elastomers," Structural Health Monitoring, Nov. 2024, doi: https://doi.org/10.1177/14759217241296831
6. T. Čamo and D. Waldmann, "Damage level assessment using DAD method and model updating," Engineering Structures, vol. 336, p. 120498, Aug. 2025, doi: https://doi.org/10.1016/j.engstruct.2025.120498

IV Table of Contents

V List of Figures

VI List of Tables

VIIAbbreviations

1-D-CNN - one-dimensional Convolutional Neural Network

ADB - area between the DILC and the beam

ADC - Displacement Assurance Criterion

AE - Acoustic Emission

ANN - Artificial Neural Networks

ASCE - American Society of Civil Engineers

B-WIM - bridge-weigh-in-motion

BOTDA - Brillouin Optical Time Domain Analysis

CAD - computed aid design

CNN - Convolutional Neural Network

CO-MAC - Coordinate Modal Assurance Criterion

CRP - Close-Range Photogrammetry

DAD - Deformation Area Difference

DAD IL - Deformation Area Difference Influence Line

DBI - Displacement-Based Index

DDR - Damage Detection Range

DIC - Digital Image Correlation

DI-CD - damage-induced chord-wise deflection

DIL - deflection influence line

DILC - displacement influence line change

DMRB - Design Manual for Roads and Bridges

DFOS - Distributed Fiber Optic Sensors

DT - displacement transducers

DT - Digital Twin

FEMU - Finite Element Model Updating

FOS - Fiber Optic Sensors

FBG - Fiber Bragg Grating

FE - Finite Element

FEA - Finite Element Analysis

FFT - Fast Fourier Transform

GPR - Ground-Penetrating Radar

GRC - Grey Relational Coefficient

GSM - Gapped Smoothing Method

HGV - Heavy Goods Vehicles

IAS - Instantaneous Amplitude Squared

IB - Inner Boundary
IL - Influence Line
IQR - interquartile range
LPF - Load Participation Factor
MFI - Moving Force Identification
ML - Machine Learning
MSAD - Modeshape Area Differences
MU - Model Updating
NARX - Nonlinear Autoregressive with eXogenous Inputs
NBIS - National Bridge Inspection Standards
NDT - Non-Destructive Testing
NULS - Normalized Uniform Load Surface
NURBS - non-uniform Rational B-Splines
OB - Outer Boundary
PBIL - Positive-Bending-Inspection-Load
POM - Proper Orthogonal Mode
Q1 - 25^{th} percentile
Q3 - 75^{th} percentile
RelDif - Relative Differences
RIL - Rotation Influence Line
SAD - Strain Area Difference
SHM - Structural Health Monitoring
SLS - Serviceability limit state
SPMT - Self-propelled modular transporter
SS - simply supported
TLS - Terrestrial Laser Scanning
TL - Transfer Learning
UAV - Unmanned Aerial Vehicle
VB - Vision Based
VBI - Vehicle-Bridge Interaction
VoI - value of information
WBA - Wavelet-Based Analysis

1 Introduction

1.1 Background and Motivation

Infrastructure maintenance is becoming an increasingly important global challenge, particularly with respect to bridge structures that are experiencing the effects of aging and are subject to increased loads from modern traffic [1]. Many of these critical structures were not originally designed to accommodate the significant traffic volumes they now support. This problem is particularly prevalent in Europe, where extensive and aging road networks are a major concern. Two main factors are responsible for the deterioration of bridges: the age of the infrastructure and the increasing volume of traffic, particularly Heavy Goods Vehicles (HGVs) [2]. These combined pressures place considerable stress on bridge structures, which were often not designed to accommodate the weight and frequency of today's traffic.

The European Commission has identified a growing number of maintenance challenges across the European Union, particularly in the context of road and bridge infrastructure. The convergence of aging infrastructure and insufficient financial resources has resulted in a significant backlog of unmet maintenance needs, as outlined in reference [3]. Furthermore, a series of projects has been initiated with the objective of standardizing maintenance and safety protocols, with a particular emphasis on the importance of monitoring and predictive maintenance[4]. The limited resources and capacity for preservation and maintenance have resulted in a growing backlog of maintenance needs [4]. This growing gap underscores the necessity to address the condition of aging bridges, with a significant number of road bridge structures built in the post-World War II reconstruction with an age of over 50 years [5], and more than 35% of EU railway bridges over 100 years old [6] facing the end of their lifetime. A significant number of these structures are approaching the end of their design life and require immediate maintenance to prevent deterioration or failure.

The European Union's extensive bridge network constitutes a pivotal component of the continent's transportation infrastructure, encompassing over 1,234 km of road bridges exceeding 100 meters in length, thereby ensuring the safety of these structures [7]. Furthermore, the prevalence of freight traffic has increased twofold from 1995 to 2015 [8], thereby compounding the complexity of the problem. The rise in heavy vehicle traffic exerts considerable pressure on bridges that are nearing the end of their design life, hastening their deterioration and necessitating repairs. The confluence of increased traffic and aging infrastructure presents a challenge to EU countries, who must reconcile the imperative for immediate maintenance with budgetary constraints and mounting demands on their infrastructure.

A substantial proportion of the 39,500 federal highway bridges in Germany were constructed during the post-war economic expansion between the 1950s and 1970s. These structures are now exhibiting indications of material deterioration as a consequence of their advanced age [9]. This was tragically exemplified by the collapse of the Carola Bridge in Dresden in September 2024

shown in Figure 1 [10]. The bridge, constructed in the early 1970s, experienced a partial collapse into the Elbe River, resulting in the disruption of traffic and public transportation. However, it is fortunate that no injuries were sustained. Preliminary investigations indicate that chlorine corrosion, which originated during the bridge's construction in East Germany, may have been a contributing factor. The issue is further compounded by the exponential growth in traffic, particularly that of trucks, which has significantly accelerated the deterioration of older bridges. The volume of traffic on Germany's roads has increased steadily over the decades, and the additional load is contributing to the deterioration of the country's bridges. Traffic volumes, particularly those of trucks, have increased twofold over the past three decades [11], exerting considerable pressure on infrastructure that was not designed to accommodate such substantial and continuous usage. The projected cost of maintaining and upgrading Germany's highway bridges over the next decade is estimated at €8.4 billion. This figure reflects the combined impact of aging infrastructure and increased traffic. Approximately €1.4 billion is allocated annually for the modernization of approximately 5,000 bridges by 2032 [12].

Figure 1. Collapse of the Carola Bridge (Radio Dresden)

France is similarly confronted with the broader challenges facing European bridge infrastructure, including the aging and deterioration of its bridges. France is estimated to have between 200,000 and 250,000 bridges, with approximately 25,000 deemed to be in a state of disrepair. Of these, approximately 10% require prompt repair due to structural deficiencies[13]. A 2019 Senate report underscored the chronic underfunding of bridge maintenance, which has resulted in a considerable number of bridges, particularly those managed by smaller municipalities, being in a state of disrepair. Despite the French Senate's recommendation of an annual investment of €130 million, the government has only allocated €40 to €55 million per year, a figure that falls significantly below

the amount required to address the growing backlog of repairs [14]. This funding shortfall, coupled with the increasing demands placed on the country's transportation infrastructure, highlights the urgent need for more comprehensive maintenance strategies to prevent further deterioration of France's vital bridges and other transportation infrastructure.

Italy's bridge infrastructure, constructed primarily in the mid-20th century, is experiencing accelerated deterioration due to a combination of factors, including material fatigue, environmental exposure, and increased traffic demands [15]. The collapse of the Morandi Bridge in 2018 (Figure 2), which resulted in the loss of 43 lives, has brought the fragility of these structures into sharp focus [16]. In response, the Italian Ministry of Transport and Infrastructure has introduced new monitoring and assessment guidelines, which are currently in a trial phase [17]. While regular inspections and comprehensive maintenance strategies are of paramount importance, significant challenges persist, particularly in regions with high seismic activity, where the risk to bridge infrastructure is elevated [18], [19]. Despite the introduction of advanced monitoring tools, the urgent necessity to address the pervasive structural vulnerability of Italy's bridges remains unmet.

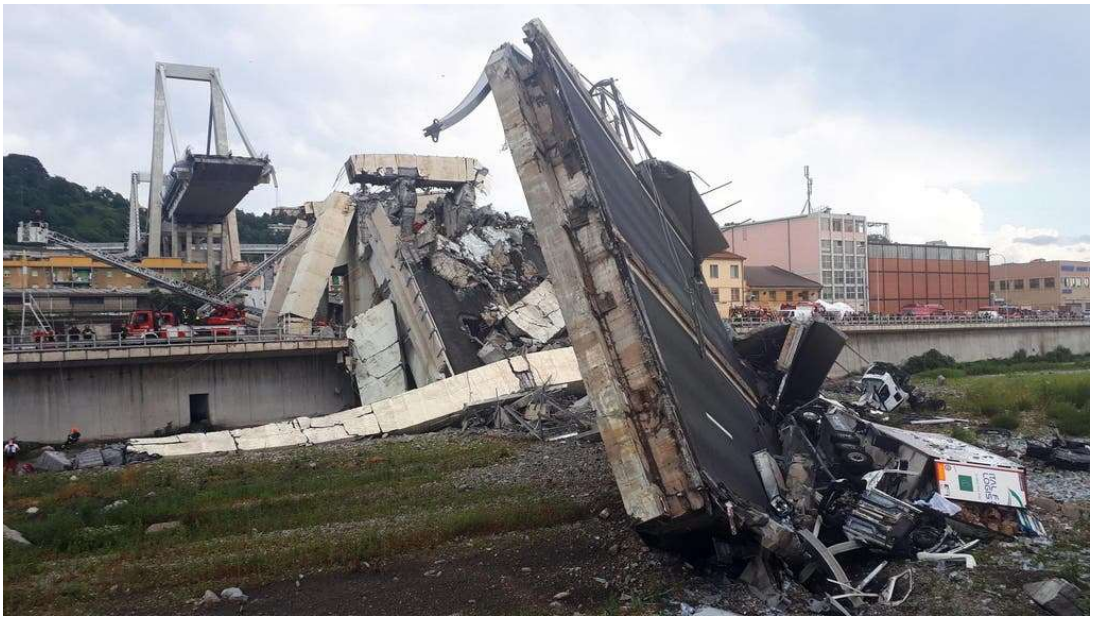

Figure 2. Collapse of the Morandi Bridge (St. Galler Tagblatt)

Similarly, in Spain, the condition of bridges and their ability to accommodate increasing traffic demands has become a key concern in recent years and warrants further study. The rapid development of rail and road infrastructure, particularly with the expansion of high-speed rail and urban road networks, has put considerable pressure on existing structures. For example, the Rande Strait Bridge, built in the late 1970s, experienced a significant increase in daily traffic, reaching 55,000 vehicles in 2006. This increase in traffic resulted in a significant increase in congestion. To address this issue, a pioneering widening project was initiated that included the addition of two new external decks to increase capacity without interrupting traffic flow [20]. Similarly, historic steel

railway bridges in northern Spain, some of which date back to the early 20th century, are now facing structural challenges. Inspections have revealed significant hidden damage that has required immediate traffic suspensions, highlighting the growing need for costly retrofits to ensure safety and service continuity [21]. Increased traffic and aging infrastructure underscore the urgent need for significant investment in repairs and upgrades to ensure the continued functionality of Spain's vital bridge network.

In parallel, Poland is also facing challenges with its bridge infrastructure. Growing demand for transport infrastructure has had a significant impact on the country's bridge network, both in terms of traffic loads and the condition of existing structures. As the number of vehicles, especially heavy trucks, has increased, so has the traffic on key bridges. For example, the Grota-Roweckiego Bridge in Warsaw, Poland's busiest bridge, recorded a daily traffic flow of more than 185,000 vehicles in 2017. This led to a major reconstruction effort to widen and strengthen the structure to meet the growing demand [22]. The increase in traffic has led to a significant deterioration in the condition of many older bridges. For example, bridges built 60 years ago that have not yet reached the end of their design life are already showing signs of fatigue damage due to the increased loads they are carrying [23]. As a result, managing the backlog of needed repairs and upgrades has become a pressing issue, with costs rising as Poland attempts to maintain and modernize its aging bridge infrastructure in the context of increased traffic demands.

Similarly, while Luxembourg's bridges are in good condition, the bridge network is under strain from increasing traffic demands. The significant increase in traffic, largely due to a large commuting workforce, has led to a significant increase in the daily traffic volume on Luxembourg's roads [24]. Consequently, the increase in traffic requires more frequent maintenance and increased monitoring to ensure the long-term safety and functionality of the bridge network. This trend reflects a broader need observed across Europe, where increasing traffic volumes require greater attention to infrastructure maintenance and monitoring to maintain structural integrity [25].

Across the Atlantic, the United States faces a similarly pressing issue. The condition of the bridge infrastructure has become a matter of urgent concern, with over 617,000 bridges included in the national inventory. Of these, 46,154 bridges are classified as structurally deficient [26], representing a significant portion of the nation's bridges in need of urgent repair or upgrade [27]. The American Society of Civil Engineers (ASCE) estimates that $70.9 billion is needed to address the current backlog of deficient bridges [28]. Furthermore, the increasing volume of traffic on U.S. bridges, particularly from heavy freight vehicles, is exacerbating the deterioration of many of these aging structures, requiring more frequent maintenance and improvements to ensure public safety and infrastructure resilience [29]. A poignant example of the consequences of inadequate maintenance is the collapse of the I-35W Mississippi River Bridge in 2007 (Figure 3). This tragedy was attributed to the use of under-designed gusset plates that succumbed to increased loads and corrosion, resulting in the loss of 13 lives and injuries to 145 people [30].

Figure 3. Collapse of the I-35 Mississippi River Bridge (NBC news)

Similarly, Japan faces significant challenges in maintaining its extensive bridge network. Japan has an estimated 730,000 road bridges, nearly 43% of which will exceed 50 years of age by 2023, highlighting the urgent need for maintenance and repair [31]. The deterioration of these bridges is primarily due to environmental stresses, such as the use of deicing chemicals and increased traffic loads from larger vehicles, which accelerate wear and tear on these aging structures [32]. Local governments, which are responsible for maintaining many of these bridges, often lack the financial resources and personnel to perform necessary maintenance and repairs in a timely manner [33]. In addition, Japan's aging population has led to significant debt and declining revenues, further limiting the ability of local governments to invest in infrastructure maintenance [34].

China also faces maintenance challenges on a large scale. As of 2013, China had 860,000 bridges, a number that surpassed that of the United States and is projected to exceed one million by 2025 [35]. By 2011, 689,417 highway bridges had been constructed with a total length of 33,494 km [36]. Long-span bridges often experience performance issues, including deflection, cracking, and corrosion, which raise concerns about the safety, durability, and life-cycle costs of such structures [37]. These issues are exacerbated by increasing traffic loads and environmental factors. Despite government initiatives for new construction and rehabilitation, the extensive bridge network poses significant maintenance challenges [38]. In 2011, the SIE2011 standard was introduced to improve the quantitative assessment of bridges; however, further calibration of empirical coefficients is needed to more accurately assess material deterioration [39].

Globally, aging infrastructure and increasing traffic volumes are converging to create unprecedented challenges for bridge maintenance. The increasing prevalence of heavy vehicles places disproportionate stress on older structures that were not originally designed to handle such loads. In response, many countries are turning to advanced monitoring technologies such as Structural Health Monitoring (SHM), photogrammetry, and FEA to detect structural problems early and manage maintenance more effectively. However, as traffic volumes continue to increase, ensuring the long-term safety and functionality of bridge infrastructure will require not only continued investment, but also innovation in monitoring and repair strategies.

In addition to structural risks, bridge deterioration poses significant environmental challenges. Increased CO_2 emissions are a primary consequence, particularly due to traffic diversions during repair and maintenance activities. For example, Ma et al. [40] showed that traffic diversions during bridge repairs contribute significantly to global warming, with CO_2 emissions accounting for over 75% of the total environmental impact, affecting both ecosystems and human health. Similarly, Pang et al. [41] highlighted that maintenance-related traffic diversions account for about 50% of the total environmental impact during bridge strengthening, leading to increased energy consumption and emissions. Gokasar et al. [42] emphasized that CO_2 emissions from traffic diversions should be a primary consideration when prioritizing bridge maintenance projects. Yang and Frangopol [43] further emphasized that bridge failures result in significant traffic delays and increased vehicle operating costs, exacerbating emissions and environmental degradation. Furthermore, Hou et al. [44] emphasized that inadequate maintenance can necessitate the demolition and reconstruction of bridges, resulting in far greater environmental impacts. Even with advanced low-emission demolition techniques such as Self-propelled modular transporter (SPMT) technology, the environmental impact remains significant, primarily due to material waste and emissions. Therefore, timely maintenance is essential to avoid the environmental costs of complete reconstruction. To mitigate these impacts, it is critical to improve monitoring strategies and prioritize early damage detection to ensure timely maintenance and reduce the need for environmentally costly demolition and reconstruction.

1.2 Aim of the study

The aim of this dissertation is to enhance the Deformation Area Difference (DAD) Method for SHM of bridge structures by addressing its current limitations. The research primarily focuses on improving the method's accuracy in detecting local damages by analyzing how key factors—such as deflection values, noise levels, measurement point density and the type of bridge structures—affect its performance. By investigating these influences, the study seeks to advance the DAD method's practical application for real-world SHM scenarios.

A significant aspect of the research is exploring how the integration of strain-based curvature analysis can augment the DAD method's precision. Specifically, the study examines whether

incorporating strain measurements can enhance damage localization and overall accuracy, particularly in cases where the DAD method is limited by noise sensitivity and low deflection values.

Furthermore, the research aims to broaden the applicability of the DAD method to support more comprehensive SHM frameworks, extending its capabilities to higher-level monitoring. This includes enabling damage level assessment, which opens for predictive maintenance, which are crucial for modern infrastructure monitoring. Through these improvements, the study aims to offer a more flexible and reliable SHM tool, benefiting the field of structural engineering by providing enhanced damage detection and monitoring capabilities.

The research is guided by the following key questions:

1. **What are the limitations of the DAD method regarding deflection values, noise levels, measurement point distances and bridge structure types in detecting local damages?**
2. **How can the noise sensitivity of the DAD method be reduced to improve damage detection accuracy, particularly in low-deflection scenarios?**
3. **Can strain-based curvature analysis be integrated to improve the precision and practical applicability of the DAD method in SHM applications?**
4. **How can the DAD method be extended to support more advanced SHM levels, including damage level assessment?**

These research questions provide a focused pathway for systematically addressing the challenges and opportunities in optimizing the DAD method for modern SHM applications.

1.3 Outline of the thesis

This dissertation is organized into five chapters, each of which systematically addresses the research questions and presents the key advancements made in enhancing the DAD method for SHM of bridge structures. The outline of the thesis is visualized in Figure 4.

The **Introduction** chapter provides a detailed background on the growing global challenge of infrastructure maintenance, with a particular focus on bridge structures. The chapter highlights the global character of the problem and the circumference of the problem. The chapter addresses the need for reliable damage detection methods and SHM strategies. Additionally, the chapter discusses the influence of bridge conditions, maintenance, demolition, and rebuilding on the environment.

The **Literature Review** chapter offers a comprehensive analysis of existing methods for bridge condition assessment. It begins with a discussion of traditional approaches, including manual inspection techniques, followed by an in-depth review of modern SHM methods, such as vibration-based, static load deflection, and strain-based techniques. The review highlights the limitations of these methods, particularly in their sensitivity to noise and the influence of variable deflection values on accuracy. A critical evaluation of the DAD method is presented, identifying its strengths and weaknesses, which form the foundation for the improvements proposed in this research. It

introduces the levels of SHM, and the use of Close-Range Photogrammetry (CRP), Unmanned Aerial Vehicles (UAV), and Machine Learning (ML) in SHM. The Literature Review describes the research gap that this study tries to fill.

The **Results** chapter is structured around three key studies, each presented in the form of published papers that contribute to the advancement of the DAD method. Each paper is summarized as follows:

- **Publication I** addresses the limitations of the DAD method concerning deflection values, noise levels, measurement point distances, and different types of bridge structures. The study provides a detailed analysis of how these factors impact the method's accuracy in detecting local damages, and it proposes strategies to mitigate these challenges, improving the practical applicability of the DAD method in real-world SHM scenarios.
- **Publication II** explores the integration of strain-based methods into the DAD framework. By incorporating strain measurements, the research examines whether the precision of the DAD method can be enhanced, particularly in situations where noise sensitivity and deflection variabilities pose significant constraints. This paper demonstrates how the integration of strain data improves the localization of damage and increases the overall accuracy of the method.
- **Publication III** investigates the expansion of the DAD method to higher levels of SHM, with a focus on damage level assessment. The research develops the method further to support Level 4 SHM and opening predictive capabilities that extend beyond simple damage detection to lifecycle assessment and proactive maintenance strategies.

The **Discussion** chapter provides a critical evaluation of the findings from the three studies, drawing connections between the results and the overarching research questions. It reflects on the contributions of this research to the field of SHM, particularly in relation to the improvements in the accuracy and applicability of the DAD method. The discussion also considers the broader implications of integrating strain-based methods, expanding SHM to level 3, and enabling real-time monitoring, highlighting the potential impact of these advancements on bridge management.

The **Conclusion and Future Outlook** chapter summarizes the key contributions of the dissertation. It reflects on the research questions and discusses how the findings of the thesis address the limitations of the DAD method. The chapter also provides an outlook on future research directions, including the potential for further refinements of the DAD method, the integration of AI and machine learning for automated SHM, and the application of these advancements to broader infrastructure monitoring challenges.

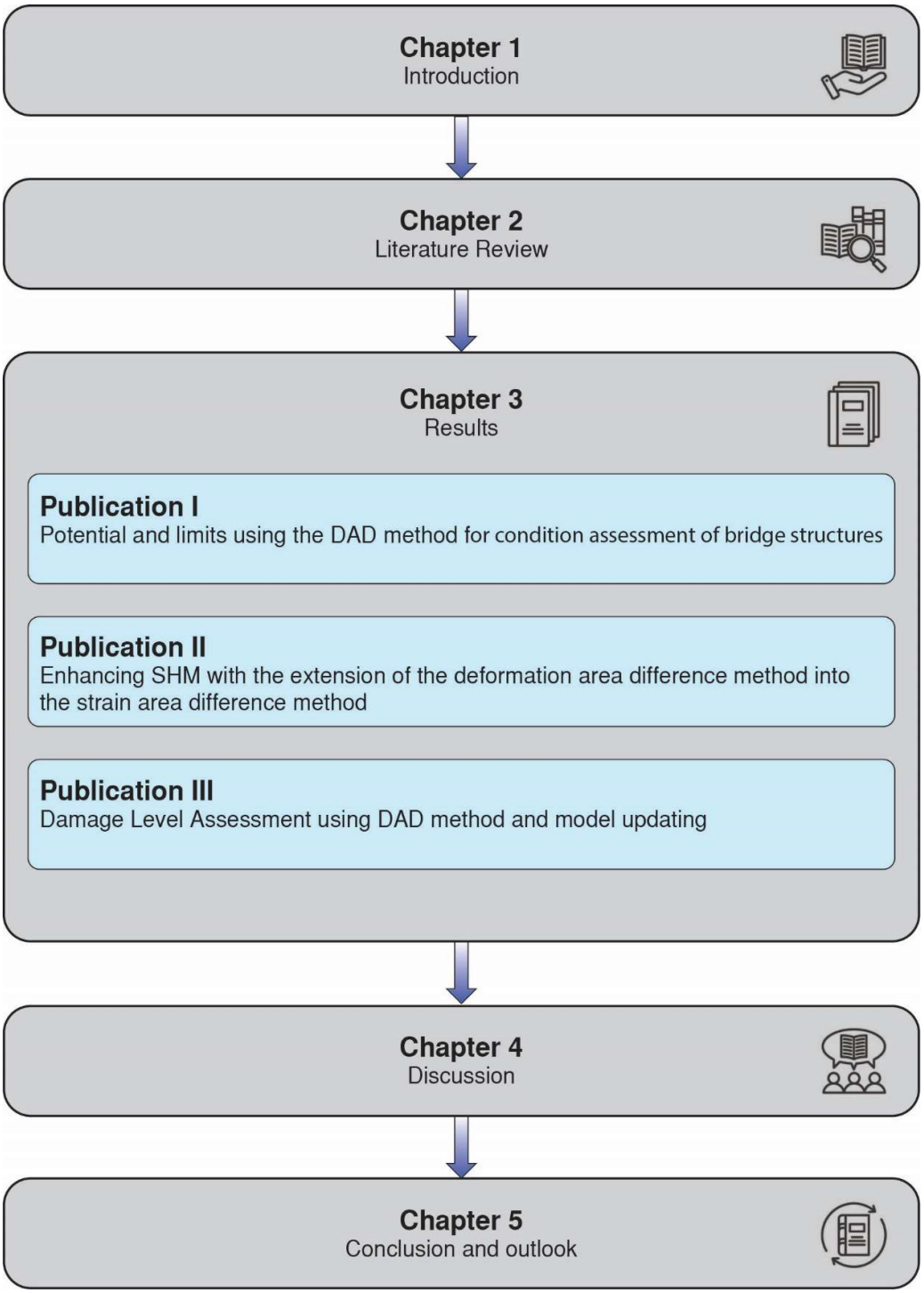

Figure 4. Outline of the thesis

2 Review of the Literature

2.1 Bridge Condition Assessment: An Overview

The assessment of bridge condition represents a fundamental aspect of infrastructure management, being indispensable for guaranteeing the safety, reliability, and durability of bridge networks [45]. Bridges are subjected to increasing traffic loads, more severe environmental loads (e.g., wind, temperature, snow, and earthquakes), and material deterioration. Consequently, it is imperative to conduct regular assessments of their structural condition to prevent damages that could result in closure or collapse, optimize maintenance, and extend the service life of aging infrastructure. The assessment of bridge condition is a matter of regulatory concern, with different countries adopting varying standards to ensure structural safety and reliability. In Luxembourg, bridge inspections are conducted by the Administration des Ponts et Chaussées in accordance with European standards. In the United Kingdom, the Design Manual for Roads and Bridges (DMRB) CS 450 is followed, while in Switzerland, the SN 640 820b standard is utilized for civil engineering inspections. In the United States, the National Bridge Inspection Standards (NBIS) are followed in accordance with Title 23 of the Code of Federal Regulations. In Germany, inspections are conducted in accordance with DIN 1076, with the authorities placing a particular emphasis on the necessity for reliable, uniform, and comprehensive assessment methods to ensure the safety and integrity of the country's infrastructure as outlined in the Federal Transport Infrastructure Plan [46].

Historically, visual inspections have been the primary method for assessing bridge health. While these inspections provide a direct, hands-on evaluation of visible damage, they are inherently limited in their ability to detect early-stage deterioration or structural issues inside the structure. Engineers are often tasked with identifying surface-level damage such as cracks, spalling, or corrosion, but internal damage can go unnoticed until it reaches an advanced stage [47]. Additionally, as bridge networks expand and grow more complex, the reliance on manual inspections alone becomes increasingly impractical due to time, cost, and labor constraints [48].

To address these limitations, advancements in technology have led to the development of sensor-based SHM systems. These systems allow for continuous or periodic monitoring of critical parameters such as vibration, strain, and deflection, providing early detection of potential problems. SHM complements traditional inspection methods by offering objective data and reducing the reliance on subjective visual assessments. As bridge structures become more complex and traffic loads continue to increase, the integration of SHM is becoming essential for proactive, data-driven maintenance strategies [49]. Today, bridge condition assessment is moving towards a hybrid approach, combining manual inspections with SHM systems. This combination enables more comprehensive monitoring, with SHM addressing the limitations of manual methods by providing real-time data on structural behavior. Looking forward, the future of bridge condition assessment will likely involve further advancements in SHM technology, including the use of machine learning

algorithms for predictive maintenance and more widespread adoption of non-contact methods like UAV-based inspections and photogrammetry [50].
For each paper, a literature review was conducted that compliments this chapter.

2.2 Research context on condition assessment of bridge structures

To put the research in the context of the current research, a VOSviewer map shown in Figure 5 was designed using the key words of over 2,000 publications related to condition assessment of bridge structures. The search engine of the bibnet.lu library network was used to analyze the co-occurrence of key words to creating maps based on network data for visualization. Each node represents a keyword or topic, with node size indicating its occurrence frequency in the literature. Clusters, distinguished by color, group related topics based on their co-occurrence and link strength, highlighting research subfields such as SHM, deformation, and FEA. The proximity of nodes reflects the strength of their relationship, with closer nodes indicating stronger thematic connections. This map provides a clear overview of the research landscape, contextualizing the DAD method within the broader framework of bridge damage detection methodologies. The DAD method primarily aligns with the keyword **'deformations',** as it focuses on static deflection analysis to assess the condition of bridge structures. By analyzing the connected research themes in the VOSviewer map, including SHM, FEA, and noise processing, it becomes evident how the DAD method bridges experimental data and computational tools. Each cluster highlights complementary aspects that enhance the applicability of DAD, from refining deformation measurements to integrating advanced monitoring and modeling techniques. This interconnected framework situates the DAD method as a crucial component within the broader landscape of bridge damage detection methodologies.
The VOSviewer map offers a visual representation of the interconnectivity between research themes pertaining to condition assessment for bridge structures. Each cluster represents a discrete focus within the field, offering insights into the manner in which methodologies such as the DAD method are situated within the broader research universe. By examining clusters such as SHM, FEM, and measurement techniques, it is possible to contextualize the relevance and role of the DAD method. This approach illustrates the manner in which the DAD method interacts with and contributes to these established themes.

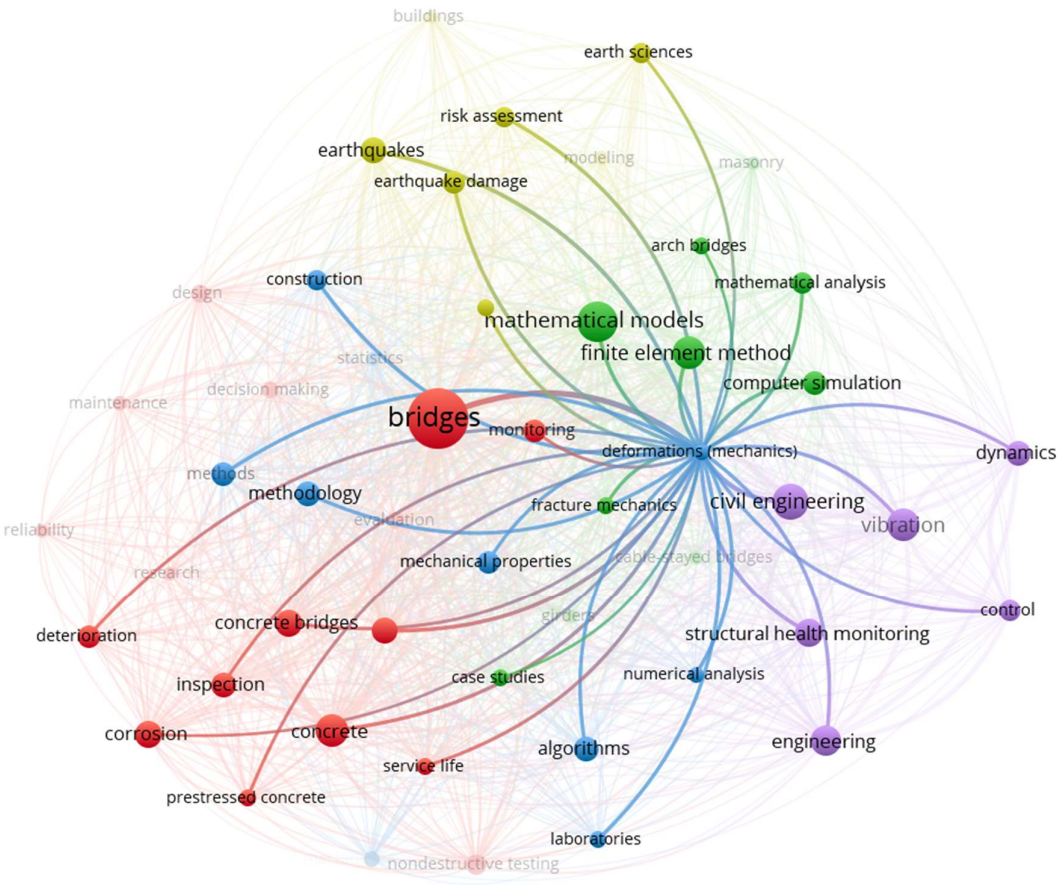

Figure 5. VOSviewer map of the keyword 'condition assessment'

- **Structural Health Monitoring**

The cluster on SHM emphasizes various methodologies aimed at assessing structural integrity. The field of SHM encompasses a range of methodologies, including dynamic, acoustic, and static methods. In this context, the DAD method can be classified as a static load deflection method, which employs deformation measurements under static loads to assess structural stiffness and damage.

Static methods, including DAD, offer distinctive advantages when compared to alternative SHM approaches. In contrast to traditional methods, which often rely on visual inspections or simple deformations and dynamic property measurements, the DAD method offers a more sophisticated approach by analyzing local deformation behavior under controlled static loads and comparing the results with a FEM model. This allows for the precise localization of damage and the assessment of damage levels.

- **FEM and Computational Tools**

The cluster on FEM demonstrates the increasing reliance on computational tools for structural analysis. The DAD method is inherently reference model-based, with FEM calculations forming a

central component of the approach. By integrating the FEM and comparing the results with measurements, the DAD is able to localize damage and assess its severity.

This reliance on FEM distinguishes the DAD method from statistical models that do not require a computational reference. Such models necessitate the acquisition of sufficient data over time and are therefore unsuitable for use as a sole condition assessment method, as is the case with the DAD method. This integration serves to illustrate the DAD method's alignment with advanced computational practices within the domain of SHM.

- **Measurement Techniques and Deformation Mechanics**

The cluster on measurement techniques and deformation mechanics is concerned with the tools and principles used to capture structural behavior. Conventional deformation-based methodologies frequently depend on fundamental instrumentation to monitor deflections, such as levelling or laser scanning. In contrast, the DAD method employs precise deformation measurements under static loads to calculate changes in structural stiffness. As it relies on high precision, advanced methods such as photogrammetry are employed for the DAD method and FOS for the SAD method.

This distinction situates the DAD method within a more advanced category of measurement techniques. It employs high-precision deformation data for the assessment of structural condition, thereby bridging the gap between raw measurements and meaningful condition indicators.

- **Emerging Opportunities in Monitoring**

Although the VOSviewer map includes clusters such as automation and AI, these technologies have yet to be directly applied in the DAD method. Nevertheless, these represent potential avenues for future investigation. As an illustration, image processing and UAV inspection could serve to supplement the DAD method, facilitating remote deformation monitoring. Similarly, the application of artificial intelligence could facilitate more sophisticated data interpretation, although this remains outside the current scope of the DAD method's implementation.

The VOSviewer map illustrates the interconnectivity of SHM research, demonstrating how the DAD method unites diverse themes, including static deflection methods, FEM-based modeling, and advanced measurement techniques. Rather than supplanting traditional methodologies, the DAD method serves to complement and refine existing approaches, offering a precise and reliable tool for structural condition assessment. This positions it as a valuable addition to the array of techniques available for bridge condition assessment, without overstating its scope beyond its current methodological boundaries. This contextualization underscores its role within the broader landscape of SHM research. In the following, this will be more detailed and discussed in the literature review. An overview of the coherence of the presented different research topics is shown in Figure 6.

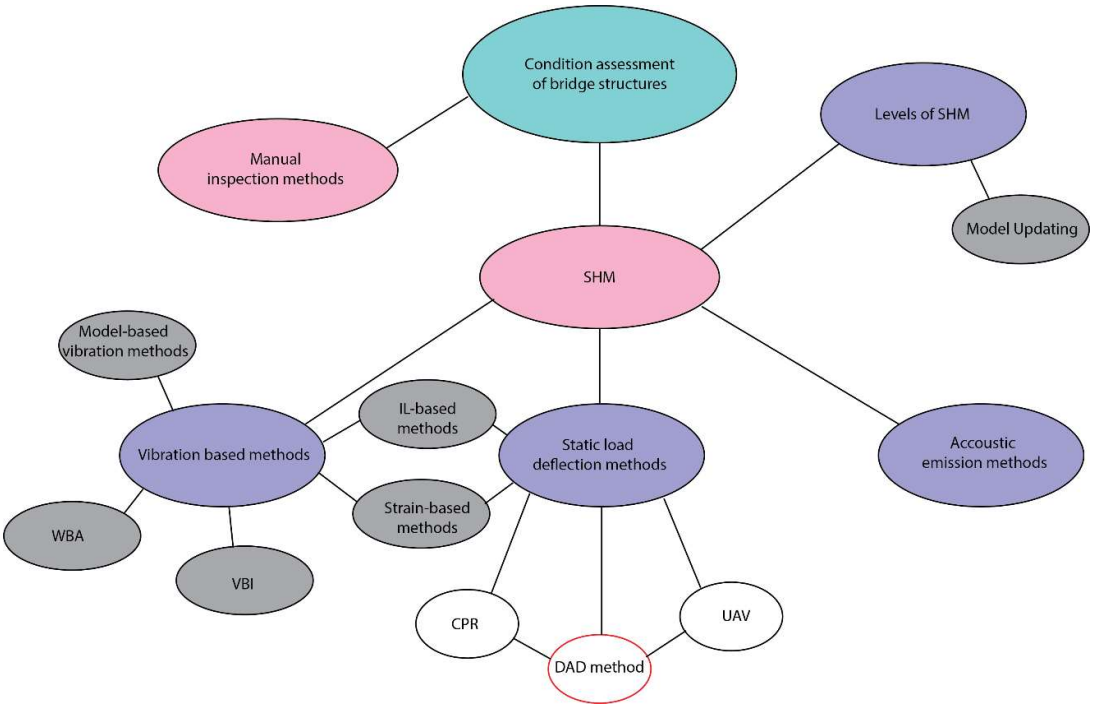

Figure 6. Literature review overview

2.3 Manual Inspection Methods

Manual inspection methods have long been the foundation of bridge condition assessment, largely due to their simplicity and the direct nature of visual evaluations. In practice, these inspections are typically conducted by experienced engineers who assess the physical condition of bridges based on observable signs of damage, such as cracks, spalling, corrosion, or misalignment of structural elements. In Germany for example, inspections are regulated by the DIN 1076 standard, which requires periodic visual inspections, with more detailed checks scheduled for critical structures or those nearing the end of their design life [51].

Despite their widespread use, manual inspection methods have inherent limitations, particularly when it comes to detecting internal damage or early-stage deterioration. Cracks, for example, often develop from micro cracks inside the structure and may only become visible on the surface once they have progressed significantly. Similarly, corrosion in steel components can be hidden, making it difficult to detect without invasive testing [52]. This reliance on surface-level observations means that internal structural issues may go undetected until they manifest as more severe problems, potentially compromising the safety of the bridge.

Another major drawback of manual inspections is their subjective nature. The accuracy of an inspection can vary depending on the experience and expertise of the engineer conducting the assessment. Studies have shown that even experienced inspectors may overlook subtle signs of deterioration, leading to inconsistent evaluations [53]. Furthermore, manual inspections are time-

consuming and labor-intensive, especially for large or complex bridge structures where access to all areas may be challenging. In many cases, scaffolding or special equipment is required to reach certain parts of the bridge, adding to the cost and duration of the inspection process [54].

In response to these challenges, many engineers now incorporate non-destructive testing (NDT) techniques alongside visual inspections to improve the accuracy of their assessments. NDT methods such as ultrasonic testing, ground-penetrating radar (GPR), and infrared thermography allow inspectors to identify hidden defects that may not be visible to the naked eye [55]. For example, GPR can detect delamination in concrete decks, while ultrasonic testing is effective at identifying internal cracks in steel components. However, these techniques also have their limitations, particularly in terms of the equipment and expertise required for proper implementation. Moreover, NDT methods still rely on manual data collection and interpretation, which can introduce variability and limit their effectiveness in large-scale assessments.

The limitations of manual inspection methods underscore the need for more objective, data-driven approaches to bridge condition assessment. While manual inspections will likely remain an important part of bridge maintenance programs due to their regulatory requirements and the familiarity of engineers with these techniques, the growing integration of SHM systems provides a valuable complement. SHM technologies can offer continuous, real-time monitoring of structural health, addressing many of the gaps in traditional manual inspections by providing more accurate, consistent, and early detection of damage.

2.4 Structural Health Monitoring (SHM) Methods

SHM systems offer periodic, and continuous monitoring of bridges, reducing reliance on manual inspections and providing real-time data on structural performance. SHM systems are typically classified into several categories based on the type of data they collect and the method of assessment. The three main categories of SHM methods are vibration-based methods, static load deflection methods, and acoustic emission methods, each addressing different aspects of bridge behavior and damage detection.

a) **Vibration-Based Methods**: These methods monitor the dynamic response of a structure by measuring vibrations. Damage such as cracks, stiffness loss, or joint issues often cause changes in a structure's natural frequencies, mode shapes, and damping characteristics. Vibration-based methods can be further classified into model-based approaches, Wavelet-Based Analysis (WBA), and Vehicle-Bridge Interaction (VBI) methods, each offering unique approaches to damage detection.

b) **Acoustic Emission Methods**: Acoustic-based SHM methods capture sound waves generated by cracks or other structural failures. These high-frequency emissions are particularly useful for detecting internal damage in materials like concrete or steel, where visual inspections might miss early-stage deterioration.

c) **Static Load Deflection Methods**: These methods involve applying a known static load to the structure and measuring the resulting deflections. By comparing the deflection response to baseline data, engineers can assess changes in stiffness and identify potential damage. Strain-based methods and Influence Line (IL) analysis are often employed alongside deflection measurements to provide more localized insights into damage.

Together, these methods provide a comprehensive framework for understanding the condition of a bridge and detecting early-stage damage before it becomes critical.

2.4.1 Vibration-Based Methods

Vibration-based methods are fundamental in SHM for detecting structural damage by monitoring changes in dynamic properties. These methods measure how a structure responds to external forces, particularly vibrations induced by environmental factors like wind, traffic, or artificial excitation. Any damage to a structure, such as a loss of stiffness or the development of cracks, typically alters its natural frequencies, mode shapes, and damping characteristics. Vibration-based methods can be subdivided into model-based approaches, WBA, VBI, and other hybrid approaches.

- **Model-Based Vibration Methods**

Model-based vibration methods rely on finite element (FE) models that simulate a bridge's expected dynamic behavior. Engineers use these models to predict how the structure should respond to loads, comparing these predictions with real-world data. Discrepancies between predicted and measured responses can indicate damage. A key advantage of model-based methods is the ability to not only detect but also quantify damage by updating the FE model as new data becomes available. This model updating process involves continuously refining the model's parameters to reflect the real-time condition of the bridge [56]. Gonen et al. [57] explore by means of a numerical model a hybrid method for bridge damage detection and localization that combines data from conventional accelerometers and computer vision-based measurements (Figure 7). The study shows that this hybrid approach improves damage detection accuracy, especially near bridge supports, by enhancing spatial resolution. Despite that, the method's accuracy can be affected by the need for high-resolution sensors and the difficulty in capturing small vibrations near supports. The authors also state that modelling uncertainties can also affect the damage detection problem in real applications. Nguyen et al. [58] present a method combining the Gapped Smoothing Method (GSM), which is a modal curvature-based damage detection method, and Convolutional Neural Network (CNN) for damage localization in girder bridges. The study demonstrates the effectiveness of this approach using the Bo Nghi Bridge as a numerical case study, showing that it accurately detects and localizes damage with up to 30% stiffness reduction without the need of the initial data of the intact structure. Nevertheless, the method's reliance on high-quality images for CNN training with a high number of sensors and sensitivity to noise in the data can affect its accuracy. Model-

based vibration methods usually struggles with the quality of the FE model, as support conditions, joints, and other details influence the dynamic behavior significantly.

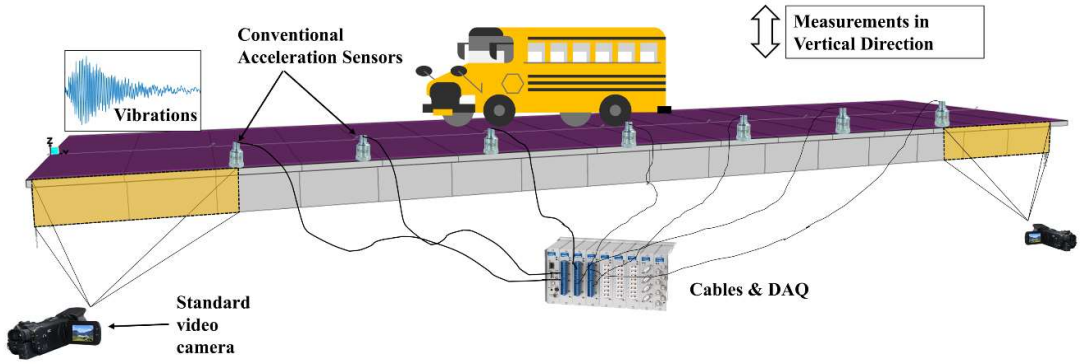

Figure 7. Proposed methodology illustrated on an isolated one-span bridge deck. Gonen et al. [57]

- **Wavelet-Based Analysis (WBA)**

WBA methods are used to detect localized damage by examining how wavelets—mathematical functions that can capture both frequency and time information—propagate through the structure. When waves encounter discontinuities, such as cracks or other defects, their characteristics (e.g., speed, amplitude, and frequency) are altered. WBA methods are highly sensitive and can detect small-scale damage that might go unnoticed by traditional vibration analysis. Das et al. [59] successfully applied WBA to monitor structures, demonstrating its ability to detect early signs of structural damage. Zhang FL et al. [60] propose an efficient Bayesian Fast Fourier Transform (FFT) method for bridge damage detection using ambient vibration data. It constructs a likelihood function and prior probability density function based on Gaussian distribution to integrate modal parameters and their uncertainties. The method demonstrated high accuracy in both numerical simulations and real-world applications, such as a simply supported bridge and a steel truss bridge. The numerical study considers damage with a bending stiffness reduction from 5% to 50%. As there is no outlier boundary defined, the detectable damage level is not specified. The field tests were conducted whereas damage on the bridges were successively detected and however no information is given about damage level or measurement noise. However, the approach's dependence on accurate prior information of the undamaged structure for constructing the Bayesian model and the sensitivity to noise in the ambient vibration data can affect its robustness as a high number of mode shapes is needed for damage detection, a disadvantage that all WBA methods have in common.

- **Vehicle-Bridge Interaction (VBI) Methods**

VBI methods leverage the dynamic interaction between a bridge and the vehicles that cross it. As vehicles induce dynamic loads on the bridge, the structure's response—measured through accelerometers, strain gauges, or displacement sensors—can reveal changes in stiffness or potential damage. VBI methods are particularly advantageous because they utilize traffic as a natural source of dynamic loading, making them well-suited for long-term, non-intrusive monitoring [61]. A

noteworthy approach by O'Brien et al. [62] employs a Moving Force Identification (MFI) algorithm within a two-dimensional VBI model. This method entails the simulation of vehicle fleets traversing the bridge, with subsequent analysis of the resultant force patterns to identify any variations that may indicate structural damage. By observing shifts in frequency within these force patterns, the algorithm can identify reductions in stiffness as minor as 6% of the beam depth, thereby demonstrating a sensitivity that surpasses that of traditional displacement-based methods. However, O'Brien et al. recognize a significant challenge in implementing this method in real-world settings: differentiating damage-induced forces from ambient traffic forces. Building on the sensitivity of VBI-based methods, Zhang et al. [63] propose an innovative approach that focuses on the vehicle's contact-point response rather than solely on bridge forces or displacements (Figure 8). In their methodology, the authors utilize Instantaneous Amplitude Squared (IAS) peaks, calculated using the Hilbert transform, as indicators of damage. This study demonstrates that IAS peaks remain consistent even when subjected to challenging conditions, such as road roughness, measurement noise, and multi-damage scenarios. These findings underscore the robustness of this approach in detecting both localized and distributed damage. However, the study reveals a limitation in scenarios involving random traffic. The presence of extraneous IAS peaks generated by non-damaging vehicles may interfere with damage-related signals, thereby impeding the precise identification of damage locations.

Another contribution to the field of VBI-based damage detection is presented by Mousavi et al. [64], who introduce a baseline-free, physics-based approach utilizing static condensation transformation matrices. This method is distinctive in that it does not require a baseline from an undamaged structure, thereby enabling the analysis of incomplete VBI data and the direct detection of changes in structural stiffness. By averaging the results of multiple experiments, the method is able to effectively identify both the location and severity of bridge damage, even when road roughness and noise are present. While Mousavi et al. emphasize the method's adaptability, a potential limitation emerges from its dependence on repeated experiments to mitigate noise, rendering it less suitable for rapid or real-time assessments. While VBI-based damage detection methods can offer high sensitivity to structural changes, they are inherently susceptible to environmental noise, road surface variations, and, particularly, random traffic interference.

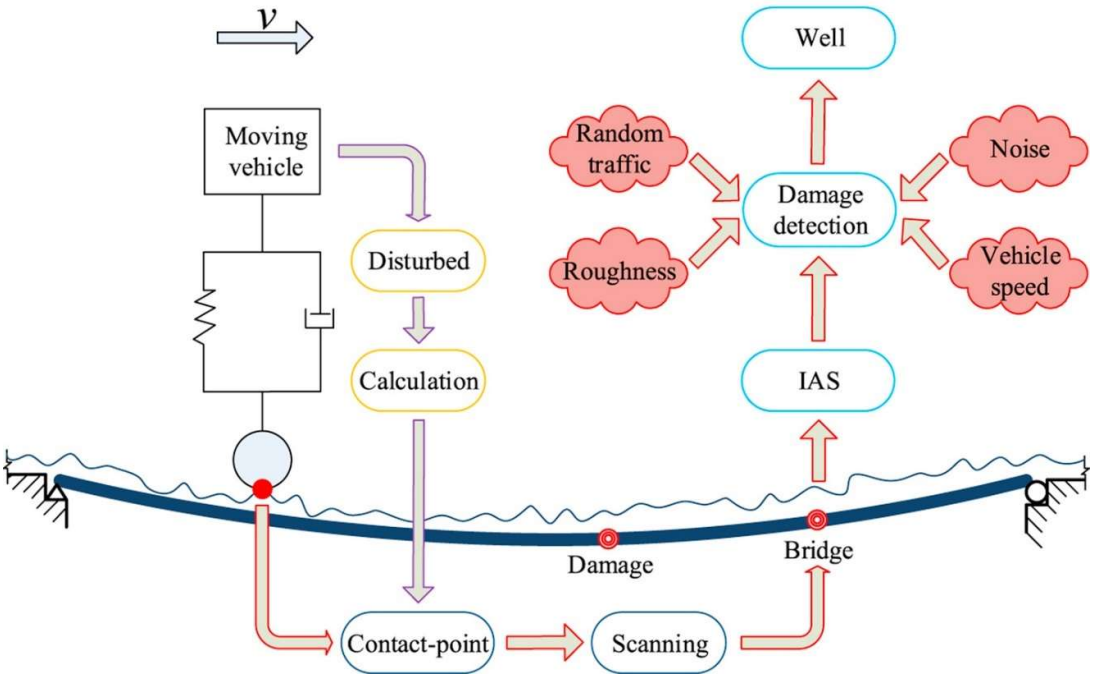

Figure 8. Contact point response of a moving test vehicle [63]

- **Influence Line (IL) methods**

IL-based analysis, traditionally used in static load deflection methods, is also applicable in vibration-based methods. ILs map how a structure deflects or strains under a moving load, such as a vehicle, and can be used to assess the dynamic response of bridges. For example, by comparing ILs over time, engineers can track changes in the structure's behavior, revealing areas where stiffness has decreased due to fatigue or damage [65], [66]. In Sun et al. [67], a damage detection algorithm was introduced which calculates the dynamic curvature of displacement responses induced by moving vehicles. By isolating the damage-induced component through filtering techniques that utilize the bridge's natural period, the method can identify both the location and severity of damage. The algorithm was tested through FEM under simulated noise, road roughness, and VBI, and it was found to reliably detect single and multiple damage scenarios. However, the authors identified a potential limitation for future studies, namely the possibility that higher local modes or torsional modes in real bridges might impact the accuracy of the results. Wang et al. [68] proposed a method for the extraction of ILs from dynamic bridge responses, which employs a mixed fitting function comprising piecewise polynomials and harmonic sinusoids. By separating quasi-static and fluctuating components, the method is able to effectively localize damage through the identification of deviations in the IL curves. The robustness of the method was validated by means of numerical simulations and field tests, even in the presence of varying vehicle speeds. However, the study explicitly noted that noise, road roughness, and vehicle speed variability could compromise the accuracy of IL extraction, particularly in uncontrolled environments. While vibration-based IL methods offer significant promise for detecting and quantifying bridge damage

with high sensitivity, they share common limitations in practical implementation. Both studies highlight the challenges of noise, road surface irregularities, and environmental variability, which complicate precise measurement and signal interpretation.

- **Strain-Based Methods**

Strain-based methods are often used in conjunction with vibration-based methods to measure how much deformation occurs in response to dynamic loads. Strain gauges or Fiber Optic Sensors (FOS) are deployed to capture localized strain in critical areas of a structure. Strain-based methods provide additional insight into areas where vibration measurements alone may not be sufficient, particularly for detecting early-stage damage in specific components of the structure. By integrating strain measurements with vibration data, engineers can improve the precision of damage localization and quantification [69]. This hybrid approach enhances the accuracy of structural assessments and damage detection. Wu et al. [70] developed a damage assessment methodology that employs long-gauge Fiber Bragg Grating (FBG) sensors to monitor strain histories under dynamic vehicular loads. By establishing a correlation between strain history data and stiffness coefficients, the study was able to effectively quantify structural damage in a bridge-vehicle system that was scaled to a 1:10 ratio. The method exhibited high sensitivity to reductions in stiffness and demonstrated robust performance under varying loading scenarios. Although this method is effective on a scaled model, its application to large bridges necessitates meticulous sensor placement and substantial computational resources for real-time data processing. Furthermore, potential instability in strain measurements near the supports may present challenges in implementing this technique. In a separate study, Lee et al. [71] presented a method utilizing distributed fiber optic sensors (DFOS) for the collection of both static and dynamic strain data. The dynamic strain data were subjected to analysis using a neural network algorithm that had been trained to detect and localize damage. Validation on a cracked cantilever beam demonstrated that the method accurately identified both the location and severity of damage. The distributed sensing approach yielded high-resolution strain data, thereby enhancing the model's predictive accuracy. Nevertheless, the study identified two significant challenges: the method's dependence on high-quality strain data and the extensive dataset necessary to train the neural network. The presence of noise in strain measurements and variability in operational conditions necessitate the use of robust preprocessing techniques to ensure reliable application. While fiber optic sensors offer exceptional sensitivity and resolution, both studies highlight the necessity for extensive sensor arrays and advanced computational techniques, which can increase the complexity and cost of large-scale bridge applications.

Recent advances in SHM have also focused on integrating machine learning algorithms to analyze the large datasets generated by traffic-induced vibrations. These algorithms can detect subtle patterns in the vibration data that may indicate early-stage damage, further enhancing the sensitivity and accuracy of vibration-based methods [72]. In conclusion, despite the extensive applications of vibration-based methods for damage detection and their notable advancement in research, all

studies consistently highlight common challenges: vibration-based techniques typically necessitate extensive data, are vulnerable to noise interference, and experience global structural response to dynamic excitation, which complicates damage detection and, more crucially, its localization.

2.4.2 Acoustic Emission (AE) Methods

AE methods are widely used in SHM for detecting internal damage in bridge structures. AE is based on capturing high-frequency sound waves generated by stress-induced events within the material, such as crack formation, crack propagation, or material degradation. These sound waves, often referred to as "emissions," can be detected by strategically placed sensors that monitor changes in the material's acoustic behavior. When damage occurs, such as a crack opening or a fiber break in a tendon, it releases energy that propagates through the structure as an acoustic wave. The detection and analysis of these waves allow engineers to localize and assess damage before it becomes critical [73].

AE methods are particularly effective in materials like steel and concrete, where internal cracking or other forms of damage may not be visible during traditional visual inspections or deflection-based monitoring. AE has a high sensitivity to active damage, making it a powerful tool for detecting early-stage deterioration that could otherwise go unnoticed. By capturing and analyzing the waveform characteristics of acoustic emissions, engineers can determine the location, type, and severity of the damage [74].

One of the primary advantages of AE methods is their ability to provide real-time monitoring. Unlike periodic inspections, AE can continuously monitor the structural integrity of a bridge, allowing for immediate detection of any stress-induced events. This makes AE particularly valuable for monitoring critical structures, such as long-span bridges or bridges subjected to high traffic volume, where early detection of damage is essential for preventing catastrophic failure [75]. In addition, advances in sensor technology and signal processing algorithms are continually improving the accuracy and reliability of AE methods, making them an increasingly important component of modern SHM systems [76].

- **Steel Bridges**

In steel bridges, AE methods have proven to be highly effective in detecting internal fatigue cracks, which often form at stress concentrations, such as welded joints or bolted connections. A study by Aggelis et al. [77] demonstrated the use of AE sensors in detecting fatigue crack initiation in steel bridge components. The sensors captured acoustic emissions generated by micro-crack formations long before these cracks became visible, allowing engineers to take preventative maintenance measures.

- **Concrete Bridges**

In concrete bridges, AE methods are used to monitor the development of cracks caused by factors such as creep, shrinkage, or thermal expansion. AE can detect the onset of micro-cracking, which can eventually lead to significant structural issues if left untreated. A comparative study by Ohtsu et al. [78] compared AE monitoring with strain-based methods in concrete bridges, finding that AE was more sensitive to detecting early micro-cracking, while strain measurements were more effective for identifying larger, more developed cracks. This comparison underscores the complementary nature of AE and other SHM techniques in providing a comprehensive assessment of a structure's health. In another study, Mahmoudkhani et al. [79] proposed an acoustic emission-based method for the detection of wire breaks in post-tensioning tendons of bridge structures. The method employs piezoelectric AE sensors to record acoustic signals generated by the breaking of wires, cracking of grout, and environmental noise. Subsequently, these signals are processed using a fuzzy C-means clustering algorithm, which enables the differentiation of wire-breaking events from other noise sources. To enhance robustness, the algorithm incorporates a pre-recorded database of environmental noise and grout crack signals from an actual bridge. The study demonstrated the effectiveness of the method through experimental tests, achieving 100% accuracy in distinguishing wire-breaking signals from unrelated acoustic events, even under noise-polluted conditions. However, the authors identified a significant limitation: the approach relies on a well-curated database of noise and grout-specific signals to achieve reliable clustering. This dependency presents a challenge for its application in bridges with highly variable environmental conditions or unique grout properties.

While AE methods offer significant advantages in terms of real-time monitoring and high sensitivity to active damage, they also have limitations. One challenge with AE monitoring is the presence of environmental noise, which can interfere with the detection of genuine acoustic emissions. Traffic, wind, and other external factors can generate acoustic signals that may be mistaken for damage-related emissions, complicating the interpretation of the data [74]. To address this, advanced filtering techniques are often employed to distinguish between damage-related acoustic events and environmental noise.

Another limitation of AE is its reliance on active damage. AE sensors can only detect acoustic emissions when damage is occurring in real time, meaning that pre-existing damage, such as dormant cracks or corrosion, may not generate the necessary emissions to be detected. This makes AE less effective for monitoring long-term, non-active damage compared to methods like static load deflection or strain-based monitoring, which can assess the overall condition of the structure without requiring active deterioration [73].

2.4.3 Static Load Deflection Methods

Static load tests have constituted a fundamental methodology for the assessment of structural capacity since antiquity. Initially, they served to substantiate the robustness of empirically designed structures prior to their inauguration. By the 17th century, advancements in the fields of statics and material mechanics transformed these tests into a quantitative tool for validating theoretical models. In the present era, static load tests are an indispensable tool for assessing novel designs, evaluating the condition of aging structures, and verifying the efficacy of rehabilitation efforts. Contemporary applications are focused on both diagnostic load testing, which is employed to refine theoretical models and evaluate performance under service loads, and proof load testing, which assesses safety under extreme conditions in non-destructive testing. These methodologies ensure precise insights into structural behavior, guiding engineering practices across a range of scenarios. These methods are particularly effective for detecting global structural changes, such as reductions in stiffness or deformations caused by damage like cracking or corrosion. Deflection measurements, when compared to baseline data, can provide valuable insights into the health of the bridge, revealing changes in performance over time [80].

Static load deflection tests often use displacement transducers or non-contact laser sensors to record the movement of critical elements, such as girders and bridge decks, under load. Recent advances in optical measurement techniques, such as photogrammetry and Terrestrial Laser Scanning (TLS), have significantly improved the accuracy and resolution of deflection measurements, enabling engineers to detect even small changes in structural behavior [81]. However, while static load deflection methods are effective in capturing global stiffness changes, they may struggle to detect early-stage localized damage, which can go unnoticed until it affects the overall structure. Comparative research conducted by Boumechra [82] demonstrated the advantages and limitations of static load deflection methods compared to dynamic monitoring techniques. While dynamic methods, such as vibration-based monitoring, are more sensitive to early-stage damage, static load deflection methods are often more reliable for detecting significant structural changes under real-world load conditions. In another comparative study, Tian et al. [83] found that static load deflection measurements were particularly effective for long-span bridges, where challenges such as the necessity for supplementary scaffolding and the constraints of diverse measurement transducers exist, and where deflection profiles can reveal distributed damage along the structure. These studies highlight the complementary nature of static and dynamic monitoring approaches.

Meng et al. [84] proposed a method for identifying corrosion damage in beam-like structures incorporating shear deformation using Timoshenko's beam theory, addressing the inaccuracies of Euler-Bernoulli's theory. By minimizing an objective function based on the discrepancy between analytical and measured displacements, the method improved damage identification accuracy. The approach was validated through numerical tests on a multispan beam structure, demonstrating significant improvements in detecting corrosion depths. However, the accuracy of damage detection

can degrade with small data errors, if shear deformation effects are not precisely modeled. Xiao et al. [85] developed a damage identification method for large-scale truss structures by enforcing stiffness separation and simplifying the objective function. The high-dimensional structure is separated in substructures for damage identification reducing the number of unknown parameters using displacement measurements as additional boundary conditions. Then, strain error functions are calculated for each subsection. The method was validated on truss structures, showing accurate stiffness measurements. However, it is currently limited to specific truss structures, necessitating further research for broader application.

- **Strain-Based Methods**

Strain-based methods are commonly used alongside static load deflection tests to provide more localized assessments of structural performance. Strain gauges or FOS are placed on key structural elements to measure the deformation caused by applied loads, allowing engineers to detect localized damage, such as cracks or material degradation [86]. The combination of strain-based and deflection measurements enables a more detailed understanding of how individual components of a bridge are responding to stress. For example, research by Abdel-Jaber & Glisic [87] compared strain-based methods with deflection-based measurements in assessing the health of a prestressed concrete bridge. Their results showed that strain gauges were able to detect localized damage, such as cracking in the deck, even when global deflection measurements remained within acceptable limits. The study concluded that strain-based methods could provide early warnings of structural distress before it significantly impacts overall bridge behavior, making them a valuable complement to deflection tests.

Figure 9. Optical fiber for strain measurement of a bridge structure [88]

Oskoui et al. [88] introduced a method for distributed damage detection along the lengths of multi-span continuous bridges using Brillouin Optical Time Domain Analysis (BOTDA) FOS (Figure 9). The approach effectively identified and localized damage by monitoring and normalizing distributed strains, comparing them with theoretical influence lines, and formulating a damage index. Evaluated through load testing on a five-span bridge, the method successfully pinpointed damage locations verified by visual inspections. However, the method requires careful calibration

and normalization of strain measurements to accurately detect damage, as on one side the measured distributed strains include contribution from thermal effects and on the other side also changes in operation such as e. g. traffic disturbance of other vehicles, varying axle configurations, and varying axle weights can affect the measurement results.

- **IL Methods**

IL-based methods, which analyze how a bridge responds to moving loads, are another powerful tool used in static load deflection testing. ILs provide a representation of how measurement data, - such as deflection or strain – changes as a load moves across the bridge. By analyzing these lines, engineers can assess the structure's stiffness and identify areas where damage may have compromised its load-bearing capacity [89]. IL-based methods are especially effective for multi-span bridges, where localized damage in one span can alter the load distribution across the entire structure. Research by Yunkai et al. [90] demonstrated that IL analysis is highly effective for tracking changes in stiffness in continuous beam bridges. By comparing ILs over time, they were able to localize areas where stiffness reductions had occurred due to fatigue. In a comparative study, Boumechra [82] examined the use of IL-based methods alongside traditional deflection tests and found that ILs provided more detailed information about the distribution of loads and stiffness along the length of the bridge, making them particularly useful for detecting damage in complex bridge systems.

Chen et al. [91] present a novel method for damage detection and quantification in beam structures using Deflection Influence Lines. By reconstructing DIL matrices by applying the matrix decomposition of the stiffness and flexibility matrices of the structure, the relationship between structural damage and corresponding changes in DILs was derived. The study shows in numerical and experimental case studies under laboratorial conditions that this approach accurately localizes and quantifies the damage level in simply supported, continuous beams through numerical simulations and laboratory experiments. The drawback in the method's effectiveness and accuracy on damage localization again relies on the number and location of sensors and their distance from the damage position. The authors note that only beam structures were investigated, and complex bridge structures would bring further challenges with greater matrix size, modelling uncertainty.

The study by Marasco et al. [92] explores a method that combines genetic algorithms and neural networks to analyze ILs, effectively localizing structural damage in bridges. In this study, midspan DIL, and support Rotation Influence Line (RIL) were used. The study demonstrates the method's robustness through numerical simulations, showing improved performance in terms of computational time, improved accuracy localization of critical elements using fewer measurement points, and improved versatility of the approach. However, the approach's reliance on high-quality data for neural network training and the complexity of genetic algorithm optimization can affect its efficiency and scalability.

In general, IL-based methods rely on analyzing changes in the course of the IL. This is typically the case for most static load methods. As a result, it is not possible to detect damage that has already occurred. Only damage that arises when the bridge is already monitored can be identified. This highlights the need for methods that can assess the structure without requiring knowledge about its current condition.

2.4.4 The Deformation Area Difference (DAD) Method

In order to address the previously described need for knowledge regarding the condition of bridge structures and the necessity of long-term monitoring for effective damage detection, the DAD method was developed as an innovative and efficient technique for the assessment of bridge structures. This method, belonging to the static load deflection methods, is designed to detect local stiffness reduction by analyzing the deflection lines of the investigated structure under static loading. In contrast to traditional visual inspections, the DAD method is capable of detecting stiffness-reducing damage that is not discernible from the exterior. In comparison to numerous dynamic monitoring techniques, the DAD method is not influenced by global factors such as temperature or asphalt layer effects. The DAD method can identify damage without prior measurements, and a single measurement can already detect damage, making it an effective approach for rapidly assessing the condition of existing bridge structures.

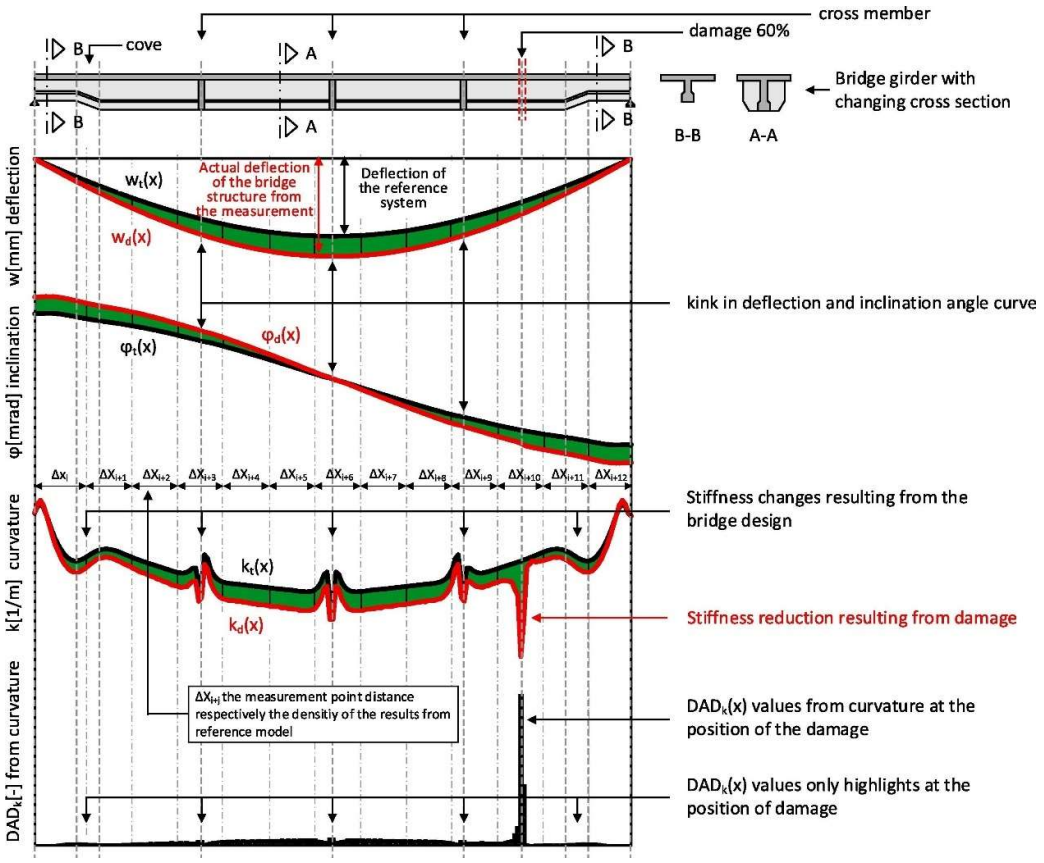

Figure 10. Principle of the Deformation Area Difference (DAD) method [93]

The fundamental tenet of the methodology is founded upon the principles of static load deflection measurements, as illustrated in Figure 10. A continuous deflection line is measured on the actual bridge structure under static load. A reference deflection line is then calculated using a numerical model. The curvature of the two deflection lines, derived from the in-situ measurements and the numerical reference model, is calculated using the double derivation of the deflection line. Given that the determined can be expressed as the ratio between the bending moment and the stiffness, each local change in the stiffness can be identified using the curvature and the bending moment. The area between the curvature lines is subjected to analysis. The area is then subdivided into smaller sections. Subsequently, each difference area is squared and divided by the sum of the squared areas, with the objective of filtering out the known stiffness changes from the reference. As a result of this normalization, the effect of damage is reinforced, thereby allowing for an increase in the sensitivity of the method.

The DAD method is a particularly useful tool for damage detection, as it is highly sensitive to localized changes. This makes it ideal for identifying cracks, local material degradation, and other issues that could compromise the bending stiffness of a bridge structure. [94]. The method is further detailed in the Results section.

The DAD method was initially evaluated on a reinforced concrete beam in a controlled laboratory experiment. The girder was subjected to incremental loading, the onset of cracking was monitored, and the DAD method was employed. Deflection measurements were obtained using CRP. The DAD method facilitated the detection of damage within the serviceability limit state [94].

These experimental findings were further validated through laboratory experiments on another reinforced concrete beam and on a steel beam. The effect of camera calibration on measurement precision and, consequently, on damage detection quality was demonstrated, and the smoothing of the deflection line was introduced using polynomial regression. It was shown that CRP can be used to achieve highly accurate measurements with a precision of 0.06 mm [95].

Following its successful implementation in laboratory settings, the DAD method has been applied to a real-world bridge structure. A static load deflection measurement was conducted on a prestressed concrete slab bridge in Altrier, Luxembourg, utilizing six heavy trucks as the loading apparatus. To capture the bridge's response, modern deflection measurement technologies, including UAV-based photogrammetry, laser scanners, levelling, and displacement sensors, were employed. Given the relatively recent construction of the bridge, it was not anticipated that it would have sustained any damage. The objective of the study was not to detect damage, but rather to test the applicability of the method and to assess different techniques for deflection line measurement. The applicability of the method on real bridge structures was demonstrated, and photogrammetry in combination with UAVs was shown to have a high degree of precision (0.12 mm) and to be a highly practical solution for the method's application compared to displacement transducers. [93].

The primary advantages of the DAD method are its insensitivity to global influences such as temperature, the absence of a prerequisite knowledge of the bridge condition, and the capacity to detect damage with a single measurement. Furthermore, the method's foundation in static load-deflection measurements, coupled with the straightforward yet efficacious photogrammetry-based measurement technique, enables the DAD method to be deployed with greater ease than dynamic monitoring systems, which frequently necessitate the use of specialized equipment and more intricate data interpretation processes [96].

However, despite the evident advantages of the DAD method, it is not without limitations. Previous studies have demonstrated that the accuracy of the method is contingent upon the precision of the deflection measurements. To minimize the impact of noise and ensure reliable results, highly accurate measurements are required. Even minor errors in measurement can affect the outcomes, reducing the reliability of the method for real-world applications. The deflection value and the position of the damage have been shown to have an essential effect on damage detection, which requires further investigation [93].

Although the DAD method offers a promising approach for detecting localized damage in bridge structures, its reliance on high-precision measurements and the significant influence of various parameters underscores the necessity for further investigation and refinement. Addressing these challenges will be crucial for fully realizing the potential of the DAD method in SHM. A more detailed discussion is located at the end of the literature review.

2.5 Levels of SHM

The classification of SHM into different levels is a widely accepted framework introduced by Rytter [97]. This classification defines the capabilities of a monitoring system in terms of its ability to detect, localize, quantify, and assess damage in a structure (Figure 11). Understanding these levels is essential for selecting appropriate methods based on the complexity of the structure, the severity of potential damage, and the monitoring objectives.

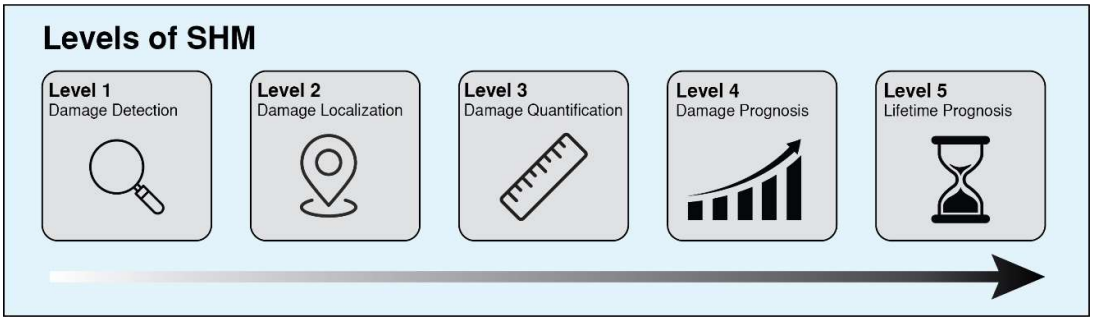

Figure 11. Levels of SHM

- **Level 1: Damage Detection**

At this basic level, the SHM system is tasked with detecting the presence of damage. The system signals that something in the structure has changed, but no further information about the location

or type of damage is provided. Vibration-based methods, such as modal analysis, are commonly used at this level to detect changes in the structure's dynamic properties, which may indicate damage. These changes in vibration frequencies, mode shapes, or damping ratios serve as early indicators of structural degradation. Rytter [97] originally established Level 1 methods as critical for early warning systems, which can trigger further investigations if anomalies are detected [98].

- **Level 2: Damage Localization**

Level 2 SHM extends the capability of detection to include the localization of damage within the structure. This involves determining the specific area or component where damage has occurred. Techniques such as the DAD method fall into this category, as they can precisely localize stiffness reductions within a bridge by comparing deflection curvatures from load tests. The DAD method's strength lies in its ability to localize damage even when global deflection changes are minimal, making it particularly useful for identifying local damages [93]. Additionally, strain-based methods and IL-based techniques contribute to this level, providing localized information about structural performance under varying loads.

- **Level 3: Damage Quantification**

In Level 3 SHM, the focus shifts from simply detecting and localizing damage to quantifying its severity. This is an important step, as knowing the extent of the damage helps engineers determine whether repairs are immediately necessary or if the structure can continue to function safely for some time. Techniques such as model updating allow engineers to refine FE based on real-world data from sensors, such as strain gauges or displacement sensors. By continuously updating these models, the severity of damage—such as a reduction in stiffness or the extent of cracking—can be quantified more accurately [99].

- **Level 4: Damage Prognosis**

Level 4 SHM systems not only quantify damage but also predict how it will evolve over time. This involves using predictive models to simulate the progression of damage under future load conditions, providing engineers with a forecast of the remaining service life of the structure. Prognostic capabilities are particularly useful in long-term maintenance planning, enabling more efficient resource allocation and proactive interventions. Machine learning algorithms, in particular, are increasingly being integrated with SHM systems at this level to analyze large datasets and generate predictive insights [100]. Prognosis at this level helps decision-makers plan more accurately, thereby reducing both financial costs and the risk of structural failures.

- **Level 5: Lifetime Prognosis**

The highest level of SHM, Level 5, focuses on the lifetime prognosis of the structure, predicting its future performance and estimating when and where failure is likely to occur. This requires not only a comprehensive understanding of the current state of the structure but also sophisticated modeling of how various factors—such as expected traffic loads, environmental conditions, and material

degradation—will affect the structure over time. Advanced techniques, including full-scale simulations and extensive sensor networks, are used at this level to provide a complete assessment of the structure's long-term behavior and its eventual failure modes. The application of data-driven methods, such as semi-supervised learning, is especially promising for addressing the uncertainty of long-term predictions [101].

2.6 Model Updating (MU) in SHM

Model updating (MU) is a fundamental technique in SHM used to refine predictive models of structural behavior by incorporating measurement data gathered from sensors. This approach is essential for improving the accuracy of damage detection, localization, and quantification. The core principle of model updating is to adjust the parameters of an existing FE model based on discrepancies between the model's predicted responses and actual sensor data. By continuously refining the model in this way, engineers can obtain a more accurate representation of the structure's real-time condition, enabling more precise assessments of structural health [102].

The primary goal of model updating is to reduce the discrepancies between the predicted and actual responses of a structure, which often arise due to changes in material properties, environmental conditions, or errors in the initial design assumptions, especially for support conditions and joint stiffnesses. By incorporating measurements from SHM systems, such as strain gauges, accelerometers, and displacement sensors, engineers can continuously refine their FE models to reflect the current state of the structure [102]. Model updating has been widely applied in bridge structures for SHM, enhancing damage detection accuracy. In a study by Zong et al. [103], a response surface-based FE model updating technique was applied to a prestressed concrete bridge, significantly improving the alignment between predicted and actual structural responses under operational conditions.

Several studies have demonstrated the effectiveness of model updating in improving SHM systems. Teughels & De Roeck [104] applied model updating to a prestressed concrete bridge and improved the localization and quantification of damage by comparing vibration data with the updated model's predictions. Sanayei et al. [105] conducted FE model updating on a scale bridge, integrating static and modal test data, and improved the structural performance model. This helped to detect stiffness and mass parameter deviations and allowed more accurate predictions for future damage assessment. Similarly, Garcia-Palencia et al. [106] used dynamic data to update the model of an in-service bridge, successfully identifying stiffness and damping parameters that reflect the actual condition of the structure. This protocol offers great potential for regular SHM activities.

Despite the advantages of model updating, several challenges remain. The process can be computationally intensive, especially for large-scale structures with complex geometries, requiring significant processing power to continuously update FE models with up-to-date measurement data. The FE model needs to be designed in such way, that it is suitable for model updating, e.g.

segmentations and parametrization. Furthermore, data quality is a critical factor. Noisy or incomplete data can lead to erroneous model adjustments, compromising the SHM system's accuracy. Recent advancements aim to address these challenges through optimization techniques. Zhao et al. [107] proposed an improved response surface method for FE model updating, combining the radial basis function with annealing algorithms, which significantly enhanced both the convergence speed and accuracy of the model for a highway bridge.

- **Model Updating for increasing SHM Levels**

Model updating plays a critical role in various levels of SHM, particularly at Level 3, where the goal is to quantify the damage level. By integrating measurement data into the FE model, engineers can assess the extent of damage, such as stiffness loss or crack propagation, in a structure. This enables more accurate tracking of damage progression and informs maintenance decisions, making MU a very useful tool for SHM level enhancement.

At Level 4 and Level 5, model updating is critical for predicting future structural behavior and estimating the remaining service life. By continuously refining the model with up-to-date data, future loading conditions can be simulated and when and where failures are likely to occur can be predicted. This predictive capability is crucial for implementing proactive maintenance strategies.

2.7 Photogrammetry in Bridge Condition Assessment

Photogrammetry is a powerful non-contact technique for measuring and monitoring the structural condition of bridges. By capturing images from multiple angles, photogrammetry allows for the generation of point-clouds, and three-dimensional models of structures, which can be used to assess deformations, cracks, and corrosion. Photogrammetry has become particularly valuable in recent years due to advances in digital photography, image processing algorithms, and the increasing use of Unmanned Aerial Vehicles (UAVs) for data collection.

Photogrammetry operates by using two-dimensional images taken from different viewpoints to create a three-dimensional representation of an object. The accuracy of this method depends on the quality of the camera, the resolution of the images, and the geometry of the object being measured. The technique involves measuring the displacements and deformations of visible features on a structure by comparing images taken over time or under different loading conditions [108]. Unlike traditional sensors, which often only capture one-dimensional measurements, photogrammetry provides a comprehensive view of a structure's condition by capturing data from multiple dimensions. There are different forms of Photogrammetry. One of the most common forms is aerial photogrammetry, which involves capturing images from aircraft or drones to create detailed maps and 3D models of terrain and structures. Another popular form is terrestrial photogrammetry, which utilizes ground-based cameras to capture images from various angles, allowing for precise measurements and detailed modeling of objects and environments. Close-range photogrammetry is

another variant that focuses on capturing images from a very short distance, often used in applications such as architecture, engineering, and cultural heritage documentation to ensure high levels of detail and accuracy.

- **Close-Range Photogrammetry (CRP)**

Close-Range Photogrammetry (CRP) is particularly well-suited for bridge condition assessments, where the distance between the object and the camera is typically less than 300 meters. CRP is used for detailed deformation measurements, structural modeling, and condition monitoring, offering a high degree of accuracy at a relatively low cost [109]. In bridge assessments, CRP has proven effective in capturing small deflections and other changes in the structure under static loads. The ability to create highly detailed three-dimensional models from CRP data has made it a key tool for detecting damage in areas that are difficult to access or not visible to the naked eye [110].

A study by Valença et al. [110] showed that CRP could achieve results comparable to traditional displacement transducers or LVDTs in bridge monitoring applications while offering greater flexibility and ease of use. Additionally, the hardware independence of photogrammetry, along with its rapid data collection and processing capabilities, makes it particularly attractive for large-scale infrastructure assessments. Photogrammetry systems can be easily mounted on UAVs, providing an efficient solution for monitoring extensive bridge spans without interrupting traffic or requiring manual inspections [109].

- **Applications in Structural Health Monitoring (SHM)**

In SHM, photogrammetry has been applied to measure bridge deflections under load, track crack development, and monitor structural movements over time. For instance, CRP by Mirzazade et. al [111] has been employed to monitor geometrical deviations in bridges, as demonstrated in the Pahtajokk Bridge in Northern Sweden. This method, which involves comparing point cloud datasets generated from scans taken a year apart, has shown potential for accurately monitoring both large-scale and small-scale damage, although its accuracy depends on the quality of equipment and environmental conditions. Similarly, studies of Hu et al. [112] have investigated structural deformation monitoring using CRP combined with image recognition technology, achieving high accuracy in calibrating measuring points. Moreover, innovative methods like photogrammetry-based structural damage detection by tracking a visible laser line have been developed by Xu et al. [113]. This technique projects a laser line onto a structure's surface and tracks it to measure deformations, successfully identifying structural damage by analyzing anomalies in the curvature mode shapes, whereas the curvature mode shapes are calculated by converting the time-domain data of the measured laser line into frequency-domain data. The technique requires precise alignment and calibration of the laser line and camera setup and may be sensitive to environmental conditions affecting the visibility of the laser line, which can be challenging for bridge structures. Reagan et al. [108] developed a UAV-based photogrammetry system for bridge deflection measurements, showing that the technique could provide highly accurate data on structural

deformations under live loads. Their system was able to capture deflections to an accuracy of within 0.01 mm, demonstrating the potential of photogrammetry as a non-contact method for monitoring the health of bridge structures. Riveiro et al. [114] validated the use of photogrammetry for measuring vertical underclearances and beam geometry in bridge inspections. The study found that photogrammetry was effective in capturing small deformations and provided an accurate representation of the structure's geometry, making it a valuable tool for ongoing SHM efforts. Photogrammetry is also widely used in crack detection. Yang & Xu [115] improved digital photogrammetry techniques to monitor the development of cracks in concrete bridges. By analyzing the changes in crack patterns over time, engineers can assess the progression of damage and determine whether immediate maintenance or further monitoring is required. The method's non-contact nature allows for efficient monitoring without interrupting the structure's operation, which is a significant advantage over traditional crack detection methods.

Photogrammetry offers several advantages in the context of bridge condition assessment. It is cost-effective, non-invasive, and capable of capturing detailed data over large areas. Moreover, the technique can be employed using UAVs, making it easier to monitor remote or difficult-to-access areas. The use of UAVs also enables photogrammetry to cover larger structures, such as long-span bridges, while still maintaining a high degree of accuracy [116].

However, there are some limitations to photogrammetry. The accuracy of the measurements can be affected by environmental factors such as lighting, shadows, and weather conditions, which can introduce noise into the images. Additionally, the method requires careful calibration of the cameras and equipment to ensure precision, and post-processing of the data can be time-consuming. Despite these challenges, ongoing advancements in image processing algorithms and sensor technology are continually improving the reliability and efficiency of photogrammetry for SHM [114].

2.8 UAVs for Bridge Condition Assessment

UAVs have revolutionized the field of SHM, providing a cost-effective and flexible approach to bridge condition assessment. UAVs offer distinct advantages, including the ability to access difficult-to-reach areas without the need for expensive scaffolding or temporary traffic disruptions. Recent technological advancements have made UAVs a versatile tool for gathering data on various aspects of a bridge's condition, including deflection measurements, crack detection, and corrosion. UAVs are remotely or automated piloted aircraft equipped with various sensors, cameras, and non-destructive testing equipment to capture high-resolution imagery and data. UAV systems consist of the drone itself, a payload (camera or sensor), a ground control station, and data processing software. UAVs can either be fixed-wing or rotor-based, with rotor-based systems like quadcopters being more commonly used in SHM due to their ability to hover and capture detailed images at close range [117].

In recent years, UAVs have been integrated with various sensing technologies, including LiDAR, infrared thermography, and photogrammetry. These technologies enable the collection of highly accurate data, facilitating the creation of three-dimensional models of the bridge. UAV-based systems can also be used to monitor structural deflections, measure crack dimensions, and assess other critical parameters of structural health [116].

- **Applications in Bridge Condition Monitoring**

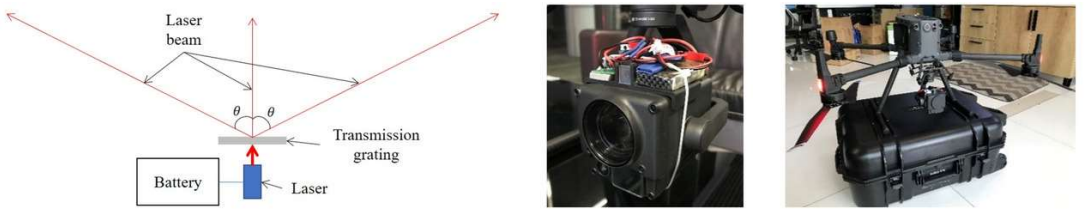

(a) Schematic diagram of the coplanar laser indicator.

(b) Physical picture of the coplanar laser indicator fixed on the Zenmuse H20 gimbal and camera.

(c) M300 equipped with the coplanar laser indicator.

Figure 12. System overview of the UAV equipped with the coplanar laser indicator [118]

UAVs have been extensively used for various applications in bridge inspection. Xu et al. [119] propose a crack detection method using large-scene images acquired by UAVs. The approach involves a UAV-based scheme based on the acquisition of large-scene images, followed by a background denoising algorithm and a maximum crack width calculation algorithm. The method significantly improved detection efficiency and achieved an accuracy of up to 93.4% in crack detection. However, this method is a visual method and thus cannot identify damage inside the structure. Zhuge et al. [118] describe a noncontact deflection measurement using multi-UAV systems that also can demonstrate high precision in monitoring bridge deflections, showing good agreement with traditional methods, despite the challenges related to UAV coordination and environmental factors (Figure 12). A study by Perry et al. [120] demonstrated the use of a UAV system for non-contact deflection measurement, achieving high precision in monitoring bridge deformations without interrupting traffic (Figure 13). This method showed excellent agreement with traditional methods, highlighting the efficiency of UAV-based deflection measurements in real-world applications. UAV systems have also proven useful in inspecting areas that are typically difficult to access, such as underneath bridge decks and other remote areas [116]. In crack detection, UAVs equipped with high-resolution cameras capture images of large areas of the bridge structure. Peng et al**.** [121] demonstrated the application of UAVs for detecting cracks in bridge concrete components, achieving high accuracy using image processing algorithms.

One of the primary advantages of UAVs in SHM is their ability to capture large quantities of high-resolution data efficiently. UAVs significantly reduce the time and cost associated with traditional bridge inspections, which often require extensive manual labor and equipment setup. Their flexibility in accessing hard-to-reach areas and their ability to operate in hazardous environments make UAVs particularly valuable in bridge inspections where safety and accessibility are concerns

[117]. However, there are some limitations to the use of UAVs in SHM. UAVs are susceptible to environmental factors such as wind, rain, and poor visibility, which can impact the quality of the data collected. Additionally, the battery life of UAVs is limited, restricting the duration of data collection during a single flight. Another limitation is that while UAVs equipped with photogrammetry and visual imaging can detect surface damage, they may not capture subsurface damage without integrating more advanced sensors such as acoustic emission or infrared thermography [122]. No fly zones and application for flight permission with authorities also needs to be considered, which can be restricting and time-consuming.

As UAV technology continues to evolve, its role in SHM is expected to expand. Future developments may focus on integrating UAVs with machine learning algorithms to automate data analysis, enabling real-time damage detection and assessment. Additionally, advances in UAV payload capacity and battery life could enable longer flights and more comprehensive inspections. Combining UAVs with ground-based sensor networks and other SHM technologies will likely improve the overall accuracy and reliability of bridge monitoring systems [116].

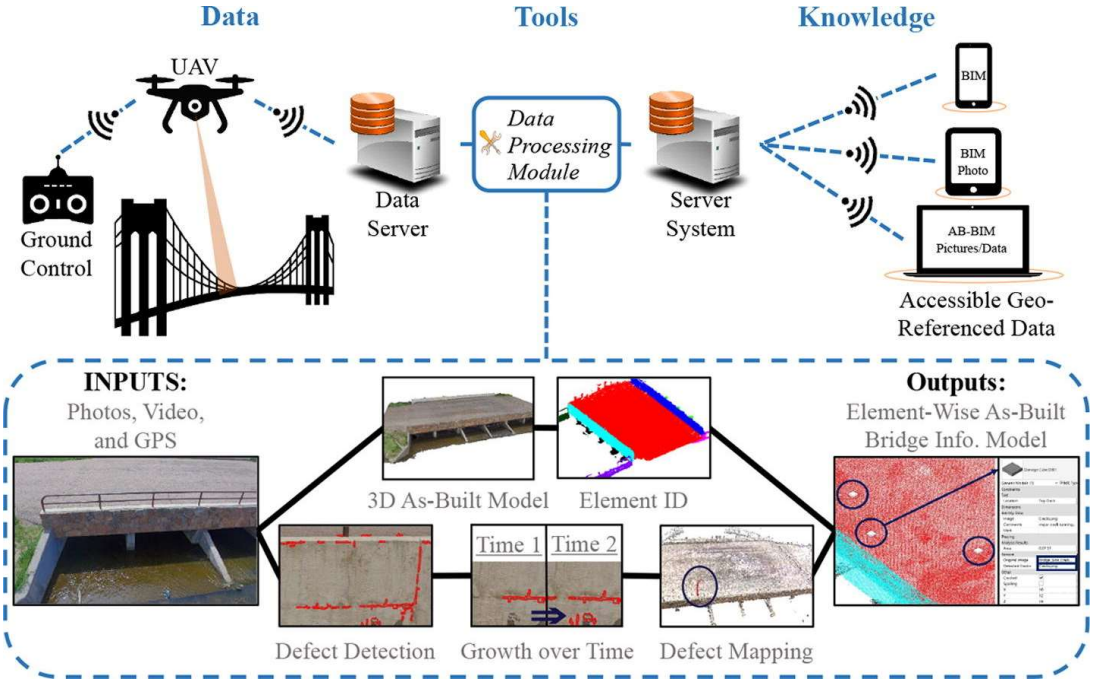

Figure 13. Streamline bridge inspection system [120]

2.9 Enhancing the DAD method: Addressing key limitations for advanced SHM applications

The presented literature review highlights the significant advancements and limitations in SHM methodologies, including the DAD method. While the DAD method demonstrates substantial potential for localized damage detection in bridge structures, its limitations underscore the necessity for further research. These constraints primarily relate to the method's sensitivity to noise,

dependency on deflection values, and challenges in adapting to diverse structural types. This study is based on the need for innovative approaches to address these challenges.

Although it has been demonstrated that the DAD method is theoretically capable of detecting a reduction in bending stiffness of 1%, the influence of noise was identified as a limiting factor. Additionally, [93] demonstrated the limiting nature of the deflection value for damage detection. These limitations present a significant obstacle to the practical implementation of the method in real-world applications. Accordingly, the initial objective is to gain insight into the current limitations of the DAD method with relation to deflection values, noise levels, measurement point distances, and the influence of damage position along the longitudinal axis. Although the method has been successfully tested in a laboratory setting on reinforced concrete and steel girders, its application to bridge structures and the influence of local damages within these cross-sections remains unexplored. Given that real bridge cross-sections exhibit a far more complex load-bearing behavior than simple beam girders, it is essential to investigate precisely how local damage affects the curvature.

In consideration of the identification of noise as a critical limiting factor, particularly in scenarios with low deflection values, this study aims to enhance the damage detection potential of the DAD method. However, the current approach relies on curvature lines derived from measured deflections, which amplifies the influence of noise. To address this limitation, the study aims to eliminate the need for derivation by exploring alternative methods for obtaining curvature lines, particularly through strain measurements, thereby enhancing the method's precision.

Furthermore, the current implementation of the DAD method has primarily concentrated on its application at the detection and localization levels of SHM. Although the method is effective in identifying damage and its location, its capability to quantify the severity of damage remains underexplored. The size of the damage is necessary for determining the residual load-bearing capacity and for determining the remaining service life. Therefore, this study will also focus on enhancing the DAD method to a higher level of SHM.

In conclusion, this study addresses the principal shortcomings of the DAD method, with the objective of transforming it into a more sophisticated SHM tool, capable of being deployed on actual bridge structures in realistic conditions. By enhancing its precision and expanding its capabilities, this research contributes to making the DAD method a modern and powerful SHM tool for condition assessment.

3 Results

This chapter will introduce the papers that have been published containing the results and studies related to this research project. The outcomes of this research are documented in a total of three journal articles. Collectively, these publications offer in-depth insights into the findings and investigations of this study.

3.1 Introduction to the publication I

The first paper addresses the inaugural research question by investigating the limitations of the DAD method to achieve a comprehensive understanding of its potential and to inform subsequent research strategies. This investigation is conducted through a numerical parametric analysis, focusing on parameters such as deflection values, noise levels, and measurement point distances. Additionally, the paper examines the applicability of the DAD method for different bridge structure types to explore its full potential. For the first time, the influence of local changes within the cross-section on the performance of the DAD method is explored. This novel aspect provides deeper insights into how structural characteristics affect damage detection capabilities and informs strategies for optimizing the method.

3.2 Publication I: Potential and limits using the DAD method for condition assessment of bridge structures

T. Čamo, D. Waldmann, "Potential and limits using the DAD method for condition assessment of bridge structures", Engineering Structures, vol. 308, 1 June 2024, 117972, doi: https://doi.org/10.1016/j.engstruct.2024.117972

AUTHORS CONTRIBUTIONS:

T. Čamo, Conceptualization, Methodology, Software, Validation, Formal Analysis, Investigation, Resources, Data Curation, Writing - Original Draft, Visualization, D. Waldmann, Conceptualization, Methodology, Validation, Resources, Writing - Review & Editing, Supervision, Project Administration, Funding Acquisition

ABSTRACT:

In the last years, the age of the bridge contingent is in all countries constantly increasing while in addition the bridges are solicited by an increased load level and an increased load frequency. This leads to an urgent need for defining efficient bridge structure condition assessment methods. Here, the Deformation Area Difference (DAD) method has already proven to be reliable and practicable. This has been shown in recent research in which it has been tested on real bridge structures using photogrammetry and compared with other highly precise measurement techniques.

In order to further develop this method and to analyze the potential and limits of the DAD method in practical experiments, in the present study different parameters are varied such as e.g., the loading position along the longitudinal axis of the bridge structure, the damage position along the longitudinal axis of the bridge structure and the damage position in the cross-section. In addition, the method is analyzed on different bridge structure types. The results of the current study allow to determine set-ups for in-situ experimental investigations of existing bridge structures using the DAD method. A novel DAD Influence Line (DAD IL) is introduced to identify necessary load positions for the experiments. The Damage Detection Range depends on different damage levels, precisions, and deflection values. It is found that for local damage only one measurement line for the cross-section is not sufficient.

3.2.1 Introduction

Bridge structures are connecting the world and are essential for a functional infrastructure of a country. Due to aging and increased loading generated by augmented needs of transport, existing bridges are highly challenged. As the bridge structures were not designed for these high solicitations, their lifetime is highly affected [123]. This has resulted in over 70 collapsed bridges over the last decade, e.g., the Fern Hollow bridge in Pittsburgh (01/2022) [124], the Mexico City Metro overpass collapse (03/21) [125], the Caprigiliola bridge in Aulla (04/2020) [126] or the Ponte Morandi in Genoa (08/2018) [127]. Studies worldwide highlight the insufficient condition of bridge structures. The US national Bridge Inventory database categorizes 7.6% of the included bridges as "structurally deficient" [128]. In Germany, 15.7% of the highway bridge structures received the

category “not sufficient” in terms of their condition [129]. Similar findings have been reported for several other countries around the world [126].

Thus, the need for bridge inspections and structural health monitoring is increasing [130]. Bridge inspections are still mainly executed by visual inspection [131]. The usual inspection methods can detect mainly damages which can be seen externally or which are close to the surface however, they do not allow to detect internal damage, which might lead to failure of the structure.

Therefore, new methods for Structural Health Monitoring (SHM) are intensively investigated. The studies can be split into methods based on static loading tests, based on the analysis of the influence line, and based on modal parameters. In the field of SHM, modal parameter-based methods are gaining popularity due to their effectiveness in detecting structural changes and practicality in utilizing environmental excitations available in real-world scenarios. Koo et al. [132] developed a unique approach for detecting damage-induced chord-wise deflection (DI-CD) in beam-like structures using a Positive-Bending-Inspection-Load (PBIL) able to identify the location with the maximum deflection and an abrupt change in slope. The approach utilized modal flexibility matrices obtained from acceleration measurements. Although the study was verified through numerical and experimental studies, it only investigated beam-like structures, leaving a gap in knowledge for other types of structures. Bungard et al. [133] aimed to bridge the gap by analyzing the in-situ conditions of concrete structures, specifically through the analysis of bending modeshape curvature. The authors successfully identified discontinuities at positions of reduced stiffness and introduced the Modeshape Area Differences (MSAD) method as a tool for quantifying these changes. However, they also noted the method's sensitivity to environmental conditions, particularly temperature, which affects the dynamic properties and complicates the detection of minor stiffness changes. This highlights the need for methods that can withstand such global conditions. Catbas et al. [134] used Modal Flexibility-Based Deflection and Flexibility-Based Curvature methods for damage detection and localization. These methods utilize modal flexibility to calculate deflection and curvature for more precise damage indication. Experimental studies have validated the theory and practical application of large-scale laboratory structures and a three-span highway bridge, but the practical application of these methods requires consideration of their complexity in real-life applications, as they require extensive data collection and signal processing and the determination of the optimal sensor location combining expertise in data science. Bernagozzi et al. [135] also provided insights into truncation errors related to modal flexibility-based deflections. The authors used a Load Participation Factor (LPF), which is a factor derived analytically, to determine the relative contribution of each mode to the overall deflection and to indicate early signs of truncation effects. This method was validated through numerical models and experimental data from a steel frame structure, demonstrating its practical applicability. However, the practical application of their findings may be constrained by challenges posed by irregular structures. Sung et al. [136] proposed a Normalized Uniform Load Surface (NULS) curvature

method for damage detection, which successfully localized damage in both numerical and experimental studies of beam-like structures. The method which is based on modal flexibility uses NULS curvature changes as an indicator for damage, which only occur at damaged elements. It is important to note that this method has limitations and is only applicable to beam-like structures. However, a significant challenge persists for modal parameter-based methods: accurately detecting damage in complex structures and under varying environmental conditions. Although these methods show promise, the investigation of influence lines is becoming a crucial research area, providing complementary insights into SHM methodologies. OBrien et al [137] have developed a method using bridge-weigh-in-motion (B-WIM) to detect damage from rotation. In their approach, a B-WIM system is designed to estimate axle weights of passing vehicles, while rotation is measured at the support to provide information for the B-WIM. By calculating the influence line for rotation, this method allows for the detection and localization of damage However, there are certain drawbacks associated with this method. Firstly, the effectiveness of the method to detect damage decreases with increasing distance from the supports. Additionally, reliable results require a substantial amount of data to be analyzed over an extended period. A study combining Moses' method [138] and Quilligan's method [139] to create a unit influence line is carried out by Heitner et al. [140]. In this research, a bridge experiment is performed with a WIM system and strain transducers measuring random traffic data without the information of calibrated axle weights. Initially, a preliminary influence line is based on engineering judgement, iteratively, the Moses' algorithm is applied to calculate the axle weight, which is used to recalculate the influence line with the Quilligan's method. However, this study is limited to data collected from a single lane, and the presence of traffic in other lanes affects the obtained data significantly, leading to errors. While the method is developed to track changes in the condition of the bridge structure, it is not able to detect damage through single measurement. Martinez et al. [141] analyzed damage with means of a numerical bridge model in case of drive-by monitoring, which describes the monitoring by sensors at different locations on passing vehicles. Their approach utilizes a dynamic vehicle-bridge interaction model for deflection determination and employs a damage detection algorithm using the unit load method. However, in contrast to the usual unit load method, this study considers the variable virtual bending moment due to the moving load. The Flexural Rigidity (FR) of each finite element of the bridge's numerical model is back-calculated with absolute deflections, allowing for the calculation of FR by comparing deflections between a healthy and damaged bridge. Nonetheless, it is important to note that the method proposed by Martinez et al. is only applicable to bridges with a constant FR over the entire length of the structure. While methods based on the influence line offer valuable insights, they face challenges related to measurement noise effects which makes it necessary to make an assessment over an extended period to ensure reliable outcomes. He et al. [142] present a noteworthy approach in the realm of influence line-based methods. Their study uses a two-stage method: a quasi-static moving load is used to induce

displacement responses in beam structures. The two-stage process combines damage localization using the area of the region encircled by the displacement influence line change (DILC) in the first stage, and damage quantification based on the area between the DILC and the beam (ADB) in the second stage. While He et al.'s method has been successful in both numerical and experimental settings, however it has a significant limitation. Specifically, it requires a substantial number of measurements to accurately construct the DILC from quasi-static loads. This need for extensive data collection could lead to challenges in practical applications, particularly in scenarios where obtaining numerous measurements is impractical or too resource-intensive.

Static load deflection-based methods have demonstrated effectiveness detecting damage, characterized by a change in stiffness. Ha et al. [143] analyzed two different damage detection methods based on the displacement of a structure for determining damage in bridge structures. The first method, known as the Displacement Assurance Criterion (DAC) is used to identify the damage severity and the Displacement-Based Index (DBI) to localize damage. DAC uses the normalized displacement at an observation point and shows the degree of the relationship between the damaged displacement curve and the displacement curve of a different state of the structure resulting to a DAC, which is able to describe a stiffness loss without localization of damage. The DBI describes the point-relation degree at different points of the deteriorated and intact girder. It reaches the highest value at the position of damage. In this study, the DBI was calculated on a numerical destructive test on a prestressed concrete beam and could clearly identify damage. In their approach, noise was also simulated, and it was found that noise with a value of less than 0.1 % of the nodal displacement difference will not lead to misinterpretation of results. Another parametric study by Ono et al. [144] analyzed the DBI in comparison with the Grey Relational Coefficient Method (GRC). The GRC assesses the similarity of a reference sequence (undamaged displacement influence line) and a deteriorated sequence using the displacement values (damaged displacement influence line). The study found that both methods yield similar results; however, the DBI was found to minimize effects of noise and torsion through standardization, and the detectability of damage with a single measurement has a wider range for the GRC compared to the DBI.

Recent technical development facilitates the possibility to perform static load-deformation tests with a continuous deflection line and, thus, opens up resources for new condition assessment methods. A method using a continuous deflection line is the deformation area difference (DAD) method [94]. With a single static load deflection measurement, the DAD method can detect and localize damage from the deflection line. This changes the effort for reliable damage detection tremendously. Apart from theoretical and analytical studies, the method has been tested under laboratory conditions on a single span concrete beam and proved to be able to detect and localize damage. The method has been further developed in [95] dealing with noise removal and was also already tested on a real bridge experiment, namely a prestressed concrete slab bridge with a span of 27 m in Altrier (Luxembourg) [93]. The deflection line was measured, and the DAD method was

carried out with the aim of the study not to detect damage, but rather to show the applicability of the method on real bridge structures using photogrammetry and a drone. It was shown that the reached precision with photogrammetry amounts to 0.12 mm and realistic experimental data was successfully generated. Overall, studies of the DAD method provide evidence of a reliable damage detection method. However, these studies remain narrow in focus dealing with influences from loading position and damage position respecting noise.

The current paper presents the investigation of the potential and limitations of the DAD method in condition assessment. One of the key objectives of this study is to explore the applicability of the DAD method on different types of bridge structures. To analyze different influencing factors a parametric numerical study with the finite element (FE) software SOFiSTiK and the non-uniform Rational B-Splines (NURBS) computed aid design (CAD) software Rhinoceros is carried out. In this study, different parameters are varied such as e.g., the loading position along the longitudinal axis of the bridge structure, the damage position along the longitudinal axis of the bridge structure and the damage position in the cross-section. So far, very little attention has been paid to the role of influence of local damage. Previous studies in the field of damage detection based on static load deflections have only focused on damage in the whole cross-section. As damage usually impacts only local parts of the structure, this paper analyzes the impact of local damage on the method. A novel influence line, the DAD Influence Line (DAD IL), is introduced to investigate how many loading positions are needed for the condition assessment of a bridge structure. Furthermore, the Damage Detection Range is established to get an estimation in which range which damage level is detectable with certain parameters. Subsequently, the results for each parameter are shown and discussed. Finally, the results of the parametric studies are evaluated and their influence on the DAD method and application are assessed for consideration in future experiments. This study advances the current understanding of the DAD method and of damage influence on static behavior of bridge structures by providing the first comprehensive analysis of its application across different bridge structures and with local damage consideration, filling a critical gap in existing research.

3.3 Deformation Area Difference (DAD) method

As the DAD method can detect damage within the service limit state (SLS), the method can be used as a non-destructive method. The method aims to detect damage in structures with only one single measurement and it can be applied on different bridge types and construction materials (see section *Position of the damage in the cross-section in transversal direction*). The DAD method is based on the fact that damage is affecting the bending stiffness of a structure leading to changes in the deflection line [93], [94], [95]. Thus, the DAD method identifies local stiffness changes as damage. For the application of the DAD method, a reference deflection line from the undamaged system is required to which the deflection line of the damaged system is compared. However, for existing bridges, the initial reference line through measurement of the undamaged system is usually not available. In this case, a deformation line from a FE model can also serve as a reference. Among

the advantages of the method counts that the FE model does not have to be calibrated as the exact deformation is not needed. As the DAD method only analyses stiffness changes, this FE model needs to consider all planed bending stiffness changes like e.g., changes in the cross-section or stiffeners.

The deflection curve *w(x)* of a structure contains information about its stiffness. The first derivative of the deflection curve results in the inclination angle (Eq. (1)) of the deflection curve (*φ(x)*) and the second one for small deflections, which applies for most structures, in the curvature (Eq. (2)) (*κ(x)*). The curvature of the structure can be expressed as the ratio of the bending moment to the bending stiffness (Eq. (3)). As the curvature can be obtained by formulating the second derivation of the deflection (Eq. (4)) and as the bending moment can be obtained from the numerical reference model, stiffness changes can be identified and localized with the known information.

$$w'^{(x)} = \frac{\delta_w(x)}{\delta(x)} = \varphi(x) \tag{1}$$

$$\varphi'(x) = \frac{\delta_\varphi(x)}{\delta(x)} \cong k(x) \tag{2}$$

$$\kappa(x) = \frac{M(x)}{EI(x)} \tag{3}$$

$$w''(x) = \varphi'(x) \cong \kappa(x) \tag{4}$$

However, as deflection measurements are subject to noise effects, the measured curvature line can lead to incorrect identification of damage. Furthermore, double derivation causes further noise and planned stiffness changes of the structure's cross section also lead to a change in the curvature line. However, the DAD method can distinguish discontinuities in the curvature line caused by damage from the ones caused by noise or planned stiffness changes [94].

This research study deals with the optimization and verification of the method using a parametric FE analysis without experimental measurements. All results are theoretical results obtained with FE software. In Figure 15 the principle of the DAD method is demonstrated on a typical bridge structure. This is a steel bridge consisting of a deck-girder system with 9 girders sharing a steel plate as upper flange. Cross-girders are connecting the main girders in the quarter points of the longitudinal direction. The bridge structure is a single span with a span length of 27 m. Damage is simulated with a reduction of 10% of the bending stiffness (red area in Figure 15 shows the position of damage). In a first step, the deflection line is obtained from a static load measurement $w_d(x)$ and from a FE model as reference deflection of an undamaged system $w_t(x)$. In Figure 15 a difference between the two deflection lines becomes apparent. However, this difference is not necessarily an indication that the structure is damaged as it can also result from the assumption of different material properties, of different cross-section dimensions or of different loading. Then, in Figure 15 in a next step the first derivation of the deflection is depicted which leads to the inclination angles ($\varphi_d(x)$; $\varphi_t(x)$). In this case, slight kinks become visible in the area of stiffness changes and in the area where

loads are applied. In a third step, the curvature lines ($\kappa_d(x)$ and $\kappa_t(x)$) are calculated with the second derivation of the deflection line, represented below in Figure 15. Here, stiffness changes become clearly visible, whereas stiffness changes due to damage can already be better distinguished from other stiffness changes: the undamaged structure indicates only planned stiffness changes in the curvature line while the one from the damaged system shows additional stiffness changes from damage.

In the case shown here, the curvature line was already able to indicate the damage as the chosen damage level was very high. However, for less severe damage, the curvature line is not appropriate to be used to clearly localize damage. Therefore, in a final step, the DAD method is applied which uses the enclosed area between the damaged and undamaged curvature lines (Eq. (5)). This enclosed area is divided over the length of the structure into small sections Δx_i. Then, the identified area of each section is squared to reinforce the effect and divided by the sum of the enclosed area of all squared sections (Eq. (6)). This represents a normalization which allows to further highlight the effect of damage. For additional details regarding the method, refer to [93], [94], [145].

$$\Delta A_{k,i} = \int_{i-1}^{1} \kappa_{d,i}\,(x)dx - \int_{i-1}^{i} \kappa_{t,i}\,(x)dx \tag{5}$$

$$DAD_{\kappa,i} = \frac{\Delta A_{\kappa,i}^2}{\sum_{i=1}^{n} \Delta A_{\kappa,i}^2} \tag{6}$$

The DAD method has been primarily developed to assess the condition of bridge structures and can be applied to various structures. The following will provide a detailed explanation of how the method is applied based on real bridge tests.

The DAD method's central aspect is a static load deflection measurement on a real bridge. To perform this crucial measurement, heavy trucks (as shown in Figure 14a) are strategically positioned on the bridge according to the numerical reference model. To ensure an undisturbed bridge environment and obtain a clear contrast between the bridge's deflected state under load and its natural, unloaded state, traffic control is essential during this process.

While different deflection measurement methods can be used for the DAD method, photogrammetry was found to be a particularly effective method [93]. Using a drone-mounted camera, a series of photographs has to be taken of the bridge in both loaded and unloaded conditions. To facilitate precise bundle adjustment in image processing, targets are placed at certain intervals along the bridge (see Figure 1b), along with reference targets on the abutments. This setup enabled a continuous deflection line to be extracted by subtracting the unloaded state from the loaded state. While other methods, such as total stations, levelling, and displacement sensors, were also used in [93], photogrammetry was preferred for its ability to comprehensively cover the entire bridge with high precision. Since the method requires both, a continuous deflection line and high precision, photogrammetry was the preferred method.

a) b)

Figure 14:a) Figure 1of [93] *– Loading of the bridge by six trucks; b) Figure 7A of* [93] *– Installation of the targets*

3.3.1 Application of the DAD method

The applicability of the DAD method has already been proven [93] showing that the DAD method is independent of the construction material used, the structure and the cross-sections. This makes the application of the DAD method independent from a specific bridge type. However, for a successful application the method still needs to be further developed which can be obtained based on a profound analysis of its potential and limits. To achieve this goal, the present study focuses on numerical models, including the undamaged reference model and a simulated damaged model, without the need for experimental measurements. This research enhances the fundamental knowledge around the DAD method by addressing the gap in understanding its effectiveness on various bridge structures and in scenarios involving local damage. This study makes a significant contribution to the field of SHM by offering a comprehensive analysis of the before mentioned parameters. Therefore, in the following different parametrized numerical models are presented and discussed.

Figure 16 shows the flowchart of the procedure for the parametrical study via a numerical analysis tool allowing for a high number of different study cases. In a first step, the numerical models are built up based on real bridge structures, using the execution statics, the structural design calculations, and the execution plans (Figure 16 (A)). They are parametrized to investigate the influence of different parameters on the applicability of the DAD method (B), which will be described in *Investigated parameters of the numerical models*. Depending on the parameter, several structural beam models as well as 3D models are designed (C). However, to cover relevant parameters, further models are built based on different bridge types whereas also their static systems are varied.

The numerical models will be further discussed in the following section. For each designed structure, two numerical models are prepared: one without any damage which serves as a reference model and one with simulated damage in a specific area (Figure 16 (C)).

In case a real field experiment could be performed, only the undamaged FE model would be needed to be created as reference model. In the current study, also a numerical model for the damaged structure is used in order to be able to perform the intended parametrical analysis. Different damage types were analyzed and will be discussed in the following section. The two numerical models with loading are built with the NURBS CAD software Rhinoceros using visual programming environment Grasshopper and transferred via SOFiSTiK -Rhinoceros-interface to the structural analysis software SOFiSTiK (D). The models are calculated in the structure analysis software SOFiSTiK (E). The deformations of the structure for different load cases are extracted from the SOFiSTiK database (CDbase) (F) of the structural analysis software back to the software tool Grasshopper (G) and the deformation curves are analyzed at different positions along the longitudinal axes of the bridge. The deflection curves of the damaged and the undamaged models are compared, and the DAD values of the curvature are determined (Figure 16 (H)). As the models are all parametrized, a large parametrical study can be performed, and several variations can be investigated.

3.3.1.1 Investigated parameters of the numerical models

To further develop the DAD method and determine its potential and limits for practical experiments, based on the flowchart presented in Figure 16 a parametrical study is performed by varying the following influencing factors:

- the damage position along the longitudinal axis,
- the loading position along the longitudinal axis,
- the position of the damage in the cross-section depending on the bridge structure type,
- the damage level,
- the number of spans of a structure (isostatic versus hyperstatic systems),
- the mesh size and measurement point density,
- the measurement precision,
- the order of magnitude of the deflection.

In the following subsections all these different influencing factors are discussed.

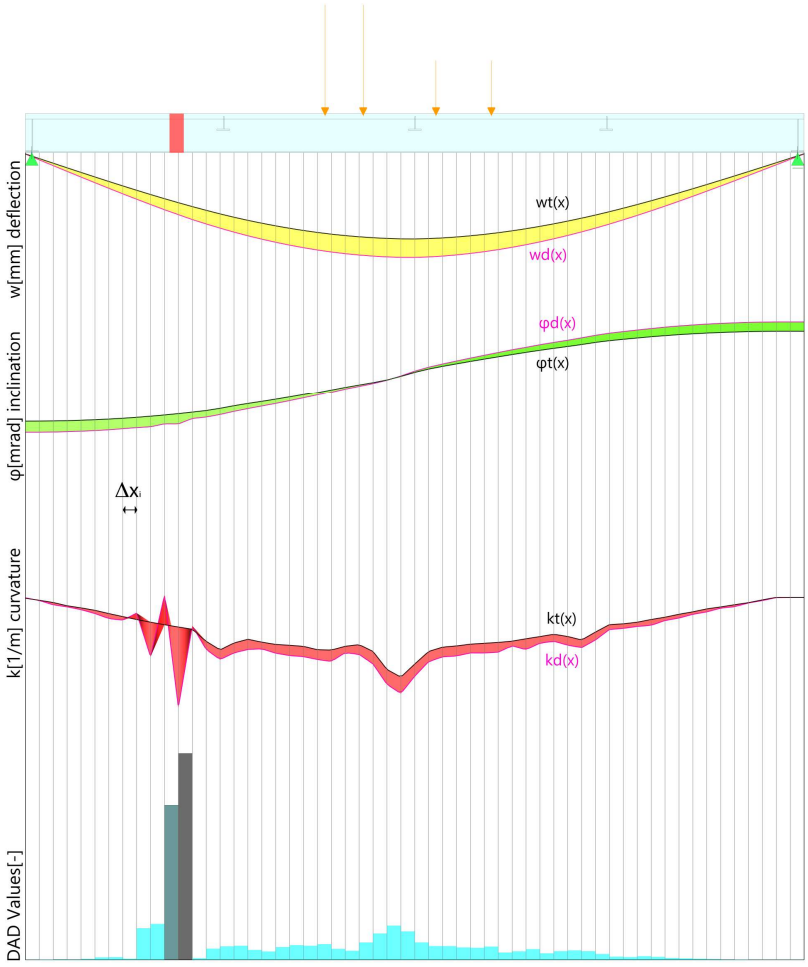

Figure 15. Principle of the DAD method

$w_t(x)$	Deflection line reference model (theoretical)
$w_d(x)$	Deflection line measurement
$\varphi_t(x)$	Inclination angle line reference model (theoretical)
$\varphi_d(x)$	Inclination angle line measurement
$\kappa_t(x)$	Curvature line reference model (theoretical)
$\kappa_d(x)$	Curvature line measurement
Δx_i	Distance between measurement points
yellow area	The enclosed area between theoretical and measured deflection line
green area	The enclosed area between theoretical and measured inclination angle line
red area	The enclosed area between theoretical and measured curvature line
$\Delta A_{\kappa,i}$	Enclosed area difference between theoretical and measured curvature line
$DAD_{\kappa,i}$	Deformation Area Difference (DAD) value from curvature line

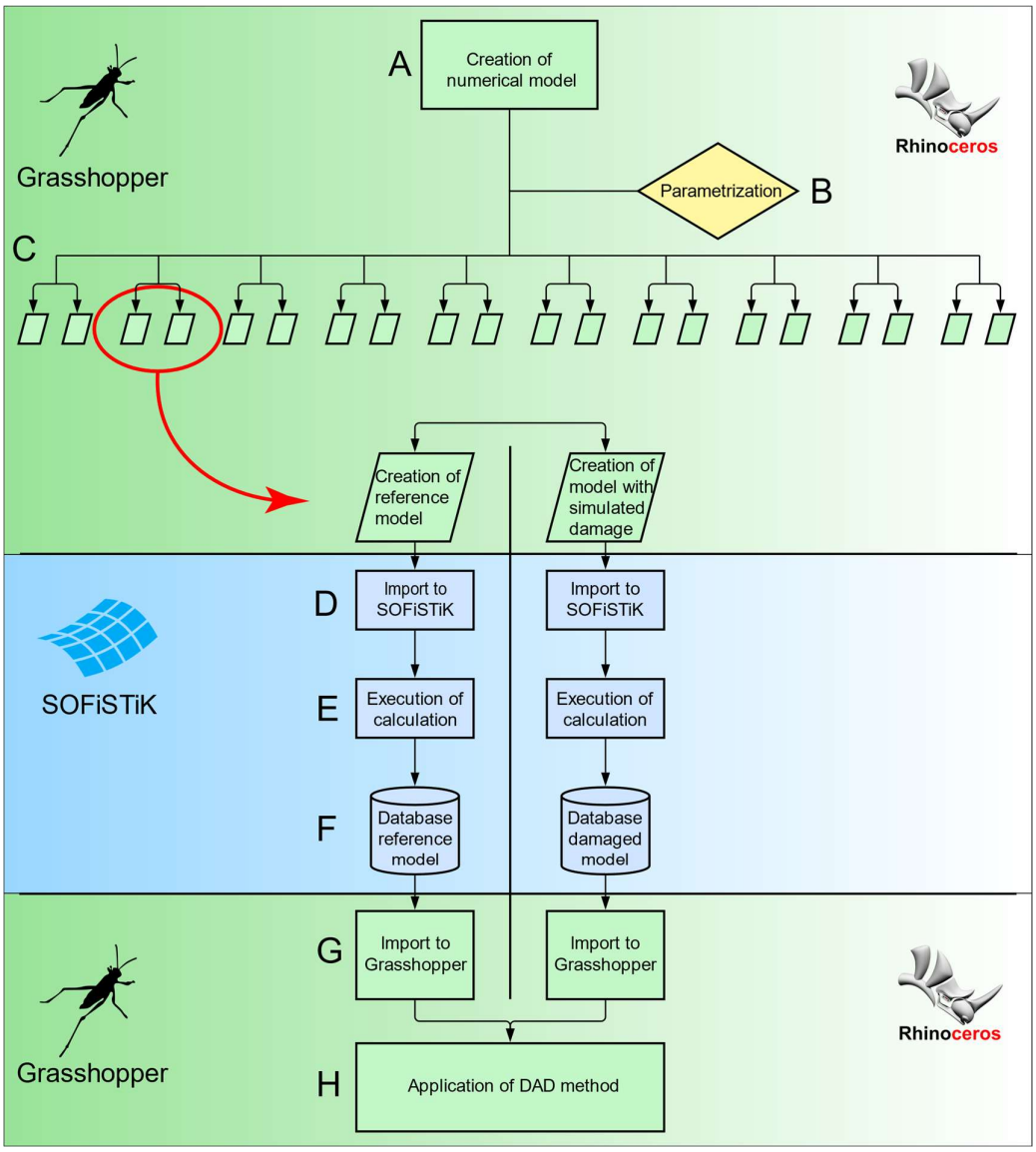

Figure 16. Flowchart of the procedure for the parametrical study via a numerical analysis tool allowing for a high number of different study cases

- **Position of damage along the longitudinal axis**

The first parameter which is varied to determine the potential and limits of the DAD method is the damage position. A beam model based on a prestressed slab bridge with a single span of 27 m is built, with the loading applied to the structure (Figure 17). The bridge structure has a width of 16.3 m and a maximum height of 930 mm. It is prestressed with 19 post-tensioned tendons. For the FE model built in the Software SOFiSTiK the structure is simplified to a prestressed concrete beam. The loading is modeled by single loads representing the axle load of the trucks from a previous field experiment. Supports are modeled as springs and connected with point constraints to the beam structure. Damage is simulated by reducing the bending stiffness by 30% over a length of 0.50 m

in longitudinal direction and over the whole width of the cross-section in transversal direction. Previous studies have already shown that that in theory the DAD method is able to detect and localize already a bending stiffness reduction of 1%[145]. Here, the damage is varied along the longitudinal axis to investigate the influence of the damage position. The DAD values for several damage positions are calculated and the respective damage detectability is analyzed.

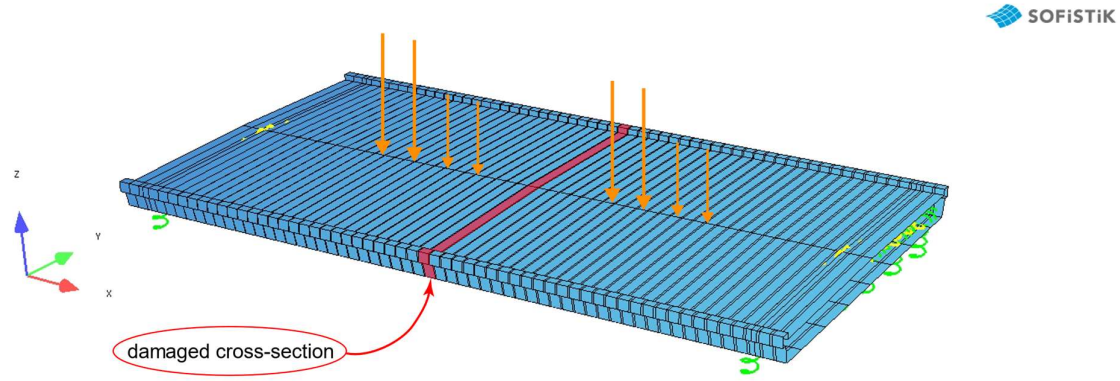

Figure 17. Beam FE model of the bridge structure with a reduction of the bending stiffness by 30% over a length of 0.50 m in longitudinal direction and over the whole width of the cross-section in transversal direction

- **Position of loading along the longitudinal axis**

The same model as described in the previous section is used to examine the potential and limits of the DAD method by analyzing the impact of different loading position along the longitudinal axis. A moving load is applied to the structure and damage is simulated again by reducing the bending stiffness by 30% over a length of 0.50 m in longitudinal direction and over the whole width of the cross-section in transversal direction. The DAD values for every load position are calculated and the detectability of the damage depending on the loading position is analyzed. A novel influence line representing the maximum DAD values in function of the different loading positions, the DAD IL, is introduced in order to show the impact of this parameter along the longitudinal axis. It can be understood like a conventional influence line, which shows the maximum DAD value for the loading position instead of a specific force or deformation value.

- **Multi-span span bridge structures**

To investigate the influence of the load position in relation to the damage position the previously discussed model is modified by adding more spans. Furthermore, different load positions and damage positions are investigated. The DAD IL is further used to investigate how damage in other spans influence the DAD values in the investigated span and to investigate how many spans can be analyzed while loading is limited to one single span.

- **Position of the damage in the cross section in transversal direction**

This section investigates the DAD values for different bridge types, the position of damage in transversal direction, and the measuring positions. While in previous studies, the stiffness of the cross-section has been reduced over the whole width of the bridge structure, here the bending

stiffness is only partly reduced in transversal direction. In the first application of the DAD method [93], the deflection measurement was carried out at the edge of the bridge structure as the targets for photogrammetry were applied at the edge to make the deflection measurement accessible. So far, very little attention has been paid to the role of the position of the damage in transversal direction and whether it is sufficient to have a single deflection curve measured at the outside front of the cross-section. Here, this influence revealing the potential and limits of the DAD method is studied on two bridges, where in situ measurements were performed. They are considered as case studies in the paper for performing only numerical analyses:

- Prestressed concrete slab bridge structure in Altrier, Luxembourg (see *Prestressed concrete slab*);
- Steel multi-girder bridge structure in Luxembourg (see *Plate girder bridge structures*).

The two bridge structures are discussed in the following subsections.

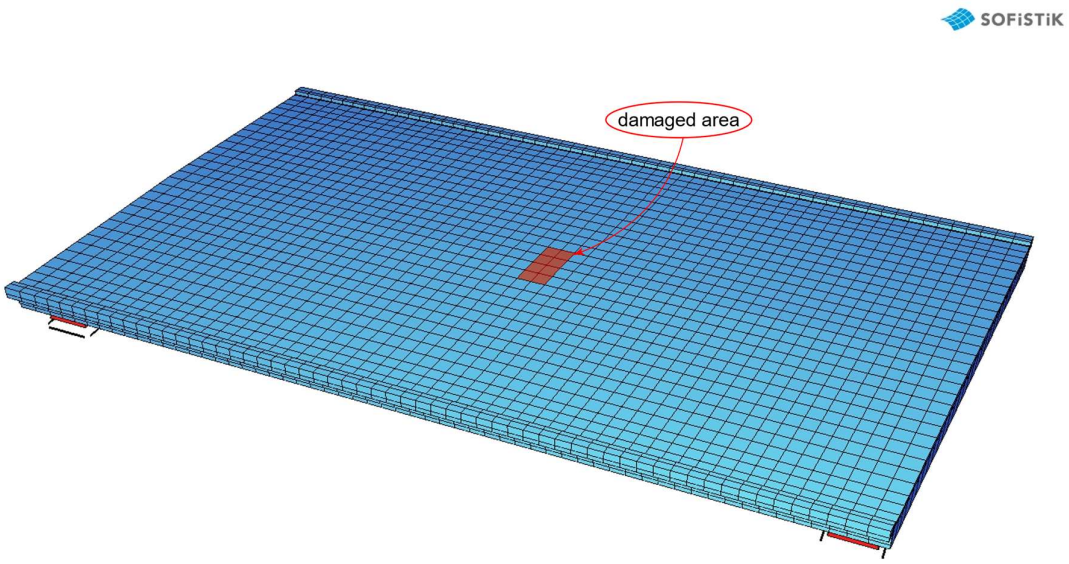

Figure 18. Quad FE model of the bridge structure for the analysis of the impact of damage position in the cross-section in transversal position

♦ **Prestressed concrete slab**

In the previous study, it was assumed that the damage reduces the bending stiffness of the whole cross-section. In reality, the impact of the damage of a bridge structure does not always influence the whole cross-section, but rather influences the bending stiffness of a locally limited part of the cross-section. However, the position of the damage along the cross-section also plays a major role in the detectability of the damage. As the DAD method is investigated by photogrammetry and deformations are measured with photogrammetric targets on the bridge structure, usually, the deflection curve will be analyzed on the outer side of the cross-section. To investigate for which damage position in transversal direction this approach is sufficient, a surface model of the same bridge structure of the previous sections is used. However, here the dimensions of the damage are

now limited in length and width. Furthermore, the damage is applied randomly to the structure and the DAD values of the curvature at different positions are analyzed to study whether the DAD method is still able to detect the implemented damage. Prestressed bridge structures are typically engineered to prevent the occurrence of tensile forces and the expectation of cracks. In the case of damage leading to cracks in the bridge structure, the damaged model needs to be calculated non-linearly. This is only necessary for the simulated damaged model, as the reference model is considered undamaged. The bridge structure is modeled with QUAD elements in SOFiSTiK (Figure 18) with a non-linear material definition for concrete in state II[146].

- **Plate girder bridge structures**

The second investigated structure is a single span steel bridge with span length of 30 m. The steel bridge consists of a steel plate that serves as upper flange of 9 identical I-sectioned girders (Figure 19). It contains stiffeners in transversal direction at the supports and in the quarter points. The bridge structure is modeled in detail with all components and connections.

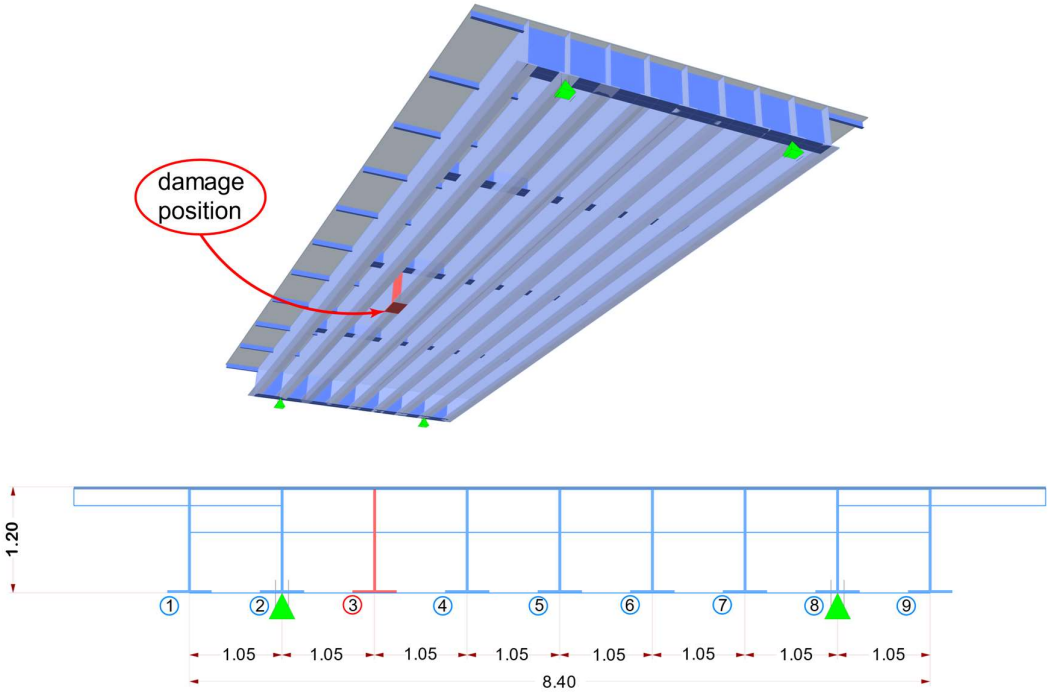

Figure 19. FE model steel bridge structure with damage position (dimensions shown in m)

Damage is simulated by reducing the flange thickness which could e.g., be caused by corrosion (stiffness reduction to 85% of the bending stiffness). The damage is simulated to a length of 1 m at the flange N° 3 according to Figure 19. Another aim of the study is the influence of the local damage to the curvature of the other girders. Therefore, the DAD method will also be applied with deflection values of the other girders, obtained from the FE model.

- **Impact of Mesh size and measurement point density**

As the DAD method compares the enclosed area differences within a defined small section Δx_i, the mesh size needs to match this length which also corresponds to the spacing of measuring points within an in-situ measurement. As already discussed in [95] the spacing of the measurement points influences the outcome of the DAD method. This will be further discussed here by varying the mesh size and investigating the influence of the measurement point spacing on the damage detection.

- **Impact on DAD values by combination of the effects generated by a variation order of magnitude of measurement precision, damage level and deflection value**

The DAD method requires high precision and is sensitive to measurement noise. This requires further investigation on the order of magnitude of the precision required within a measurement campaign which still allows the detection of damage. This also includes an analysis on which damage level can still be localized for a given damage position along the longitudinal axis. With the help of the parametric study described in chapter *Application of the DAD method*, it is possible to combine several precision levels, damage levels, and deflection values to analyze a very high number of variations.

3.3.2 Results and influence on the assessment

3.3.2.1 Different parameters

- **Position of damage along the longitudinal axis**

Previous studies showed that in theory, a stiffness reduction of only 1% is detectable with the DAD method [95]. This study now examines the influence of the position of damage on its detectability. Therefore, the damage position has been varied and the generated DAD values analyzed. Figure 20 shows exemplary the DAD bar graph for a simulated damage at midspan. The horizontal axis shows the total length of the structure with gridlines in the tenths points whereas the vertical axis shows the DAD value. The darker the color of the DAD value bar, the higher the value. The DAD values are displayed as bars for every discrete section Δx_i. As a reminder, the DAD values are normalized, so that the theoretical maximum is 1.0, which is shown in the figure as the theoretical maximum limit. It is clearly visible that although the damage is simulated by a stiffness reduction of only 30%, the method can reliably detect and localize damage. Below the DAD bar graph, the enclosed areas differences of the reference model and the damaged model are shown for the deflection line, the inclination angle, and the curvature. For these areas, only the courses are given as the values are not really of interest here.

In the following, the determination of DAD values was carried out for several damage positions located at a regular distance of every 50 cm in longitudinal direction, resulting in a bar graph for each damage position. To summarize the results in one graph, in Figure 21 the given DAD value at the position of damage is represented as one point for each damage position resulting in a line graph with values for every damage position. As already discussed in previous studies, the detectability

near the supports is limited. In theory, only damage close to supports cannot be detected. As damage is simulated as being constant within a given segment Δx_i, damage can be clearly localized even in the first segment next to the supports (see Figure 21). So, the maximum DAD value increases to a value of 0.66 at 1/10 on both sides of the span and remains stable towards midspan.

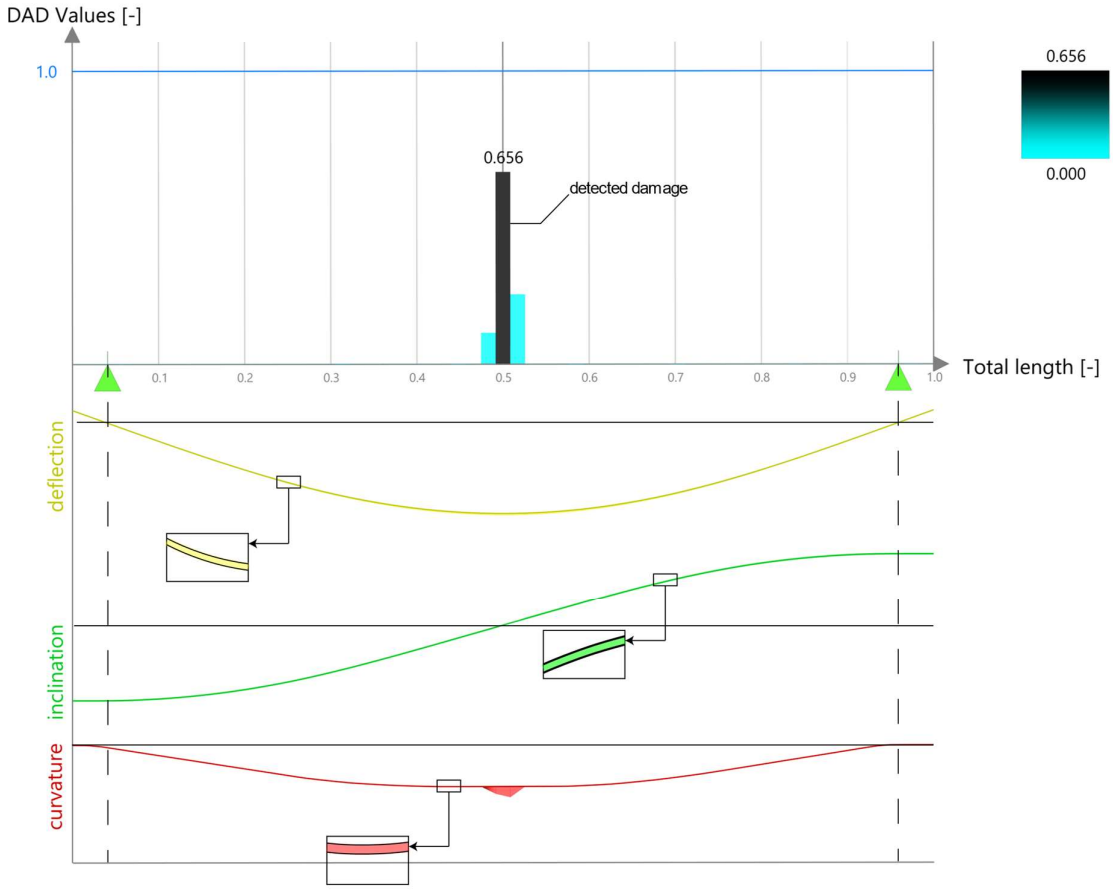

Figure 20. Comparison of the DAD values (shown in the bar graph) for damage at midspan with stiffness reduction of 30% to nearly invisible area differences for deflection, inclination and curvatures highlighting the effectiveness of the DAD method

However, the representations of Figure 20 and Figure 21 are only valid for a noise-free deflection curve. In case the DAD values are calculated from curvature, noise can falsify the results, so that discontinuities within the measurement standard deviation must not be interpreted as damage. As noise cannot be avoided in experimental test campaigns and has a significant influence on the results, it is important to find ways to consider the influence of noise. So, in the following an artificial noise has been applied on the deflection curve resulting from damage at midspan and for a stiffness reduction of 30% (see detailed description in *Impact on DAD values by combination of the effects generated by a variation order of magnitude of measurement precision, damage level and deflection value*). Noise with a standard deviation of 0.01 mm is chosen in order to make the resulting DAD-outlier clearer visible. Under laboratory conditions a precision up to 0.01 mm was

reached [94]. By comparing the maximum DAD value in Figure 22 to the maximum DAD value of the noise free study in Figure 20, it becomes apparent that the detectability is significantly reduced.

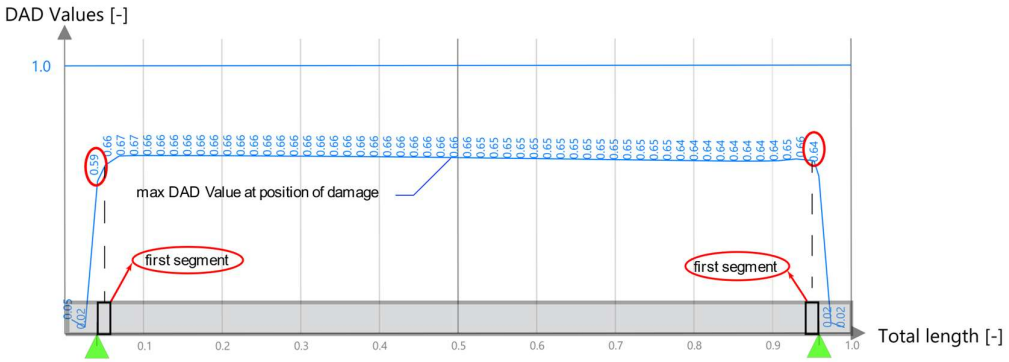

Figure 21. Maximum DAD values for different damage positions along the longitudinal axis for a stiffness reduction of 30%

The question is which level of damage can still be detected. This question will be further analyzed in the following. Here, it becomes clear that an outlier boundary condition must be defined, which specifies the level at which the DAD value indicates damage or must simple be attributed to noise effects. In the following, the outlier boundary condition is defined according to the box plot method [147]. In a first step the interquartile range (*IQR*) is calculated with the lower 25% quantile value (*Q1*) and the upper 75% quantile value (*Q3*). Inner and outer boundary (*IB* and *OB*) values are calculated according to Eq. (7) and Eq. (8).

$$IB = Q3 + 1.5 \times IQR \tag{7}$$

$$OB = Q3 + 3.0 \times IQR \tag{8}$$

The DAD values exceeding the outer boundary are considered as localized damage. In Figure 22 and Figure 23, this is applied where the outer boundary is displayed as a black curve. As can be seen from Figure 23, damage in the first 1/5 span on both sides from the supports cannot be clearly detected. In Figure 23, also a new indicator is introduced: The Damage Detection Range which can be defined as the length where the DAD values are exceeding the outer boundary and thus, damage can be clearly identified.

Due to noise effects, the results can be falsified. This can be improved by smoothing the measured deflection line and thus using only discontinuities outside the standard deviation range for the determination of the DAD values (see Figure 24). Here, the smoothing is processed with the polyline smoothing function of rhinoceros software. Adjacent vertices of the polyline segments Δx_i connecting the deflection curve are averaged resulting to a smoother polyline. What is striking about the data in Figure 25 is that the Damage Detection Range in relation to the span is 10% larger than without smoothing. Further numerical studies showed that smoothing can improve the Damage Detection Range up to 30%. However, the localization of damage at midspan by the DAD values is now increased to a larger area (see Figure 24).

- **Position of loading along the longitudinal axis**

As a next step, the damage position is varied for a structure with an increased span length of 50 m to reinforce the effect. For each damage position, the DAD values are calculated and the DAD influence line (DAD IL) representing the maximum DAD value for a given loading position is derived. Figure 26 shows the DAD IL for damage at midspan calculated from

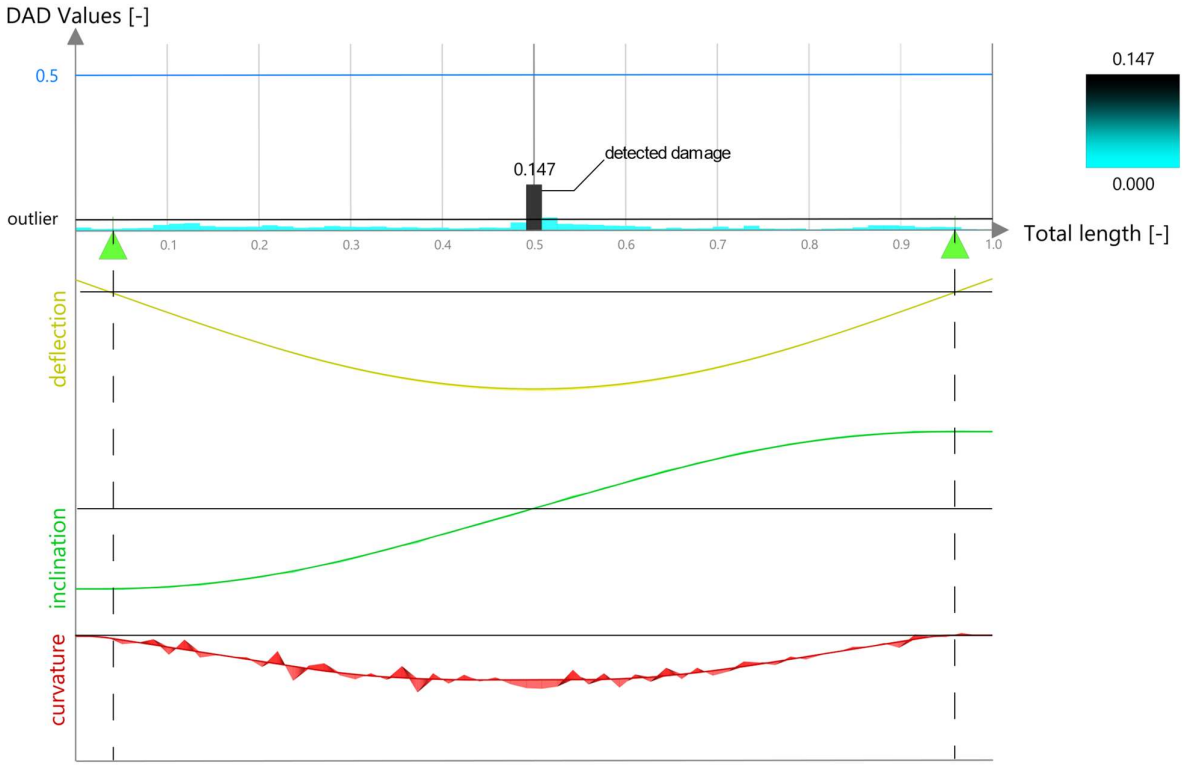

Figure 22. DAD values for damage at midspan for a stiffness reduction of 30% including artificial noise

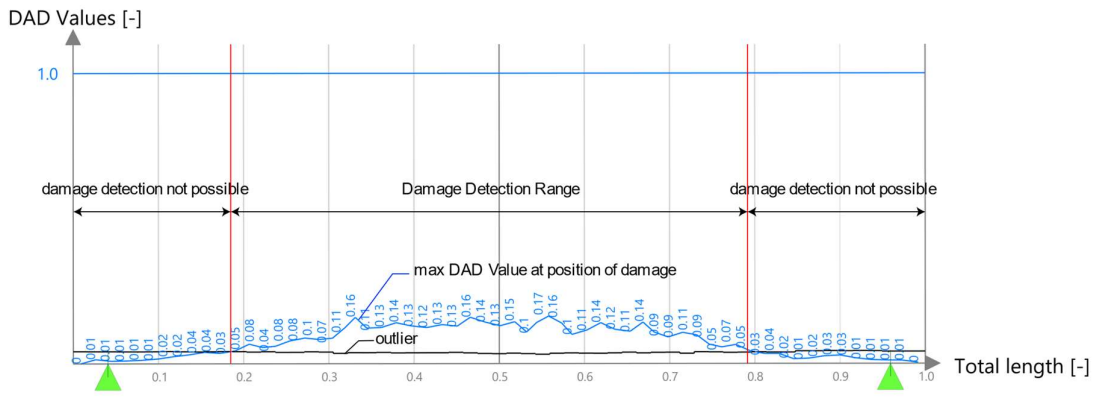

Figure 23. Maximum DAD values for different damage positions along the longitudinal axis for a stiffness reduction of 30% with artificial noise

the curvature lines including artificial noise. Below the graph, the longitudinal bridge section is shown with an indication of the damage position. As an example, for the loading position at 2/3 of

the span, the load vector is represented with its corresponding DAD values reflected as bar graph. In the same figure, also the outlier boundary is shown as a curve. Finally, the intersection points of the DAD IL and the outlier line define the load positions leading to a successful damage detection of a certain damage, here damage at midspan. It can be clearly seen that the load position leading to the highest DAD values is at midspan. As at this position the deflection value is the highest for the given load position, this result was to be expected. Previous studies have already shown that high deflection values lead to better damage detection [93].

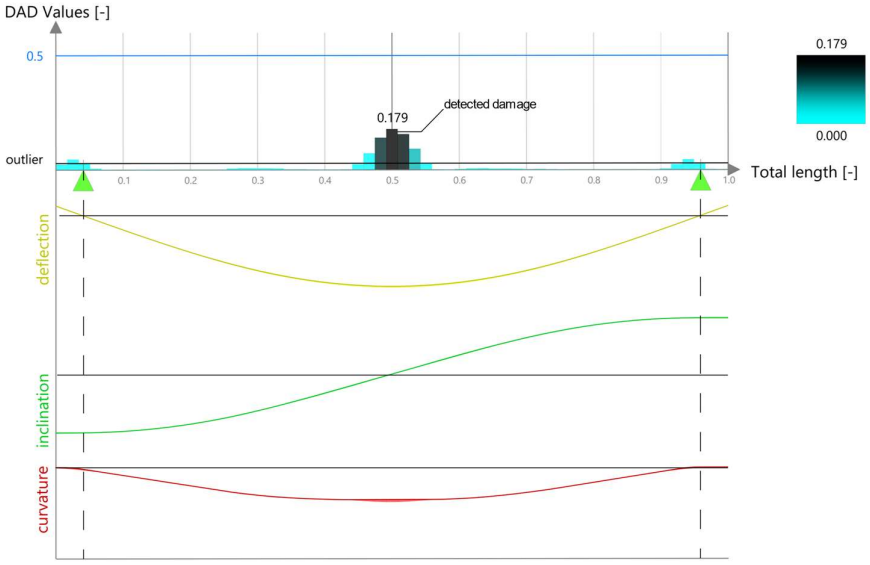

Figure 24. DAD values for damage at midspan and stiffness reduction of 30% with smoothed artificial noise

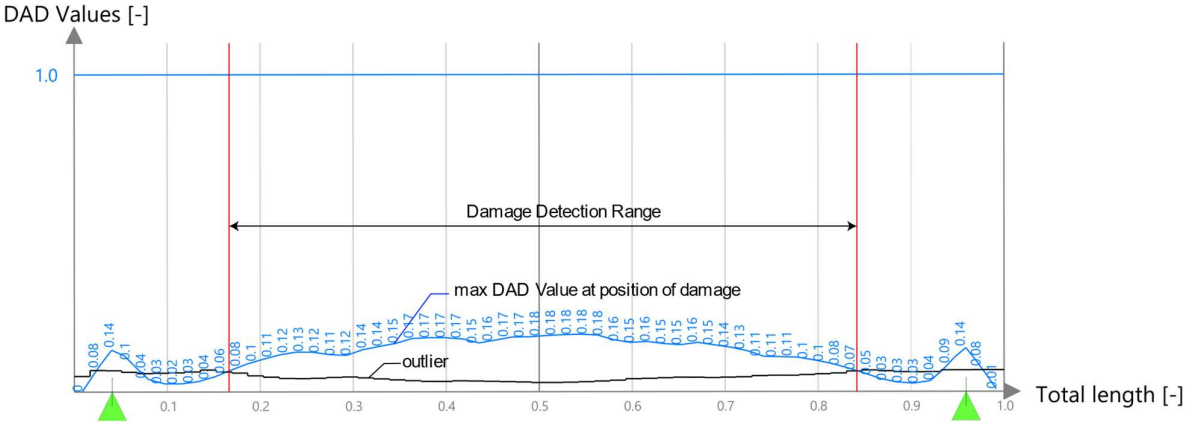

Figure 25. Maximum DAD values for different damage positions along the longitudinal axis for a stiffness reduction of 30% with smoothed artificial noise

As already shown in *Position of damage along the longitudinal axis*, damage detection becomes more difficult when damage is located close to supports [95]. Figure 27 shows the maximum DAD value for damage at 1/5 of the span length with DAD values generated for a load position at ¼ of the span length. It is noticeable that the value is high in the area of damage and decreases along the longitudinal axis. This means that damage could be detected for a loading position at ¼ of the span length while it cannot be detected for a loading position at midspan loading position, where the deflection is the highest, however.

From the previous findings, it becomes clear that for a bridge structure with a higher span, it is necessary to analyze how many loading positions need to be considered in an in-situ experiment to ensure that all possible damage in the longitudinal

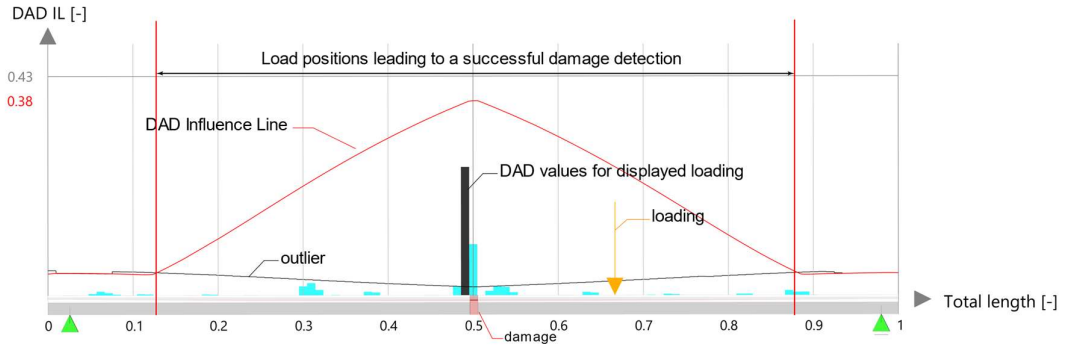

Figure 26. DAD IL for damage at midspan with DAD values generated for a loading position at 2/3 of the span

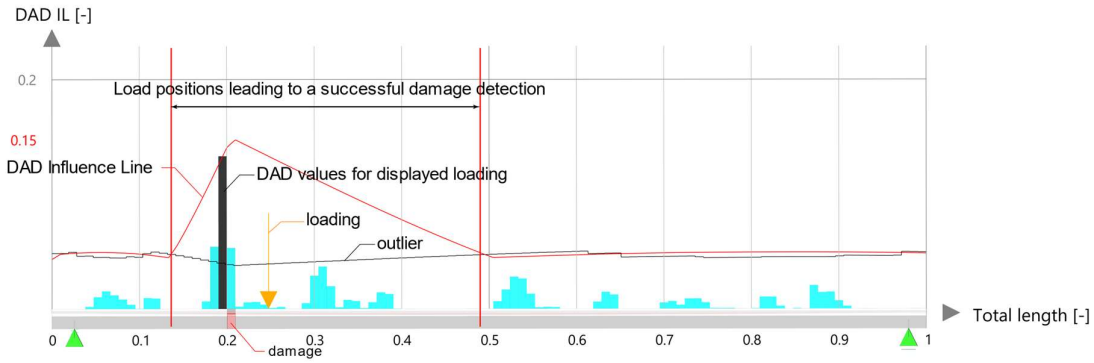

Figure 27. DAD IL for damage at 1/5 of the span length with DAD values generated for a load positioned at 1/4 span

axis of the structure is recorded. For this example, a minimum number of 3 load positions, respectively in the thirds points of the span, are needed to cover the whole length of the bridge structure. Therefore, preliminary studies, similar to those presented in this chapter, must be processed to define the required loading positions allowing for a sustainable condition assessment of the bridge structure.

- **Multi-span span bridge structures**

Previous studies have already shown that the DAD method is also valid for multi-span structures which are indeterminate systems [94]. In the following, the bridge model is now modified to a multi-span structure with four spans of equal length. At midspan of the second span, the bending stiffness is reduced to 30% to generate a high deflection and the DAD IL is calculated. The results are shown in Figure 28. Here, the DAD values for a load position located at the last span are visualized in a bar graph to show that the DAD method can also locate damage in non-loaded spans. The aim of this study here is to define the potential and limits of the practical use of the DAD method. The fact that damage in other spans can be detected would mean that, even for multi-span bridges, a single measurement could theoretically be sufficient. However, in order to achieve this goal, a noise-free deflection measurement would be a prerequisite, which is not possible. Therefore, to account for measurement inaccuracies also in this study, an artificial noise is again applied to the deflection values as described in the previous chapter. Figure 29 shows the DAD IL with DAD values as bar graph for a load position close to the damage position. As already discussed previously, the load positions leading to successful damage detection is defined by the intersection points of the DAD IL and the outlier boundary. As expected from the analysis in *Position of loading along the longitudinal axis*, damage can only be localized if the loading position is in the middle range of the same span. Load positions in other spans are neither able to localize, nor detect damage.

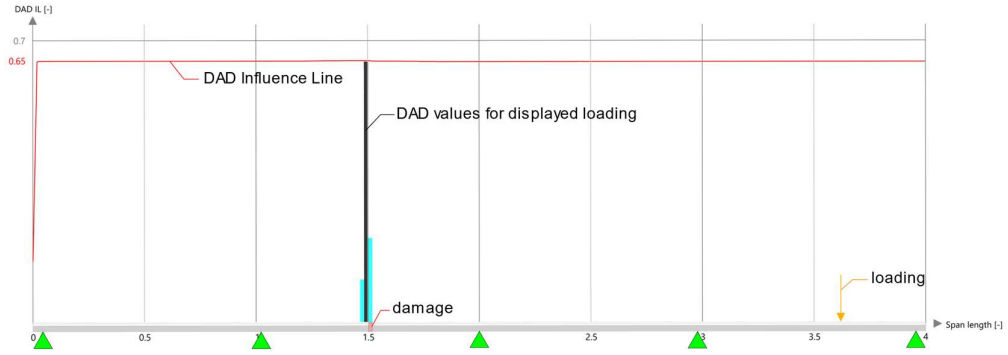

Figure 28. DAD IL for damage at the second midspan whereas loading is applied at last span

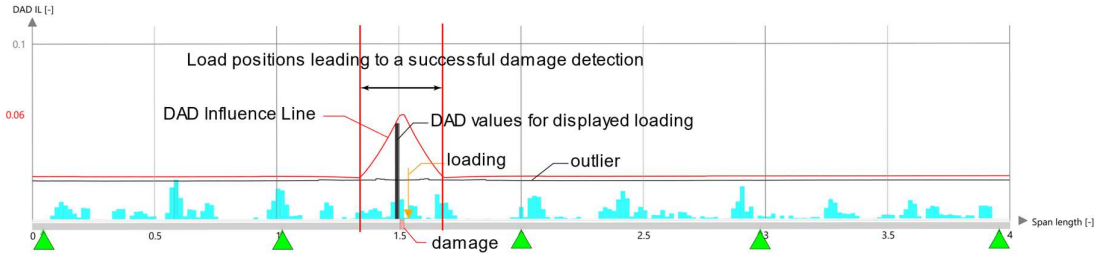

Figure 29. DAD IL for damage at the second midspan, whereas loading is also applied at the second span inculding also articicial noise effects

Again, a smoothing of the deflection values generated with artificial noise is applied and the corresponding DAD values are calculated. Interestingly, the localization of damage is still possible. These can still be clearly detected even if they occur in a field adjacent to the loaded field. However, the load should be positioned at midspan of a field, as higher deflections usually deliver more reliable results.

- **Position of the damage in the cross-section in transversal direction**

Different types of cross-sections, a prestressed concrete slab and a steel-girder bridge, were analyzed to investigate the evolution of the DAD values for the different bridge structures in function of a varying damage position in transversal direction.

♦ **Prestressed concrete slab**

In order to assess the impact of the damage position within the cross-section of the structure from *Position of damage along the longitudinal axis*, a surface model of the same bridge structure is created and analyzed. A stiffness reduction of 60% over a width of 1 m of the cross-section and a length of 0.5 m is introduced, which results to a total damage of 20% of the whole cross-section. This specification is based on empirical findings on the effects of corrosion in concrete structures. The study by Castel et al. [148]shows that corroded concrete beams have an overall stiffness reduction between 53% and 75% compared to their uncorroded counterparts. Complementing this, the study by Malumbela et al. [149] specifically reports a stiffness reduction of approximately 60% in corroded reinforced concrete beams.

Configuring the model with a 60% reduction in bending stiffness reflects these documented effects of corrosion and ensures that the simulated damage scenarios are realistically representative of typical structural damage. This parameter choice facilitates a robust evaluation of the DAD method, assessing its effectiveness in detecting damage under conditions that closely resemble those found in actual SHM cases. The DAD values are analyzed for several positions across the cross-section. Figure 30 shows the DAD values for several axes for damage in the middle of the cross-section and the middle of the span length. From the DAD values in Figure 30a) which shows all DAD axes in a 3D visualization, it becomes apparent that the DAD values are able to clearly indicate the position of damage in the axis of the damage position as a clear peak in damage position can be observed. With increasing distance from the damage position along the cross-section, the DAD values become smaller and less narrow, but localization is still possible. Figure 30b) to Figure 30d) show the DAD values in the middle of the cross-section (damage position), in ¼th of the cross-section, and the edge of the cross-section respectively.

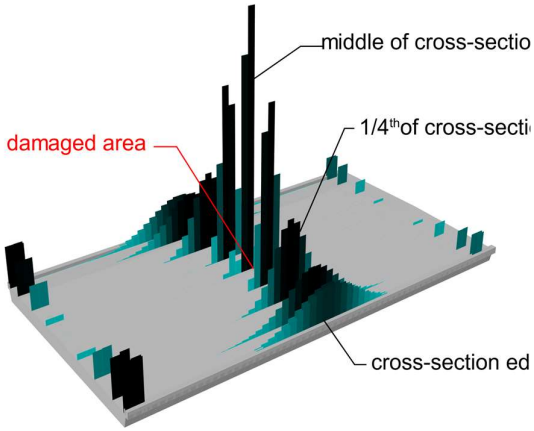

a) DAD values in all axes over the cross-section in transversal direction

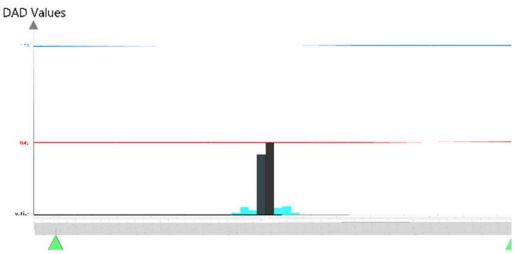

b) DAD values at the middle of cross-section in transversal direction

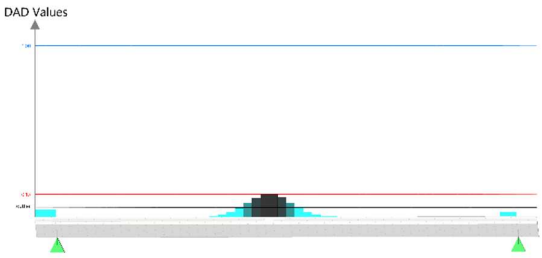

c) DAD values at 1/4th of cross-section in transversal direction

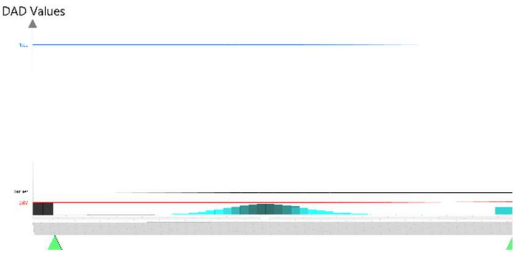

d) DAD values at the cross-section edge in transversal direction

Figure 30. a) DAD values in all analyzed axes of the prestressed concrete slab over the cross-section in transversal direction; b) DAD values at the middle of cross-section; c) DAD values at ¼th of cross-section and d) DAD values at the cross-section edge in transversal direction

In Figure 31a) to f), the same structure with same damage is analyzed. Here however, in addition again measurement noise is considered. A comparison between Figure 30a) and Figure 31a) shows that damage detection becomes in this case more challenging. While damage localization is still possible for the DAD values obtained from measurement in the axis in which the damage is located (Figure 31b)), damage detection is no longer possible for the other axes (Figure 31c)).

A significant improvement can be obtained by smoothing the DAD values (Figure 31d) and Figure 31e)). However, the smoothing cannot increase the detectability of damage in other axes (Figure 31f)), but it helps to remove wrong peaks and helps to avoid false damage identification. These results suggest that damage which is influencing the structure only locally within the cross-section can only be detected in the axis where the damage is located. The false peaks near the support in Figure 31d) result from the high inclination angle at this position which leads to an increased length of the curvature line. As previously discussed in *Position of damage along the longitudinal axis*, the method is unable to accurately detect damage close to the support and false outliers can appear.

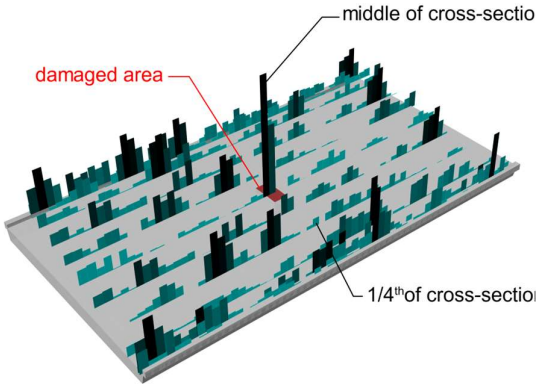

a) DAD values in all axes over the cross-section including the consideration of measurement noise

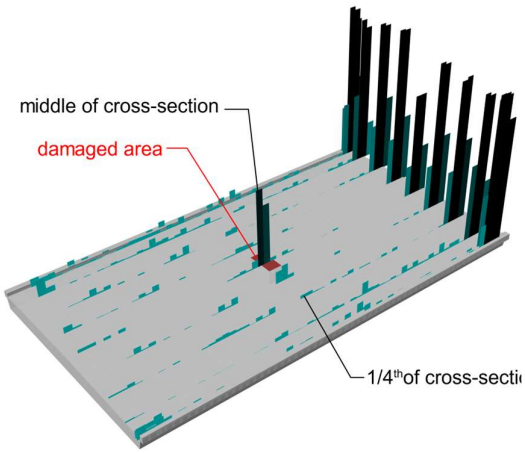

d) DAD values in all axes with smoothing of the deformation line

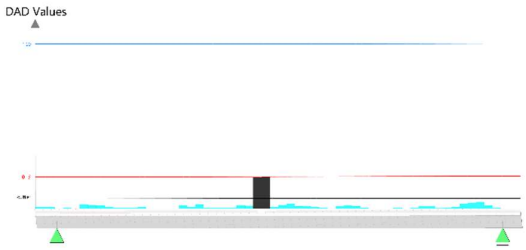

b) DAD values at the middle of cross-section width with consideration of measurement noise

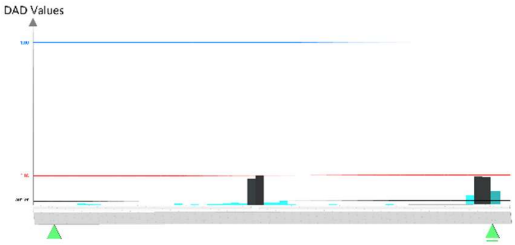

e) DAD values at the middle of cross-section width with smoothing of the deformation line

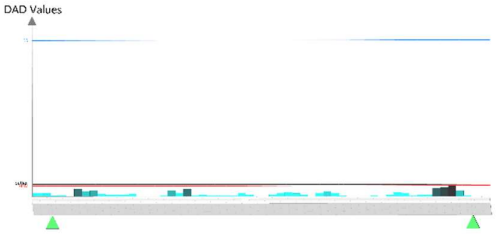

c) DAD values ¼th of cross-section width with consideration of measurement noise

f) DAD values at ¼th of cross-section width with smoothing of the deformation line

Figure 31. a)-c) DAD values from measurement with noise; d)-e) DAD values with smoothing of the deformation line

In the following, a non-linear analysis is performed to assess the behavior of a prestressed structure affected by damage leading to cracking and non-linear behavior. Damage is simulated again by reducing the bending stiffness by 60% over a length of 0.5 m and a width of 1.0 m. The damage is indicated in Figure 32 with a small area, close the edge of the cross-section nearly at 1/3rd of the width. The DAD values clearly localize the damage position indicated by peaks (Figure 32 right). Assuming now an additional tendon failure, shown in Figure 33, the cross-section is not anymore under compression and cracks may occur when reaching the tensile resistance of the concrete. The left side of Figure 34 illustrates the DAD values for the cracked system, while the right side shows the cracks in the structure. It should be noted that the cracks observed in the structure, as shown on the right side of Figure 20, are a result of tendon failure. These identical cracking patterns are also

present in the system without simulated damage, as indicated by the 60% reduction in stiffness demonstrated by the red area in Figure 34. This suggests that the reduced bending stiffness alone does not contribute to crack formation in this scenario. It can be observed that the DAD values match with the cracks that occur in the structure. It is noticeable that the DAD values clearly indicate the crack location and the cracked area. However, no clear identification is possible for the area with decreased bending stiffness as this area remains uncracked. So, the DAD values in the axes without cracks appeared to be unaffected. These results suggest that for structures reaching state II, the localization of damage such as cracks is clearly possible. However, it must be mentioned that the cause of the damage (here: tendon failure) can only be detected indirectly by the occurrence of cracks. In conclusion, while detection of cracks for concrete structures reaching state II becomes easier, the condition assessment becomes more challenging as the method fails to accurately localize in this case the cause of the damage.

- **Steel-girder bridge**

In the next, the position of the damage in the cross-section in transversal direction is also analyzed on the steel-girder bridge shown in Figure 19. A damage is applied to girder N° 3 of the cross-section in the form of a thickness reduction of the flange over a length of 1 m in longitudinal direction. The DAD values are analyzed using the deformation values from the FE model at the edge of all lower flanges. This point of the cross-section was chosen as in in-situ tests, this position offers good applicability for the measurement targets. Damage is simulated only in one girder at a time to enable a clear identification of the influence on the DAD values. In order to analyze the efficiency of damage detection, the DAD values of all girders are represented in Figure 35 at their respective girder. Only for the damaged girder a clear localization of damage was possible. The DAD values of the adjacent girder only indicate a disturbed curvature pointing out damage, but the localization of the damage is not possible. With a closer look to the DAD values of the following girders, it becomes apparent that the identification of damage is not possible anymore. Consequently, a localization of damage was possible.

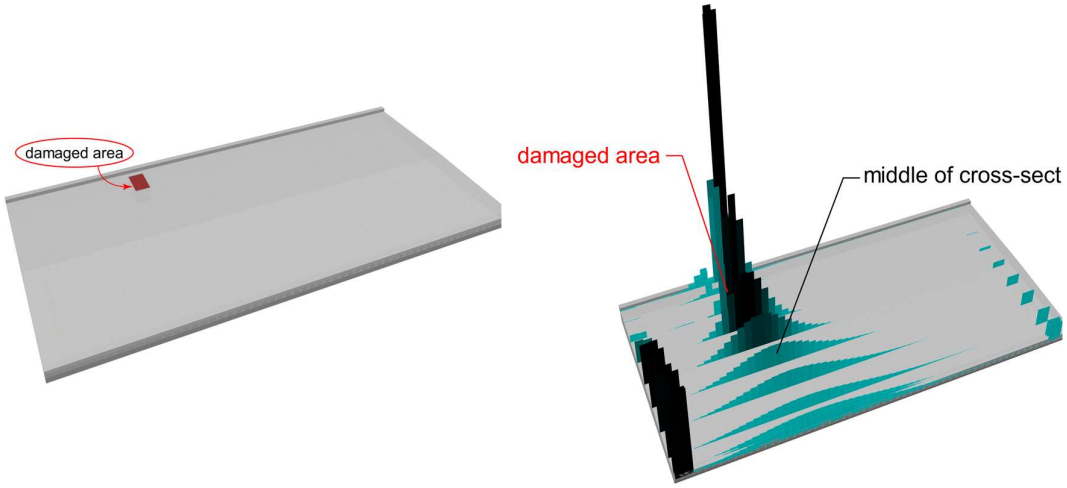

Figure 32. Damaged structure of the prestressed concrete slab(left); DAD values of the prestressed concrete slab (right)

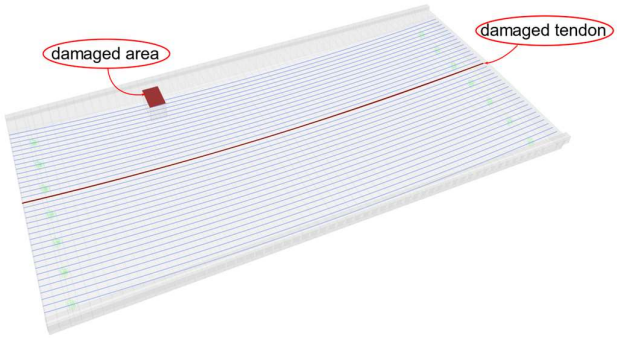

Figure 33. Tendon failure of the prestressed concrete slab shown in the Rhino model

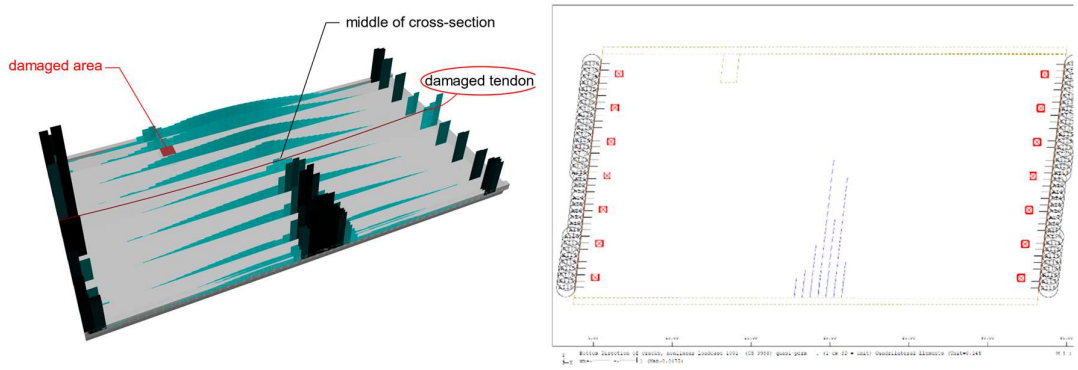

Figure 34. DAD values of the prestressed concrete slab in all analyzed axis in state II (left); numerically analyzed crack distribution of the prestressed concrete slab (right)

The DAD values of the adjacent girder only indicate a disturbed curvature pointing out damage, but the localization of the damage is not possible. With a closer look to the DAD values of the following girders, it becomes apparent that the identification of damage is not possible anymore. Consequently, a clear identification and location of the damage is only possible for the damaged girder if DAD values are obtained from measurements of this same damaged girder.

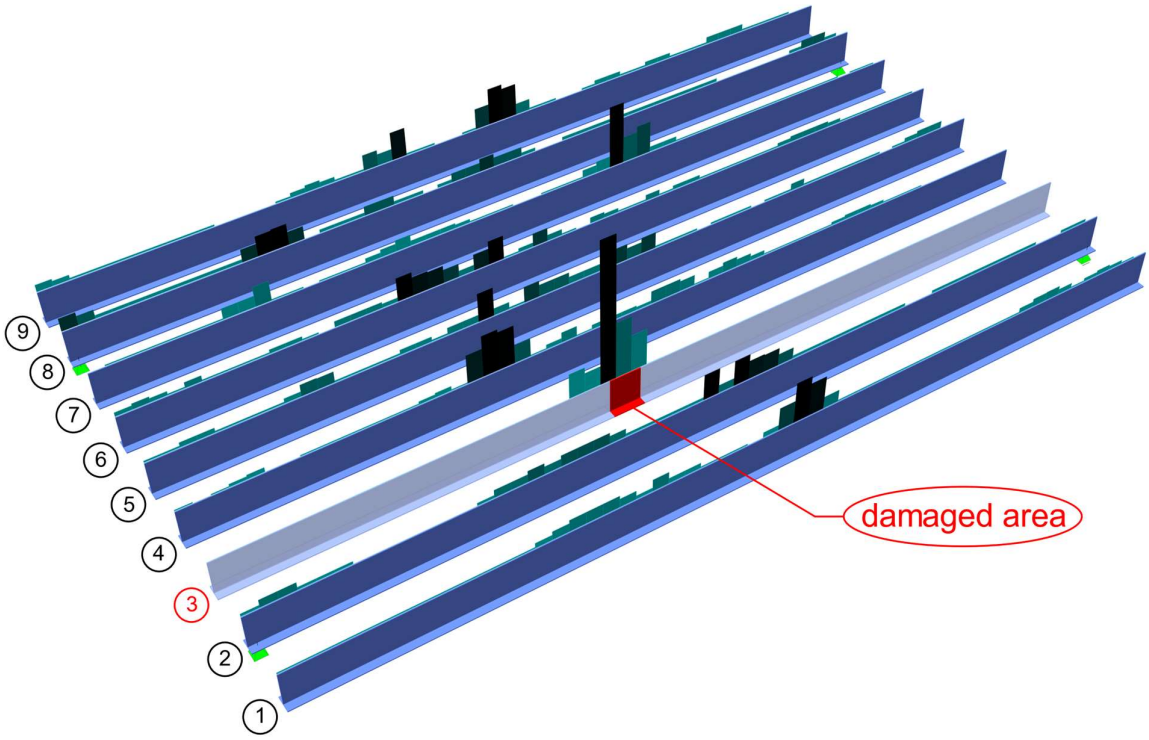

Figure 35. DAD values from curvature of all girders of the steel-girder bridge structure (exploded view)

The results make clear, that for a multi-girder bridge, it is necessary to analyze the curvature of every girder to detect every possible damage. Only by doing so, damage from all girders can be detected and localized. However, Figure 35 shows also that the application of the DAD method can clearly detect damage on one girder while generating noise effects on other girders, so, the interpretation should be done carefully, and only by analyzing the DAD values from all girders, a clear damage detection becomes possible. With the information from all girders, it is also possible to locate more than one damage.

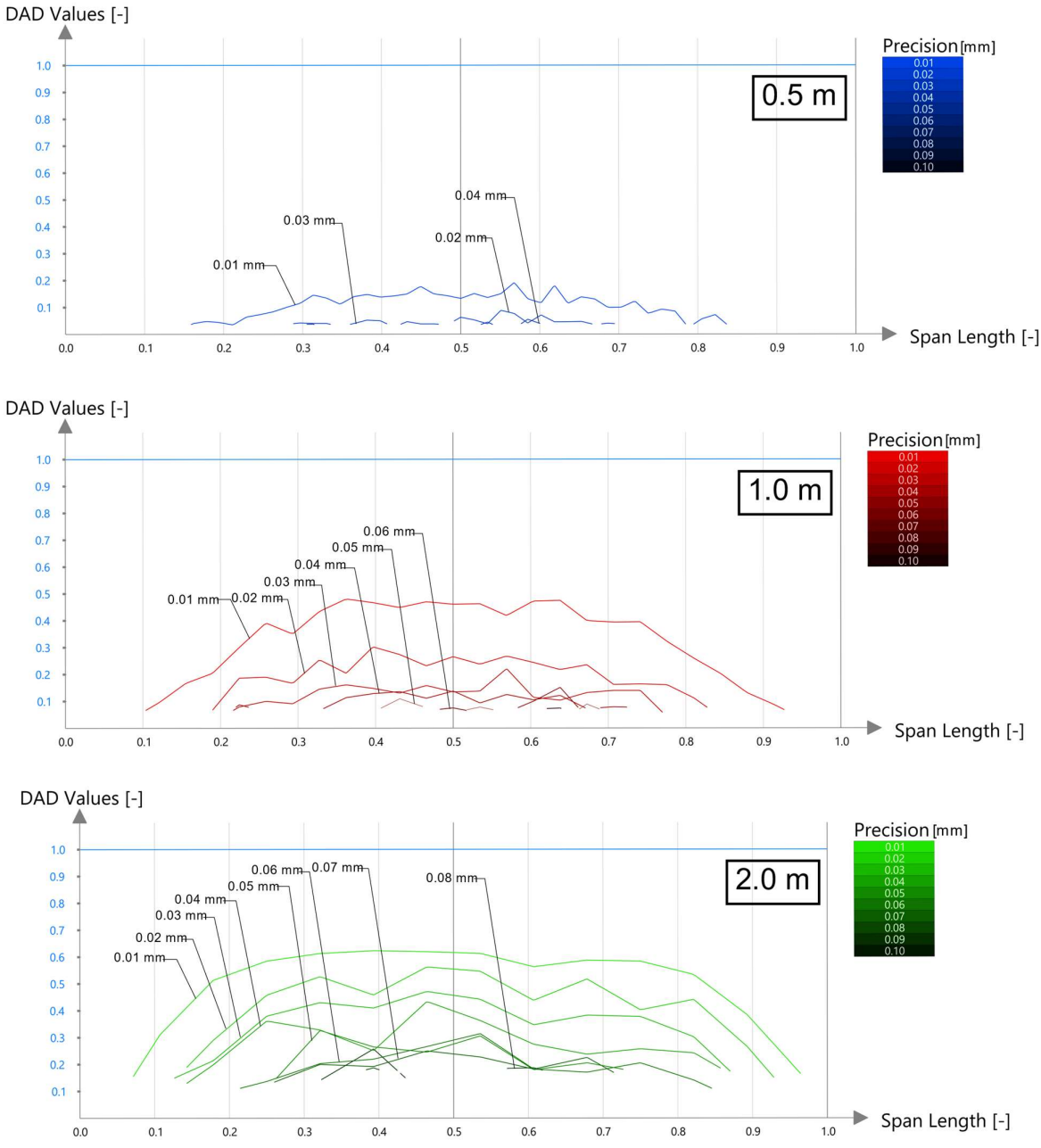

Figure 36. DAD values of the prestressed concrete slab for measurement point density of 0.5 m(top), 1.0 m(middle) and 2.0 m(bottom)

- **Mesh size and measurement point distance**

Previous studies dealt with the mesh size and the influence of the measurement point distances [95]. It was found that the denser the measurement grid, the more accurate the damage detection while denser measurement point distances are more prone to measurement noise. Thus, an optimum ratio needs to be defined based on the damage/noise effects [150]. Therefore, in this study the DAD values are analyzed for different damage positions along the longitudinal axes with different

measurement point distances with the aim to determine the Damage Detection Range. The same model with a reduction of 30% of the bending stiffness as already described in *Position of damage along the longitudinal axis* is used in addition, the precisions of the defection data is varied between 0.01 mm and 0.1 mm for several damage positions along the longitudinal axis. As already discussed in *Position of damage along the longitudinal axis*, damage is detected when the DAD value at the position of the damage is exceeding the outlier value. Figure 36 shows the DAD values for the damage positions similar to the graphs from *Position of damage along the longitudinal axis*, extended by the inclusion of different precision levels ranging from 0.1 mm (highest precision) to 0.01 mm (lowest precision) including also the consideration of artificial noise. In Figure 36, only the Damage Detection Range is represented with the values above the outlier boundary. The Normalized Damage Detection Range can be determined by the ratio of the Damage Detection Range to the total length. Comparing the Normalized Damage Detection Range of the different curves, Figure 36 provides a good representation of which damage can still be detected in function of varying measurement point distances (shown in the different graphs) and in function of varying precisions (shown in each case in the same graph for different measurement point distances). The graphs in Figure 37 summarizes the results of Figure 36 and show the Normalized Damage Detection Range for different precisions, for different measurement points distances and the equivalent maximal DAD value. The results clearly prove that the impact of precision is higher for smaller measurement point densities. However, a higher measurement point density enables also a more accurate damage location while a smaller measurement point density is less affected by noise. Figure 37 indicates that the same Normalized Damage Detection Range can be achieved with half the precision by halving the measuring point density. Therefore, it is recommended to choose a high density of measurement points for the in-situ tests, whereas afterwards the data analysis can be done with different densities by skipping measurement points. However, it must be considered that more measurement points lead also to more expenses for the installation of the measurement points and the photogrammetric calculation.

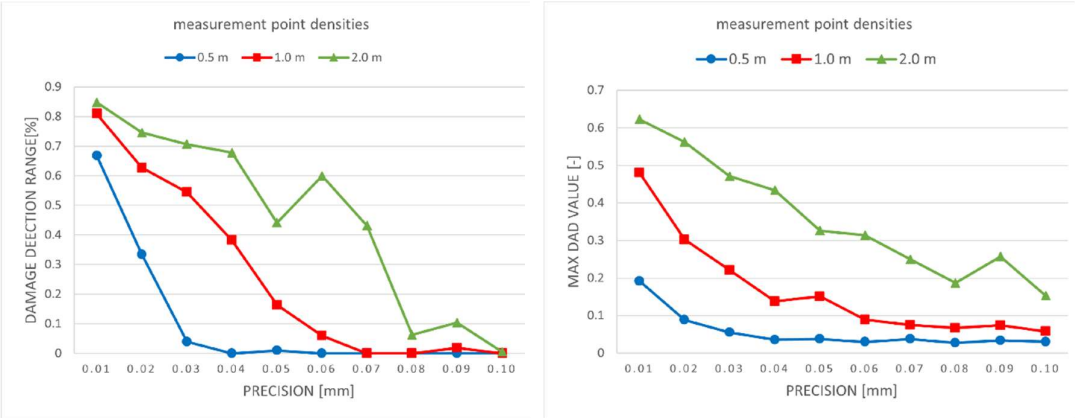

Figure 37. Normalized Damage Detection Range (left) and maximal DAD values (right) for the different measurement point densities

- **Impact on DAD values by combination of the effects generated by a variation order of magnitude of measurement precision, damage level and deflection value**

The influence of the three parameters, the order of magnitude of the precision of deflection data, of the damage level and of the deflection value have already been investigated [93]. Here now, a parametric study is performed in order to combine these different parameters and to determine the Normalized Damage Detection Range for different damage positions allowing so to analyze the least detectable damage level for a given precision and deflection value. According to [93] the deflection value should be chosen as high as possible. For street bridges no general deflection limitation is given. However, a needed clearance profile, the bridge road joints, or asphalt cracking might limit the application of a high deflection level [151]. Further, the maximum deflection value can be limited by the serviceability limit state respecting different proofs for different materials e.g. decompression proof or limitation of stresses [152], [153], [154]. In addition, here also a discussion on which position of a DAD peak represents damage and which position leads to wrong damage identification is presented.

Several models, based on the beam model from *Position of damage along the longitudinal axis*, are damaged with a length of 0.5 m at different positions. Artificial noise is generated with a normal distribution pseudo value produced with the Numerical Python (NumPy) function 'numpy.random.normal' [155] according to Eq. (31).

$$p(x) = \frac{1}{\sqrt{2\pi\sigma^2}} e^{-\frac{(x-\mu)^2}{2\sigma^2}} \tag{9}$$

p(x)	probability density for the Gaussian distribution
σ	standard deviation
μ	mean deviation

10 different series of noise are applied, and the DAD values are analyzed. Figure 38 shows the DAD values at the position of the damage for simulated bending stiffness reduction 30% and a precision of 0.01 mm. The different noise series are shown as dots. The median of the 10 different series is calculated and shown as a continuous line. The outlier is calculated for every model according to the previously described box plot method in *Position of damage along the longitudinal axis*, and shown at every position of the damage resulting to a curve (Figure 38). The DAD values for damage at midspan are shown exemplary as a bar graph in Figure 38. When the DAD value curve intersects the outlier curve, damage can be considered as detected. The Normalized Damage Detection Range is determined in numerous models with damage levels between 10% and 70% of bending stiffness reduction, for different deflection values between L/500 and L/2000. The Normalized Damage Detection Ranges for different damage severities, precisions, and deflection values are shown in Figure 39. The graphs allow to define the necessary data precision in function of a given deflection value and of different damage levels. The results are combined in a bee swarm

plot in Figure 40, where the horizontal axis represents the data precisions, the vertical axis represents the different deflection values. The results of the different damage levels are shown as dots, each representing a different precision and deflection value, with the Normalized Damage Detection Range represented by the size of the dots and the maximum DAD value written inside of the dots. So, the bigger the dot, the higher the Normalized Damage Detection Range. In case damage detection was not possible, no dot is represented in the graph. By combining the results in a bee swarm plot, the influence of the three different parameters on the detectability becomes more apparent and comparable. Overall, the results show that higher deflection values can compensate for lack of precision. For example, with a 50% reduction in bending stiffness with a deflection value of L/500, the same Normalized Damage Detection Range is achieved as with a 70% reduction in bending stiffness with a deflection value of L/2000.

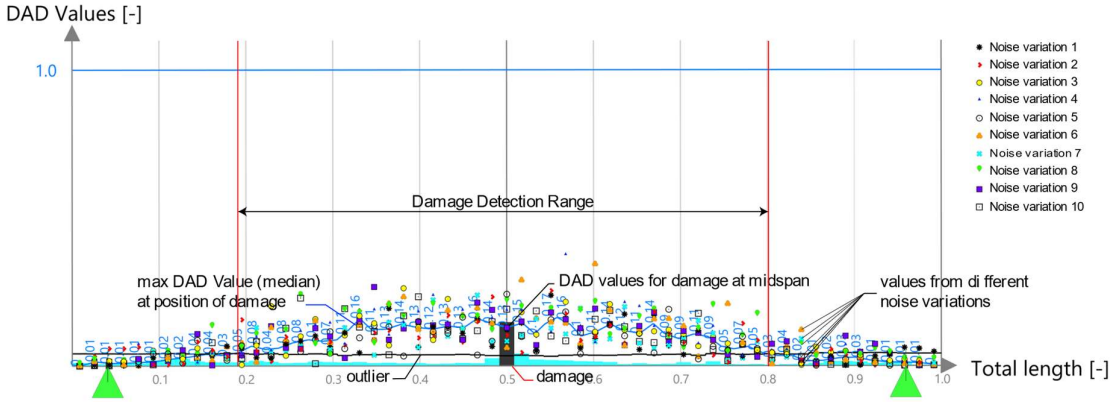

Figure 38. DAD values at the position of damage with exemplary DAD bar graph for damage at midspan for the prestressed concrete slab with a stiffness reduction of 30% with 10 different noise levels

3.3.2.2 Recommendations for the application of the DAD method

The parametric numerical FE analyses aim to investigate different parameters on the influence of the DAD method and figure out the potential and limits for the execution of in-situ experiments. As already shown in previous studies, the closer the damage is to the supports, the less likely it is to be detected. Considering the influence of noise on the DAD values, damage detection becomes more challenging, and the Damage Detection Range decreases noticeably. Smoothing is shown as very effective for extending the Damage Detection Range. High DAD values near the supports should be treated carefully as they might be leading to a wrong interpretation. However, as the curvature line is very steep at the supports, small deviations in the curvature lines already lead to a high area difference due to the length of the curvature line. Therefore, to avoid false peaks, values close to the support can be omitted for the DAD method. In summary, damage is more likely to be detected the farer damage is distant from the supports leading to more reliable results.

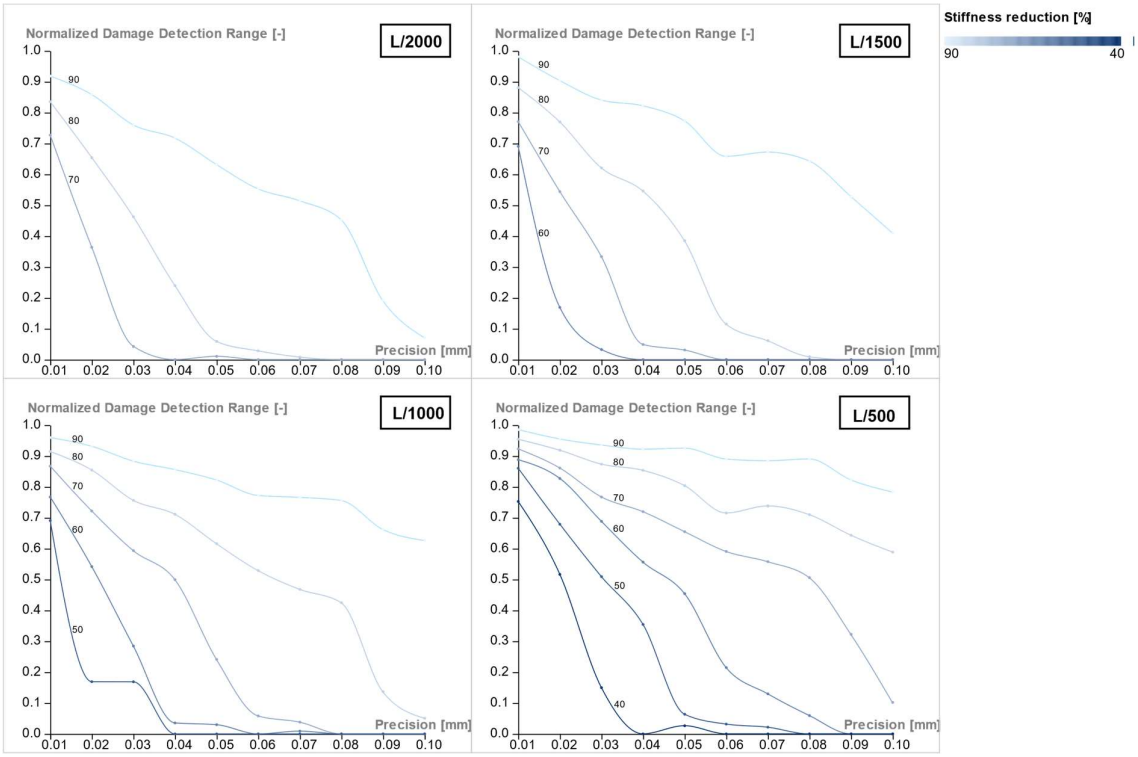

Figure 39. Normalized Damage Detection Range for different damage levels, precisions, and deflection level

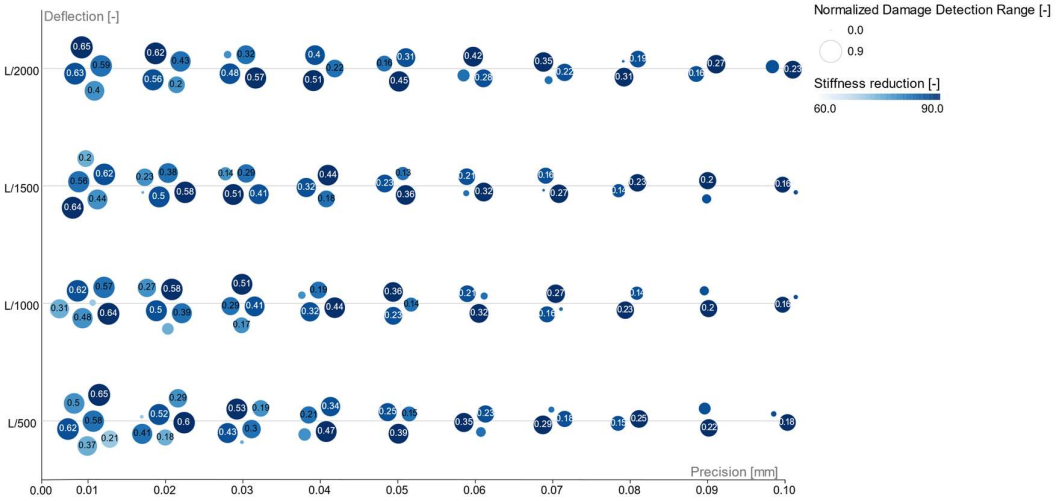

Figure 40. Damage Detection Range with maximal DAD value for different damage levels, precision, and deflection level

The novel DAD IL provides a good understanding of the correlation between the damage detection and the loading position for both, single span and multi-span structures. As shown *in Mesh size and measurement point distance* a high deflection value is reinforcing damage detection. Thus, it is obvious that a loading position somewhere in the middle of the span delivers a reliable damage detection for different damage positions. The different DAD ILs show that different loading positions should still be considered for damage detection in different parts over the span length, especially for longer spans to improve the Damage Detection Range of the structure. Although the

studies on continuous multi-span structures show, that damage detection is still possible with the DAD method for damage in other spans than the loaded span, it is highly recommended to investigate every span separately considering noise in the measurement data.

The next big section of the studies deals with local damage in different structure types. Two different structure types are presented in this paper, a prestressed concrete slab bridge and a multi-girder steel bridge. It is shown that every bridge structure behaves differently and should be handled differently. A focus is put on necessary measurement positions for different damage positions. Overall, the more compact the cross-section is, the more likely damage can be detected at many measurement positions. For the structure of the multi-girder steel bridge, it was shown that every girder behaves very independently and that damage influences only the DAD values of the damaged girder. Therefore, measurements should be taken at every girder to be able to detect damage at all positions. It becomes apparent that the more compact a cross-section is, the fewer measurement positions are necessary. The testing and analysis effort for a T-Beam section, which behaves in a more compact manner, is therefore significantly lower than for a multi-girder system, where all the different girders have independent curvature curves in case of local damage. Also, the density of the measurement points should be varied during data analysis to identify the best results considering the measurement noise and damage localization accuracy. As a higher density can localize more precisely the damage and as a lower density is less effected by noise, it makes sense to analyze with both, higher and lower measurement point density.

Analyzing several models with varying data precisions, deflection values, and damage levels highlight the importance of precision. It is a prerequisite for a successful damage location for a maximal possible Damage Detection Range. The higher the deflection value is, the less precision is needed for leading to the same results. These findings suggest that for bridge experiments, the deflection should be increased as far as possible. Then, the presented parametric model can be used to analyze the Damage Detection Range for an expected precision and deflection value for different damage levels. Thus, when damage is found with the DAD method, the minimum damage level which can still be detected, can be estimated.

3.3.3 Conclusion

The current study aims to determine the potential and limits of the DAD method for bridge assessment. The DAD method relies on a single static load deflection measurement to detect and locate damage. The findings of this study significantly contribute to the body of knowledge on SHM by providing a deeper understanding of the DAD method's potential and limitations across varied bridge types and damage parameters. This research not only validates the method's effectiveness but also illuminates its applicability in more complex and realistic scenarios, thereby advancing the field of bridge structure assessment. The method is further investigated using a parametric FE model where different parameters and different bridge structure models are analyzed. The position of

damage along the longitudinal axis is varied to analyze the Damage Detection Range for given damage positions and damage levels considering a given precision. The influence of the loading position on the DAD values is shown with the novel influence line DAD IL. The presented study examines the position of the damage in the cross-section for a prestressed concrete bridge structure and a steel-girder bridge structure. Further, the mesh size the measurement point distance, data precision, the damage level and the deflection values are varied to investigate their influence on the Damage Detection Range.

The following main conclusions can be drawn:

- For every bridge structure, a previous analysis is necessary to prepare the experimental setup. With the help of a parametric model, possible damage detection can be located, and the Damage Detection Range and detectable damage level estimated.
- The Damage Detection Range can be analyzed for different damage levels, precisions, and deflection values. Based on the expected precision and the selected deflection value, the detectable damage level can be analyzed for every area. This enables an estimation of minimum damaged level for detected damage. The nearer the damage to the support, the less detectable it is. Smoothing the curvature line can improve the Damage Detection Range up to 30% of the span length.
- The novel DAD IL can identify the load positions necessary in an in-situ experiment to get a reliable damage localization. It has been demonstrated that, depending on the static system and damage position, one load position is not sufficient, and a minimum number of load positions has to be determined based on the span length of the structure and the deflection value.
- The study shows that for local damage only one measurement line for the cross-section is not always sufficient. The number of necessary measurement lines for the different cross-sections can be determined from a parametric model. The more compact the cross-section is, the greater is the influence of local damage on the overall cross-section needing fewer measuring positions.
- A higher measurement point density can localize more precisely damage, but a lower density is more affected by noise. So, the same Normalized Damage Detection Range can be achieved with half the precision by halving the measuring point density. When combining the effects generated by a variation order of magnitude of measurement precision, damage level and deflection value, it becomes apparent that the precision of the measurement has a major role in the damage assessment with the DAD method. However, the results show that higher deflection values can compensate for lack of precision. For example, with a 50% reduction in bending stiffness at a deflection value of L/500, the same Normalized Damage Detection Range is achieved as with a 70% reduction in bending stiffness at a deflection value of L/2000.

The DAD method is an interesting method which can detect damage based on a single static load deflection measurement. The potential of the method is that a calibration of the existing bridge

structure is not necessary. It can be applied to every bridge structure and can already detect a damage level corresponding to 1% bending stiffness reduction. Theoretically, every damage position can be located with the method. However, this study also points out the limits of the method. The measurement requires high measurement precision. Measuring noise reduces the Damage Detection Range leading to the fact that only high damage level can be detected, especially for small deflection values. The research has also shown that smoothing has a major influence on the study and can improve damage detectability. Overall, the study shows a reliable application of the DAD method for condition assessment when considering the limitations discussed in this study.

3.4 Transition to publication II

The first paper successfully identified the limitations and potential of the DAD method, thereby addressing the initial research question. It highlighted that measurement precision represents the most limiting parameter for the method's performance. Building on these findings, the subsequent paper focuses on overcoming the noise sensitivity of the DAD method to improve damage detection accuracy in low-damage and low-deflection scenarios. This transition addresses the second research question by investigating strategies to mitigate noise sensitivity and enhance the method's reliability and effectiveness.

3.5 Publication II: Enhancing SHM with the extension of the Deformation Area Difference (DAD) Method into the Strain Area Difference (SAD) Method

T. Čamo, E. Apostolidi, and D. Waldmann, "Enhancing SHM with the extension of the deformation area difference method into the strain area difference method," Structural Concrete, 2024, doi: https://doi.org/10.1002/suco.202400779

AUTHORS CONTRIBUTIONS:

T. Čamo, Conceptualization, Methodology, Software, Validation, Formal Analysis, Investigation, Resources, Data Curation, Writing - Original Draft, Visualization. E. Apostolidi: Writing – Review & Editing. D. Waldmann, Conceptualization, Methodology, Validation, Resources, Writing - Review & Editing, Supervision, Project Administration, Funding Acquisition

ABSTRACT:

This study contributes to the fields of Non-Destructive Testing (NDT) and Structural Health Monitoring (SHM), which are pivotal for extending the service life of infrastructure and aligning with sustainability goals in construction. The study emphasizes an advanced application of the Deformation Area Difference (DAD) Method, focusing on the comparative analysis of curvature lines derived from photogrammetry-assisted deflection measurements and direct strain measurements. The novel Strain Area Difference (SAD) Method is presented.

The research includes numerical simulations and practical experiments. A laboratory experiment with a steel beam demonstrates the method's effectiveness by comparing curvature lines from strain and deflection data. Additionally, an on-site application on a composite bridge using photogrammetry and drone technology is described with a comparative numerical analysis.

The investigations' results shed light on the potential of integrating diverse data sources in NDT/SHM practices. For instance, the integration of deflection measurements and strain measurements for SHM. The comparative analysis provides crucial insights into the accuracy and applicability of the DAD and SAD method in various structural scenarios, improving the precision of condition assessments in reinforced concrete structures.

The findings have significant implications for the sustainable maintenance and operation of infrastructure. They support efficient decision-making in the maintenance and repair of structures, contributing to their longevity and reducing the need for extensive interventions. They present a robust framework for decision-making in predictive maintenance.

KEYWORDS: Deformation Area Difference Method, Non-Destructive Testing, Structural Health Monitoring, Photogrammetry, Drone-Assisted Monitoring, Sustainability in Construction

3.5.1 Introduction

Bridge structures are critical components of infrastructure, and their timely and proper maintenance is essential for their longevity that also ensures public safety. However, aging bridges often suffer from various forms of deterioration that cannot be easily detected through visual inspection, making accurate and efficient condition assessment vital. Traditional inspection methods can be labor-

intensive, costly, and sometimes detect the problem when the asset is already in a very bad structural condition, highlighting the need for innovative techniques to enhance Structural Health Monitoring (SHM).

Studies on SHM can be categorized according to the applied methodologies and test methods. Interesting literature can be subdivided as follows: (i) SHM with dynamic excitation analysis based on modal parameters, (ii) SHM based on influence lines under moving loads as well for static as for dynamic analyses, and (iii) SHM based on static in-situ loading tests. Soo Lon Wah et al. [156] explore a regression-based method for structural damage detection that uses modal parameters, in particular natural frequencies. The study demonstrates the method's effectiveness in accurately detecting damage in both a numerical beam model and the Z24 Bridge in Switzerland, even under varying operational and environmental conditions. However, the method's accuracy depends on precise initial measurements and relies on the availability and quality of vibration data. However, this method is not able to localize the exact position of the damage. Delgadillo et al. [157] explore non-modal vibration-based methods for bridge damage identification using empirical parameters. The study demonstrates the robustness of these parameters for detecting and localizing damage under ambient and vehicle-induced excitations. However, these methods face challenges such as sensitivity to environmental and operational conditions, which can impact their accuracy. Methods based on modal parameters usually show high sensitivity to noise.

Methods based on Influence Lines (IL) of moving loads also play a crucial role in SHM. Yunkai et al. [158] investigate a multi damage identification method for multi-span bridges using deflection influence lines (DILs). The study finds in numerical analysis and a small-scale experiment that by analyzing their first and second derivatives the location and severity of structural damage can be effectively identified. However, the accuracy of the method relies to a large extent on the precision of measurement instruments and the complexity of data processing, particularly for the second derivative. Zhang Y. et al. [159] present a method for multi-damage identification in multi-span bridges using DILs. The study demonstrates the effectiveness of DIL and its derivatives for accurately detecting and localizing damage in continuous beam bridges in a numerical simulation. The method’s accuracy can be affected though by low measurement precision and complexity of interpreting the IL differences.

Static experiments without a need of a moving load provide another reliable approach to SHM. Ma and Solis [160] proposed a two-step model-independent method for identifying multiple nearby cracks in beams. First, they use trend filter functions to locate damage by comparing deflection lines of undamaged and damaged systems. Second, they determine crack depths using rotational spring models. The method, validated experimentally via close-range photogrammetry, successfully detects cracks of varying depths, and accurately differentiated nearby cracks. Minor modeling discrepancies were noted but had minimal impact and the method requires an initial measurement Le et al. [161] devised a damage identification method based on changes in static

deflection lines of Euler-Bernoulli beams, avoiding optimization algorithms or FE modeling. The method, applicable for both short- and long-term monitoring, effectively localized and quantified single damage but struggled with double damage of varying magnitudes as only one damage was localized, and the damage level was overestimated. Furthermore, the method is limited to the application on simply supported (SS) Euler-Bernoulli beams.

Strain-based SHM methods also show significant potential and are used for all three aforementioned categories. Ayad et al. [162] conducted a study on damage identification in reinforced concrete bridges using strain-based methods and visual inspections. They employed eigenfrequency change, eigenstrain change (using the Coordinate Modal Assurance Criterion – CO-MAC), and strain energy change methods on a 3D finite element model. Strain sensors were used to capture detailed dynamic characteristics. The study demonstrated that strain energy change effectively localized damage. However, a high number of sensors covering the whole bridge is necessary for the method and the accuracy is influenced by environmental noise, similar to other methods relying on modal parameters. Rageh et al. [163] propose an automated strain-based, output-only framework for bridge damage detection using continuous stream of SHM data. The study utilized measured strains from an optimized sensor set deployed on a double track steel railway truss bridge. The methodology focuses on the deterioration of the connection between stringers and floor beams, a common deficiency, but can be applied to various structural elements and details. The framework used Proper Orthogonal Modes (POMs) as damage features and Artificial Neural Networks (ANNs) to infer damage location and intensity from the POMs. The proposed method successfully detected artificial deficiencies imposed on measured signals under operational conditions, demonstrating its robustness against noise and variability in input data, though it requires high-quality strain data, accurate positioning of the sensors strategically chosen based on a numerical sensitivity analysis, and substantial computational resources for ANN training and data analysis. The study was also conducted without accounting for modelling errors and environmental variability.

The integration of photogrammetry and drones into SHM has emerged as a powerful technique, offering non-contact, high-resolution measurements of structural deformations. (Mirzazade et. al [111], Hu et al. [112]) However, CRP based methods rely on the quality of the photogrammetric equipment and the accessibility of a bridge structure.

The usage of drones or Unmanned Aerial Vehicles (UAV) further enhances these capabilities, enabling efficient data collection over large areas. For instance, UAV-based crack detection methods, which acquire large-scene images and apply algorithms for noise reduction and crack width calculation, have significantly improved detection efficiency and accuracy. (Lorenz et al. [119], Zhuge et al. [118])

The integration of these methods in SHM has led to significant advancements in damage detection and localization. Among these [164], [165], the Deformation Area Difference (DAD) method has been introduced as a robust approach for assessing bridge health, focusing on the analysis of

deflection lines under static loads. The DAD method, introduced by Erdenebat et al. [94], offers a novel means of detecting local damage by comparing deflection lines derived from theoretical models and actual measurements. Initial studies demonstrated its effectiveness in laboratory settings, particularly in identifying stiffness reductions in reinforced concrete beams. In [95] the DAD method was further refined by addressing the impact of measurement noise. Through theoretical analyses and laboratory experiments, this study introduced data smoothing techniques that enhanced the sensitivity and robustness of the DAD method. Building on this foundation, in [93] the DAD method was extended to real-world applications, examining its efficiency in a prestressed concrete bridge. This study highlighted the practical challenges and advantages of using photogrammetry and UAV-based data acquisition, which were found to be essential for achieving the necessary precision in measurements. Most recently, a comprehensive parametric numerical study was conducted to optimize the DAD method for different bridge types [166]. This research introduced concepts such as the DAD Influence Line (DAD IL) and Damage Detection Range (DDR), which expanded the method's applicability across various structural configurations and damage scenarios. The study's findings underscored the versatility and effectiveness of the DAD method, emphasizing the need for tailored experimental setups to maximize its utility in diverse bridge structures. However, the recent study also showed the limits of the DAD method: although achieving high accuracy, the measurement noise still limits the method to the detection of high level damage.

Methods based on modal parameters often face challenges due to global and environmental influences and modeling uncertainties. In contrast, methods utilizing static parameters are generally more robust against these issues. Methods based on ILs under moving loads are typically restricted to simple beam structures, require continuous measurements, and are affected by operational environments. Static methods, however, are capable of detecting damage with fewer such limitations. The DAD method stands out by detecting damage with a single measurement, without needing prior knowledge of the bridge structure's condition. So, unlike many other methods, the DAD method does not require the reference model to be calibrated or initial measurements of the undamaged structure. It combines CRP and UAVs to provide a simple and cost-effective measurement technique, leveraging the advantages of static load experiments.

The current paper introduces the Strain Area Difference (SAD) method, which compares the area between the curvature line of a damaged structure and the curvature line of an undamaged reference structure, as in the DAD method. The difference lies in how the curvature line is obtained. The two methods are compared with a parametrical numerical Finite Elements (FE) model of a steel girder using the DDR concept, presented in [166]. The results of the numerical analysis are verified through a laboratory experiment on a steel girder. Finally, the DAD method is carried out on a real bridge structure in Vianden (Luxembourg) with a numerical comparison between the DAD and the SAD method.

3.5.2 Extension of the DAD into SAD method

As already mentioned above, the DAD method is an innovative Non-Destructive Testing (NDT) method developed to detect damage in structures, particularly bridges, within the SLS. The core idea of the DAD method is that damage affects the bending stiffness of a structure, which consequently locally changes its deflection line. By identifying local changes in stiffness, the DAD method can localize areas of damage.

The DAD method can be categorized as short-term SHM technique as it requires only one single in-situ measurement of the deflection line [167]. As, the application of the DAD method requires however a reference deflection line from an undamaged system, an initial measurement of the undamaged structure, if such measurements are unavailable, or alternatively the deflection line from a FE model of the undamaged structure can be used. It is important to note that the reference model does not require precise calibration to the actual deflection. However, it is necessary that the model accurately reflects the planned stiffness variations inherent to the structural design. This approach ensures that any observed deviations can be attributed to unplanned stiffness changes that may have been caused by damage. By concentrating on relative differences in curvature patterns rather than absolute values, the DAD method is able to identify local stiffness reductions, so that the FE model does not need to be finely calibrated to the exact deformation [94]. A calibration using Model Updating (MU) could yield an improved damage detection, especially for low damage levels at early stage with low measurement precision.

The SAD method is similar in principle to the DAD method, with the only difference in its approach to obtain the curvature line. In the SAD method, the curvature is derived from strain measurements. In Figure 41, both methods are presented on the example of an end span of a bridge structure under the static loading of two trucks. The main steps are described in sections 2.1 und 2.2 for DAD and SAD, respectively.

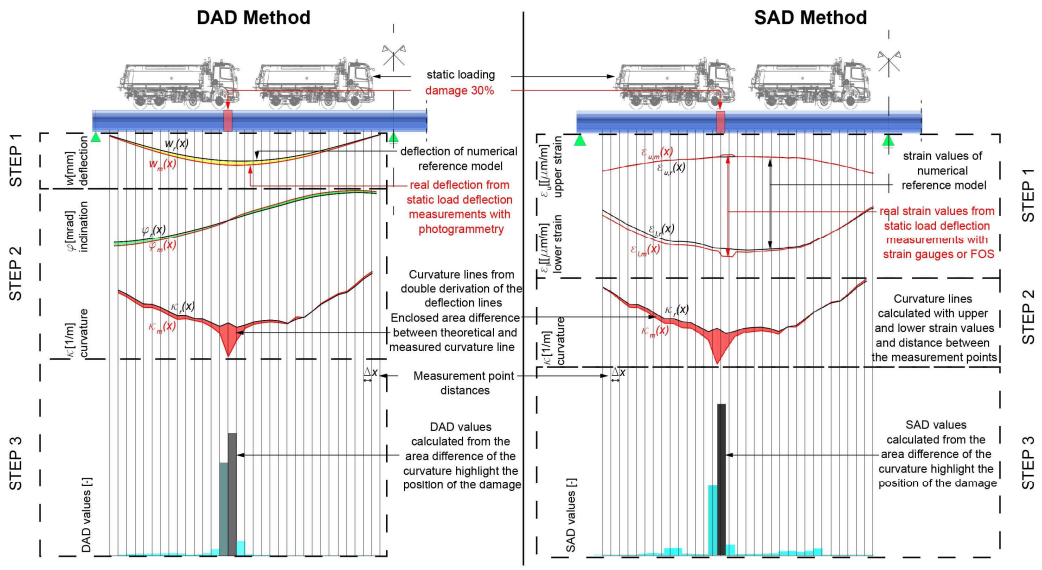

Figure 41. Principle of the DAD method (left) and the SAD method (right)

$w_r(x)$	Deflection line reference model (theoretical)
$w_m(x)$	Deflection line measurement
$\varphi_r(x)$	Inclination angle line reference model (theoretical)
$\varphi_m(x)$	Inclination angle line measurement
$\varepsilon_{u,r}(x)$	Upper strain line reference model (theoretical)
$\varepsilon_{u,m}(x)$	Upper strain line measurement
$\varepsilon_{l,r}(x)$	Lower strain line reference model (theoretical)
$\varepsilon_{l,m}(x)$	Lower strain line measurement
$\kappa_r(x)$	Curvature line reference model (theoretical)
$\kappa_m(x)$	Curvature line measurement
Δx_i	Distance between measurement points
$\Delta A_{\kappa,i}$	Enclosed area difference between theoretical and measured curvature line

3.5.2.1 DAD Method

In Figure 41 the main principles of the DAD method are shown, and they involve the following steps:

- Step 1 (a) - Deflection Measurement: A continuous deflection curve $w_m(x)$ of the structure under a static load is measured. A practical application involves performing a static load deflection measurement on a bridge structure using heavy trucks as loading. Photogrammetry, particularly when combined with drones, has proven effective in capturing high-precision continuous deflection lines. This method involves taking a series of photographs of the bridge under loaded and unloaded conditions, using photogrammetric targets placed along the bridge with certain distances and reference targets on the abutments (as presented in Section 3.5.5). The coordinates of the photogrammetric targets are

calculated with photogrammetric software for the loaded and unloaded state. The continuous deflection line is then extracted by subtracting the unloaded state from the loaded state.

- Step 1 (b) - Reference Deflection Curve Calculation: A linear FE model is designed considering all planned stiffness changes and the loading applied on the static load deflection measurement. The deflection line $w_r(x)$ is calculated with numerical analysis software.
- Step 2 - Curvature line calculation: The calculated deflection curve contains critical information about the structure's stiffness. The first derivative of the deflection curve provides the inclination angle $\phi(x)$, and the second derivative gives the curvature $\kappa(x)$, as shown in Eq. (10) to Eq. (12). The curvature lines $\kappa_m(x)$ and $\kappa_r(x)$ are calculated from the second derivative of the deflection lines of the measured and the calculated deflection, respectively. The curvature of the structure can also be expressed as the ratio of the bending moment to the bending stiffness (Eq. (13)). Therefore, any stiffness change should be reflected on the respective curvature line.

$$w'^{(x)} = \frac{\partial_w(x)}{\partial(x)} = \varphi(x) \tag{10}$$

$$\varphi'(x) = \frac{\partial_\varphi(x)}{\partial(x)} \cong \kappa(x) \tag{11}$$

$$w''(x) = \varphi'(x) \cong \kappa(x) \tag{12}$$

$$\kappa(x) = \frac{M(x)}{EI(x)} \tag{13}$$

- Step 3 - DAD Calculation: The DAD method calculates the area between the curvature lines of the damaged and undamaged structures. This area, divided into small sections Δx_i, is used to identify, and quantify damage (Eq. (14)). The size of Δx_i, which also needs to correspond to the measurement point distances, have to be chosen dense enough to be able to localize the damage precisely, but also not too dense so that the influence of noise can be kept to a minimum (25, 26). The stiffness changes within the area Δx_i are compared to the stiffness differences of the whole structure's length. The area difference for each section $(\Delta A_{\kappa,i})$ is normalized to further highlight the effect of damage and squared to reinforce the visibility of damage effects through Eq. (15). High DAD values pinpoint damage.

$$\Delta A_{k,i} = \int_{i-1}^{1} \kappa_{d,i}\,(x)dx - \int_{i-1}^{i} \kappa_{t,i}\,(x)dx \tag{14}$$

$$DAD_{\kappa,i} = \frac{\Delta A_{\kappa,i}^2}{\sum_{i=1}^{n} \Delta A_{\kappa,i}^2} \tag{15}$$

The method's robustness lies in its ability to differentiate between discontinuities caused by damage and those due to noise or planned structural changes.

3.5.2.2 SAD Method

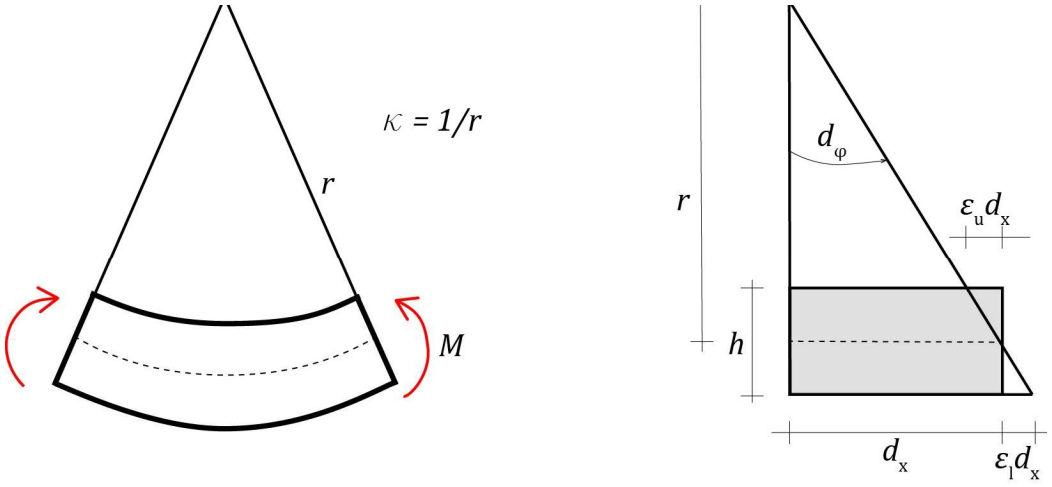

Figure 42. Bending Curvature and Bending Rotation for an infinitesimal element. Adopted from [168]

r	Radius
κ	Curvature
M	Bending moment
d_φ	Angle between two infinitesimal elements
h	Height of the cross-section
d_x	Infinitesimal element length
ε_u	Upper strain
ε_l	Lower strain

Although in theory the DAD method can already detect a bending stiffness reduction of 1%, measurement noise has a big influence on the damage detectability [166]. Therefore, a measurement method less prone to noise is needed to improve the method and detect smaller levels of damage even for small deflection values.

The term local strain refers to a dimensionless quantity that describes the lengthening/shortening of a beam, which can be described as the proportion of the change in length to its original length. In addition, for linear systems the strain can also be defined via the Hooke's law as the quotient of the normal stress to the Modulus of Elasticity [169]. Eq. (16) describes both strain-relations.

$$\varepsilon = \frac{\Delta L}{L_0} = \frac{\sigma}{E} \tag{16}$$

The stress at any point in the cross-section is calculated using the bending moment (M) and the section's moment of inertia (I), as presented in Eq. (17), where z is the distance from the neutral axis.

$$\sigma = \frac{M}{I} \times z \tag{17}$$

For the simplified case of a beam or girder with a constant cross-sectional area *A* and predefined bending stiffness *EI*, it would experience a curvature in the case of a bending load as visualized in Figure 42 on a global scale (left) and as an infinitesimal element (right) [168]. The curvature ($\kappa=1/r$) can be derived by Figure 42 and is expressed by Eq. (18) above:

$$\kappa = \frac{1}{r} = \frac{\varepsilon_l - \varepsilon_u}{h} \tag{18}$$

This way the curvature can be obtained with strain measurements that can be compared to the reference curvature and lead to the SAD values though the application of the SAD method, similarly to the DAD method.

The process is again described on the same example of a bridge structure in Figure 41 right) and the key steps and principles of the SAD method are as follows:

- Step 1 (a) - Strain Measurement: Strain is measured at two points over the height of the cross-section of the structure. In practice, strain measurements can be obtained using strain gauges placed along the span of the bridge with given sensor distances or using advanced Fiber Optic Sensors (FOS). These sensors provide high-resolution strain data essential for accurate curvature calculation and damage detection.
- Step 1 (b) - Reference Strain Calculations: A FE model is designed considering all planned stiffness changes and the loading applied on the static load deflection measurement. The strain lines are calculated with a numerical analysis software.
- Step 2 - Curvature Calculation: The curvature (κ) of the structure is derived from the strains at the top and the bottom of the cross-section using Eq. (18).
- Step 3 - SAD Calculation: The SAD method calculates the area between the curvature lines of the damaged and undamaged structures. This area, divided into small sections Δx_i, is used to identify, and quantify damage. The area difference for each section ($\Delta A_{\kappa,i}$) is squared and normalized to enhance the visibility of damage effects, as shown in Eq. (19). High SAD values pinpoint damage.

$$SAD_{\kappa,i} = \frac{\Delta A_{\kappa,i}^2}{\sum_{i=1}^{n} \Delta A_{\kappa,i}^2} \tag{19}$$

The SAD method can also be used as short-term SHM method, although it could be classified as a long term SHM method with strain measurement systems like strain gauges or FOS providing real-time-data for an application of a data-driven solution.

3.5.3 Numerical Verification and Comparison of the DAD and SAD Methods on a Steel Beam Model

To evaluate and compare the effectiveness of the DAD and SAD methods, a parametric model of a steel beam was developed using Rhino's Grasshopper plugin and was further analyzed with

SOFiSTiK software. The steel beam model has a cross-section of HEB 220 and a steel grade S355. The beam is simply supported, with a span of 5.60 meters and a total length of 6.00 meters.

For this study, a beam made of steel was selected to enable precise control of damage and simplify the analysis within a linear elastic system. Damage was simulated by reducing the bending stiffness by 30% over a length of 20 cm. Various single damage locations were applied along the longitudinal axis of the beam for all locations over the whole length. The load was applied at midspan, chosen to produce a deflection of w= L/300. This setup allows for a comprehensive comparison of the DAD and SAD methods under controlled conditions.

To quantify and assess the efficiency of the DAD and SAD methods, DAD and SAD values were calculated for each simulated damage position in the numerical steel beam model, as described in section *Extension of the DAD into SAD method*. For the DAD values, different noise levels were applied to the calculated deflections, with a chosen feasible range based on literature values ranging from 0.01 mm to 0.1 mm [93] and [170]. For the SAD values, the highest possible precision and accuracy in strain measurements had to be ensured. Several studies demonstrated that the accuracy of strain gauges can achieve precision levels of around one micro strain (1 με = 0.000001) whereas Lee et al. [171] report among others, this to be an optimal strain measurement accuracy. Middleton [171] highlights stable performance under high strain conditions for Digital Image Correlation (DIC) systems, thereby validating the accuracy of 1 με for multiple measurement techniques to accurately perform strain - measurements. Eichinger-Vill [172] postulates that the accuracy of strain gauges is between 1 με and 50 με. Consequently, for the presented numerical model, an artificial noise level of 50 με was selected on the safety side and generated using a normal distribution pseudo-random value with the numpy.random.normal [173] function. To describe damage detectability, an outlier boundary was defined using the box plot method [174]. In the initial stage of the process, the interquartile range (*IQR*) is determined by calculating the lower 25% quantile value (*Q1*) and the upper 75% quantile value (*Q3*). Subsequently, the inner and outer boundary (*IB* and *OB*) values are calculated in accordance with Eq. (20) and Eq. (21), respectively. Damage was considered to have been detected when the outlier boundary was exceeded.

$$IB = Q3 + 1.5 \times IQR \tag{20}$$

$$OB = Q3 + 3.0 \times IQR \tag{21}$$

Figure 43 to 5 illustrate the DDR for the DAD method considering a simulated bending stiffness reduction of 30% at noise levels of 0.02 mm, 0.04 mm, and 0.1 mm, respectively. The study by Valença et al. [175] demonstrated that a precision of 0.03 mm can be achieved in photogrammetry, justifying the use of 0.02 mm and 0.04 mm noise levels in this study. These two values are chosen here also to demonstrate the huge difference for the DDR when applying these two noise levels of small difference. The 0.1 mm was chosen as a realistic value of in-situ experiments, which was reached in previous studies [93]. Several cases were conducted with damage introduced at every section along the longitudinal axis of the structure. For each case, the DAD value at the position of

the damage is calculated. These DAD values for all damage positions are plotted as a blue curve, while the black curve represents the outlier boundary corresponding to each position. Given that noise exerts a greater influence on DAD values at the supports than at the midspan, and that different noise series were calculated for each damage position, the outlier boundary is subject to change depending on the position of the damage. This implies that the noise's impact on DAD values varies with the location of the damage, with noise sensitivity being higher at the supports. Furthermore, for each specific damage position, a separate noise series was employed, which explains the observed variation in the outlier boundary curve. When the DAD value exceeds the outlier boundary, damage can be detected. This indicates that in the range where the max DAD value-curve exceeds the black outlier boundary curve, damage is detectable. This range is referred to as the DDR (26). In correlation, a respective Figure 46 with the DDR for the SAD method at an artificial noise level of 50 με is presented.

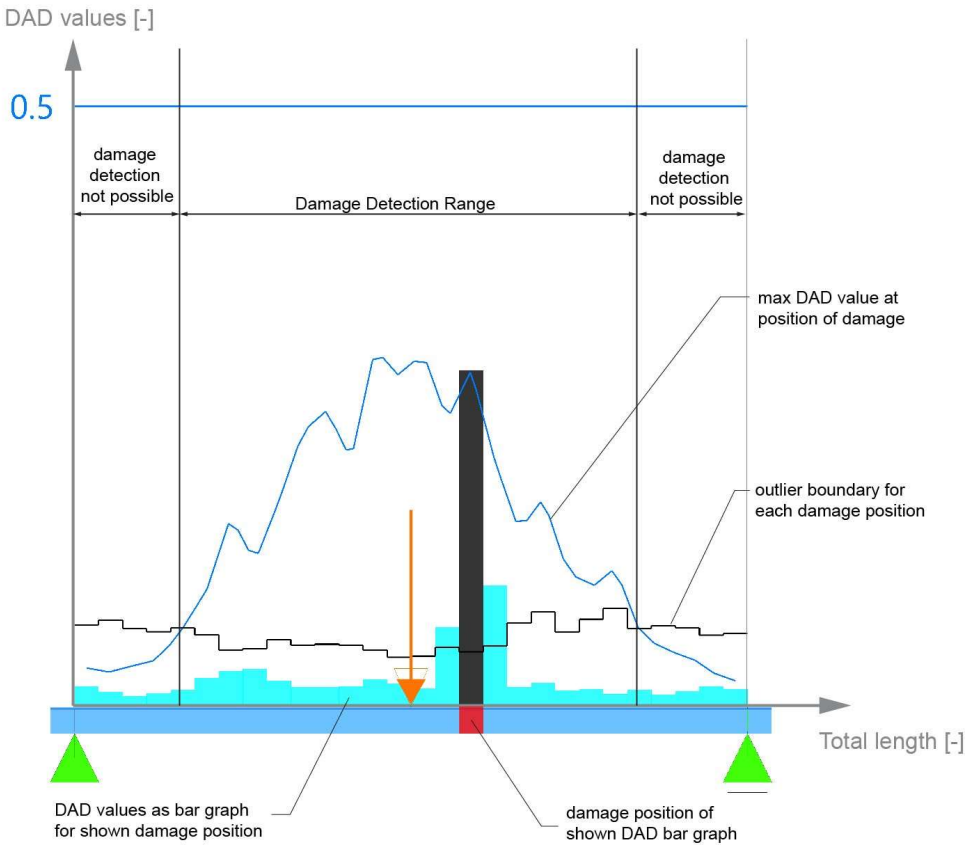

Figure 43. Damage Detection Range for DAD method for a damage of 30% reduction of bending stiffness with artificial noise of 0.02 mm

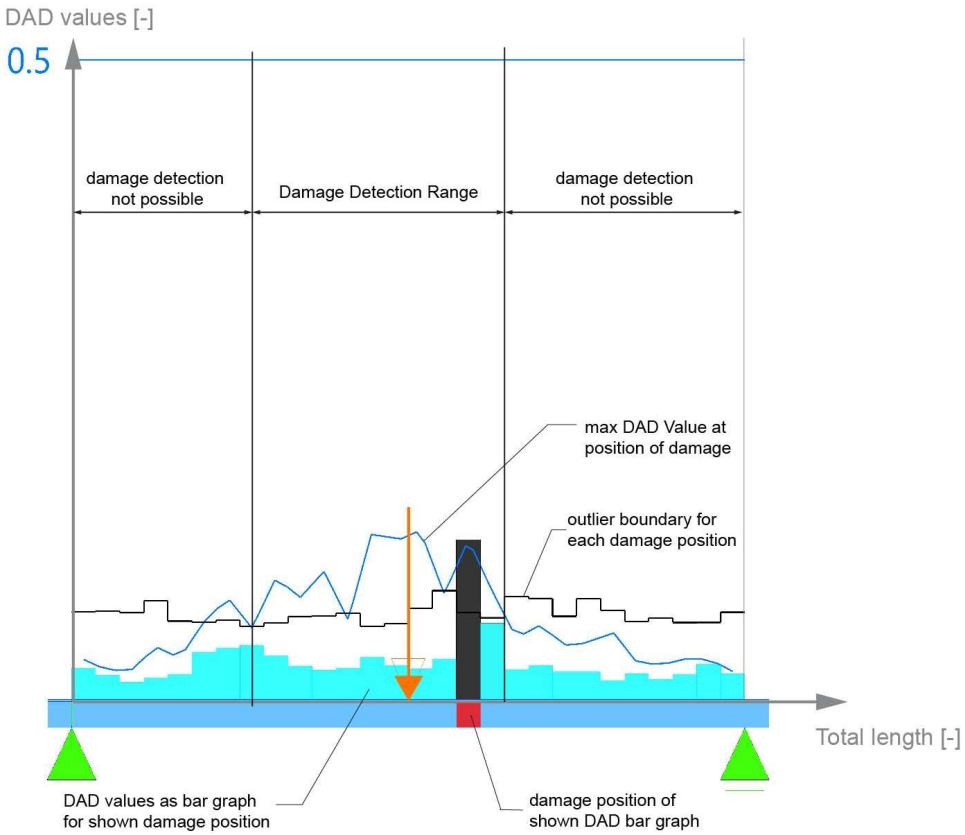

Figure 44. Damage Detection Range for DAD method for a damage of 30% reduction of bending stiffness with artificial noise of 0.04 mm

For example, the cyan bar graph in Figure 43 to Figure 45 shows DAD values for damage located 60 cm away from the midspan on the right-hand side of the girder as indicated with the red area. For Figure 43 to Figure 45, the following observations could be made regarding the influence of the noise levels on the numerical results of the DAD method:

- At a noise level of 0.02 mm (Figure 43), damage near the midspan is clearly detectable. However, detectability decreases toward the supports due to the fact that smaller deflection values are more affected by noise.
- With a noise level of 0.04 mm (Figure 44), the Damage Detection Range decreases significantly, indicating a less reliable damage detection area.
- At a noise level of 0.1 mm (Figure 45), which is realistic for in-situ experiments, no damage positions led to successful detection, highlighting the need for high precision in damage detection and the limitations of the DAD method with current precision levels for small damage. However, smoothing the deflection line and measurement repetition can significantly improve the method [93].

As far as the noise influence in the SAD method is concerned, Figure 46 demonstrates that nearly every damage at each position can be located using the SAD method, indicating a significant

improvement over the DAD method. The higher precision of the SAD method in detecting damage underscores its potential for more accurate structural health monitoring.

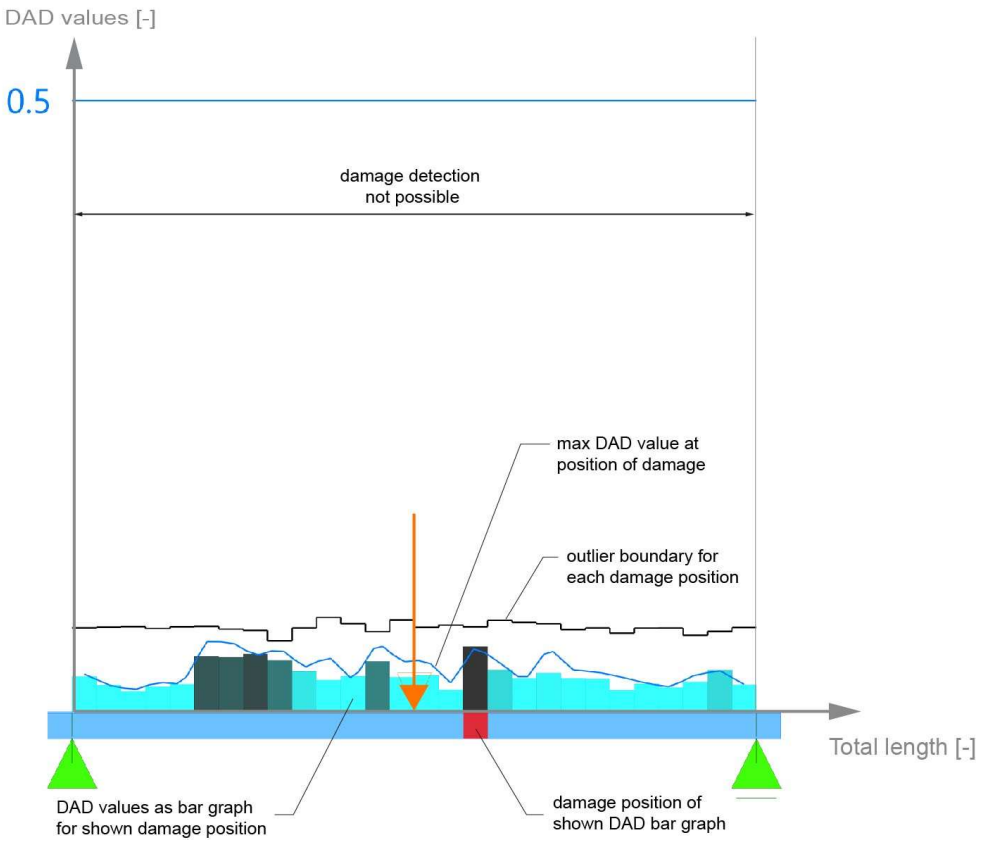

Figure 45. Damage Detection Range for DAD method for a damage of 30% reduction of bending stiffness with artificial noise of 0.1 mm

3.5.4 Experimental Verification and Comparison of the DAD and SAD Methods on a Steel Girder in the laboratory

3.5.4.1 Description of the experiment

To validate the results obtained from the parametric numerical model, a laboratory experiment was conducted. The experimental setup is depicted in Figure 47. The setup involved a steel beam HEB 220, consistent with the numerical model described in Section *Numerical Verification and Comparison of the DAD and SAD Methods on a Steel Beam Model*, with a span length of 5.60 meters. Photogrammetric targets were placed every 20 cm along the beam's flange using stickers. Additional reference targets (see Figure 47) were placed on rigid parts within the laboratory, and auxiliary targets for enhanced bundle block adjustment were affixed to extra steel plates on the top and bottom of the girder.

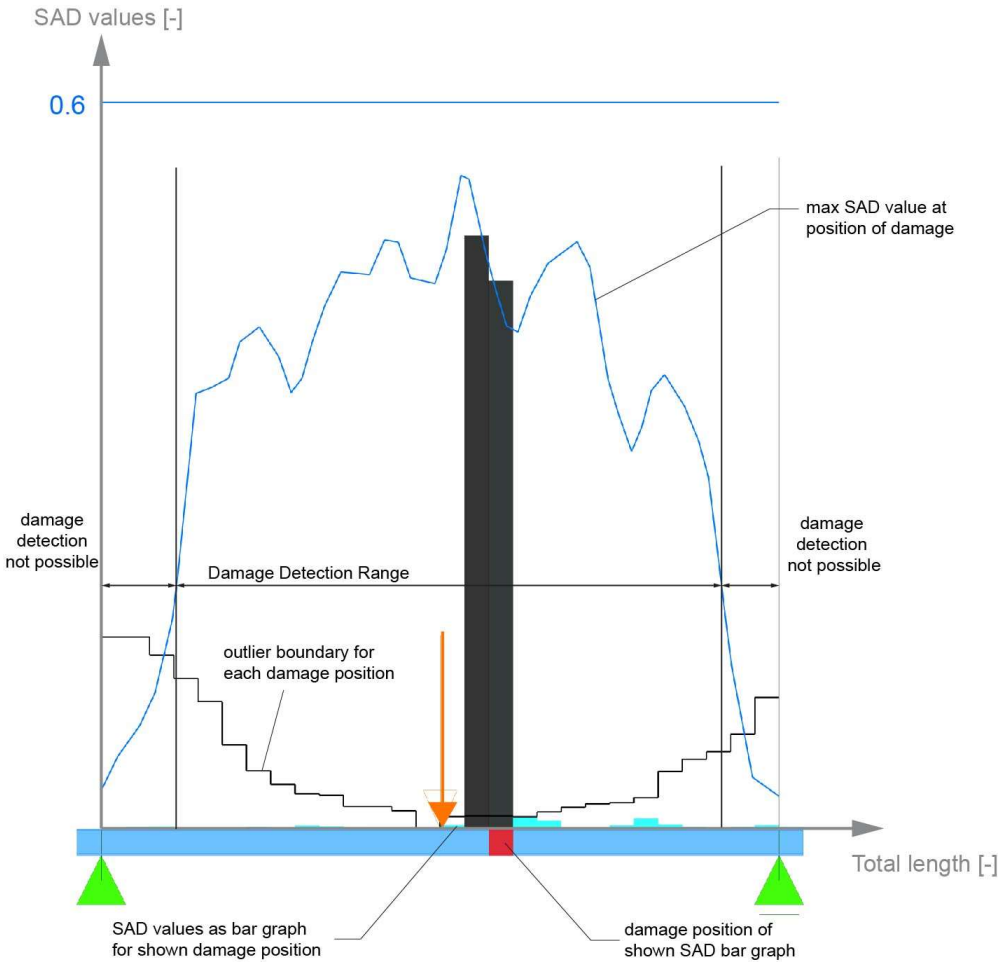

Figure 46. Damage Detection Range for SAD method for a damage of 30% reduction of bending stiffness with artificial noise of 50 με

Strain gauges were installed on one half in the longitudinal direction of the steel girder (leveraging the system's symmetry) on the top and bottom flanges every 20 cm. Three displacement transducers (DT) were also used to verify the deflection values at midspan and at the third points of the right half. A point load was applied at midspan of the girder in five loading steps outlined in Table 1. The maximum load of 80 kN resulted for the undamaged girder in a deflection of approximately $w \approx L/300$, ensuring that the steel girder remained within the Service Limit State (SLS).

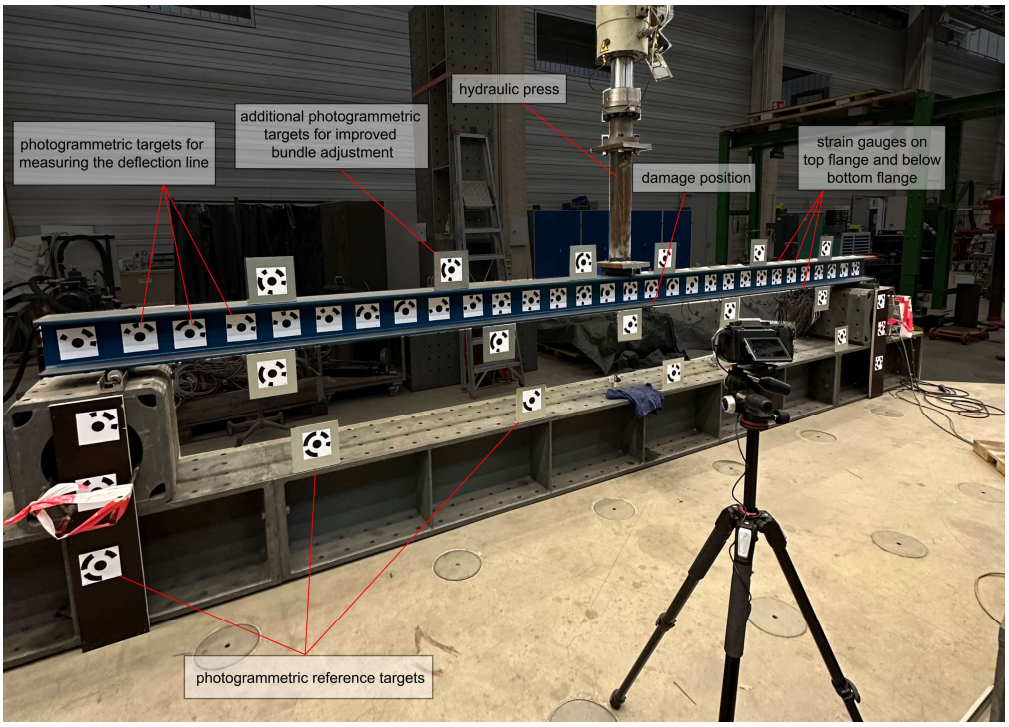

Figure 47. Experimental set up of steel beam HEB 220 S355

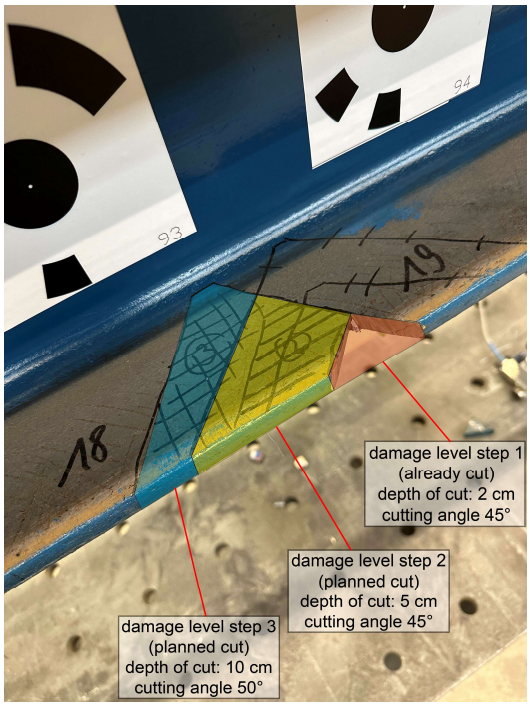

Figure 48. Damage level 1 applied and damage level 2 and 3 sketched on lower flange

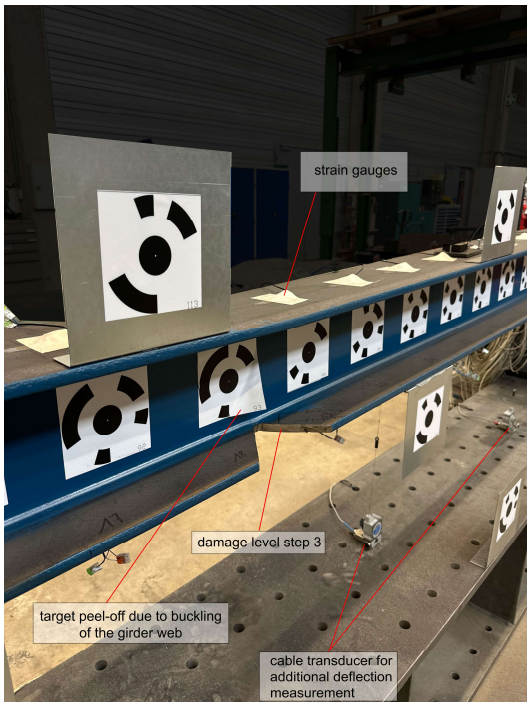

Figure 49. Damage level 3 applied by cutting the lower flange

Table 1. Load steps with deflection values

Load steps	Measured deflection	Deflection value
Undamaged girder		
10 kN	2.2 mm	≈ L/2.550
20 kN	4.5 mm	≈ L/1.240
40 kN	9.4 mm	≈ L/600
60 kN	14.4 mm	≈ L/340
80kN	19.4 mm	≈ L/290
Damage level 1		
10 kN	2.2 mm	≈ L/2.550
20 kN	4.6 mm	≈ L/1.220
40 kN	9.5 mm	≈ L/590
60 kN	14.4 mm	≈ L/390
80kN	19.4 mm	≈ L/290
Damage level 2		
10 kN	2.2 mm	≈ L/2.550
20 kN	4.6 mm	≈ L/12.20
40 kN	9.5 mm	≈ L/590
60 kN	14.6 mm	≈ L/390
80kN	19.7 mm	≈ L/290
Damage level 3		
10 kN	2.4 mm	≈ L/2.330
20 kN	5.0 mm	≈ L/1.120
40 kN	10.2 mm	≈ L/550
60 kN	15.7 mm	≈ L/360
80kN	21.7 mm	≈ L/260

After unloading the undamaged reference stage, damage was induced in three levels by cutting triangles from both sides of the lower flange, creating a 2 cm, 5 cm and 10 cm deep and 4 cm, 10 and 16.8 cm long notch, respectively, 60 cm away from midspan. The damage levels' introduction is shown in Figure 48, with orange, yellow and blue areas, respectively. Figure 49 illustrates the final damage state. This damage configuration resulted in a maximum bending stiffness reduction of 12% at the tip of the triangle for the first damage level. While the flange is cut out in a triangular way, the damage is the highest in the middle of the damage, as here the biggest part of the flange is missing, and the bending stiffness increases constantly towards the end of the cut. By averaging the stiffness reduction linearly, the average reduction results to 4% over the whole damaged length. In Table 2, the maximum and average stiffness reduction values for all three steps are presented. To show the influence of the stiffness reduction, the increase in deflection for load step 80 kN is presented in Table 2.

Table 2. Damage level steps with damage values

	Depth of the cut (per flange side)	Maximum reduction of the bending stiffness	Length of damaged section	Average reduction of bending stiffness	Increase in deflection for load step 80 kN
Damage level 1	2 cm	12 %	4 cm	4%	0%
Damage level 2	5 cm	28 %	10 cm	9%	1.5%
Damage level 3	10 cm	73 %	16.8 cm	24%	11.9%

3.5.4.2 Results

- **Results of DAD method**

For each loading step and each damage level, images were captured using a Fujifilm GFX 50S from various positions (see Figure 47). These images were analyzed using bundle block adjustment with the photogrammetric suite Elcovision. The software provided coordinates for each photogrammetric target. By subtracting the coordinates of the loaded girder from the unloaded girder, the deflection line was obtained. The measurements of the DT confirmed the photogrammetric measurements in submillimeter range. The DAD method was then applied for each load step according to Table 2 and each damage level. The results are presented in Figure 50.

- First Damage Level: No damage was detected using the DAD method regardless of the loading step due to the minimal damage level.
- Second Damage Level: Damage was detectable and locatable for load steps of 60 kN (with deflection w= L/390) and 80 kN (w= L/290). Lower load steps resulted in small deflection values, which were insufficient for damage detection.
- Third Damage Level: Damage was detectable already at a load step of 40 kN (approximately $w\approx$ L/600).

Figure 51 presents the load deformation diagram for damage level 3 of strain gauge 19, located adjacent to the damage on the bottom of the lower flange. At a load of about 40 kN, the girder began to yield. At higher loads between 60 kN and 80 kN, the photogrammetric sticker near the damage started to peel off (as shown in Figure 49), making photogrammetric analysis for the last load step impossible. This peeling is caused by the observed buckling of the girder's web. The deflections measured with photogrammetry are presented in Figure 52 and Figure 53 for the load steps of 60 kN, respectively 80 kN for the undamaged girder and damage levels 1 and 2. As previously mentioned, no photogrammetric measurements were performed for damage level 3 at 80 kN. Figure 53 shows the deflections measured with the DT for damage level 3. The deflection lines for the undamaged girder, damage levels 1 and 2, exhibit only small differences. However, a more pronounced divergence is evident in the deflection line for damage level 3.

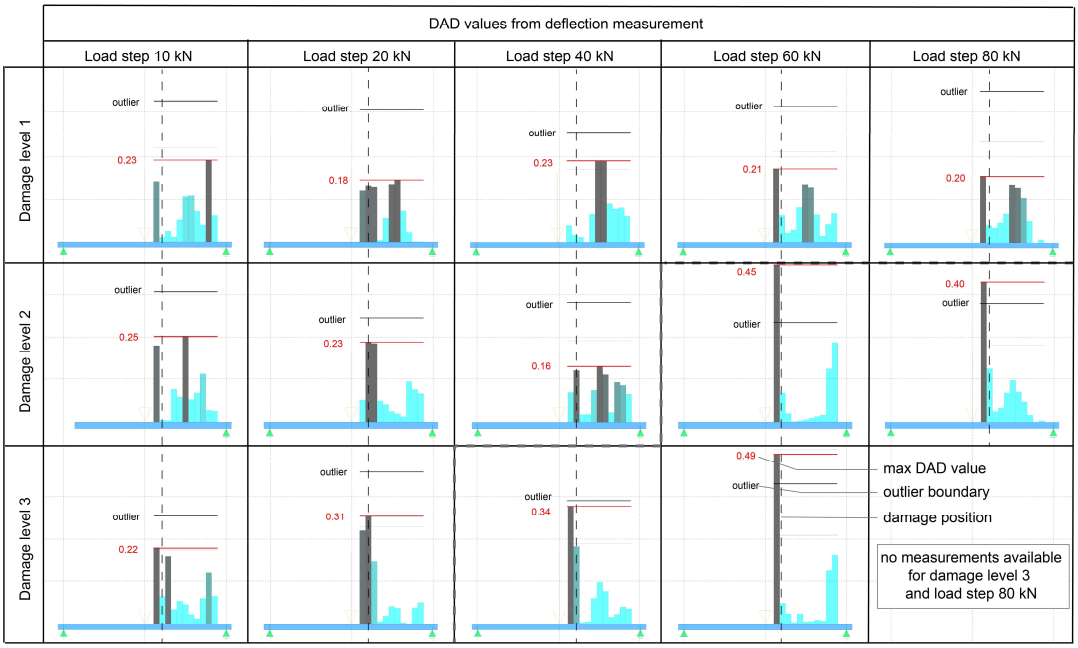

Figure 50. Overview of DAD values of all damage levels and load steps

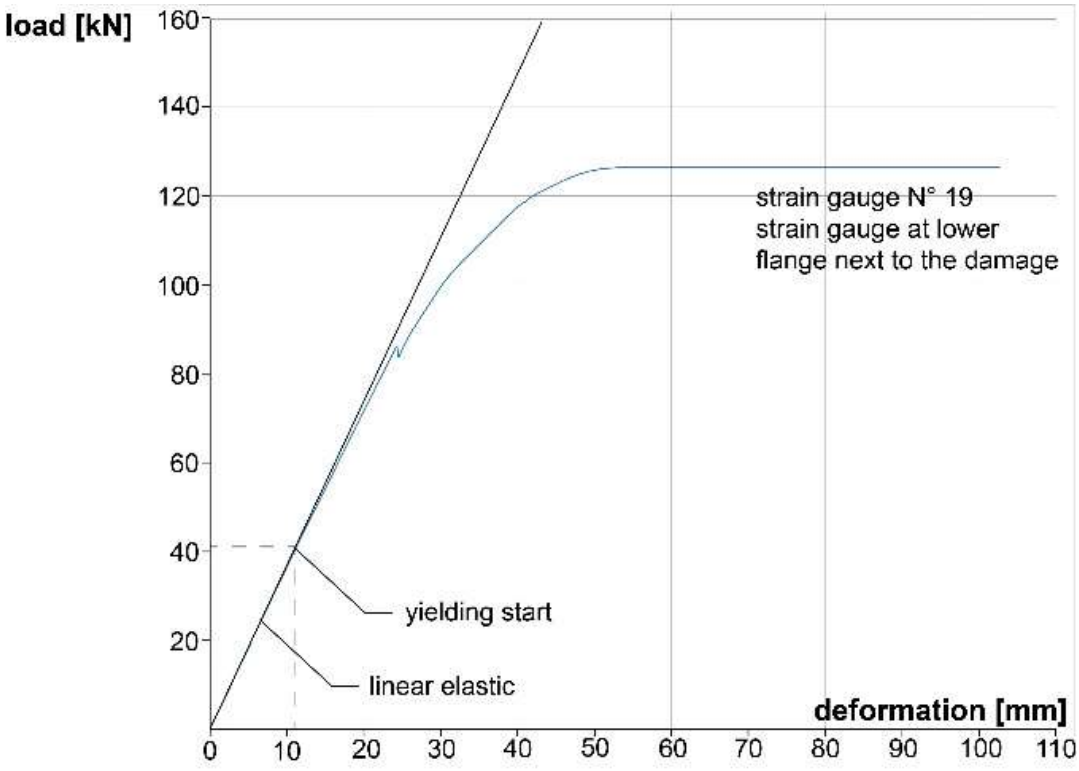

Figure 51. Load-deformation-graph of strain-gauge next to the damage on the lower flange for damage level 3

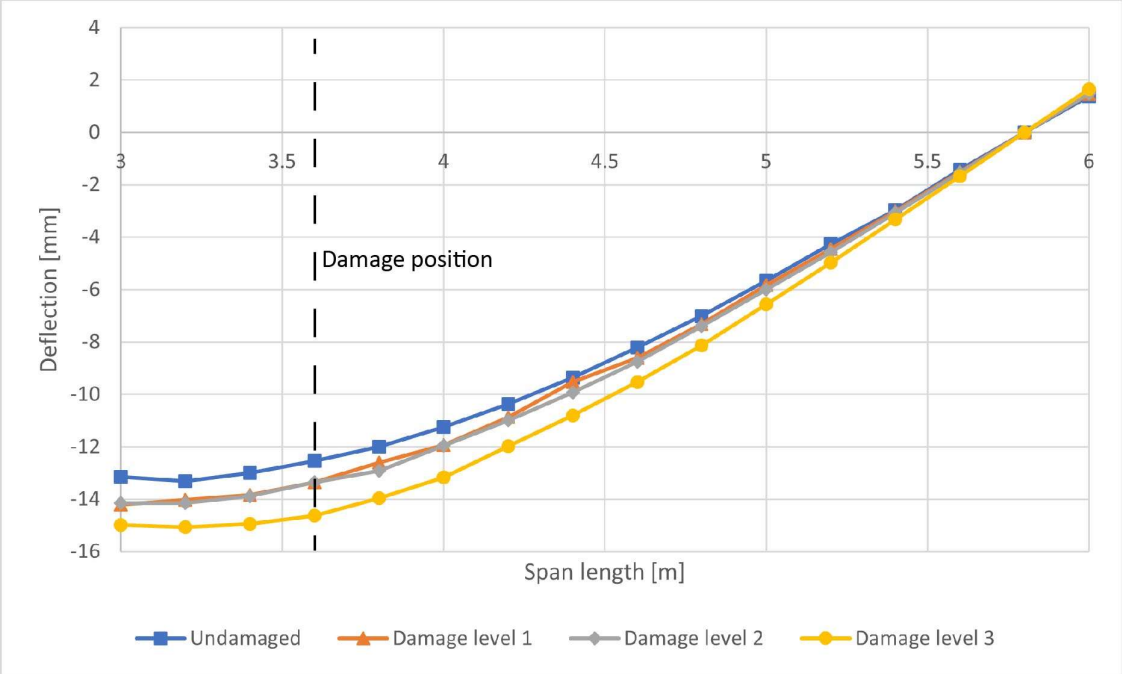

Figure 52. Measured deflection line for all damage levels at load step 60 kN (only half of the girder)

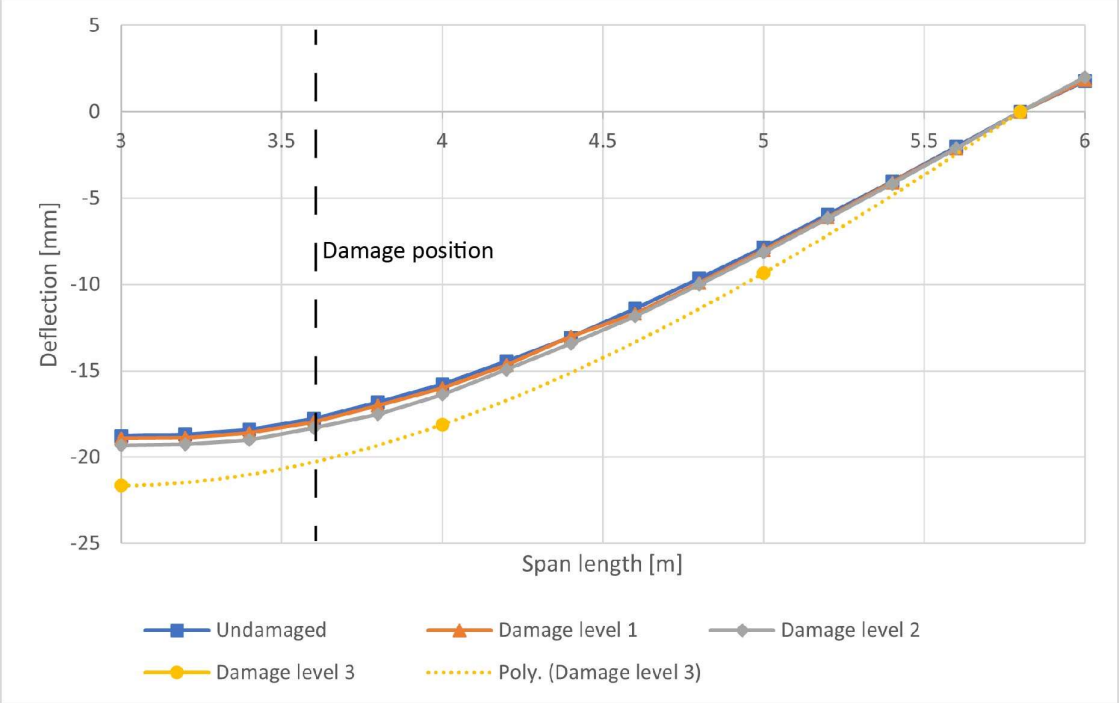

Figure 53. Measured deflection line for all damage levels at load step 80 kN (only half of the girder)

- **SAD Method Results**

The strains were measured with the strain gauges on the upper and lower flange of the girder. With these measured strains, the SAD method was applied for each load step and each damage level. Figure 54 shows the SAD values for each load step and damage level step. The results demonstrate that:

- Even at the lowest damage level and deflection value, the SAD method successfully located the damage, highlighting its superiority over the DAD method.
- For damage level steps 2 and 3 and load step 80 kN, increased SAD values, although still below the inner boundary, were observed. This anomaly could indicate a secondary damage or a malfunctioning strain gauge.

The experiment clearly underscores the advantages of the SAD method, showing improved performance and reliability compared to the DAD method. The ability of the SAD method to detect damage even at lower deflection values and damage levels makes it a more robust tool for damage detection. Here, the same DDR was achieved for the SAD method as for the DAD method with a noise of 0.01 mm. It is important to note that these results of the SAD method are limited to a linear elastic state. Further investigation is required to understand the influence of nonlinear behavior in the cracked state on concrete structures. Cracks can significantly impact strains at the crack position, making interpretation challenging. In contrast, the DAD method relies on deformation and is not sensitive to the behavior of concrete in a cracked state. It has been successfully applied to concrete structures.

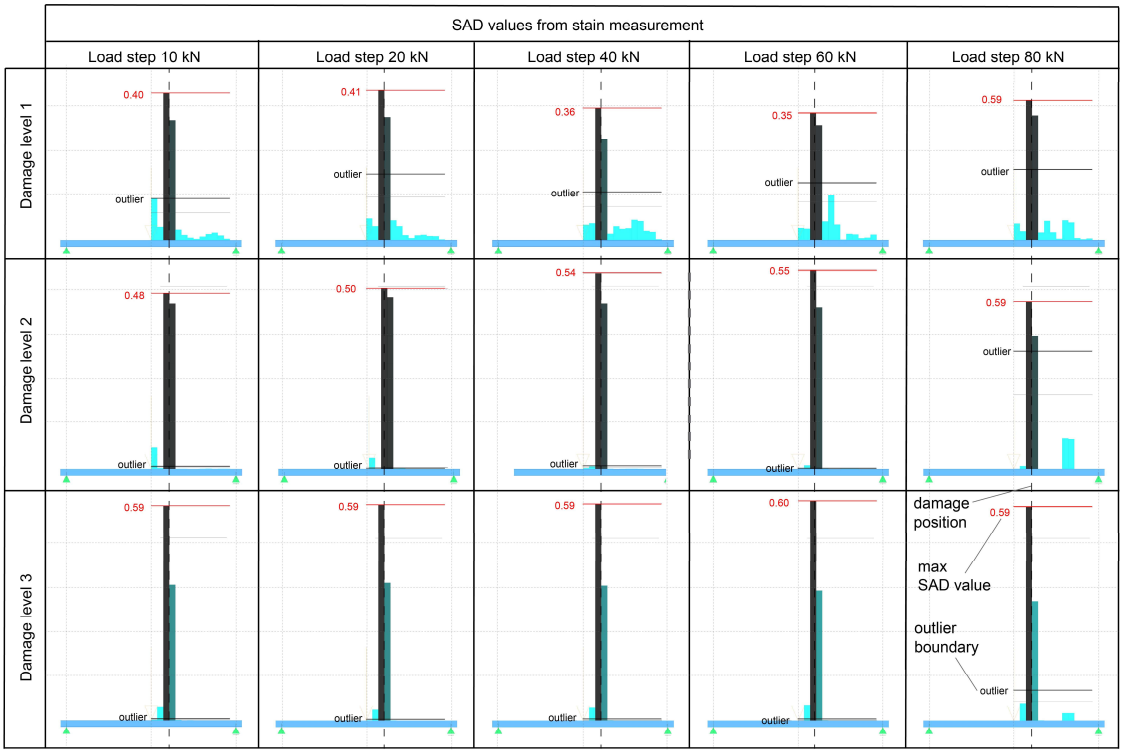

Figure 54. Overview of SAD values of all damage levels and load steps

3.5.5 Case Study on a real bridge structure in Vianden

The DAD method is also applied on a real bridge structure for a sensitivity analysis. The bridge to be studied was built in 1960 and is a road overpass over the river Our with two tracks and two pedestrian lanes (Figure 55). It is a continuous bridge with two spans of 17.5 m. The superstructure

is a RC – structural steel composite, with a cross-section as shown in Figure 56. The cross-section consists of three steel girders completely concreted within reinforced concrete beams connected through two concrete slabs of 16 cm thickness. The height of the bridge cross section is 1.0 m and the total width 9.5 m. The bridge is supported at the three girders and has cross members in the third points. The concrete and the steel grade are not documented. The skew angle of the bridge compared to the alignment of the river is 45°.

Figure 55. The Vianden bridge during the execution of a measurement with a UAV

3.5.5.1 Experimental Set-Up and Loading of the Bridge

For the application of the DAD method a continuous deflection line is needed. Previous studies [166] have shown that three measurement lines would be required for an analysis of the complete bridge structure, one for each girder, and it would be optimal to obtain additional measurement lines, one for each bridge edge. Due to time constraints, only one outer girder is equipped with measurement targets over the entire length and the inner girder only for one span. Previous studies have also shown that two load positions need to be applied and measured, one for each span, respectively. However, time constraints due to minimal road closure, only one span was loaded. The positions of photogrammetric targets are shown in Figure 56 and Figure 57. They have been applied on steel plates, which are bolted on the structure. The outer targets are directly bolted on the girder, while the inner targets were attached with rods, to be lower, so that they are still visible from a height (Figure 58). Additional reference targets are attached to the bridge abutments and on the bridge pier, as they are required for the reference coordinate system of the photogrammetry software.

As already mentioned, and demonstrated in the previous sections of the current paper, accurate deflection values have a great influence on the detectable damage level [166]. However, the loading level is limited on bridge structures, as the structure needs to remain within the SLS. As heavy trucks are usually used to load bridges, especially for the smaller bridges, the area of the bridge is limited which leads to a limitation of the trucks that can be positioned on the bridge deck. In this

experiment, four heavy trucks could fit on one span, (see Figure 59) with each truck having eight tires and a total load of 35 tons. The position of each tire was measured and used to simulate a realistic loading in a FE reference model. A by-product of the photogrammetric survey is a detailed point cloud, which can also help to more easily transfer the geometry of the structure to the FE reference model. Furthermore, the point cloud is also used to confirm the exact position of the loading on the bridge structure.

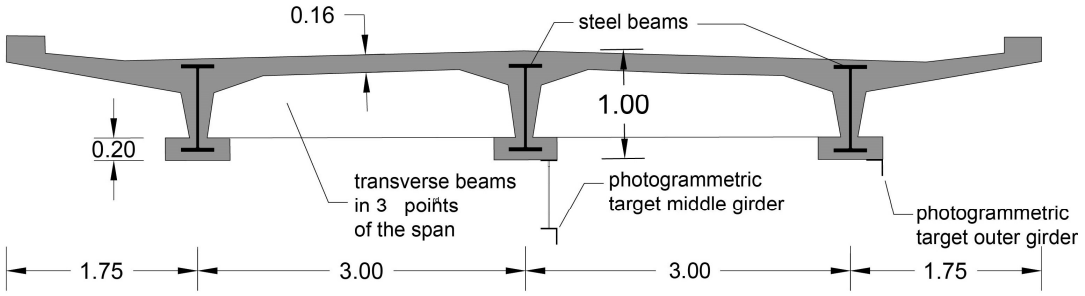

Figure 56. Cross-section of the Vianden bridge

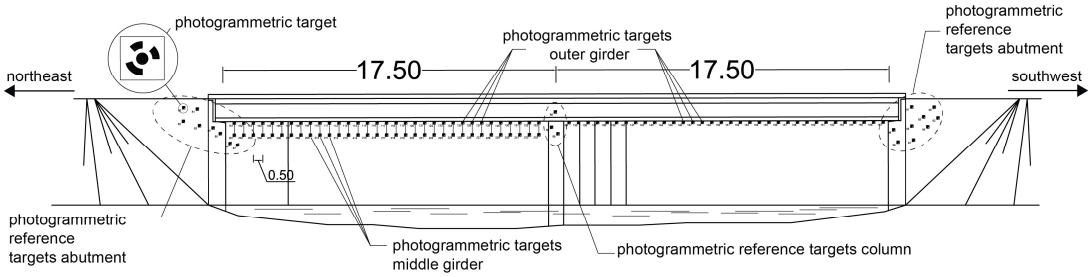

Figure 57. Elevation of the bridge with experimental set-up

Figure 58. Photogrammetric targets attached on outer and middle girder with bolts

3.5.5.2 Finite Element Model of the bridge

A reference model is required for the application of the DAD method. Therefore, a numerical FE reference model of the structure is developed using the commercial software SOFiSTik. The girders of the bridge are modelled as composite I-beam cross-section, whereas the concrete plate is realized in addition as an orthotropic surface slab structure without normal force stiffness and without Elastic Modulus in longitudinal direction so that the slab only bears loads in transversal direction. In addition, the slab is designed with no self-weight to ensure that the dead weight of the concrete slab is not applied twice. The load was applied as point loads for each tire of the four heavy trucks. The position of the trucks was measured, and, additionally, the position of the loading has been verified with the Point Cloud of the bridge structure (Figure 59). The bridge model does not have to be calibrated for the application of the DAD method. However, the model needs to be a realistic representation of the static system with the respective span lengths and to include all stiffness changes as variation of cross-section dimensions or other local stiffness variation. The deflection results of the model are determined at the positions of the photogrammetric targets to achieve the best possible comparison with the UAV measurements.

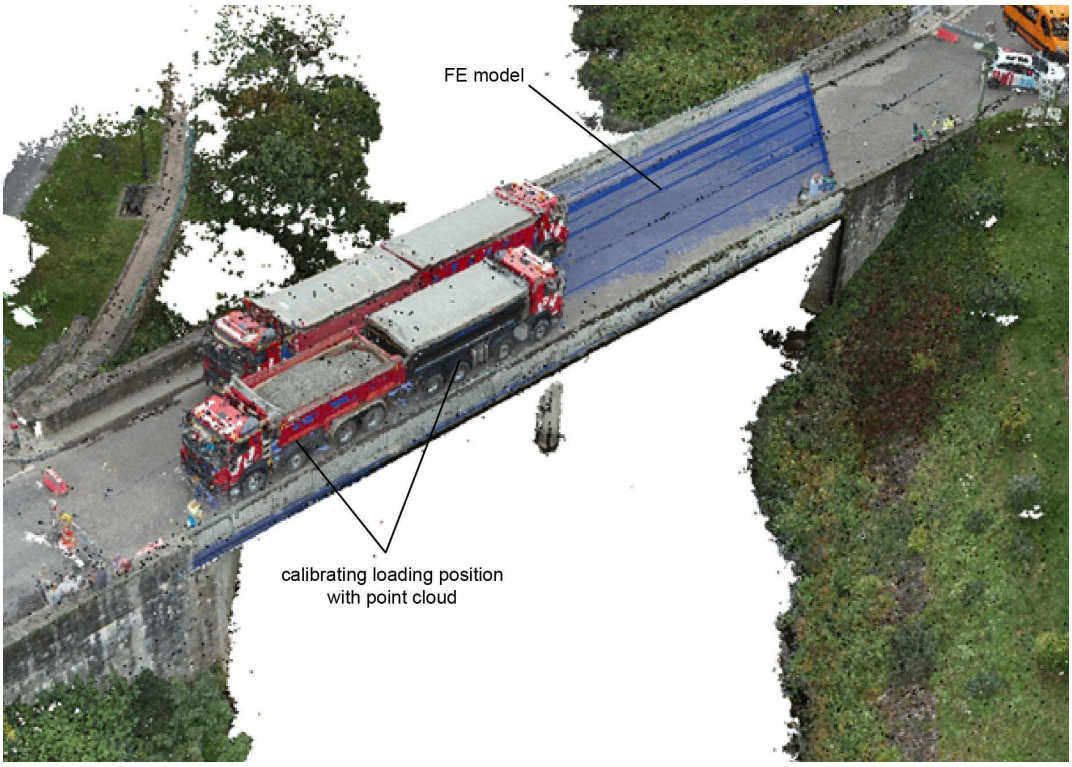

Figure 59. Point cloud of the bridge overlayed with FE-model

3.5.5.3 Experimental results

The effectiveness of the DAD method has been previously validated in laboratory experiments [94], [95] and its applicability has also been demonstrated on a real bridge structure in Altrier, Luxembourg [93]. Parametric studies [166] have shown that bridges with a more coherent cross-section like the Vianden bridge are more suitable for the DAD method as less measurement lines are needed as mentioned in *Experimental Set-Up and Loading of the Bridge*. In Figure 60, the DAD values for the outer girder and first span from direction northeast are shown. It can be observed that the highest DAD value does not exceed the lower outlier boundary. The following process have been applied to smooth the deflection line: First, a polynomial regression is determined based on the deflection curve, which is affected by noise. Subsequently, the raw deflection curve is filtered within the measurement standard deviation, resulting in a smoothed deflection curve. The detailed process is described in [95].However in this case, the described smoothing process did not improve the results. Further smoothing of the deflection line by averaging adjacent vertices as described in [166] and repeating the measurements, which reduces the outlier caused by measurement noise by averaging values from different measurements according to [93] could improve the results.

Increasing the deflection value would also have a significant influence on which damage level would be detectable as shown in previous studies [93], [166].

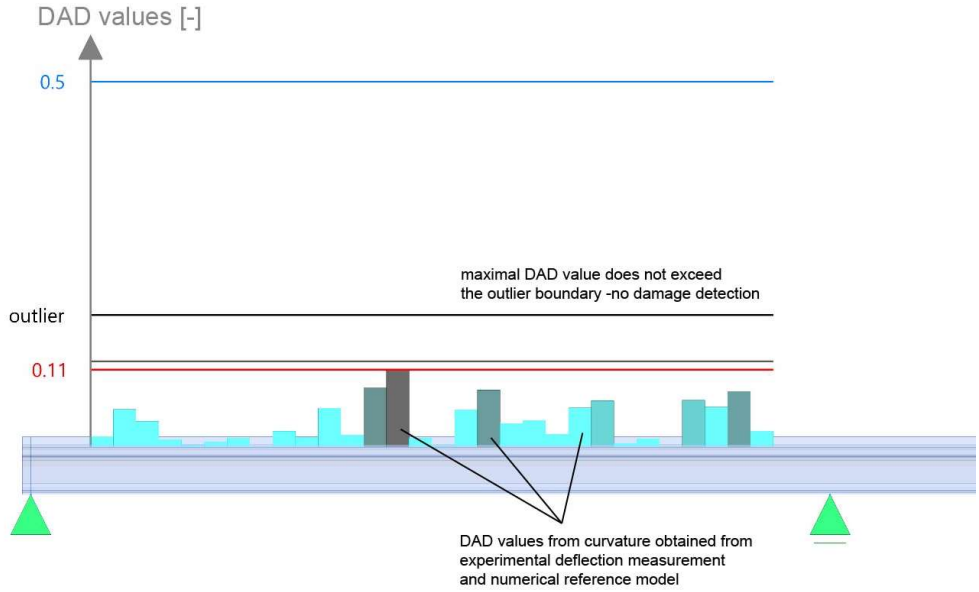

Figure 60. DAD values of the experimental deflection measurement and the FE reference model for the first span and the outer girder

3.5.5.4 Numerical analysis of the DAD and SAD method with artificial noise

To better classify the experiment's results, a numerical finite element (FE) reference model with simulated damage at midspan was developed. The experiment reached a deflection level of about $w \approx$ L/2500 with a standard deviation of 0.08 mm. The damage levels were varied, starting with a 10% reduction in bending stiffness in 10% increments, until the DAD method was able to localize the simulated damage. Due to the low deflection value and in agreement with previous studies [93], [166] (Figure 61), a high damage level with 80% reduction in bending stiffness was reached in order to detect the damage with the given deflection value and a precision of 0.08 mm. The corresponding DAD values are shown in Figure 62. Visual inspection of the bridge confirmed the absence of any such high-level damage. Although the experiment's precision was high, damage levels below 80% bending stiffness reduction could not be detected with the achieved precision.

With an increased deflection value, the detectable damage level would decrease significantly as shown in Figure 61.

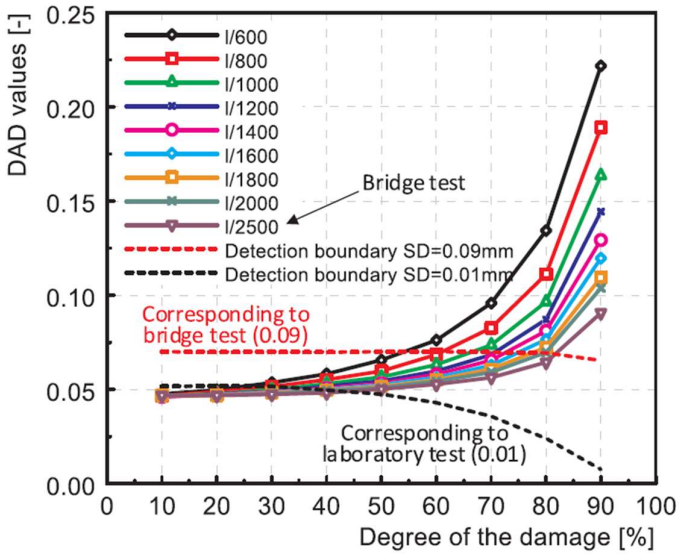

Figure 61. Damage identification based on deflection size and measurement precision. [93]

The strains from the numerical model with simulated damage were further analyzed using the SAD method for different damage levels, starting from a reduction of 10% in bending stiffness, with the same deflection value as reached in the in-situ experiment and an artificial noise of 50 με (Figure 63). A damage level of 20% was sufficient to successfully localize the damage, showcasing the superior precision of the SAD method. The height between the upper and the lower strain measurement position significantly influences the results—the greater the distance, the higher the strains and the better the precision. This is usually limited by the height of the cross-section and the accessibility of the bridge structure. The optimum sensor placement would be the lower and the top surface of the cross-section. While the lower surface should be well accessible, the top surface is located under the bridge deck. Here, the position below the bridge deck would be a good position.

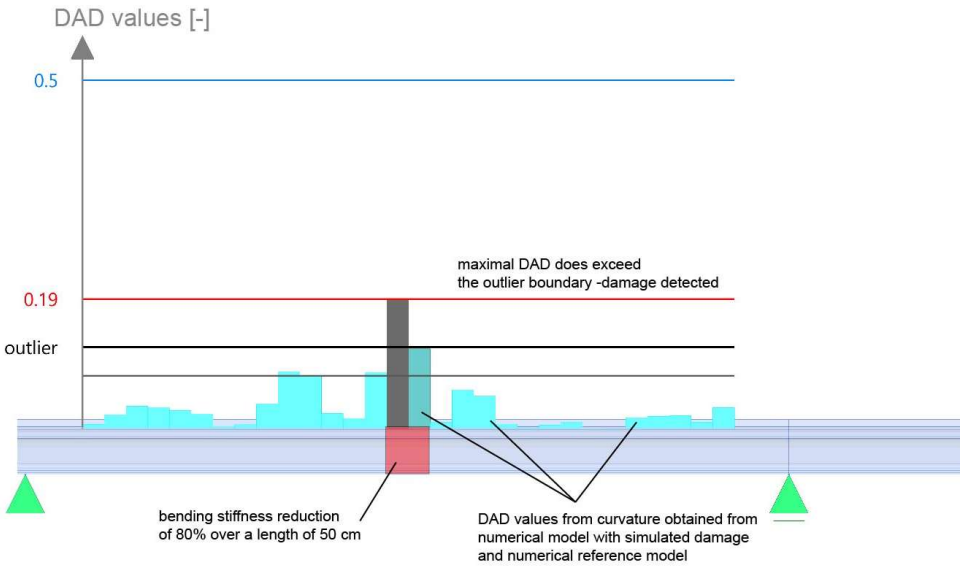

Figure 62. DAD values with deflections of numerical models with simulated damage of 80% and artificial noise with a standard deviation of 0.08 mm for the first span and the outer girder

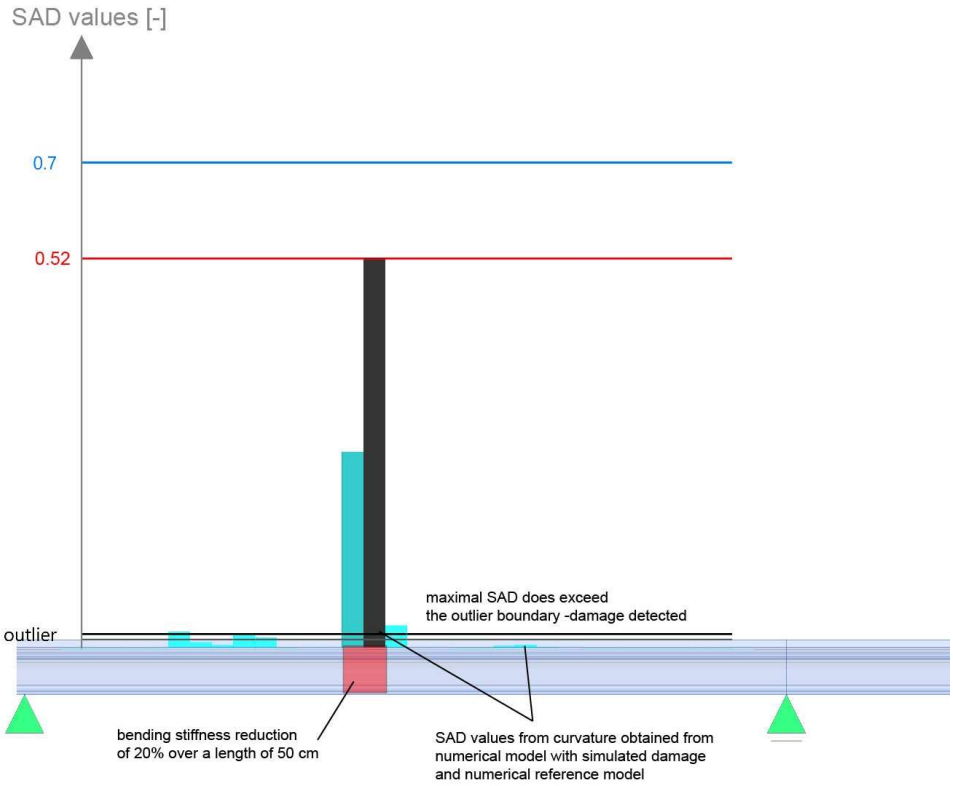

Figure 63. SAD values with strains of numerical models with simulated damage of 20% and artificial noise with a standard deviation of 0.00005 for the first span and the outer girder

3.5.5.5 Comparative Analysis

Compared to the high performance of the SAD method, the information obtained from the deflection line measurements appears to be limited and less useful for this bridge structure. Figure 64 illustrates the relationship between the information provided by the two measurement

techniques. Using photogrammetry and drones, the deflection line can be measured, and then the DAD method is applied. Strain measurements and the obtained yield strain values enable the application of the SAD method. From both techniques the curvature line is derived, either through double derivation of the deflection line or by using strain measurements (see section 3.5.2).

According to Bertola et al. [176], the value of information (VoI) can be assessed for each type of measurement technique used in structural performance monitoring. For direct measurements, such as non-destructive testing, the detection ranges are primarily influenced by measurement precision and repeatability. For indirect measurements, such as those derived from inverse analysis after bridge load testing, the posterior parameter distributions are determined by the structural identification process, which links sensor data with model predictions. Additional benefit can be achieved by updating the numerical finite element (FE) reference model using the results from these measurements, thereby refining the model and enhancing the accuracy of structural assessments.

In contrast to the measurement of strains, the DAD method can be performed at a relatively low cost. For cost and time reasons, no strain measurements with strain gauges or FOS were carried out during the in-situ bridge test. However, the strains can be calculated by measuring the distance differences between the points according to Eq. (16), whereas the distance difference is calculated by subtracting the distance between two targets in the unloaded measurement from the loaded measurement.

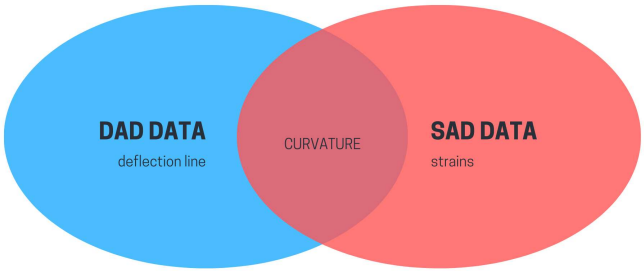

Figure 64. DAD and SAD method data correlation

The maximum expected strain from the experiment, based on the numerical reference model, is approximately 0.00012. With a standard deviation of 0.08 mm for the measurement points, the calculated strain deviation at point spacing differences of 1.0 m is approximately 80 με, which is high compared to the expected strain value. At distances of 4.0 m, the expected deviation is 20 με, which offers greater precision but results in fewer strain values and a less accurate strain line. It is noteworthy that with FOS a precision of up to 1 με is reachable as previously mentioned.

Figure 65 shows the strain values at the bottom of the cross-section over the first span of the bridge. The strain values originate either from point-to-point spacing differences of the photogrammetric targets at the bottom of the cross-section with measurement distances of 1.0 m (rectangular marker)

and 4.0 m (triangular marker) or from the finite element (FE) reference model with strains calculated at the bottom of the cross-section and extrapolated to the position of the photogrammetric targets (dashed marker). The curve with the triangular markers, which was derived from measurements at a distance of 4.0 m in longitudinal direction, deviates from the calculated strain curve due to the limited number of measurement points. However, when comparing the polynomial trend line of the measured strain values at a distance of 1.0 m with the numerical model, a better agreement with the calculated strain curve can be obtained. The numerical reference model assumes a pinned support at the bridge abutment, while the extrapolated trend line of the measurements indicates a small restraint at the support. Using the information from the deflection measurements, the numerical model was updated by adjusting the spring stiffness of the restraint until the deflection value of the numerical reference model matched the deflection measurement. The strain curve of the updated reference model (rhombic markings) agrees well with the trend line of the measurement. Consequently, the deflection line measurements obtained from the experiment can help eliminate modelling uncertainties and thus increase the value of the monitoring technique. However, it is worth repeating that the strains measured here with photogrammetry do not reach a high accuracy, and therefore the results of the strain measurements must be considered with care. If the strain were measured with strain gauges or FOS, the accuracy would be much higher.

By combining deflection measurements with strain measurements, the application of the SAD method with an updated reference model can improve its effectiveness, aiding in the detection of smaller damage. The updated reference model, informed by direct and indirect measurement outcomes, allows for a more precise and effective structural assessment.

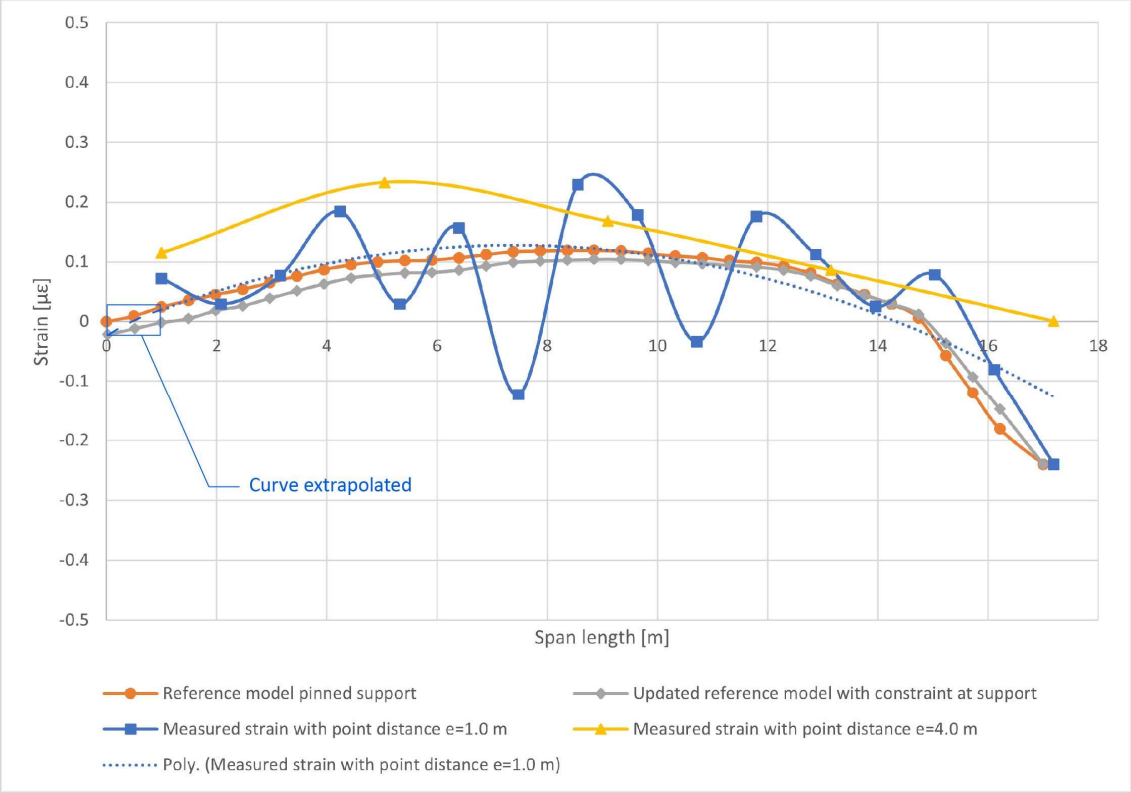

Figure 65. Comparison of measured strains, calculated from point distance differences of the photogrammetric targets at the bottom of the cross-section and strains of the reference FE-model

3.5.6 Discussion

The comparative analysis of the DAD and SAD methods reveal several significant advantages for each technique in terms of SHM.

The DAD method is recognized for its cost-effectiveness and practical applicability. It is a low-cost solution, making it feasible for projects with budget constraints. The method provides a clear deformation line, which is useful for various damage assessment methods and for model updating. The use of drone technology in the DAD method allows for efficient visual inspections [177], [178], [179]. Additionally, the use of drones for the DAD method can also be used to generates detailed point clouds through photogrammetry, which are valuable for high-resolution 3D modeling and analysis [180], [181]

Another significant advantage of the DAD method is its simplicity in data management. Unlike methods that generate large volumes of data requiring extensive storage and processing, the DAD method produces manageable data sets, making it easier to handle and analyze, and therefore, is in that aspect also less cost intensive [182], [183]

The SAD method, on the other hand, if the strains can be directly measured in situ, stands out for its high precision, allowing to the detection of smaller damage levels with lower deflection values compared to the DAD method. This precision is crucial for identifying minor structural issues that might not be apparent through deflection measurements alone. Using FOS could even improve the

precision of the strain measurements. [184], [185]. Furthermore, the ability of the SAD method to provide real-time data is a major advantage. As a continuous monitoring system, the SAD method offers the potential of providing near-real-time alerts whenas deterioration mechanisms evolve [167]. This is essential for proactive maintenance to enhance the safety and longevity of infrastructure.

In this study the SAD method is only applied for the steel girder under laboratory conditions. For a concrete structure, the applicability of the SAD method still needs to be verified. The positioning of the strain sensors could influence the results, as the position of cracks affects the results, and thus influences the measured strains locally and makes interpretation more challenging. A crack influences the strain mainly at the position of the crack. Further investigations on concrete structures are necessary to ascertain the applicability of real bridge structures, while the DAD method has already been demonstrated to be independent of the material and suitable for use in real bridge structures.

3.5.7 Conclusions

This study comprehensively examined the effectiveness of the DAD and SAD methods in structural health monitoring. Initially, these methods were evaluated and compared through a parametric numerical FE model, observing and comparing the damage detection range. This was verified through a laboratory experiment on a steel girder. Subsequently, an in-situ experiment on a real bridge structure was conducted, measuring deflection with photogrammetry and UAVs. The DAD method was applied, and additionally, strains were analyzed with the measured points. A model updating was performed based on the deflection line and validated through the comparison of measured strains and calculated strains of the reference model.

The comparative analysis of the two methods highlighted several key advantages for and practical applications:

- The SAD method was introduced as an extension of the DAD method using strain measurements.
- To achieve a similar damage detection range as the SAD method, an accuracy of 0.01 mm is required for the DAD method.
- The SAD method demonstrated in numerical investigations and in a laboratory experiment high precision in strain measurements, and its insensitivity to noise allowing it to detect smaller damage levels with lower deflection values compared to the noise sensitive DAD method
- In a laboratory experiment, the SAD method could identify a bending stiffness reduction of 12% with a deflection value of w= L/2550. In contrast, the DAD method could only detect a damage of 28% with a deflection value of w= L/390 and a damage of 73% with a deflection value of w= L/600.

- In the presented in-situ experiment on the Vianden bridge with a small deflection value of w= L/2.500, a damage of 80% would be necessary to be located with the DAD method for the reached precision, while the SAD method could already localize a damage of 20%.
- For cross-sections with an increased height (e.g. box girder bridges with a height of over 2 m), strains can be obtained with photogrammetry. The measurement precision remains significantly inferior to that of strain gauges or FOS.
- The DAD method provides a clear deformation line, which is useful for various damage assessment methods and modal updating.
- The DAD method is recognized for its cost-effectiveness and practical applicability. Its low-cost nature makes it accessible for projects with budget constraints.

In conclusion, the findings of this study underscore the unique advantages of both the SAD and DAD methods. The SAD method's high precision and real-time monitoring capabilities make it ideal for continuous structural health monitoring, while the DAD method's cost-effectiveness and detailed visual data collection are valuable for routine inspections. By integrating both methods, a comprehensive and efficient Structural Health Monitoring (SHM) strategy can be developed, enhancing the reliability and safety of infrastructure. This approach ensures early detection and effective management of potential structural issues, ultimately contributing to the sustainable maintenance and operation of critical infrastructure.

ACKNOWLEDGEMENT:

The authors would like to express their gratitude to the "Administration des Ponts et Chaussées" of Luxembourg for providing the opportunity to carry out experiments on a real bridge and providing the under-bridge inspection unit and the loading with heavy trucks. Furthermore, the authors would like to express their gratitude to Mr. Harald Krause for the support with the photogrammetric software Elcovision. The authors would also like to acknowledge Mr. Cédric Bruyere and his Team for providing the point coordinates for the reference points. The GGE Laboratory supported this work with specialized instruments. Special acknowledgements are expressed to the technical support team of the University of Luxembourg for their expertise and helpful contributions to the realization of the large-scale experiment. Finally, special acknowledgements are expressed to the technical support team of the Institute of Solid Structures of the Technical University of Darmstadt for their contribution to the laboratory experiment.

DECLARATION OF COMPETING INTEREST:

I hereby declare that the authors have no affiliation or involvement in any organization or entity with any financial interest or non-financial interest in the subject matter or materials discussed in this manuscript.

DATA AVAILABILITY:

The data that has been used is confidential.

3.6 Transition to publication III

The second paper, which introduced the SAD method, notably enhanced damage detection capabilities by integrating strain-based curvature analysis into the DAD framework. Furthermore, the second paper addressed both the second and third research questions, thereby demonstrating how strain-based methods enhance the precision and applicability of the DAD method.

The third paper represents a further advancement of the DAD method, with the objective of enhancing its capacity to support more sophisticated SHM levels. In particular, it investigates the integration of model updating techniques, with the aim of enabling detailed damage severity assessments and aligning numerical models with real-world structural behavior. By addressing these aspects, the third paper seeks to demonstrate the DAD method's potential for supporting high-level SHM frameworks and broader structural evaluation processes.

3.7 Publication III: Damage Level Assessment using DAD method and model updating

T. Čamo and D. Waldmann, "Damage level assessment using DAD method and model updating," Engineering Structures, vol. 336, p. 120498, Aug. 2025, doi: https://doi.org/10.1016/j.engstruct.2025.120498

AUTHORS CONTRIBUTIONS:

Tarik Čamo: Conceptualization, Data curation, Formal analysis, Investigation , Methodology, Resources, Software, Validation, Visualization, Writing - original draft.

Danièle Waldmann: Conceptualization, Funding acquisition Methodology, Project administration, Resources, Supervision Validation, Writing - review & editing.

ABSTRACT:

Aging infrastructure, particularly bridges, requires reliable methods for assessing structural integrity. Structural Health Monitoring (SHM) provides a proactive approach to damage detection and maintenance, but traditional methods often lack the capability to assess the severity of detected damage. This paper introduces an enhancement to the Deformation Area Difference (DAD) method, specifically designed to enable Level 3 SHM for damage severity assessment. Traditionally, the DAD method focuses on detecting and localizing damage by analyzing the deflection of structures under static loads, but it does not provide a means for quantifying damage severity. To address this limitation, a model updating (MU) technique is integrated into the DAD method, allowing for assessment of the severity of localized damage. The method involves deriving curvature differences from the deflection data and applying an inversion-based MU algorithm to quantify the extent of structural damage. The research includes numerical simulations and experimental investigations, showcasing the potential of the enhanced approach for real-world applications. The results highlight the potential of the enhanced DAD method for damage level assessments while maintaining computational efficiency. However, real-world applications remain influenced by noise and deformation magnitudes, requiring further refinement. These findings suggest that the enhanced method has potential for SHM applications, particularly in assessing structural integrity and guiding maintenance decisions in real-world applications.

AUTHOR KEYWORDS: Structural Health Monitoring (SHM), Bridge condition assessment, Static load deflection experiment, Model Updating (MU), Photogrammetry, Deformation Area Difference (DAD) method

NOTATION LIST:

$DAD_{\kappa,i}$	DAD values from curvature lines
$EI(x)$	Flexural rigidity
IB	Inner boundary
L	Total length of span
$M(x)$	Bending moment
OB	Outer boundary
$w_m(x)$	Measured deflection line
$w_r(x)$	Reference deflection line
$\Delta A_{\kappa,I}$	Area difference between curvature lines
Δ_{xi}	Incremental length for DAD calculations
$\varphi_m(x)$	Inclination angle line derived from measured deflection line
$\varphi_r(x)$	Inclination angle line derived from reference deflection line
$\kappa_m(x)$	Curvature angle line derived from measured inclination angle line
$\kappa_r(x)$	Curvature angle line derived from reference inclination angle line

3.7.1 Introduction

Bridges are indispensable elements of transportation networks, facilitating economic activity and public safety by enabling the movement of goods and people. In the United States, there are over 617,000 bridges, with approximately 42% of them being over 50 years old and more than 46,000 classified as structurally deficient (American Society of Civil Engineering [186]). Similarly, in Europe, the issue of aging infrastructure is becoming increasingly pressing. A significant number of bridges constructed in the post-World War II era are now in need of substantial repairs. In Germany, for instance, nearly 46.8% of bridges are overdue for maintenance, with an estimated annual maintenance backlog of €7.2 billion (European Commission [187]). The combination of aging infrastructure and increasing traffic loads, along with environmental stresses, such as corrosion of steel parts or of reinforcement steel, has given rise to concerns regarding the safety and serviceability of these structures.

Traditionally, the assessment of bridge condition has relied on visual inspections and periodic evaluations. While these methods have proven useful, they are often limited by subjectivity, infrequency, and the inability to detect internal or early-stage damage. Structural Health Monitoring (SHM) for bridge structures addresses these limitations by providing continuous, real-time assessment of the structural integrity and performance of bridges. In the context of aging infrastructure and increasing load demands, SHM offers a proactive approach to bridge maintenance. This is achieved through the use of sensors, data acquisition systems, and advanced algorithms to detect damage, assess deterioration, and predict future performance.

A method of classifying different categories of SHM is through the utilization of three principal categories: Vibration-Based Methods (i), Static Load Deflection Methods (ii), Acoustic Emission (AE) Methods (iii) and Vision-Based (VB) methods (iv). Among these, vibration-based methods

(i) can be further subdivided into model-based methods, and data-driven approaches. Model-based approaches rely on the utilization of predefined structural models for the analysis of changes in dynamic characteristics, such as natural frequencies or mode shapes, for the identification of damage. Conversely, data-driven approaches extract information directly from measured response data, thus obviating the necessity for an underlying physical model. Often used within data-driven approaches, Wavelet-Based Analysis (WBA) employs wavelet transforms for the purpose of damage detection in structural response signals. Vehicle-Bridge Interaction (VBI) methods, which utilize vehicle response data for the indirect assessment of bridge conditions, can incorporate both data-driven and model-based elements depending on the methodology applied. One example of model-based methods is the work of Teng et al. [188], who employed a one-dimensional Convolutional Neural Network (1-D CNN) for the purpose of vibration-based structural damage detection. This approach entailed the establishment of a population of bridges with single damage scenarios, pre-training of a CNN model, and subsequent application of Transfer Learning (TL) for the adaptation of the model to diverse damage scenarios. The results demonstrated that TL enhanced accuracy by approximately 47% and accelerated convergence by a minimum of 50%. However, while TL has the potential to enhance the generalization ability of CNNs, the paper underscored the challenge of insufficient training samples, which can limit generalization when applied to new or significantly different data domains. This highlights the complexity of adapting machine learning techniques for SHM when data from different bridge types or conditions are limited. Similarly, Umar et al. [189] investigated a sensor clustering-based methodology for damage detection using time-series data from ambient vibrations, which were modelled by Nonlinear Autoregressive with EXogenous Inputs (NARX) models. The approach demonstrated success in detecting and localizing damage in a scaled steel arch laboratory model, exhibiting high sensitivity to damage severity. However, as with numerous methodologies that necessitate dense sensor networks, the precision of this approach depends on the sensor density and the quality of the NARX model. In environments where sensor distribution is sparse or subject to environmental noise, the applicability of such methods is limited. In contrast to these model-based methods, WBA employs wavelet transforms to analyze dynamic responses and identify damage. For example, Soleymani et al. [190] employed wavelet analysis to examine modal excitation responses of reinforced concrete beams, successfully identifying and localizing damage. However, the researchers discovered that selecting an appropriate wavelet function was of paramount importance to the accuracy of the analysis, representing a potential complication in the overall process. To address some of WBA's challenges like noise sensitivity and calculation complexity, Miao et al. [191] integrated wavelet analysis with a neural network optimized by genetic algorithms, thereby improving both the speed and accuracy of damage detection in beam structures. Although this integrated approach yielded improved results, its increased complexity restricts its practical applicability in scenarios where computational simplicity is paramount. Another approach is offered by VBI methods, which focus on the

interaction between vehicles and bridge structures for the purpose of detecting damage. In a separate study, Zhan et al. [192] presented a method for identifying damage in adjacent box-beam connections using VBI analysis and Model Updating (MU). The method was found to be effective in identifying damage based on the height of cracking and residual bending stiffness. However, this approach is highly sensitive to factors such as vehicle speed, path, and road conditions, which limits its applicability to specific bridge types. Similarly, Zhou et al. [193] investigated various damage modeling techniques for beam-like structures, concluding that the crack spring element method had the most pronounced impact on VBI responses. This indicates that selecting an appropriate damage model is essential when employing VBI-based health monitoring. However, VBI methods are frequently constrained by their reliance on vehicle response data, which may not always be accessible or sufficiently detailed for precise monitoring. Although Vibration-Based methods provide valuable insights, they typically require extensive dynamic data and are often sensitive to environmental factors such as temperature, traffic, and wind. This sensitivity can affect the accuracy and reliability of the results, especially when used in real-world conditions where such factors vary significantly.

AE Methods (iii) are capable of detecting acoustic signals generated by structural damage, such as crack propagation, thereby providing real-time monitoring of damage progression. For example, the work of McCrory et al. [194] and Boniface et al. [195] demonstrated how AE methods could track crack development. However, one limitation of AE techniques is that they can only monitor damage progress in real time and are unable to detect pre-existing damage. Furthermore, signal attenuation over distance can make AE signals difficult to interpret, thereby complicating their practical use in large or complex structures. VB methods (iv) use computer vision and image processing techniques to non-invasively assess structural health, offering a promising alternative to traditional sensor-based monitoring. Recent advances in real-time video processing and edge computing have significantly improved the feasibility of vision-based SHM for large-scale applications (Peng et al. [196]). Despite their advantages, vision-based SHM methods are inherently limited to surface-level assessments, making them ineffective for detecting subsurface or internal structural damage - a critical drawback when compared to techniques such as ultrasonic or acoustic-based methods (Feng et al. [197]).

In contrast, Static Load Deflection Methods (ii) provide a more straightforward approach to damage detection by measuring the structural response under static loads. For example, numerous methods, such as those based on Influence Lines (IL), frequently rely on static parameters to detect structural changes. Yan et al. [198] introduced a frequency-domain approach for the extraction of ILs from static measurements, employing Bayesian inference to address uncertainties inherent to both data and model errors. This approach reduced the computational complexity of the method, but it was contingent upon the availability of a high-quality reference IL. Furthermore, IL-based methods typically necessitate a multitude of loading positions, rendering them more data-intensive in terms

of measurement configuration. In recent times, there has been a notable increase in the popularity of Strain-Based Methods, which have been enabled by advancements in measurement techniques such as Fiber-Optic Sensors (FOS). This is due to the high precision with which they can detect damage and their ability to provide localized detection. Ghahremani et al. [199] combined static strain measurements with Finite Element Analysis (FEA) to monitor bridge health, successfully detecting damage over a two-year period. However, the reliance on high-quality baseline data, along with sensitivity to environmental interference, represents a significant challenge for the widespread adoption of this approach. Furthermore, the cost and volume of data produced by these strain-based systems can be prohibitive for large-scale deployment.

Traditional deflection measurements remain a fundamental aspect of SHM applications, with the advent of new approaches serving to enhance their utility. For example, Lu et al. [200] employed sparse regularization and eigenparameter decomposition for damage identification, while Wu et al. [201] used a stochastic approach with homotopy analysis to account for measurement errors and model uncertainties. Both methods have demonstrated high accuracy in detecting damage. However, the reliance on sparse data in the Lu et al. approach may limit its effectiveness for complex structures and damage scenarios. Furthermore, the complexity of the Wu et al. approach may restrict its application, particularly when dealing with large-scale structures or extensive datasets.

The Deformation Area Difference (DAD) method (Erdenebat et al. [94]) is a static load deflection-based technique developed for the purpose of detecting and localizing damage with a single measurement. Furthermore, when used with photogrammetry, the DAD method eliminates the necessity for an excessive number of sensors by providing deflection measurements over large, continuous areas making it well-suited for complex structures. Nevertheless, attaining the requisite high precision for the DAD method necessitates the utilization of photogrammetric targets. Furthermore, the procurement of a continuous deflection line demands a substantial number of targets distributed evenly, which can be a laborious undertaking. However, other measurement techniques could be used to provide the required deflection data. The DAD method, as proposed by Erdenebat et al. [94], compares deflections from in-situ measurements with a numerical reference model. Its efficiency has been demonstrated through validation in both laboratory and real-bridge structures (Erdenebat et al. [93], [94], [95]). By analyzing the area between the curvature lines of the measurement and reference systems, the DAD method identifies reductions in stiffness which are an indication of damage. In a first application, Erdenebat et al. [94] tested the method on a reinforced concrete beam subjected to increasing loads. The primary objective of the experiment was to facilitate the identification and precise location of the damaged area through the analysis of deflection values. The DAD-values enabled a reliable localization of the crack pattern. Notably, the identification of the cracked area was achieved even at the load steps beneath the SLS, thereby validating the DAD-Method's efficacy as a non-destructive inspection technique for assessing the

condition of bridge structures. Photogrammetry revealed the DAD method's considerable potential, exhibiting a standard deviation of 0.17 mm, while the measured deflection was recorded at 9.3 mm for a load step of 20 kN under the SLS. Consequently, the impact of the measurement technique's accuracy was found to be minimal, with an influence of only 2%. A subsequent study by Erdenebat et al. [95] validated the method through two experiments: one on a reinforced concrete beam and another on a steel beam. The reinforced concrete beam was tested to evaluate the stiffness reduction due to cracking, confirming that the method is applicable to reinforced concrete structures. In the steel beam experiment, predefined damage was introduced at three locations, gradually increasing in severity to evaluate how damage intensity affects detection accuracy. The results showed that larger damage was consistently detected, while smaller damage was more difficult to detect, especially under high noise levels. This observation was conducted for the damage combination of 49% for the initial damage and 23.8% for the secondary damage, and 71.5% for the primary damage and 49% for the secondary and tertiary damage. However, the precise transition of the detectable degree of damage, contingent on the achieved measurement accuracy ranging from 0.06 to 0.11 mm, is situated within the range of 23.8% to 49.0%. The study also demonstrated that for a measurement point density of 30 cm the influence of the standard deviation is reduced to 23.7 % compared to the measurement point density of 10 cm, while the localization accuracy is limited to smaller than 30 cm. In addition, the study proposed polynomial regression smoothing to mitigate the influence of noise. The recent study by Erdenebat et al. [93] was the first application of the DAD method to a full-scale bridge structure. The structure studied was a prestressed concrete slab bridge with a span of 27 m, tested under static load-deflection conditions. Loads were applied using six heavy trucks, and deflections were measured using UAV-based photogrammetry, laser scanning, total stations, and displacement sensors. The primary objective of the study was to evaluate the achievable measurement accuracy on a full-scale structure under outdoor conditions. The results confirmed that stiffness variations could be detected in real conditions, but the accuracy of localization was affected by measurement precision and small deformation magnitudes. Numerical simulations with artificially introduced noise showed that smaller deformations lead to higher relative measurement errors, reducing the accuracy of damage localization. For instance, when a maximal deflection of L/600 is considered, the reliable identifiable damage degree commences at a 60% reduction in bending stiffness, with a measurement accuracy of 0.09 millimeters. Conversely, for a deflection of L/2,000, the identifiable damage degree initiates at 80%. This study confirmed the findings of previous work and emphasized that, while the DAD method is effective, high-precision measurements are critical for reliable real-world applications. The influence of different parameters such as influence of local damage, noise, deflection value and bridge structure type are extensively investigated in [166]. A key contribution is the introduction of the Damage Detection Range (DDR), which describes the range, where damage can be detected using the DAD method considering a given deflection value, precision, and damage level. It also

highlights that for localized damage, a single measurement line across the cross-section may not be sufficient. The findings provide a structured approach for designing in-situ tests and assessing the method's applicability to different bridge types. Traditionally, curvature is derived from the second derivative of deflection; however, the DAD method can also incorporate strain data from across the cross-section, a process known as the SAD method [202]. This hybrid approach enhances noise resistance and improves the method's overall reliability in damage detection. A numerical study and experimental validation on a steel beam demonstrate the method's effectiveness compared to DAD. Additionally, an in-situ case study on a composite bridge in Vianden evaluates the feasibility of both methods in real-world conditions. The results suggest that while DAD is cost-effective and practical, SAD provides higher precision, particularly for low deflection scenarios and early-stage damage detection.

Rytter [97] present a framework for the progression of damage detection and assessment in structures with different levels of SHM:

- Level 1: Damage Detection – This level identifies whether damage is present in the structure, without specifying its location or severity.
- Level 2: Damage Localization – This level identifies the specific location within the structure where damage has been detected.
- Level 3: Damage Severity Assessment – Quantifies the extent or severity of the localized damage, thereby providing insight into the level of structural degradation.
- Level 4: Prognosis – This level of structural health monitoring predicts the remaining useful life or future performance of the structure based on the damage identified and its progression over time.
- Level 5: Decision Support – Furnishes actionable data for maintenance or repair decisions, prioritizing interventions based on risk or cost-benefit analysis.

Each level provides increasingly detailed information, with Level 3 (Severity Assessment) being of particular importance for understanding the extent to which a structure's integrity has been compromised, and for informing necessary repairs or interventions (Falcetelli et al. [203]). Many existing methods focus on one or two SHM levels, but there is a need for more integrated techniques that encompass multiple levels (Gres et al. [204]). To illustrate, while the DAD method is able to detect and localize damage (Level 2), its integration with model-updating techniques could enable it to reach Level 3 (Severity Assessment), which is a critical step in assessing the degree to which a structure's integrity has been compromised.

MU refers to the application of algorithms that refine structural models based on observed data, thereby rendering them valuable tools for the assessment of damage severity. Bud et al. [205] integrated numerical data with machine learning algorithms for damage classification, demonstrating that such methodologies can evolve from damage detection to severity classification.

Nevertheless, the dependence on numerical data for training introduces constraints, as real-world damage scenarios frequently exhibit greater complexity. In a related study, Nguyen et al. [206] employed strain data obtained from static load tests to update the finite element model of a reinforced concrete bridge using a genetic algorithm, thereby enhancing the accuracy of load limit predictions. Although this method is effective, its reliance on precise strain data and the computational intensity of genetic algorithms present challenges for widespread real-time application. Although methods based on the FEM can offer significant insights into the severity of damage, the accuracy of these methods is contingent upon the quality of the input data. This quality is itself susceptible to noise. Errors in the measurement of deflection data can introduce uncertainties in the updated model. Furthermore, the methods themselves are computationally intensive, as they necessitate iterative optimization to refine stiffness parameters and minimize discrepancies between measured and simulated structural responses. Integrating them with static load deflection methods may help overcome some of these challenges, but further research is needed to fully realize their potential.

Despite the recognized potential of DAD for damage detection and localization (Levels 1 and 2 of SHM), there remains a critical gap in quantitatively assessing damage severity (Level 3). While traditional Finite Element Model Updating (FEMU) methods are capable of severity estimation, they frequently necessitate highly refined FEMs and become computationally prohibitive for large-scale applications (Ye et al. [207], [208]. Additionally, measurement noise has been shown to compromise the reliability of damage severity estimation (Tu et al. [209]). In addressing these challenges, this paper presents an extension of the DAD method to enable Level 3 of SHM. This is to be achieved by the introduction of a simple MU technique for damage level assessment. The MU technique presented in this paper is inversion-based and specifically designed for damage level assessment that simultaneously (i) keeps computational demands low by using simplified "sub-models" of the structure, and (ii) explicitly quantifies the influence of measurement noise on severity assessment. The method functions by means of an iterative adjustment of the bending stiffnesses of discrete segments of a surrogate numerical model. The surrogate model is a simplified representation of the structure, comprising finite segments corresponding to the distances between measurement points. The process commences with the construction of an initial surrogate model, wherein the bending stiffness values for each segment are established as the initial parameters. Subsequently, these values are adjusted iteratively using an optimization solver. The solver's objective is to minimize the discrepancy between the curvature lines of the surrogate model and the numerical reference model. The fitness function that guides this optimization process is defined as the absolute difference in curvature areas. Convergence is achieved when the area between the curvature lines of the surrogate model and the reference model matches the area between the curvature lines of the measurement and the numerical reference model. The output of this approach is the updated bending stiffness values for each segment of the surrogate model. A reduction in

stiffness corresponds to the presence and severity of structural damage. The proposed method, which integrates static load deflection measurements with low computational complexity, is demonstrated through numerical and laboratory experiments. Finally, two case studies on real bridge structures are presented to demonstrate the practical application of the enhanced DAD method.

3.7.2 Deformation Area Difference (DAD) method

The DAD method represents a sophisticated analytical approach that has been developed with the objective of detecting and localizing structural damage through the assessment of changes in bending stiffness [94]. This method assesses the deflection curve of a structure under static load, providing a systematic procedure for accurate damage identification while effectively mitigating the influence of noise and planned structural stiffness changes. The method will be illustrated using the example of a steel bridge structure with the cross-section presented in Figure 67, which will later be further described in a case study. The DAD method can be divided into three steps, which are shown in Figure 68.

- **Step 1: Measurement and Calculation of Deflection Curves**

The initial step in the DAD method is to measure the structure's deflection curve, which is denoted as $w_m(x)$ under a known static load. High-precision techniques, such as photogrammetry—often augmented with drone technology—are employed to capture continuous deflection lines. A comparative study by Erdenebat et al. [93] demonstrated that photogrammetry achieved a precision of 0.1186 mm in an in-situ measurement on a real bridge structure when using a drone-mounted medium-format camera, making it one of the most accurate non-contact measurement techniques available for deflection monitoring. This level of precision renders photogrammetry particularly well-suited for applications requiring detailed deflection analysis, such as the DAD method. For instance, in bridge assessments, a sequence of photographs is taken in both loaded and unloaded states using photogrammetric targets strategically positioned along the bridge. The comparison between these states yields the continuous deflection line, which is essential for subsequent analysis.

Concurrently, a reference deflection curve, designated as $w_r(x)$, is calculated using a linear Finite Element (FE) model of the structure. This model incorporates planned stiffness variations and the applied loading conditions, thereby ensuring that the reference curve accurately represents the structure's behavior in an undamaged state. It is noteworthy that precise calibration of the FE model is not required, as the DAD method is designed to detect relative changes in stiffness rather than absolute deflections.

- **Step 2: Derivation of Curvature Lines**

The deflection curve of a structure is fundamentally connected to its stiffness characteristics. By deriving the deflection curve, the inclination angle $\varphi(x)$ is obtained through the first derivative (Eq. (22)), and the curvature $\kappa(x)$ through the second derivative (Eq. (23) and Eq. (24)).

$$w'^{(x)} = \frac{\partial_w(x)}{\partial(x)} = \varphi(x) \tag{22}$$

$$\varphi'(x) = \frac{\partial_\varphi(x)}{\partial(x)} \cong k(x) \tag{23}$$

$$w''(x) = \varphi'(x) \cong k(x) \tag{24}$$

The curvature is of particular significance as it is directly proportional to the structure's bending moment and bending stiffness, according to the relationship between the bending moment $M(x)$ and the flexural rigidity $EI(x)$ (Eq. (25)).

$$k(x) = \frac{M(x)}{EI(x)} \tag{25}$$

The curvature lines $\kappa_m(x)$ and $\kappa_r(x)$ are derived from the measured and reference deflection curves, respectively, and provide valuable insight into local stiffness changes, which may indicate the presence of damage. In order to obtain curvature from discrete deflection points (x_i, w_i), it is first necessary to interpolate a single continuous, piecewise polynomial curve $C(t)$, where t is the internal curve parameter used to evaluate derivatives Although t is not identical to the physical coordinate x, it follows the same ordering and spacing, and the curve is constructed to respect the geometry of the measured deflection profile along the beam axis. The first and second derivatives $\frac{dC}{dt}$ and $\frac{d^2C}{dt^2}$ are then computed at each parameter value t. This parametric approach inherently smooths out local fluctuations in the raw data, thereby reducing the noise that can occur if one calculates derivatives directly from consecutive data points $\left(\frac{dw}{dx} \approx \frac{w_{i+1}-w_i}{x_{i+1}-x_i}\right)$. Consequently, the curvature estimates remain more stable and consistent for the damage detection process.

Eq. (4) reflects the baseline (elastic) relationship between curvature and bending stiffness. In a real structure with cracking or other inelastic effects, the measured curvature typically exceeds what the purely elastic reference model predicts, thus signaling a local stiffness drop. If a crack is very small, that local curvature increase may be slight—so small cracks may not be flagged as *damage* unless they produce a sufficiently large curvature deviation relative to noise levels. Conversely, more severe cracking or inelastic effects generate a visible jump in curvature relative to the elastic baseline, as shown in Figure 66, a difference that is discerned by the DAD method. In principle, when considering inelastic behavior, a distinct κ characterized by its varying EI in relation to cracking is employed.

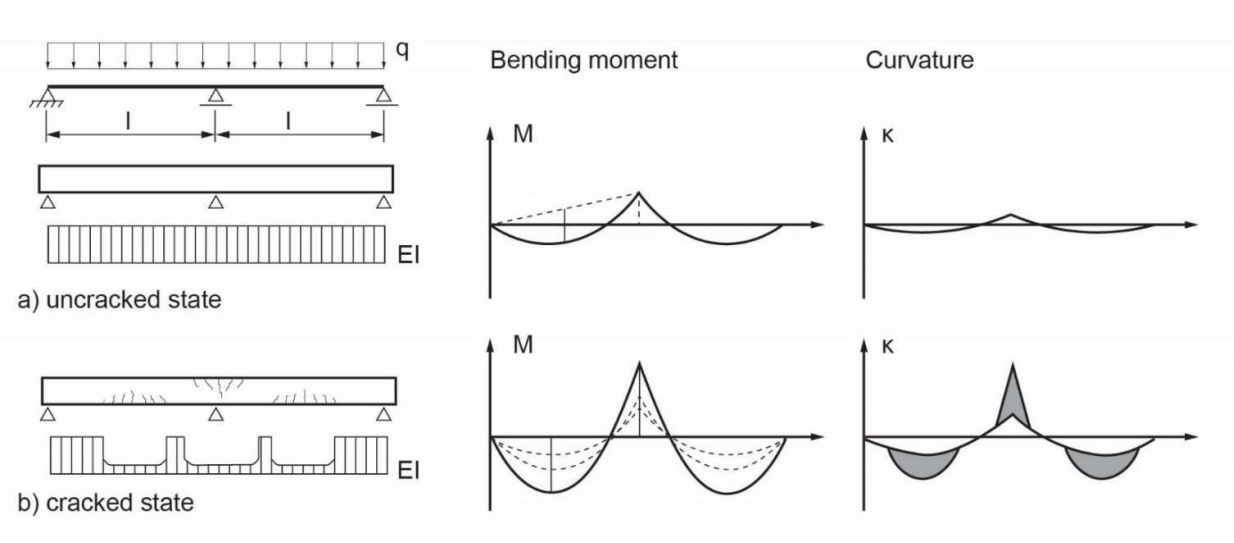

Figure 66. Relationship between crack state, bending stiffness EI, bending moment M and curvature κ (adopted from Zilch and Zehetmaier [210])

In summary, the DAD method remains applicable with an elastic reference model whose curvature is computed according to Eq. (4), even for inelastically behaving structures. However, once inelasticity manifests, the actual curvature, as measured, is larger. This discrepancy from the reference, irrespective of its origin, is identified by the DAD method. Consequently, minor cracks or inelastic effects result in only minor curvature changes. Conversely, significant damage leads to substantial stiffness reductions and substantial curvature deviations, which the method can detect.

- **Step 3: DAD Calculation**

The fundamental principle of the DAD method is the calculation of the area between the measured curvature line, designated as $\kappa_m(x)$, and the reference curvature line, represented by $\kappa_r(x)$. This area difference, denoted as $\Delta A_{\kappa,i}$, is calculated for discrete sections Δ_{xi} along the length of the structure Eq. (26). The size of these sections is selected to be sufficiently dense to accurately localize damage while avoiding the amplification of noise. The area differences are squared to enhance the detectability of damage-related effects and normalized across the entire structure Eq. (27). The following equations express this process:

$$\Delta A_{k,i} = \int_{i-1}^{1} \kappa_{m,i}\,(x)dx - \int_{i-1}^{i} \kappa_{r,i}\,(x)dx \tag{26}$$

$$DAD_{\kappa,i} = \frac{\Delta A_{\kappa,i}^2}{\sum_{i=1}^{n} \Delta A_{\kappa,i}^2} \tag{27}$$

Normalization is a vital step in this process, as it allows for the accentuation of areas where the squared area differences are disproportionately large, thereby signaling potential damage. The resulting DAD values serve as a clear indicator, with higher values indicating locations where there has been a significant reduction in stiffness within the structure. To evaluate the detectability of

damage, an outlier boundary is established using the box plot technique (Williamson et al. [174]) Initially, the interquartile range (*IQR*) is determined by subtracting the 75th percentile (*Q3*) values from the 25th percentile (*Q1*). Subsequently, the inner and outer boundaries (*IB* and *OB*) are computed based on Eq. (28) and Eq. (29), respectively. Damage is considered detected when the outlier boundary is surpassed.

$$IB = Q3 + 1.5 \times IQR \tag{28}$$

$$OB = Q3 + 3.0 \times IQR \tag{29}$$

The DAD method is robust in its ability to differentiate between discontinuities in the curvature line caused by actual damage and those due to noise or planned structural modifications, such as changes in cross-sectional dimensions or material properties. The versatility of the method is demonstrated by its applicability to a range of bridge types and construction materials. Furthermore, the efficacy of the DAD method with a single deflection measurement underscores its utility as a non-destructive tool for SHM. The DAD method thus allows for the assessment of the structure, identification of potential damage, and informed decision-making regarding maintenance and safety. The method's precision in detecting even minor changes in stiffness ensures its reliability for maintaining the structural health of bridges and similar infrastructure.

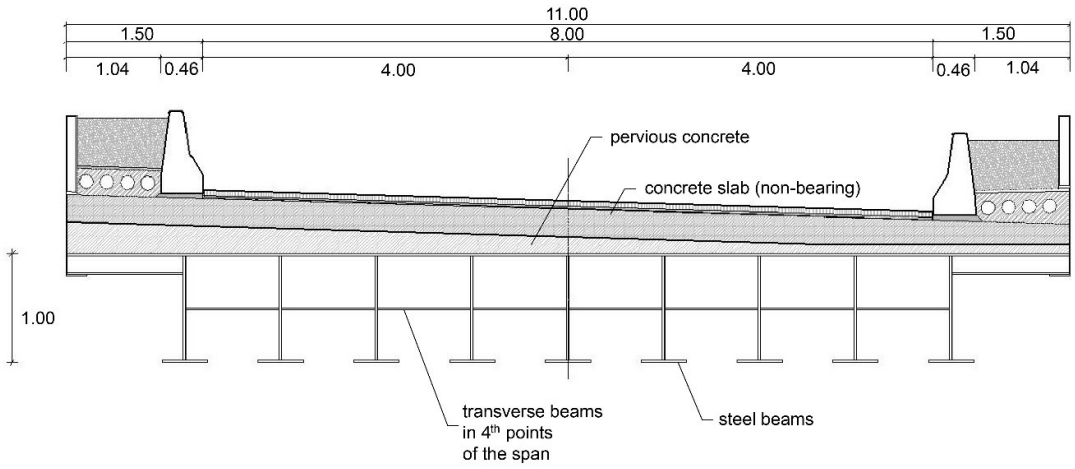

Figure 67. Cross-section of steel bridge in Soleuvre [m]

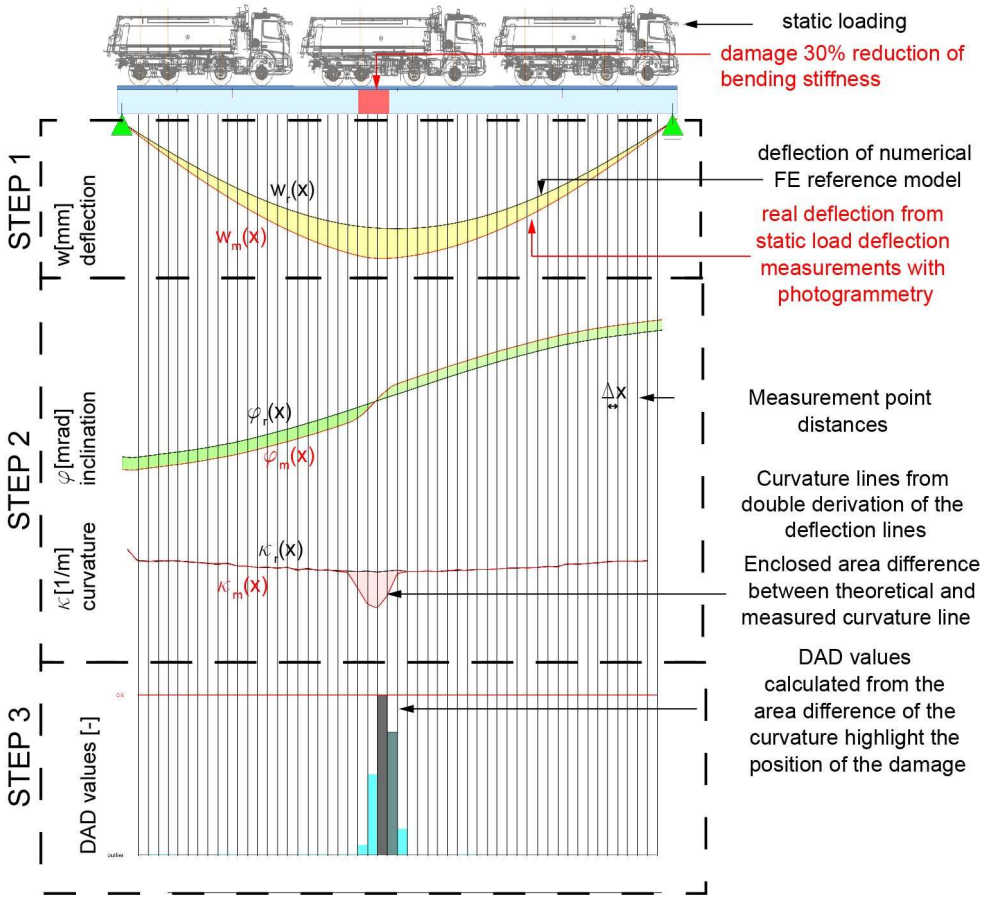

Figure 68. Principle of the DAD method with step 1 – measurement and calculation of the deflection curves, step 2 – derivation of curvature lines, and step 3 – calculation of the DAD values

3.7.3 Damage assessment using Inversion-Based MU

Although the DAD method is an effective means of detecting and localizing damage within a structure, it does not inherently provide information regarding the severity of the damage due to the normalization of DAD values. To enhance the SHM capabilities of the DAD method, the curvature area between the measured curvature line and the numerical reference model can be employed to assess damage severity. This section presents a straightforward algorithm designed to quantify damage severity using the existing data from the DAD method, as illustrated in Figure 70.

The algorithm is comprised of three distinct steps, visualized in Figure 71. The DAD method is initially applied using in-situ measurements and a numerical reference model (Step I). To establish a baseline (undamaged state) for the structure, a reference numerical model is employed that reflects the nominal, undamaged configuration. This reference captures the essential global geometry, boundary conditions, and expected material properties without incorporating damage or localized deterioration. It is built with the NURBS CAD software Rhinoceros [211] using the visual programming platform Grasshopper[212] and calculated with the FEA software SOFiSTiK [213].

Subsequently, a surrogate numerical model is generated (Step II). This model is a simplified beam representation, developed using the parametric engineering tool Karamba3D [214], which is

implemented inside the Grasshopper environment. In practice, a simplified beam representation of the structure is implemented, with each segment of the beam corresponding to a measurement interval and assigned the nominal cross-sectional properties of the undamaged state with the corresponding bending stiffness EI(x). This approach omits secondary details and intricate bracing elements, reducing computational complexity while retaining the core deflection behavior. By subsequently varying the segment stiffnesses to match measured deflections, localized damage can be pinpointed. This streamlined model is considerably less complex than a full 3D representation, yet it retains sufficient fidelity to detect deviations from the undamaged baseline. The beam is then divided into discrete sections, each corresponding to the measurement point distances. The cross-sectional properties of each section are varied using the optimization tool Galapagos. This tool adjusts the cross-sections iteratively—defined as "genomes"—until the curvature line of the surrogate model closely matches with the curvature line of the detailed undamaged reference model, minimizing the area difference between two undamaged systems. Once the substitute cross-sections representing local stiffness of the bridge are determined, the surrogate model is established, allowing the algorithm to proceed to the next step. The local stiffness includes not only the stiffness of the girders themselves but also the contribution of the transversal beams, which influence the overall bending stiffness. An initial cross-section is defined for each section, and the height of the cross-sections for each segment is introduced as individual variable parameters in Galapagos. The fitness function, defined as the area difference between the curvature lines, serves as the guiding principle for the optimization process. By employing an evolutionary solver, the algorithm engages in an iterative search to adjust these heights and minimize the fitness function. In the field of optimization, the term "objective function" is frequently employed, as evidenced by the extensive literature on the subject (Re et al. [215]). Within the paradigm of evolutionary algorithms, the term "fitness function" traditionally signifies the metric by which the efficacy of a candidate solution is evaluated. Evolutionary algorithms emulate biological principles such as mutation, selection, and inheritance. Virtual individuals, representing potential solutions, are generated, and evaluated based on their performance. High-performing individuals are "bred" to produce offspring with improved characteristics, with stochastic elements guiding the selection and variation processes. A schematic representation is shown in Figure 69 representing the progression of an evolutionary solver within a phase space. The term "phase space" represents all possible solutions to a given problem, while the boundaries indicate the evolving population of solutions across generations. In the initial generation (Generation 1), the population is dispersed throughout the phase space, exploring a vast range of potential solutions. As the algorithm progresses through subsequent generations (Generation 2 and Generation 3), the boundaries contract, indicating a shift in focus towards increasingly refined regions of the phase space. This contraction is a consequence of the evolutionary solver's progressive optimization of solutions based on the fitness function, whereby "high performing" candidates that better satisfy the objective are favored. In the final generation, a

concentrated cluster of solutions is observed around the most optimal regions, reflecting the algorithm's ability to converge towards a peak in the fitness landscape. This process is analogous to natural selection, whereby only the best-performing solutions (individuals) survive and "evolve" through iterative breeding, mutation, and selection.

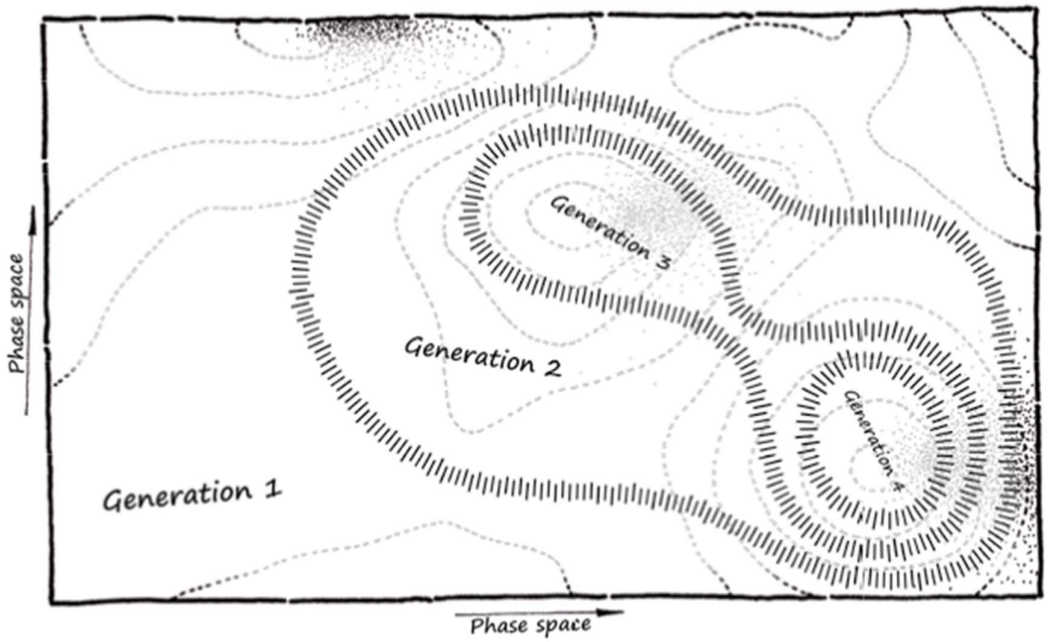

Figure 69. Schematic representation of an evolutionary solver run [216]

In the final step, the bending stiffness of the surrogate model is adjusted iteratively until the area difference between the updated surrogate model and the reference model is equal to the area difference between the reference model and the in-situ measurement (Step III). This approach, while similar to traditional model updating, can be considered an inversion technique since it uses measured data to directly infer changes in bending stiffness. This localized refinement allows for the precise identification of damage severity. While this study focuses on single damage scenarios, previous research has investigated multiple damage cases using the DAD method [95]. These studies indicate that the method primarily detects the most prominent damage, while the DAD value of the smaller damage may not exceed the outlier boundary. However, the DAD value still shows superior prominence compared to other values and a damage can be assumed by looking at the DAD values more closely zooming in the vertical axis. Further, excluding the already detected damage from the analysis, would lead to the detection of the second highest damage. So basically, a multiple application of the DAD method, excluding the detected damage will lead to the detection of multiple damages as long as they are detectable under the given precision, deflection value and measurement point distances. Since the proposed approach follows a sequential process - first damage detection and localization, followed by severity assessment - only the detected damage is considered for quantification. In principle, however, the model updating approach remains

applicable to multi-damage scenarios, as it is based on comparing the area between curvature lines. If multiple damages are detected, the severity assessment can still be performed.

By implementing this algorithm, practitioners can enhance the SHM framework, providing not only the location of structural damage but also a quantitative measure of its severity based on bending stiffness reduction. The proposed method quantifies damage based on changes in bending stiffness, which is primarily influenced by bending damage. However, other structural failure mechanisms, such as web buckling or shear failure, can also lead to a reduction in overall stiffness. In such cases, the DAD method would still detect a reduction in stiffness, but it does not inherently distinguish between different types of failure. This is a common characteristic of SHM-based damage detection methods (An et al. [217]; Svendson et al. [218]). The integration of model updating using optimization tools facilitates the efficient and precise calibration of the surrogate model, ensuring that the damage severity is accurately captured and can be effectively used in structural assessments.

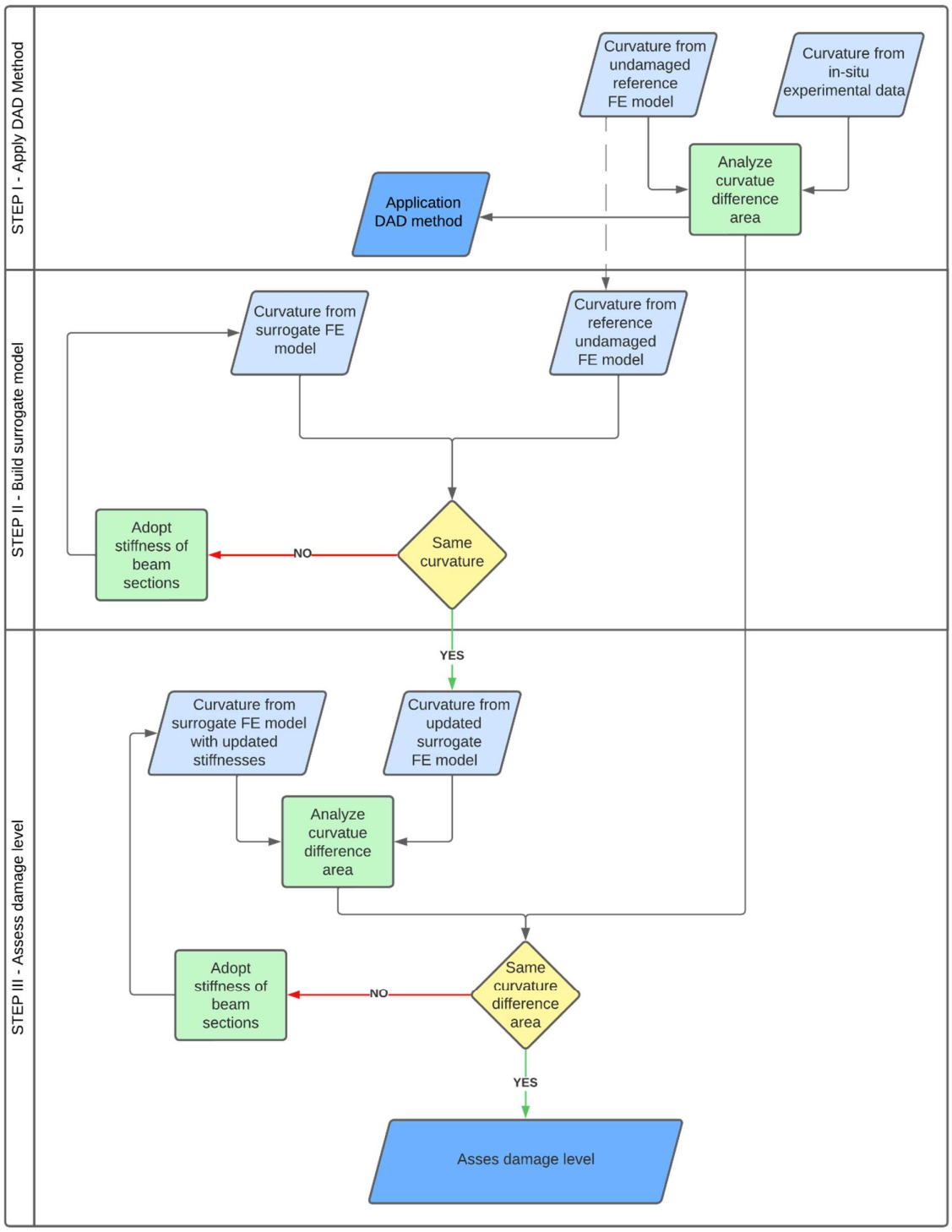

Figure 70. Flowchart of MU-based inversion technique for damage level assessment

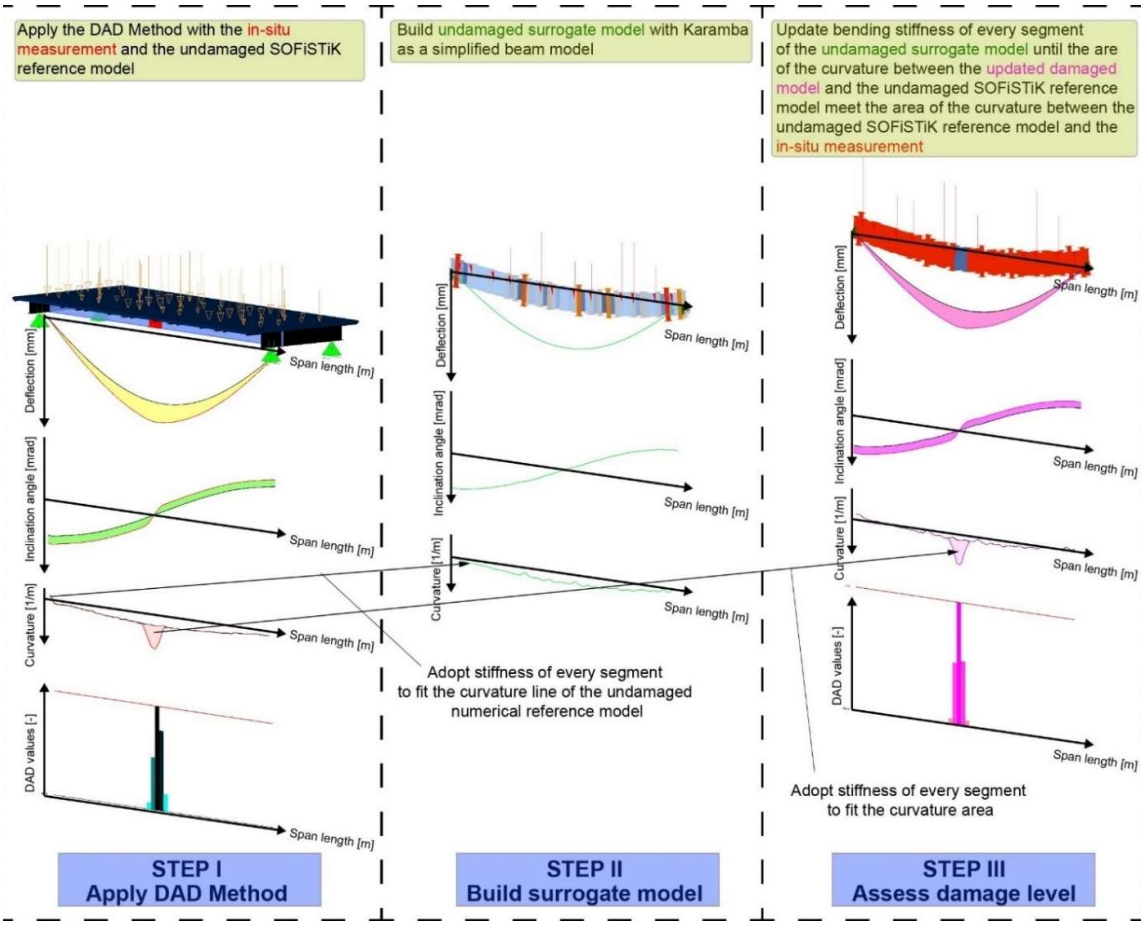

Figure 71. Visualization of the damage level assessment process

3.7.4 Mitigating missing points in photogrammetry with nonlinear regression

An in-situ measurement is achieved through the utilization of photogrammetry. The photogrammetric software is capable of automatically recognizing the photogrammetric targets and subsequently generating the 3D coordinates through the utilization of a bundle block adjustment. In the event of inadequate image quality or the presence of obstacles in the line of sight of the targets, some targets may not be automatically recognized. Nevertheless, the option exists to add these targets manually. One disadvantage of this method is that the quality of the measured point coordinates is relatively poor. Such an outcome may result in erroneous damage detection. This issue can be overcome by either not analyzing the part of the structure where the target is not recognized or by increasing the measurement point distance. However, these results are unsatisfactory in cases where the area of interest is the target area and the damage detection is narrow, or when the measurement point distance should not be enlarged. A methodology for addressing the issue of points that are not automatically recognized is illustrated in the following with a numerical example from a steel beam experiment.

The steel beam was subjected to experimental investigation in [202]. The beam has a total length of 6 meters and a cross-section of HEB 220, comprising steel grade S355. The beam is simply

supported and loaded with a point load at midspan, with a load of 80 kN, resulting in a deformation of 19.4 mm, which corresponds to a deflection value of L/290. The experimental setup is illustrated in Figure 72. The damage was simulated by reducing the bending stiffness by 30%. A simulated noise of 0.04 mm, which was reached in the laboratory experiment, is applied with a Gaussian distribution. For a measurement point in the quarter point, the noise level is increased to 2 mm, which simulates the imprecision of a manually added photogrammetric target in case the target would not have been recognized. The augmented noise level results in a larger area between the curvature lines of the undamaged and the damaged system, leading to an erroneous damage detection by the DAD method, as illustrated on the left-hand side of Figure 74. To avoid misdetection of damage, a fitted curve will be incorporated using nonlinear regression. The 3D coordinates of several deflection values are employed as input for nonlinear regression, which is used to predict the correct position of the missing measurement point. The measurement point is then projected onto the fitted curve, thereby avoiding the incorrect damage detection and localizing the simulated damage with the DAD method (right side of Figure 74). However, it is important to note that if the damage is precisely at the position of the target which is not automatically recognized, the damage will not be detected. A review of the damage level assessment reveals that the erroneous detection of damage has no impact on the damage level assessment. However, the conspicuous nature of the incorrectly identified damage means that the actual damage is not detected using the DAD method. Consequently, the damage level assessment is more likely to be classified as noise than as bending stiffness-reducing damage.

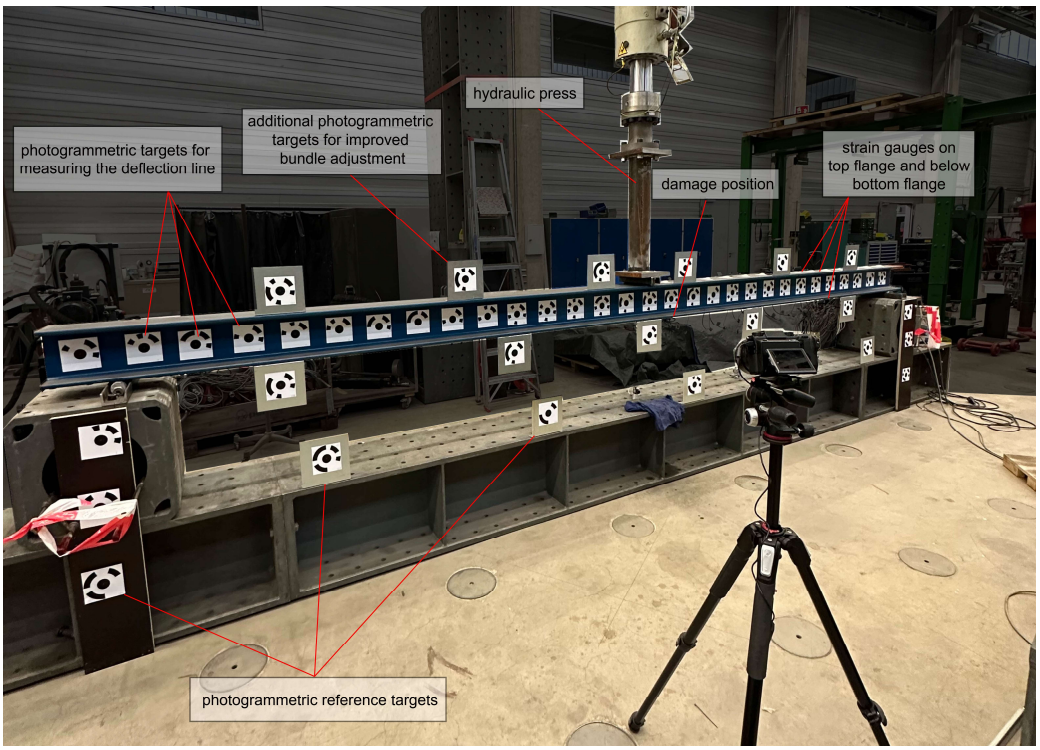

Figure 72. Experimental set up of steel beam HEB 220 S335 [202]

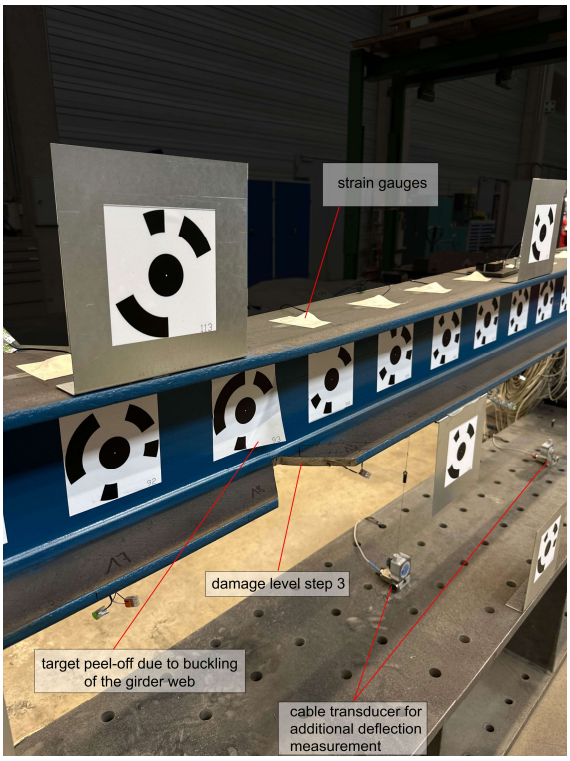

Figure 73. Applied Damage on the lower flange of the HEB 220 [202]

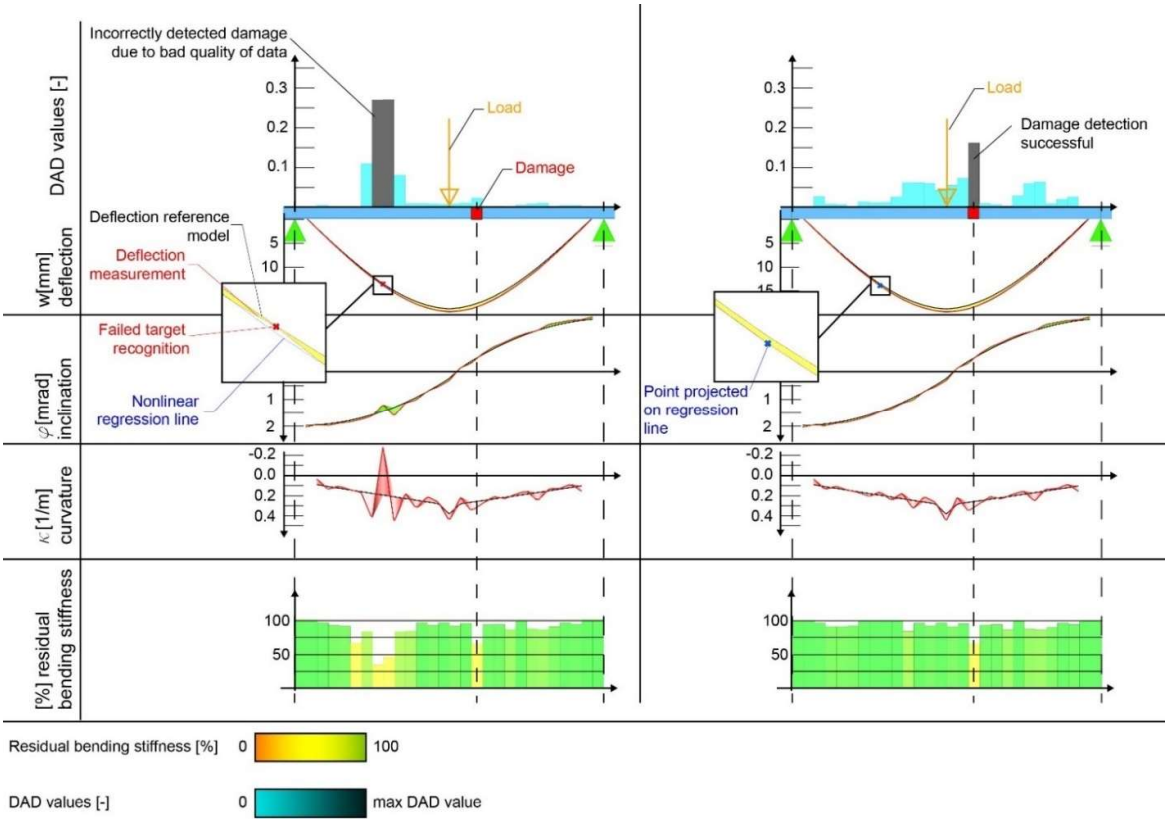

Figure 74. Projecting not automatically recognized measurement points on fitted curve using nonlinear regression

3.7.5 Noise influence on damage level error

In theory, a reduction in bending stiffness of 1% can be localized using the DAD method [93]. In practice, the impact of measurement noise on the detection of damage is considerable, as demonstrated by [166]. So, for the specific case of the steel beam HEB 220 and a deflection value of L/290, a minimum reduction in bending stiffness of 50% is necessary to detect the damage with a precision of 0.1 mm using the DAD method and a single measurement. This chapter will investigate the influence of measurement noise on damage level assessment. Although noise-induced errors in stiffness estimation are well documented (Sotoudehnia et al. [219]), our parametric studies explicitly quantify the extent to which damage severity can be misestimated for different noise levels. Furthermore, this study demonstrates practical smoothing techniques to mitigate these errors.

The numerical reference model of the steel girder, which was previously outlined in detail in chapter 3.7.4, will be employed for the assessment. The MU methodology previously described enables a precise estimation of the damage level in a theoretical model. Ten distinct noise levels, ranging from 0.01 mm to 0.1 mm, will be artificially applied to the numerical deflection values. The reached precision in the in-situ experiments ranges from 0.06 to 0.12 mm. Subsequently, the damage level assessment algorithm, described in chapter 3.7.3 will be employed. Figure 75 and Figure 77 present the outcome of the numerical investigation. Figure 75 illustrates the residual bending stiffness of the various series at different noise levels in the damaged position at x = 3.60m with a residual bending stiffness of 70 %. The box plot method is employed, with the mean value indicated by a horizontal line and the average value represented by a cross. Figure 77 illustrates the damage level error, which quantifies the extent to which the residual bending stiffness at the damaged position of the steel beam has been either underestimated or overestimated. The damage level error demonstrates a linear increase with elevated noise levels. While the damage error is 6% for a noise level of 0.04 mm, it increases to 21% for a noise level of 0.1 mm, which is not useful for damage level assessment. The application of a smoothing technique to the deformation line has already demonstrated its efficacy in the context of the DAD method, as evidenced in [166]. Subsequently, a smoothing technique will be employed, whereby the adjacent values of the deformation line will be averaged. The resulting graph is presented in Figure 76 and Figure 78. The damage error is observed to decrease significantly, reaching a value of only 1% for a noise level of 0.1 mm. It is noteworthy that this is the mean value derived from 10 artificial measurements. The number of measurements required to achieve a favorable outcome is inversely proportional to the damage error. The damage error increases significantly when only one measurement is used, as no mean value can be calculated. For example, for a noise level of 0.1 mm, the highest damage level error is 23% (see the lowest circle in Figure 78). Consequently, in an unfavorable situation, the damage level error with only one measurement is still high, despite the use of a smoothed deflection line. It is important to acknowledge that the findings of this study are applicable only to the specific

case under investigation and therefore cannot be extrapolated to other structures or conditions. The assessment of damage level is contingent on numerous factors, including the type of structure, the precision of measurements, the magnitude of deflection, and the density of measurement points. However, the observed trend, which suggests that smoothing and repeated measurements enhance the consistency of damage level estimation significantly, remains valid across different cases. This finding is consistent with previous research, which demonstrates that noise reduction techniques and measurement optimization techniques enhance the reliability of damage assessment. Additional influencing parameters for the damage level error are the deflection value and the ratio between the length of the simulated damage and the length of the real damage (Eq. (30)). Only if the length of the simulated damage has the same length as the real damage, the damage level assessment is exact. If the length of the damage is simulated longer or shorter, the damage is over-, respectively underestimated. Figure 79 illustrates the determined bending stiffness for different simulated to real damage ratios. The damage level is only accurate when the length is identical. As the ratio increases, the damage level error rises until it reaches a plateau at a ratio of 3. An increase in the length of the simulated damage with the same damage level results in the formation of higher curvature areas within the damaged segment. However, it should be noted that only the stiffness of the adjacent segment influences the curvature of the damaged segment. Segments situated further away from the damaged segment do not exert any influence on the curvature of the damaged segment. Consequently, the smaller the length of the simulated damage with the same damage level, the smaller the curvature area of the damage segment. In order to achieve the same curvature area, the damage must be higher, which consequently results in an overestimation of the damage.

$$simulated\ to\ real\ damage\ length\ ratio = \frac{length\ of\ simulated\ damage}{length\ of\ real\ damage} \qquad (30)$$

In the laboratory experiment, which was presented in [202], a controlled damage was applied over a length of 10 cm, as illustrated in Figure 73. The measured noise was between 0.04 and 0.08 mm. The average remaining bending stiffness was determined to be 76%. For the load step of 60 kN, which yielded a deflection value of L/340 and thus remained within the Service Limit State (SLS), the damage level was investigated with the presented algorithm. A remaining bending stiffness of 75% was determined, resulting in a damage level error of 1%, which correlates with the numerical results.

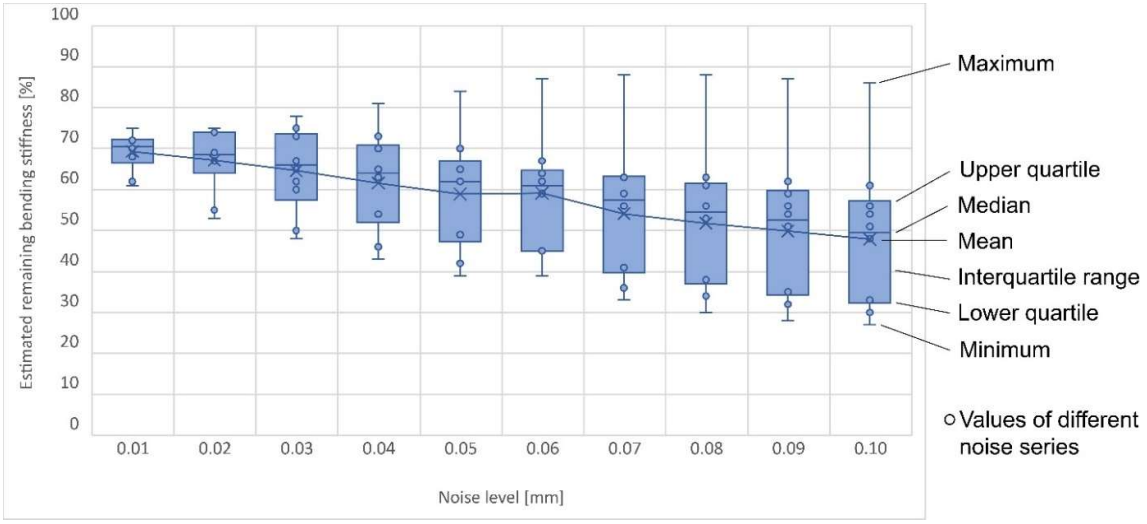

Figure 75. Influence of noise level on damage estimation

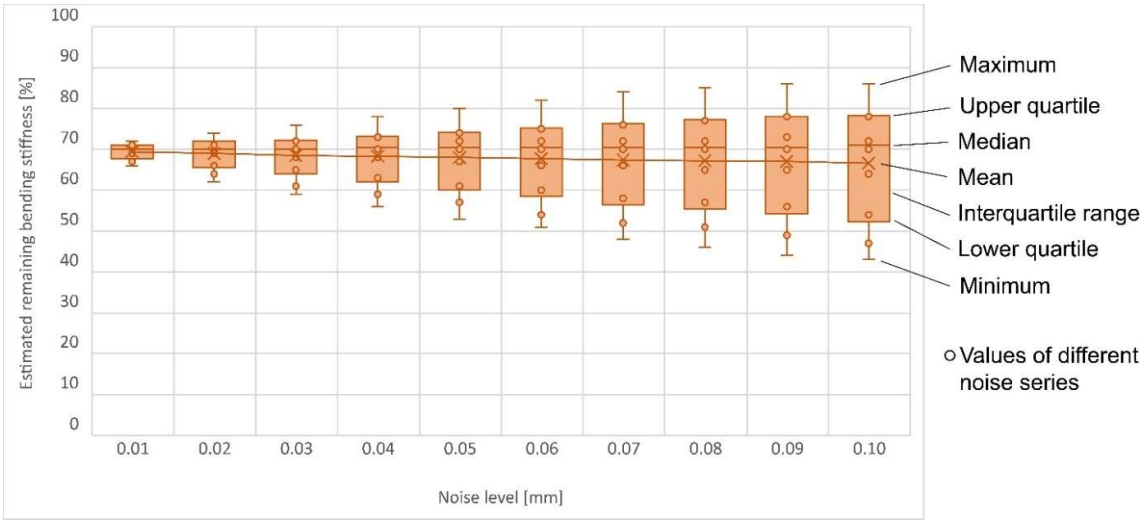

Figure 76. Influence of noise level on damage estimation for a smoothed deflection line

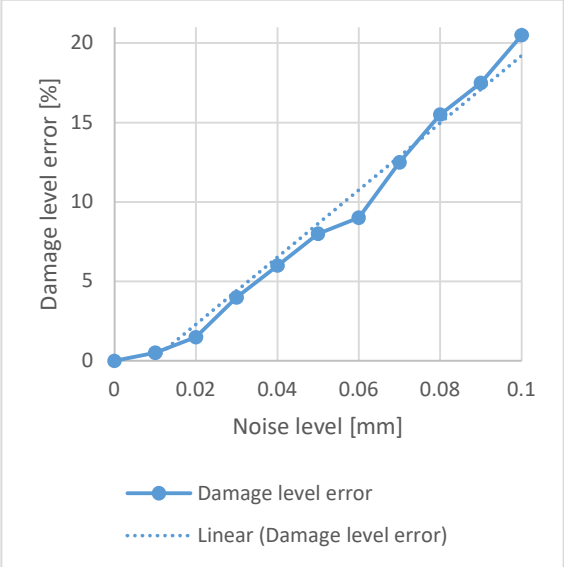

Figure 77. Error in damage level assessment

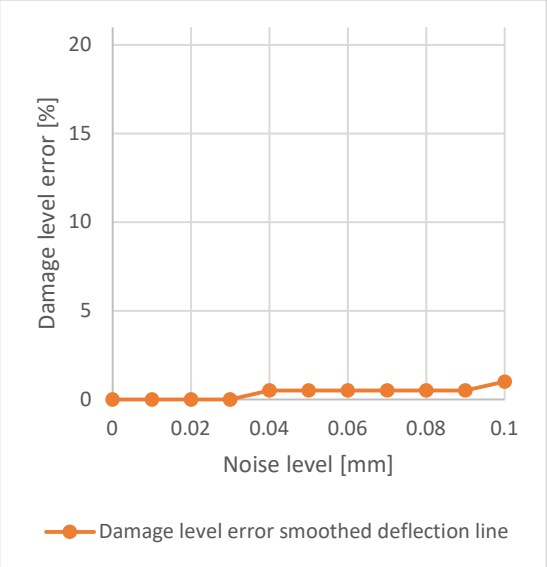

Figure 78. Error in damage level assessment for a smoothed deflection line

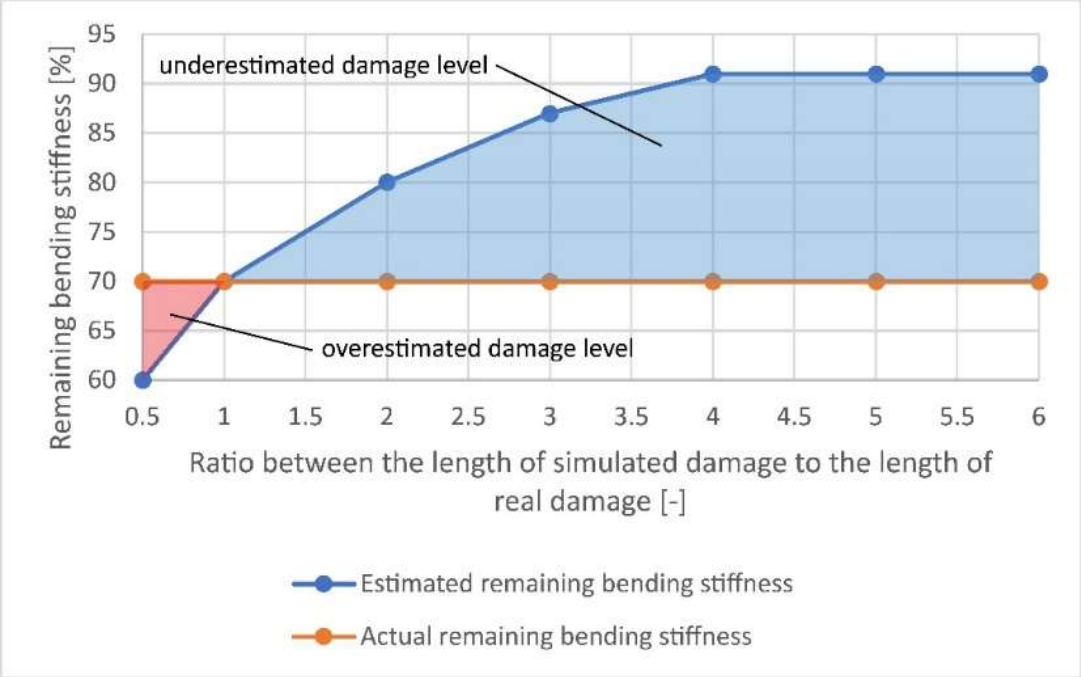

Figure 79. Influence of the ratio between simulated damage length and actual damage length on the damage level error

3.7.6 Importance of MU for damage level assessment

The DAD method uses the analysis of small segments of the area between curvature lines, thereby ensuring that the method is largely unaffected by global parameters. Consequently, the reference model does not require precise calibration for effective damage detection. However, if the global stiffness of the structure is underestimated, there is a potential risk that the curvature line may shift

by a distance that coincides with the gap between the damaged and undamaged curvature lines. In such cases, this alignment can lead to poor damage localization.

Figure 80 depicts the deflections, inclination angles, and curvatures of a damaged steel girder compared to an undamaged girder, together with the corresponding DAD values derived from the curvature analysis. As a consequence of the underestimated bending stiffness in the reference model, the curvature line is shifted, resulting in a minimal area difference at the actual damage location. This shift can lead to the damage remaining undetected. Additionally, the damage level assessment indicates that the remaining bending stiffness is analyzed incorrectly, exhibiting full bending stiffness at the location of the damage. However, a closer analysis of the curvature line and the DAD values makes it possible to draw conclusions about the stiffness change at the damaged point.

To enhance the detection of such subtle shifts, the Relative Differences (*RelDif*) of the DAD values are calculated and presented in the middle column of Figure 80. *RelDif* expresses the absolute difference as a percentage of a DAD value to the DAD value of the previous segment according to Eq. (31).

$$RelDif = \frac{DAD_{\kappa,i+1} - DAD_{\kappa,i}}{DAD_{\kappa,i}} \tag{31}$$

The DAD RelDif enables more accurate damage localization. However, when accounting for measurement noise, damage localization using the DAD RelDif can still be challenging. Furthermore, the damage level assessment remains erroneous and cannot be enhanced with the DAD RelDif.

An alternative approach to addressing this issue is through MU based on the measured deflection line. The right column of Figure 80 demonstrates damage detection using the DAD method after the reference model has been updated using MU methodology. By employing the MU methodology, the curvature lines of the measured deflection and the updated reference deflection now exhibit complete overlap, with only the damaged section remaining. This leads to a discernible damage localization, as evidenced by the clear discrepancy in the area between the curvature lines and therefore a successful damage level assessment. Beyond adjusting the bending stiffness, other parameters such as support conditions can be used for the MU methodology in the reference model. The influence of constrained support conditions on the deflection line is significant, and incorporating the measured deflection data allows for the refinement of the numerical model, thereby improving the accuracy of damage detection.

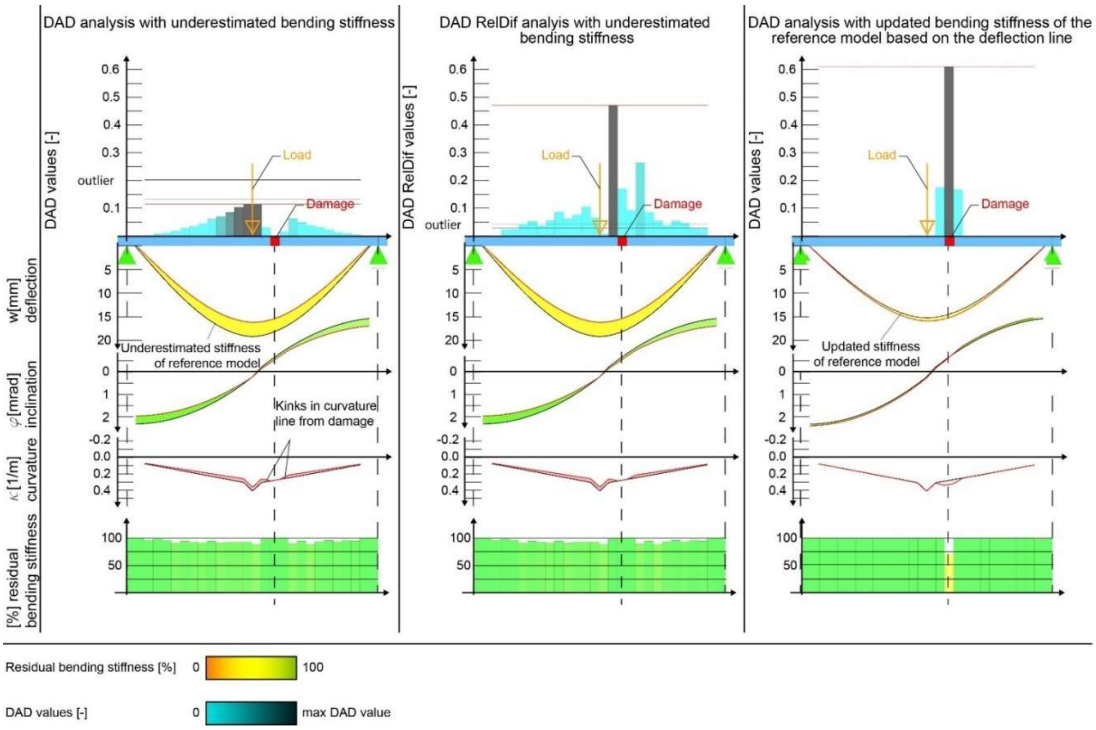

Figure 80. DAD values with deflection curves, inclination angle curves and curvature curves for a reference model with underestimated stiffness (left), DAD RelDif values (middle), and DAD values for after MU

3.7.7 Application on real bridge experiments

Two distinct case studies were conducted on real bridge structures in Soleuvre and Ettelbréck, Luxembourg to evaluate the effectiveness of the DAD method with MU methodology and the damage level assessment. The experimental workflow for these studies is outlined as follows:

- Photogrammetric target installation: While the proposed method requires displacement measurements, these can be obtained using a variety of techniques, including photogrammetry. In this study, photogrammetry was used because of its ability to provide dense, non-contact displacement data, but the method itself is independent of the specific measurement approach. The bridges were equipped with photogrammetric targets, placed at 50 cm intervals along the structure. Additionally, reference targets were installed on the abutments to serve as the reference coordinate system for the photogrammetry software Elcovision 10 [220]. The experimental setup for the Soleuvre bridge experiment is depicted in Figure 81. The photogrammetric targets were glued on steel plates, which were then attached to the lower flanges using flange clamps and bolted directly to the abutments (Figure 82 for Soleuvre bridge, Figure 87 for Ettelbréck bridge).
- Image acquisition using Unmanned Ariel Vehicle (UAV): A series of images were captured using a large UAV equipped with a full-frame camera. The UAV, a DJI Matrice 600 Pro, was outfitted with a Ronan gimbal and a Fujifilm GFX 50S camera, featuring a sensor resolution of 8256 x 6192 pixels with a sensor size of 43.8 x 32.9 mm, leading to a pixel

size of 5.30 µm. The images were taken from various positions and distances along the bridge, as illustrated in Figure 83 and Figure 87. The influence of camara quality and camara calibration on the precision of the DAD method can be found in [221]

- Measurement of the bridge under different loading conditions: The bridge was measured twice: first without any load, and subsequently under a known static load applied using heavy truck, shown in Figure 84 and Figure 88.
- Development of the reference model: A FE reference model of the bridge was developed with SOFiSTiK using existing drawings, with supplementary in-situ measurements taken where necessary.
- Calibration of the reference model: The FE reference model was subjected to the same loads as those experienced by the actual bridge. The loading positions were calibrated using the point cloud data, as illustrated for Ettelbréck in Figure 90.
- Updating of support conditions and bending stiffness: The rotational stiffnesses of the support conditions and the bending stiffness of each segment of the reference model were updated based on the course of the measured deflection line as described in chapter 3.7.6.
- Application of the DAD method with damage level assessment based on MU methodology: Ultimately, the DAD method was employed to identify and localize potential damage within the bridge structures.

3.7.7.1 Case Study on Soleuvre bridge structure

The road bridge in Soleuvre is a steel bridge with two lanes, with unknown construction year. The structure is a single span bridge structure, measuring approximately 30 meters in length and 11 meters in width. The cross-section consists of nine identical I-sections with a common upper flange, with transverse beams connecting the girders at the fourth points of the span. The height of the cross-section is 1.0 meter. On top of the bridge deck, there is a layer of pervious concrete and an additional non-bearing concrete slab, added in 1990, though the purpose of this design—potentially related to the dynamic properties of the bridge—remains unclear. The specific grade of steel is not documented while the concrete has a concrete grade of B35.

Prior research has demonstrated that for local damage, each girder exhibits independent curvature behavior, necessitating the measurement of each girder for comprehensive damage detection across the entire cross-section. However, due to temporal and financial limitations, only the first and third girders from the eastern side were assessed. The reference model for this bridge was developed using the numerical FEA software SOFiSTiK (see Figure 85), where the flanges and webs of all girders were modeled as shell elements. Furthermore, web openings were incorporated into the model to explicitly capture their influence on local stiffness and load distribution. The concrete layer was only added as additional load with no bearing capacity due to its classification as a non-structural, non-bonded element. This high-fidelity model ensures that the global and local load-

bearing behavior of the bridge is accurately represented. Given the absence of documented data regarding the precise steel grade of the bridge, an assumption was made based on the typical values (S355) observed for analogous structures. This assumption impacts the absolute stiffness of the model; however, it does not influence the damage detection process, as the DAD method is based on relative curvature differences rather than absolute stiffness values. The introduction of a global error by the assumed material properties does not affect the ability to localize damage, as this error is uniform across the structure. The MU process, which adjusts the bending stiffness and support conditions based on the measured deflection line, helps to eliminate damage levels that are falsely detected due to over- or underestimation of material properties. This phenomenon is demonstrated in chapter 3.7.6.

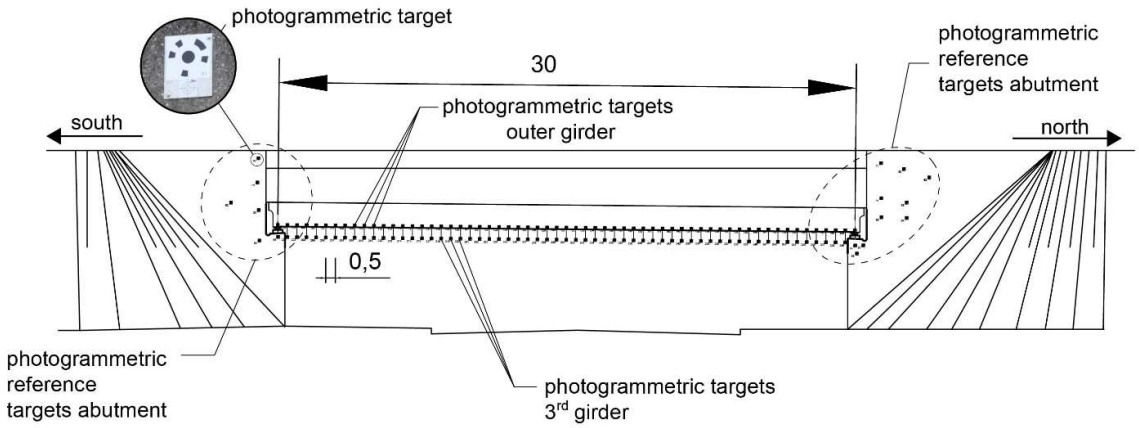

Figure 81. Experimental set-up Soleuvre bridge

Figure 82.Photogrammetric targets set-up Soleuvre Bridge

Figure 83. Image acquisition using a UAV Soleuvre bridge; unloaded state

Figure 84. Heavy trucks serve as loading for the Soleuvre bridge experiment

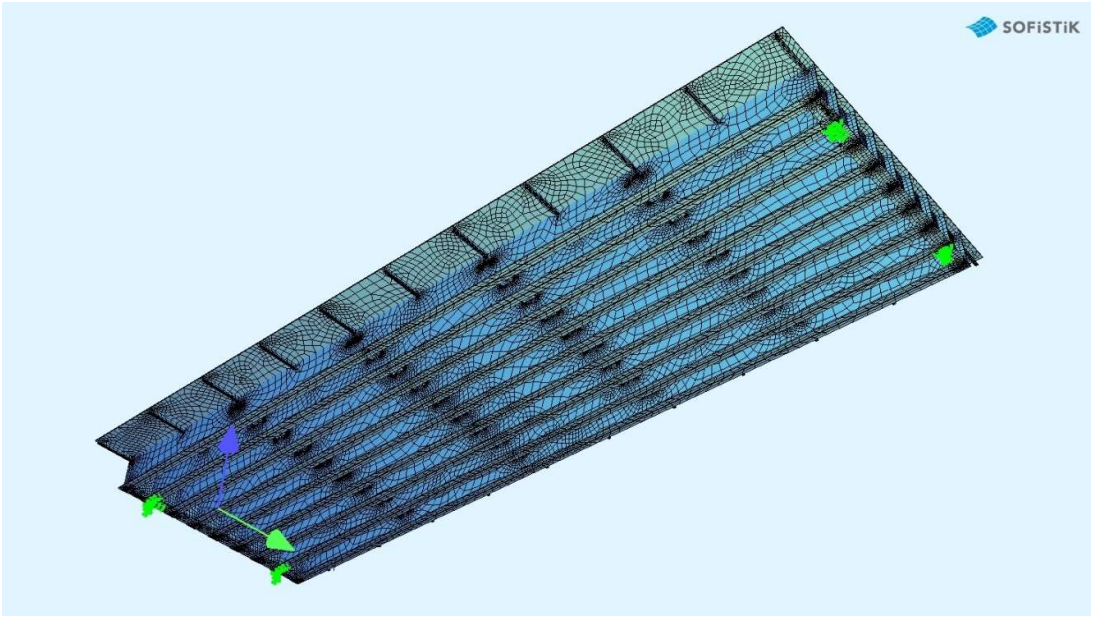

Figure 85. FE model of the Soleuvre bridge, view from below

3.7.7.2 Case study on Ettelbréck bridge structure

The road bridge in Ettelbréck represents a concrete-steel composite bridge, constructed in 1992. The bridge features two lanes for vehicular traffic and two lanes for pedestrians. The bridge is a single span bridge structure, measuring approximately 22 m in length and 12 m in width. The cross-section consists of four I-section girders integrated into a concrete slab using of stud shear connectors. Transverse beams are used to connect the girders at the third points of the span. The steel girders are 80 cm in height, while the concrete slab is 28 cm thick. The materials used include S355 steel and B35 concrete.

As with the Soleuvre bridge, measurements were restricted to one outer girder and one inner girder due to limitations, such as cost and time constraints for the application of the photogrammetric targets. The reference model for the Ettelbréck bridge, visualized in Figure 89, was also developed

using shell elements to represent the flanges, webs, and transversal girders, as well as the concrete slab, ensuring that both longitudinal and transverse stiffness contributions were included. The steel girders were modelled with couplings to the concrete slab using constraints between the two beams as infinite stiff elements that are numerically stable, thereby ensuring full composite action. This approach accurately captures the load distribution effects and overall structural response of the bridge. To accurately represent the global structural behavior and load distribution, the FE model incorporates all four girders and the concrete slab, despite the fact that deflection measurements were obtained from merely one outer and one inner girder.

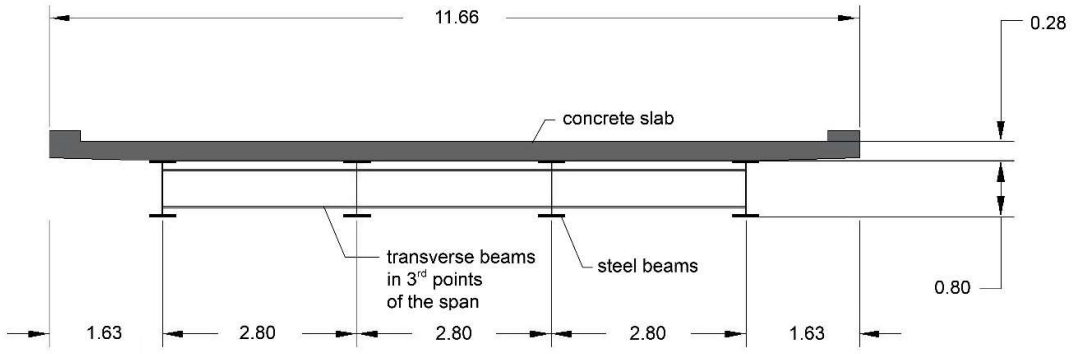

Figure 86. Cross-section of the concrete-steel-composite bridge structure in Ettelbréck [m]

Figure 87. Image Acquisition of the unloaded state of the Ettelbréck bridge

Figure 88. Heavy trucks serve as loading for the Ettelbréck bridge experiment

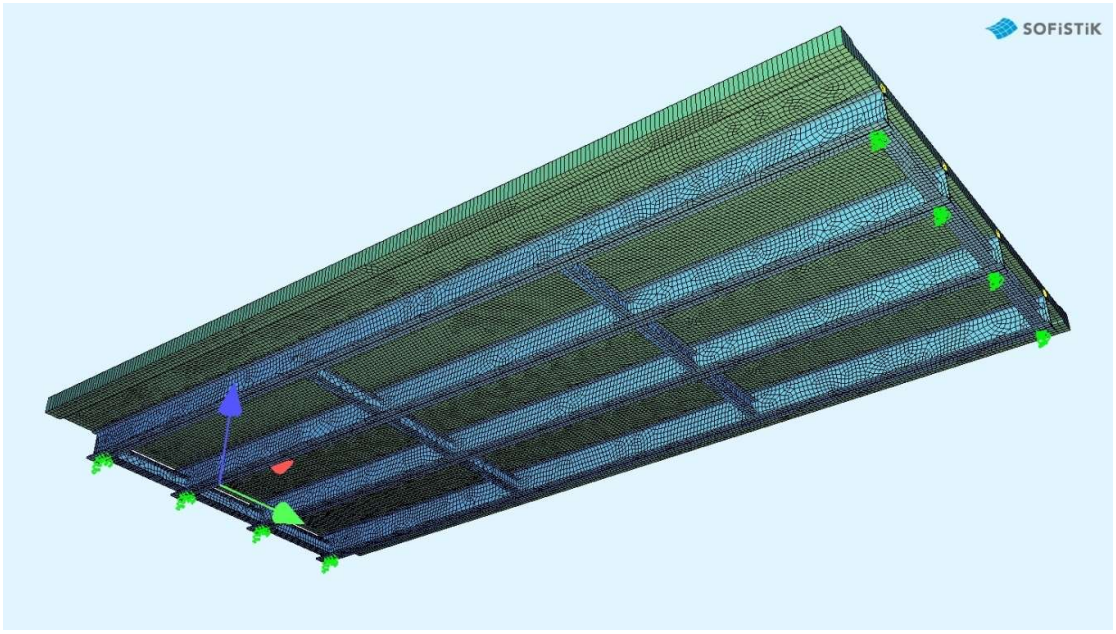

Figure 89. FE model of the Ettelbréck bridge, view from below

Figure 90. Point clout overlayed with the structural model to validate geometry and calibrate loading positions

3.7.8 Results of the real bridge experiments

3.7.8.1 Soleuvre bridge

In the case of the Soleuvre bridge, only two of the nine girders were subjected to measurement. This section presents the results for the third girder from the east side, as the first girder did not yield any significant findings since it did not present any damage. Figure 91 depicts the implementation of the DAD methodology with MU and damage level assessment on the Soleuvre bridge. The deflections derived from both the numerical model and in-situ measurements are presented below the FE model, with the inclination angle lines, curvature lines, with the respective enclosed areas, corresponding DAD values with maximum DAD value and outlier boundary and, and residual bending stiffness of each segment.

As illustrated in the first column of Figure 91, the DAD values were derived from the unsmoothed curvature lines. It is noteworthy that a DAD value, exceeding the boundary line is observed at the second fourth point of the girder. The peak near the support is not considered as actual damage but is attributed to the higher influence of noise in these regions. Like other damage detection methods (Zhou et al. [222] Cai et al. [223]), the DAD method is more sensitive to measurement noise close to the supports, making damage identification in these areas more challenging. This effect has been extensively analyzed in previous research, particularly in [166]. In the present study, only the most prominent peak was considered for evaluation, ensuring that noise-induced anomalies near the supports did not affect the results. To enhance accuracy, the deformation line from the measurement was smoothed using nonlinear regression. A fitted curve was applied through nonlinear regression, followed by shifting each measurement point within its precision range towards this fitted curve. The detailed smoothing process is described in [93]. The key difference between this process and

the aforementioned one is the use of nonlinear regression instead of polynomial regression due to the influence of stiffness from the transverse girders. In the case of a simple beam or plate, the deflection line can be approximated by a linear polynomial regression. However, the influence of transverse girders results in local stiffness jumps that prevent this approximation. In such instances, a non-linear regression must therefore be used, which is a statistical technique that helps to describe non-linear relationships in data. Non-linear regression models are parametric, where the model is described as a non-linear equation.

The second column of Figure 91 illustrates how the smoothing of measurement points with high noise levels can prevent false damage detection. The curve was further refined by averaging adjacent vertices, which reinforced the damage detection. The lower row presents the results after MU. In this case, the structure's stiffness and support conditions were adjusted to account for the influence of the concrete slab's bending stiffness, but no further improvement in the results for the damage detection was observed. Notwithstanding its classification as a non-load-bearing slab, it exerts a notable influence on the bending stiffness of the structure and possesses load-bearing capacity. This was demonstrated by the significantly reduced deflection observed in the in-situ test in comparison to that of the numerical model. However, due to the global influence of the slab's bending stiffness, the course of the curvature line does not have relative changes in the different discrete evaluation segments, and therefore, the bearing capacity of the concrete slab can be disregarded without compromising the accuracy of damage detection using the DAD method.

The overlaying of the DAD values with the point cloud data facilitated the precise localization of the detected damage, as illustrated in Figure 92 and Figure 93. For purposes of clarity, the bars with a color gradient from light blue to black, representing increasing DAD values, with light blue indicating the lowest and black the highest DAD value, have been inverted. A detailed examination of the damage site revealed the presence of corrosion in the lower portion of the web and the lower flange of the transverse girder, accompanied by scratches from vehicular impacts that exceeded the clearance profile of the bridge (Figure 94). The DAD values suggest that these damages have resulted in a reduction in the bending stiffness of the structure. However, due to the low deflection values observed, the results should be interpreted with caution, as noise can also contribute to false damage detection under such conditions.

As previously discussed in chapter 3.7.5, the damage level can be quantified through the process of inversion-based MU. The determined residual bending stiffnesses of each segment is shown below the indicated DAD values in Figure 91 as percentage of the full bending stiffness. It is important to note, however, that the influence of noise is correlated with both the damage level and the deflection value. In this experiment, the loading applied to the bridge was limited, resulting in a deflection value of only L/3,750. The low deflection value resulted in a notable increase in the influence of noise, with noise levels ranging between 0.04 mm and 0.08 mm, representing the standard deviation for each measurement point as determined from the bundle block adjustment in the

photogrammetric software. Figure 95 depicts the damage level error for a numerical 30% bending stiffness reduction damage scenario across 10 artificial measurements, with a mean damage level error of 12% for a noise level of 0.04 mm and 26% for a noise level of 0.08 mm. Due to time constraints, only a single measurement was conducted for the in-situ experiment, which may have introduced an increased damage level error. The unsmoothed curvature line shows a high degree of damage level error due to the presence of elevated noise peaks. The application of nonlinear regression for the smoothing of the deflection line yields provides a noticeable improvement in local regions where the noise level is exceptionally high. This phenomenon can be observed in the midspan region of the bridge structure. The further smoothing of the data through the averaging of adjacent values effectively eliminates the peaks, thereby enhancing the accuracy of the damage level assessment. Consequently, the residual bending stiffness reaches its minimum value at the location of the detected damage. Using the method described in chapter 3.7.3, a remaining bending stiffness of 50% was determined, which appears to be below the expected range given the visible damage. While the MU did not enhance damage detection through the adoption of structural stiffness and support conditions, it did facilitate more accurate damage level assessment, as evidenced in chapter 3.7.6. The residual bending stiffness increased to 65%, which remains below the anticipated residual bending stiffness. The combination of noise levels, low deflection values, and expected low damage level led to an inaccurately determined damage level, indicating that this method may not be suitable for cases with similar constraints.

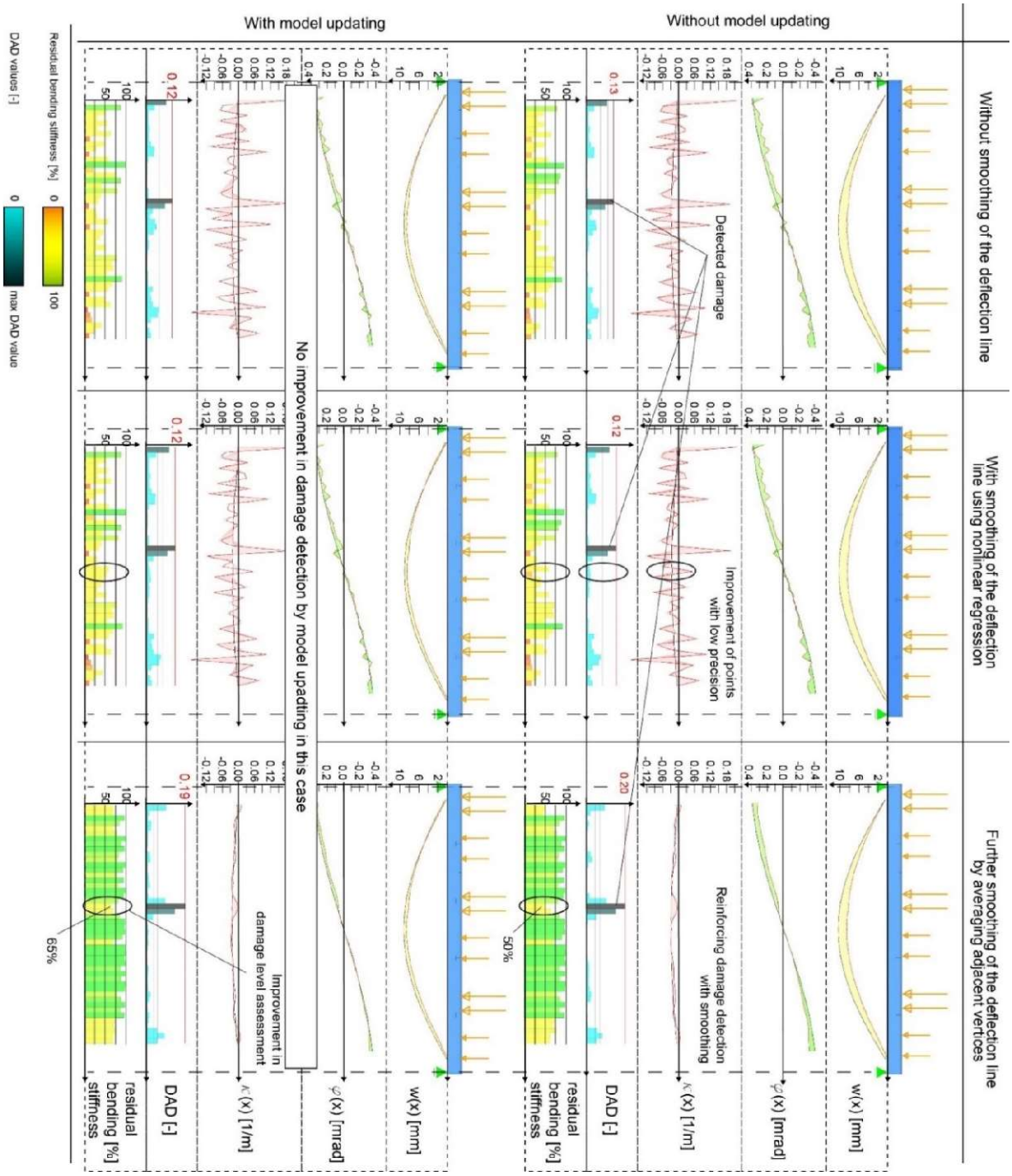

Figure 91. Results of the DAD method for Soleuvre bridge without and without smoothing of the deflection curve (first column), smoothing of the deflection curve using nonlinear regression (second column), and with further smoothing by averaging adjacent vertices (third column), without (first row) and with MU of the materials stiffness and the constraints (second row)

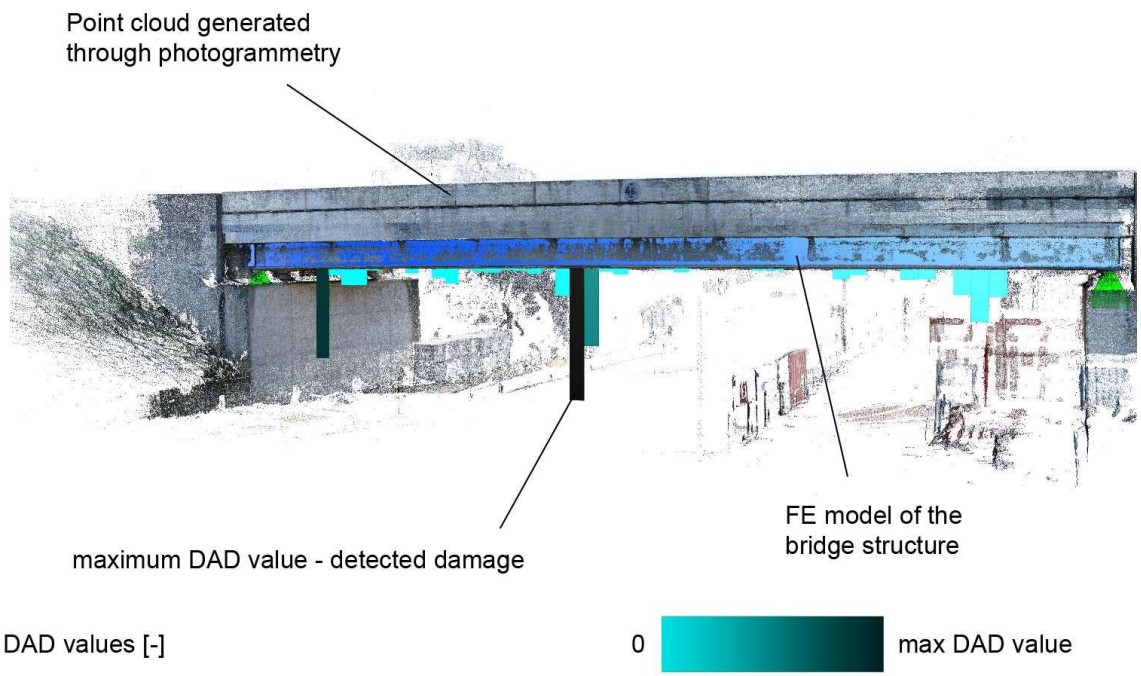

Figure 92. Overlay of calculated DAD values with the generated point cloud. The DAD values are mirrored on the horizontal axes for better representation

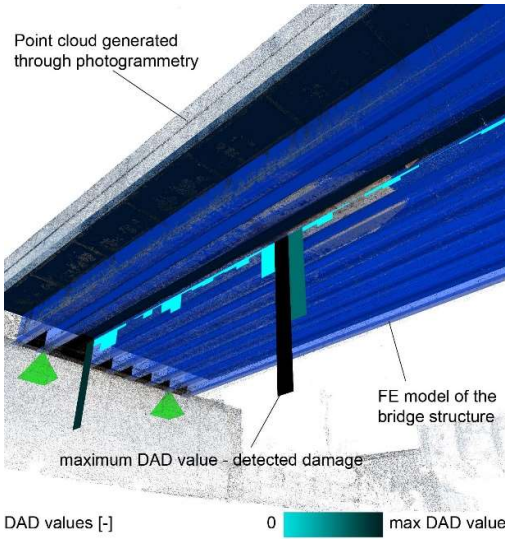

Figure 93. Overlay of the DAD values of the third girder and the generated point cloud to visualize the position of detected damage. The highest DAD value pinpointing to detected damage position

Figure 94. The position of the detected damage shows increased corrosion, especially for the transversal beams; additionally scratches from trucks colliding with the structure are visible

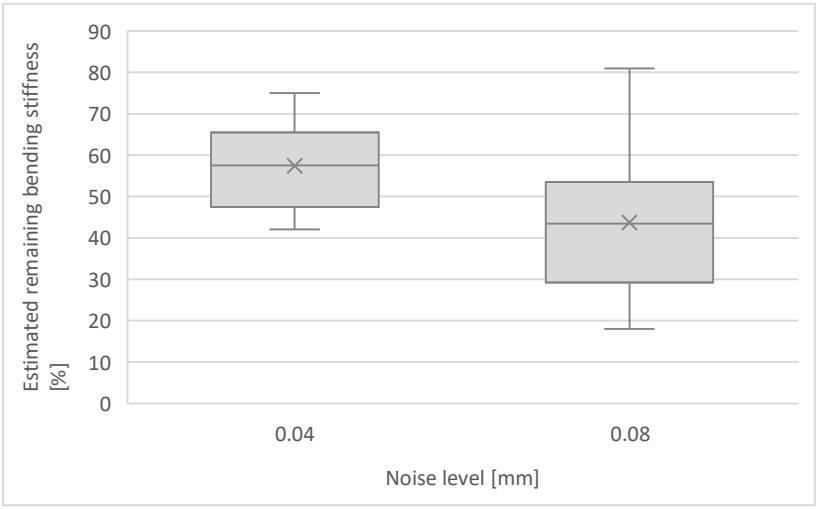

Figure 95. Influence of the present noise level on the Damage Level assessment

To validate the applicability of the method, a numerical study is conducted in which the load was increased until a deflection value of L/300 was reached. This ensured that the bridge structure remained within SLS. An artificial noise of 0.08 mm, representing the maximum measurement noise observed in the in-situ experiment, is applied. A bending stiffness reduction of 40% is simulated around the detected damage position in the in-situ experiment, and the DAD method with damage level assessment is applied. However, it is important to note that the results of this study cannot be generalized, as the position of damage influences its detectability. A comprehensive parametric study has previously been conducted on the influence of damage position along the longitudinal axis [166]. This study systematically examined how damage location affects detection accuracy and provided a thorough analysis of damage location along the span. Figure 96 illustrates the outcome of the DAD method and damage level assessment for the deflection value of L/3,750, which was attained in the Soleuvre bridge in-situ experiment and L/300. The figure illustrates the analysis based on the smoothed deflection line subsequent to MU. As illustrated on the left-hand side of the figure, the damage detection process was unsuccessful, and the damage level assessment of the segments was unable to produce accurate results, as the values displayed for most segments were exceedingly high. Upon increasing the deflection value to L/300, the damage localization was successful, and the damage level assessment, based on a single artificial measurement, yielded a residual bending stiffness of 65%, resulting in a small damage level error of 5%. This demonstrates that, with the achieved precision, the presented damage level assessment method is applicable within the SLS.

The DAD values indicated a probable damage location in the third beam near the second fourth point, consistent with visible corrosion and scratches from vehicle impacts. Application of the inversion-based MU algorithm yielded an initial estimated residual bending stiffness of approximately 50%. However, when the global stiffness and support conditions were partially updated (reflecting the non-negligible effect of the "non-supporting" concrete slab), the residual

bending stiffness increased to about 65%. These steps demonstrate how the MU process can refine the damage assessment. Additional measurements or higher loading may reduce noise and improve severity quantification.

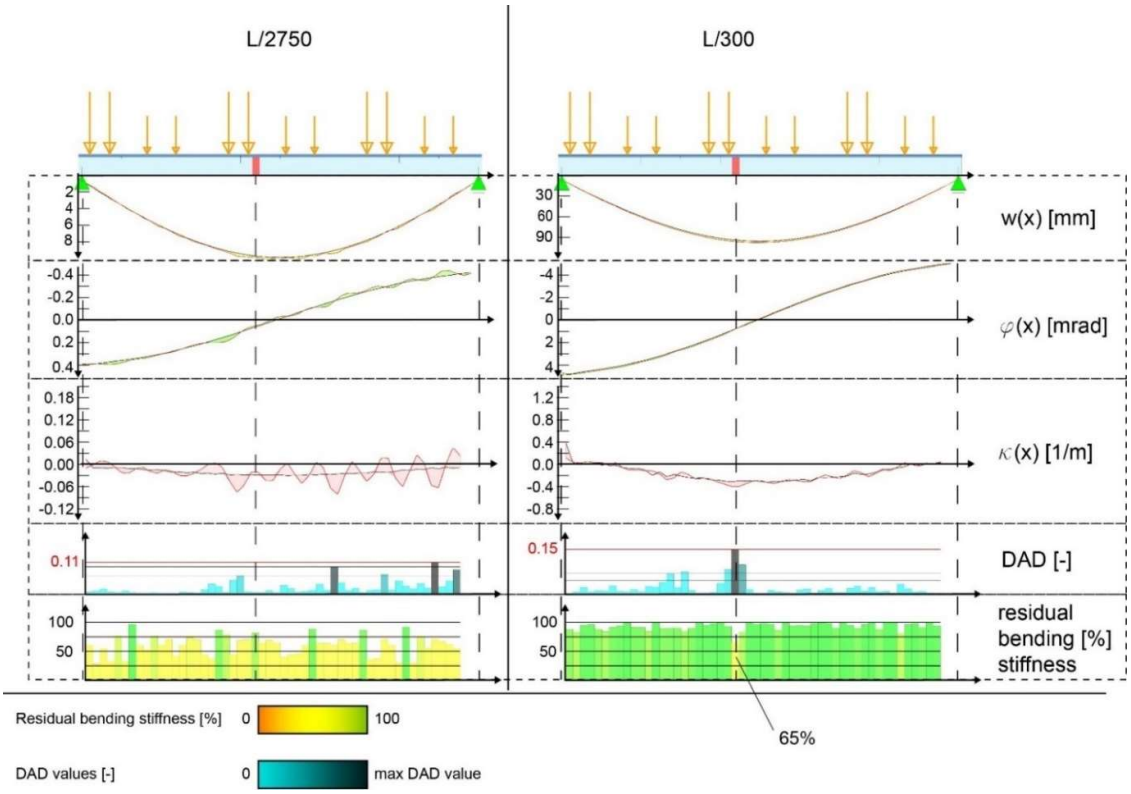

Figure 96. Results of the DAD method for numerical study on Soleuvre bridge comparing the deflection value of the in-situ experiment and in SLS with damage level assessment

3.7.8.2 Ettelbréck bridge

Similar to the Soleuvre bridge, only one outer and one inner girder were measured for the Ettelbréck bridge. In this paper, we focus exclusively on the results from the inner girder, as this component is subjected to a greater load under the applied loading pattern. Consequently, it exhibits a higher deflection value than the outer girder. Figure 97 presents the application of the DAD method using the smoothed deformation line and the updated reference model, which revealed damage near the support.

Upon closer inspection of this section of the bridge structure (see Figure 98), significant corrosion was observed. The bridge is located at a low elevation above the river, as shown in Figure 87, and is subject to frequent flooding during heavy rainfalls, which is likely to contribute to the high levels of corrosion. This corrosion could have caused a localized reduction in bending stiffness.

The recorded deflection value was L/2,450, which is relatively low. Consequently, the results of the DAD method should be interpreted with caution. Notwithstanding the low deflection value and the presence of noise, the method was able to successfully identify the location of visual damage. This serves to illustrate the robustness of the DAD method in detecting potential damage even under

conditions that are not ideal for experimental validation. In light of the low deflection value and the limited scope of measurements, the determination of the damage level will not be presented in this paper. It is recommended that more comprehensive studies will be conducted with higher deflection values and multiple measurement series to ensure a more accurate assessment of the damage severity.

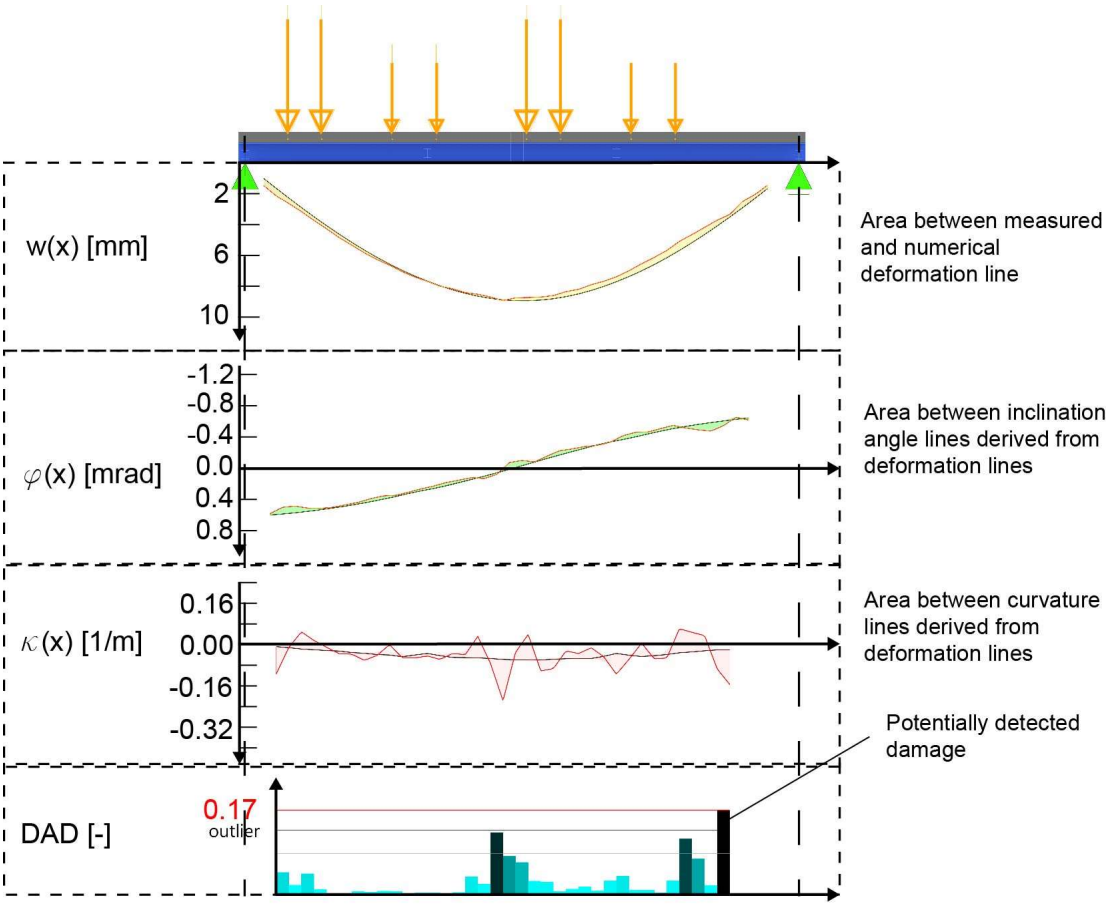

Figure 97. Application of the DAD method for the Ettelbréck bridge with a smoothed deflection curve and updated model

Figure 98. The heavily corroded area at the northern support of the middle girder

3.7.9 Conclusions

This paper presents a comprehensive extension of the DAD method, with a particular focus on its application for Level 3 of SHM. This is achieved by integrating a simple MU-based inversion technique for damage level assessment. The proposed MU approach, which has low computational intensity, has demonstrated significant improvements in damage severity detection by refining numerical models to align with real-world measurements in both, numerical and experimental studies.

A significant contribution of this paper is the method developed for handling missing measurement points, which is essential when data quality is compromised due to noise or other factors. The integration of a curve-fitting technique to replace missing points avoids false detection of damage.

Another important finding was the impact of noise on damage level estimation. The results indicated that increased noise levels resulted in increased error in the calculated damage severity, highlighting the necessity for noise mitigation strategies. In particular, the paper quantified the noise-induced errors and demonstrated how they can influence the interpretation of damage severity in SHM applications.

It is of paramount importance to emphasize the significance of MU in improving damage level assessment. Through numerical experiments, it was demonstrated that MU substantially enhances

the precision of damage detection and damage level estimation, thereby establishing it as a key component for advancing SHM methods to higher levels of functionality.

The principal findings of this study are presented as follows:

- MU-based inversion technique for Damage Level Assessment: The incorporation of a low-complexity MU-based inversion technique resulted in an enhanced Level of SHM and the accuracy was shown in both numerical and laboratory settings. However, real-world bridge applications revealed challenges related to noise and low deformations, which need further investigation.
- Replacement of Missing Measurement Points: The application of a nonlinear regression approach to replace missing data points resulted in enhanced overall accuracy of deflection and curvature analyses, thereby mitigating the adverse effects of poor data quality on damage detection.
- The influence of noise on damage level error was also investigated. It was demonstrated that noise has a significant impact on the accuracy of damage severity assessments. Therefore, effective noise reduction is essential for more reliable SHM applications.
- MU plays a crucial role in aligning numerical models with actual structural behavior, enabling more precise damage detection and damage level assessments and supporting the overall reliability of SHM systems.
- The outcomes of the case studies demonstrated the efficacy of the DAD method in detecting and localizing damage in real bridge structures. While the case studies did not fully validate the MU technique for damage level assessment, numerical analysis indicated that with different constraints (higher damage level, higher deflection value, repeated measurements), a damage level assessment is applicable to in-situ experiments. Furthermore, the case studies provided an opportunity to evaluate the method's performance under conditions that are encountered in practical assessments, providing valuable insights for further development and demonstrating the method's potential in real-world scenarios.

In conclusion, this study illustrates the increased capabilities of the DAD method for SHM, particularly in advancing to higher levels of SHM using an inversion-based model updating framework. By adopting sub-models in lieu of high-fidelity FE meshes, a substantial reduction in computational overhead is achieved. This advancement signifies a substantial enhancement in the efficiency of damage assessment and severity evaluation in practical applications, particularly in the context of real-world bridge structures. The efficiency of this approach is contingent upon the successful mitigation of noise-related challenges, which if addressed, will ensure the effective and reliable utilization of the proposed technique in bridge engineering applications without incurring excessive computational demands.

Future work will concentrate on the refinement of the MU approach for damage level assessment and the extension of its validation on real-world structures. In subsequent experiments, slender or lower-stiffness bridge structures will be selected to induce higher deflection levels, thereby enhancing the sensitivity of damage detection. Further destructive testing, analyzing and comparing the damage severity will be conducted. Additionally, the MU procedure will be integrated with the SAD method, which demonstrates reduced noise sensitivity through direct strain measurements. Through the combination of larger deflections from suitably chosen test structures with the inherently lower noise characteristics of the SAD approach, it is anticipated that more robust and earlier damage detection outcomes will be achieved.

DATA AVAILABILITY STATEMENT:

All data, models, or code that support the findings of this study are available from the corresponding author upon reasonable request.

ACKNOWLEDGEMENTS:

The authors would like to express their gratitude to the “Administration des Ponts et Chaussées” of Luxembourg for providing the opportunity to carry out experiments on a real bridge and providing the under-bridge inspection unit and the loading with heavy trucks. Furthermore, the authors would like to express their gratitude to Mr. Harald Krause for the support with the photogrammetric software Elcovision. The authors would also like to acknowledge Mr. Cédric Bruyere and his team for providing the point coordinates for the reference points. The GGE Laboratory supported this work with specialized instruments. Special acknowledgements are expressed to the technical support team of the University of Luxembourg for their expertise and helpful contributions to the realization of the large-scale experiment.

4 Discussion

This thesis aimed to enhance the applicability of the DAD method for SHM in bridge structures by addressing both its theoretical and practical limitations. This chapter presents a synthesis of findings from three individual studies, discussing the broader implications of the research and its contribution to the understanding of key parameters, including deflection values, damage level, noise sensitivity, bridge structure types, and technological integration. Furthermore, the potential of strain-based measurement techniques and model updating is investigated, with particular attention paid to their limitations and avenues for future research.

4.1 Findings from Study 1: Deflection values, damage levels, precision, and bridge structure types

The primary findings of the initial study pertain to the analysis of deflection values, damage levels, measurement precision, and the influence of bridge structure types. The objective of this study was to examine the impact of deflection values and noise levels on the accuracy of damage detection using the DAD method. The findings indicated that elevated deflection values consistently enhanced damage detection outcomes and could offset deficiencies in data quality. This finding highlighted the difficulty presented by stiffer bridge structures, which typically exhibit lower deflection values, thereby reducing the reliability of damage detection. Uncertainties regarding the materials and the structure further limit damage detection, as the proof load needs to be defined carefully, not to damage the structure. Therefore, the DAD method would benefit through a thorough investigation of the existing structure and materials to increase the deflection value. As the study revealed that the DAD method is highly sensitive to noise, its presence can impede the ability to discern essential structural alterations, thereby limiting the efficacy of the method.

Furthermore, the initial study illuminated the influence of bridge structure types on the intricacy and financial outlay associated with the implementation of the DAD method. The method proved to be more efficient and cost-effective in the context of simpler structures, such as those comprising large beams, due to the reduced number of required deflection measurements. In contrast, more intricate structures, such as those comprising multiple girders, necessitated a greater number of deflection measurements, thereby increasing both the financial burden and the intricacy of implementing the method in actual scenarios. This underscores the pivotal role of bridge structure type in determining the viability of the DAD method for practical SHM applications.

4.2 Findings from Study 2: Strain-Based Approach for Improved Precision

The second study introduced a strain-based approach to address the limitations identified in the first study, particularly concerning noise and precision in low-deflection scenarios. In contrast to deflection-based methodologies, this approach directly measured curvature from strain, thereby providing a more accurate and reliable means of detecting localized damage. The laboratory

experiments demonstrated that this strain-based method was highly resistant to noise, thereby establishing it as a promising solution for monitoring structures where low deflection values would otherwise limit the effectiveness of deflection-based approaches. Nevertheless, the study did not extend this method to real-world bridge structures due to the high cost of strain sensors. Notwithstanding this limitation, the strain-based approach offers considerable promise for future real-time monitoring applications, particularly as sensor costs decline over time.

4.3 Findings from Study 3: Model Updating for Damage Quantification

The third study aimed to further extend the DAD method by introducing model updating techniques that would enable Level 3 SHM, which would facilitate not only damage detection but also the quantification of damage severity. This constitutes a substantial theoretical advancement, as the capacity to quantify damage is indispensable for determining the extent of intervention required in maintenance and repair operations.

While the model updating framework provided a robust theoretical foundation for damage quantification, real-world experiments were constrained by the precision of the measurements and the influence of noise. Although laboratory experiments validated the potential of the model updating technique, the challenges encountered in field measurements prevented its full validation. Nevertheless, the theoretical development of model updating represents a promising step toward more advanced SHM systems in the future, especially when combined with more precise measurement techniques.

4.4 Technological Integration and Future Potential

Although previous studies have demonstrated that the DAD method can be enhanced through the use of contemporary technologies, such as UAVs and CRP, the current achievable precision in photogrammetry still exhibits certain limitations, particularly when dealing with low deflection values. This is evidenced by the real-world experiments. To investigate the influence of different parameters, including measurement precision, deflection value, damage level, and bridge structure type, the use of a parametric numerical model proved valuable. The parametric model enabled the investigation of a significantly larger number of combinations than would have been feasible without it. The parametric study yielded valuable insights for the preparation of in-situ experiments, including the requisite deflection value for the desired precision and the suitability of a bridge structure for the application of the DAD method.

As the initial study demonstrated that the DAD method is highly susceptible to noise, the incorporation of strain measurements for curvature calculation proved to be highly advantageous. This is because the SAD method, which employs curvature derived from strains rather than deflections, exhibited resilience to noise. The SAD method would be further enhanced by the

incorporation of FOS for strain measurement, as the measurement point density is exceptionally high (less than 1mm). The utilization of FOS also facilitates real-time monitoring, as the data can be directly processed.

Nevertheless, it is expected that forthcoming advances in UAV sensor resolution and image processing will address these limitations, thereby rendering UAV-based SHM a more effective instrument for the detection of minor structural alterations in bridges.

Another essential aspect for improving precision, particularly in practical applications, is the repetition of measurements. Although noise was identified as a limiting factor, the repetition of measurements can assist in the averaging out of noise, thereby producing more reliable results. This suggests that the constraints encountered during this investigation, such as road closures that limited the number of measurements that could be conducted, may be less pronounced in actual SHM scenarios, where repeated measurements are more viable. In practical applications, the capacity to undertake repeated measurements can markedly enhance the precision of deflection-based methodologies. A higher number of measurements would also allow for the implementation of noise filtering strategies using machine learning and predictive analysis. Furthermore, machine learning and AI could be employed for automation in UAV data collection, processing, and DAD analysis.

4.5 Theoretical Contributions and Implications

The findings presented in this dissertation contribute to the theoretical understanding of SHM using the DAD method in a significant manner, thereby advancing the field of SHM. The initial study's examination of deflection values and noise sensitivity reveals the limitations of the method in discerning localized damage in stiffer bridge structures. The findings pertaining to the assessment of local damages within a cross-section across different bridge structure types facilitate an understanding of the influence of local damages on the overall cross-section behavior. These insights refine the criteria for selecting bridge structures where the DAD method can be most effectively applied and provide guidance for future SHM methodologies that rely on static deflection measurements.

The second study broadens the theoretical framework of the DAD method by introducing a strain-based approach, resulting in the SAD method, which enhances precision and noise resistance. This method provides a reliable solution for the detection of localized damage in low-deflection scenarios, thereby increasing the applicability of the method to a wider range of structures.

The third study's introduction of inversion-based model updating for damage quantification represents a significant advancement in the field of SHM theory. This new approach allows for assessment of damage level (SHM level 3), which is crucial for further levels of SHM and for informing maintenance decisions.

This dissertation makes significant advancements to the DAD method, establishing it as a more effective and versatile tool for SHM of bridge structures. By addressing its limitations, extending its applicability, integrating complementary approaches, and extending its SHM level, this work enhances the method's performance in real-world scenarios, paves the way for higher SHM levels, and strengthens its practical relevance. The synthesis of findings from the three included papers is presented below.

4.6 Evaluation of Findings in Relation to Research Questions

4.6.1 Key Insights from publication I: Addressing the limitations of the DAD method

The initial paper examined the potential and limitations of the DAD method for condition assessment through comprehensive parametric numerical studies. Notable contributions include the introduction of the DDR and the DAD IL, which enhance comprehension of the interrelationships between measurement precision, damage location, and deflection values and their impact on the method's performance. The primary findings are as follows:

- **Experimental Setup:** A parametric analysis tailored to each bridge structure is essential for the design of effective experiments. Such analyses enable the identification of potential damage locations, estimation of the DDR, and determination of damage detection thresholds based on expected measurement precision.
- **Damage Detection Range:** The DDR is defined as the range for which damage can be reliably identified. The DDR is subject to the influence from a number of factors, including damage severity, measurement precision, and deflection values. Damage located near supports is less readily detectable. The application of a smoothing curvature line can result in an expansion of the damage detection range (DDR) by up to 30% of the span length.
- **Load Position Optimization:** The DAD IL identifies optimal load positions for reliable damage localization, with the number of load positions often depending on the structural system and damage location.
- **Measurement Point Density:** While an increased measurement density enhances the precision of damage localization, it simultaneously elevates the susceptibility to noise. Nevertheless, elevated deflection values may serve to offset, at least in part, the constraints associated with lower measurement precision.
- **Deflection-Damage Relationship:** An increase in deflection values facilitates the detection of damage resulting from a reduction in stiffness. To illustrate, a deflection of L/500 with a 50% stiffness reduction is equivalent to a DDR of L/2000 with a 70% stiffness reduction.

4.6.2 Key Insights from publication II: Integrating Strain-based Curvature Analysis

The second paper introduced the SAD method, which represents a strain-based extension of the DAD method. This method employs strain measurements from two lines with a vertical distance to derive curvature. The approach was validated through a combination of numerical studies, laboratory experiments, and model-updating techniques. The principal findings are as follows:

- **SAD Method Introduction:** The SAD method enhances noise resistance and precision by relying on strain measurements in lieu of deformation lines for curvature analysis.
- **Enhanced Damage Detection:** In both numerical and laboratory experiments, the SAD method exhibited greater sensitivity to smaller damage levels in comparison to the DAD method, even at lower deflection values. For example, laboratory tests demonstrated that the SAD method was capable of detecting a 12% reduction in stiffness at L/2550, whereas the DAD method required L/390 for the detection of a 28% reduction.
- **Noise Insensitivity:** The SAD method exhibits a markedly reduced sensitivity to noise, thereby enabling damage detection at lower deflection levels.
- **Photogrammetry for Large Cross-Sections:** Photogrammetry represents a viable alternative for strain measurements in large cross-sections, such as box girders. However, it is less precise than strain gauges or FOS.
- **The practicality of the DAD method is as follows:** Notwithstanding its inherent constraints, the DAD method continues to offer a competitive advantage in terms of cost-effectiveness and straightforward implementation, rendering it a viable option for budget-conscious projects.

4.6.3 Key Insights from publication III: Extending SHM to Advanced Levels

The third paper presented an extension of the DAD method for Level 3 SHM (damage severity assessment) using a low-complexity MU technique. This integration aligns numerical models with experimental data, thereby enhancing the detection of damage severity. The principal findings are as follows:

- **Advancing SHM Levels:** The MU technique markedly enhanced the DAD method to Level 3 with the detection of damage severity by improving the alignment between numerical models and observed structural behavior.
- **Data Quality Enhancement:** Nonlinear regression was successfully employed to replace missing measurement points, thereby enhancing the accuracy of deflection and curvature analyses.
- **Noise Mitigation:** The study underscored the considerable impact of noise on damage severity assessments, emphasizing the necessity for robust noise reduction strategies.

- **Real-world Applications:** The case studies demonstrated the applicability of the DAD method on real bridge structures; however, further validation of the MU approach in diverse conditions is recommended.

4.6.4 Integrated Contributions to SHM

The collective findings from the three papers contribute to a comprehensive advancement of SHM practices.

- **Optimizing Noise and Measurement Precision:** Systematic approaches were developed with the objective of optimizing DDR and mitigating the effects of noise by adjusting measurement density and deflection values.
- **Strain-measurements Integration:** The SAD method provides a noise-resistant extension to the DAD framework, thereby enhancing precision and expanding the DDR in challenging scenarios. Further, the SAD method can be used as long-term real-time monitoring, where the DAD method is used for periodical short-term monitoring.
- **Advancing SHM Levels:** The incorporation of low-complexity inversion-based MU technique facilitate enhanced damage severity detection and opens for lifecycle planning and predictive analysis, positioning the DAD method for advancement toward SHM Levels 4 and 5.

4.6.5 Addressing the Research Questions

This dissertation addressed the core research questions in an effective manner, as follows:

- **What are the limitations of the DAD method regarding deflection values, noise levels, measurement point distances and bridge structure types in detecting local damages?**
  The introduction of the DDR, DAD IL, and parametric modeling provided a systematic approach to addressing challenges related to noise sensitivity, deflection variability, and measurement density.
- **How can the noise sensitivity of the DAD method be reduced to improve damage detection accuracy, particularly in low-deflection scenarios?**
  The SAD method demonstrated superior precision in the presence of noise, offering a reliable alternative to traditional deflection-based curvature derivation.
- **Can strain-based curvature analysis be integrated to improve the precision and practical applicability of the DAD method in SHM applications?**
  A hybrid DAD-SAD framework was developed, demonstrating enhanced accuracy and broader applicability through numerical, laboratory, and in-situ validations.
- **How can the DAD method be extended to support more advanced SHM levels, including damage level assessment?**
  Integration of MU techniques enabled expansion of the DAD method's scope to encompass damage severity analysis and Level 3 SHM.

This research bridges the gap between theoretical innovation and practical implementation, providing a scalable, adaptable, and reliable SHM tool. The enhanced DAD framework addresses immediate safety concerns while supporting long-term sustainability objectives, marking a significant step toward more advanced and resilient SHM systems for bridge structures.

5 Conclusion and Outlook

5.1 Conclusions

This dissertation represents a significant enhancement of the DAD method, addressing the principal shortcomings and transforming it into a more sophisticated SHM tool for bridge structures. By addressing the inherent limitations of the method, expanding its applicability, and integrating innovative approaches, this work establishes the method as a practical solution for real-world applications and a foundation for advanced SHM levels. By synthesizing findings from three studies, this research bridges the gap between theoretical insights and practical implementation.

The initial study concentrated on elucidating the constraints of the DAD approach through a comprehensive parametric numerical analysis. The introduction of concepts such as the DDR and the DAD IL has enhanced the understanding of how factors such as measurement precision, damage location, and deflection values influence performance. Parametric analysis tailored to specific bridge structures was identified as a crucial element in the design of effective experiments. The DDR, representing the range within which damage can be reliably identified, was demonstrated to be contingent upon parameters such as damage severity and deflection levels. Damage in the vicinity of supports was observed to be less readily discernible. The application of smoothing techniques resulted in an expansion of the aforementioned range by up to 30% of the span length. The DAD IL identified optimal load positions for reliable damage localization, depending on the structural system and damage location. It was demonstrated that measurement density affects both the precision of localization and the susceptibility to noise. This limitation can be partially addressed by increasing the deflection values. A proportional relationship was observed between deflection values and damage detection sensitivity, whereby higher deflections facilitated the identification of smaller stiffness reductions.

The second study expanded the DAD framework by introducing the SAD method, which is a strain-based approach that derives curvature using measurements from two vertically spaced lines. This method exhibited substantial enhancements in noise resilience and damage detection precision. The greater sensitivity of the SAD method to smaller damage levels, even at lower deflection values, was confirmed by numerical and laboratory tests. To illustrate, while the DAD method necessitated a deflection value of L/390 to discern a 28% reduction in stiffness, the SAD method identified a 12% reduction at L/2550. The SAD method's resilience to noise further enhanced its reliability in challenging scenarios. Additionally, the study underscored the potential of photogrammetry for strain measurement in expansive cross-sections, such as box girders. However, it should be noted that the precision of this method may not reach the same level as that of strain gauges or FOS. Notwithstanding its shortcomings, the DAD method was validated as a cost-effective and straightforward solution for projects with limited resources, complementing the SAD method's advanced capabilities.

The third study advanced the DAD method toward Level 3 SHM by integrating a low-complexity MU technique. This approach aligned numerical models with experimental data, thereby enabling reliable damage severity assessments and paving the way for predictive maintenance. Nonlinear regression was employed to supplant absent measurement points, thereby enhancing the precision of curvature and deflection analyses. The study highlighted the considerable influence of noise on the assessment of damage severity, underscoring the necessity for the implementation of robust mitigation strategies. The practical applicability of the DAD method was demonstrated in real-world case studies. It was recommended that further validation of the MU approach across diverse conditions be conducted to enhance its generalizability.

In sum, the findings of these studies represent a unified advancement of SHM practices. By optimizing methodologies for the attenuation of noise and the enhancement of measurement precision, the DDR was expanded, thereby facilitating the more reliable detection of damage under varying conditions. The incorporation of strain-based methodologies constituted a noise-resistant extension to the DAD framework, thereby facilitating its application in both long-term real-time monitoring and short-term periodic assessments. The integration of MU techniques permitted the assessment of damage severity and facilitated the implementation of lifecycle planning and predictive maintenance, thereby positioning the method for advancement to SHM Levels 4 and 5. Collectively, these contributions illustrate the evolution of the DAD method into a versatile and scalable solution for modern SHM, offering sustainable and reliable infrastructure management.

5.2 Outlook

The challenges addressed in this dissertation provide a steppingstone for further developments in SHM, particularly in integrating advanced monitoring techniques into a unified framework for infrastructure management. While the DAD method has been significantly refined, the next steps lie in real-world validation, automation, and integration with complementary methodologies.

Despite the advancements made in this research, several limitations remain, which provide avenues for future research. A significant challenge associated with the DAD method is its sensitivity to noise, particularly in real-world experiments. This is especially problematic when dealing with low deflection values, which can make accurate measurements difficult. Nevertheless, technique is constantly improving which indicates the potential for overcoming this issue. The impact of new camera and UAV technologies should be further analyzed. Further, alternative methods for deflection measurements, such as profile laser scanning, or advanced radar-based displacement sensors should be investigated for the application of the DAD method.

Another critical area for future research is the exploration of the SAD method in real-world experiments, particularly focusing on concrete behavior. Real-world application on concrete structures using the SAD method will require distinguishing between cracks that do not compromise structural integrity and actual damage that necessitates intervention. Laboratory and field

experiments will be essential to validate these capabilities under realistic environmental and operational conditions. By combining SAD with FOS, the reliability of this approach can be further enhanced.

Automation is another crucial frontier for SHM. The DAD method, while powerful, currently requires considerable manual effort for data acquisition, processing, and analysis. Leveraging machine learning and AI, future research should focus on automating these processes, enabling the method to operate autonomously. This includes developing AI-driven frameworks for noise filtering, data analysis, and anomaly detection. Automated deployment using UAVs for data collection represents a particularly promising avenue, offering scalability and efficiency for large-scale monitoring projects.

To maximize its utility, the DAD method must also be integrated into comprehensive SHM systems. No single method can provide an absolute assessment of a structure's condition. A combined approach, integrating static, dynamic, and acoustic methods, can provide a more holistic perspective on structural health. This hybrid framework should be designed to leverage the strengths of each method, providing reliable condition assessments that account for both localized and global structural behaviors. It needs to be identified which methods are suitable to combine with the DAD method and complement each other.

The incorporation of the DAD method into digital twin (DT) frameworks offers a further potential for transformative change in the field of SHM. As dynamic virtual representations of physical structures, DTs facilitate real-time updates and advanced simulations. Nevertheless, their capacity to furnish immediate insights into a structure's condition remains constrained in the absence of efficacious condition indicators. The DAD method addresses this limitation by offering precise, measurement-based indicators, such as reductions in bending stiffness, that transform raw data into actionable insights. The integration of the DAD method within a DT environment would facilitate real-time localization and quantification of structural damage, enabling the seamless translation of field measurements into interpretable health metrics. Furthermore, this integration would facilitate continuous updates to FEM models, thereby enhancing their accuracy and predictive capabilities. By combining the DAD method's robust condition assessment capabilities with the predictive strengths of DTs, this approach aligns SHM capabilities with the demands of modern infrastructure management. It would facilitate proactive maintenance strategies, improve lifecycle assessments, and optimize the performance of critical infrastructure, thereby driving significant advancements in sustainability and resilience.

Achieving higher SHM levels, including Levels 4 (Damage Prognosis) and 5 (Lifetime Prognosis), remains a critical goal. These advancements require the integration of service life assessments and predictive analytics into SHM frameworks. Statistical models and machine learning algorithms must be employed to quantify the uncertainties inherent in material degradation and environmental

impacts. By addressing these gaps, SHM can evolve from a reactive to a fully proactive discipline, capable of forecasting and mitigating potential failures before they occur.

Finally, improved diagnostics and monitoring strategies can play a pivotal role in infrastructure management. The enhanced precision of the DAD method can guide the selection of monitoring techniques tailored to specific diagnostic needs. For example, the integration of photogrammetry and UAV-based approaches can complement traditional sensors, providing comprehensive data for decision-making. Collaboration with standardization bodies, such as road and bridge administration (Administration des Ponts et Chaussées) in Luxembourg or the federal highway research institute (Bundesanstalt für Straßenwesen) in Germany, can ensure that these advancements align with existing guidelines, promoting their adoption in practice.

In summary, the outlook for this research emphasizes the need for interdisciplinary collaboration, technological innovation, and real-world validation. By addressing these challenges, future work can ensure that the advancements achieved in this dissertation continue to contribute to safer, more efficient, and more sustainable infrastructure management. These efforts will bridge the gap between academic research and practical application, realizing the full potential of SHM in safeguarding critical infrastructure.

6 Bibliography

[1] B. Zhu and D. M. Frangopol, "Risk-Based Approach for Optimum Maintenance of Bridges under Traffic and Earthquake Loads," *Journal of Structural Engineering*, vol. 139, no. 3, pp. 422–434, Mar. 2013, doi: 10.1061/(ASCE)ST.1943-541X.0000671.

[2] D. Veshosky, C. R. Beidleman, G. W. Buetow, and M. Demir, "Comparative Analysis of Bridge Superstructure Deterioration," *Journal of Structural Engineering*, vol. 120, no. 7, pp. 2123–2136, Jul. 1994, doi: 10.1061/(ASCE)0733-9445(1994)120:7(2123).

[3] "DocsRoom - European Commission." Accessed: Oct. 16, 2024. [Online]. Available: https://ec.europa.eu/docsroom/documents/34561

[4] D. L. Allaix and A. Bigaj-Van Vliet, "Future perspectives of standardisation for a safe European transport infrastructure," *IABSE Symposium Prague, 2022: Challenges for Existing and Oncoming Structures - Report*, pp. 1314–1320, 2022, doi: 10.2749/PRAGUE.2022.1314.

[5] A. M. Ivanković, A. Strauss, and H. Sousa, "European review of performance indicators towards sustainable road bridge management," *https://doi.org/10.1680/jensu.18.00052*, vol. 173, no. 3, pp. 109–124, Apr. 2020, doi: 10.1680/JENSU.18.00052.

[6] J. R. Casas, "The bridges of the future or the future of bridges?," *Front Built Environ*, vol. 1, Apr. 2015, doi: 10.3389/FBUIL.2015.00003.

[7] "Keeping European bridges safe - European Commission." Accessed: Oct. 16, 2024. [Online]. Available: https://joint-research-centre.ec.europa.eu/jrc-news-and-updates/keeping-european-bridges-safe-2019-04-05_en

[8] Y. Wang *et al.*, "The volume of trade-induced cross-border freight transportation has doubled and led to 1.14 gigatons CO2 emissions in 2015," *One Earth*, vol. 5, no. 10, pp. 1165–1177, Oct. 2022, doi: 10.1016/j.oneear.2022.09.007.

[9] B. Novák, V. Boros, and J. Reinhard, "Strengthening strategies of highway viaducts in Germany," *IABSE Congress, Christchurch 2020: Resilient Technologies for Sustainable Infrastructure - Proceedings*, pp. 245–260, 2020, doi: 10.2749/CHRISTCHURCH.2021.0245.

[10] "Carolabrücke in Dresden: Korrosion ist wesentliche Ursache für Einsturz - DER SPIEGEL." Accessed: Oct. 16, 2024. [Online]. Available: https://www.spiegel.de/panorama/carolabruecke-in-dresden-korrosion-ist-wesentliche-ursache-fuer-einsturz-a-ef34a932-fa01-40ef-9ee7-0405de3f5ca8

[11] "Güterverkehr in Deutschland – Verkehrsmittel im Vergleich." Accessed: Oct. 16, 2024. [Online]. Available: https://www.dlr.de/de/aktuelles/nachrichten/daten-und-fakten/gueterverkehr-in-deutschland-verkehrsmittel-im-vergleich

[12] “Bundesrechnungshof - Homepage - Brückenmodernisierungsprogramm des Bundes für Autobahnbrücken.” Accessed: Oct. 16, 2024. [Online]. Available: https://www.bundesrechnungshof.de/SharedDocs/Downloads/DE/Berichte/2024/br%C3%BCckenmodernisierungsprogramm-volltext.html

[13] “Sécurité des ponts : trois ans après le rapport du Sénat, le compte n’y est toujours pas | Sénat.” Accessed: Oct. 16, 2024. [Online]. Available: https://www.senat.fr/salle-de-presse/communiques-de-presse/presse/cp20220616.html

[14] “État des ponts : Cinq ans après le rapport du Sénat, une situation toujours inquiétante, aggravée par le changement climatique - Public Sénat.” Accessed: Oct. 16, 2024. [Online]. Available: https://www.publicsenat.fr/actualites/territoires/etat-des-ponts-cinq-ans-apres-le-rapport-du-senat-une-situation-toujours-inquietante-aggravee-par-le-changement-climatique

[15] M. J. Fox, M. Furinghetti, and A. Pavese, “Application of the new Italian assessment guidelines to a 1960s prestressed concrete road bridge,” *Structural Concrete*, vol. 24, no. 1, pp. 583–598, Feb. 2023, doi: 10.1002/SUCO.202200884.

[16] G. M. Calvi, M. Moratti, N. Scattarreggia, V. Özsaraç, P. M. Calvi, and R. Pinho, “Numerical Investigations on the Collapse of the Morandi Bridge,” *Springer Tracts on Transportation and Traffic*, vol. 17, pp. 3–18, 2021, doi: 10.1007/978-3-030-59169-4_1/FIGURES/18.

[17] A. Gennaro, A. Caprino, V. Pernechele, F. Lorenzoni, and F. da Porto, “In-situ test and model updating of an RC tied-arch bridge,” *Procedia Structural Integrity*, vol. 44, pp. 822–829, Jan. 2023, doi: 10.1016/J.PROSTR.2023.01.107.

[18] F. Bazzucchi, L. Restuccia, and G. A. Ferro, “Considerations over the Italian road bridge infrastructure safety after the Polcevera viaduct collapse: past errors and future perspectives,” *Frattura ed Integrità Strutturale*, vol. 46, pp. 400–421, 2018, doi: 10.3221/IGF-ESIS.46.37.

[19] “Perché l’Italia crolla: ponti, viadotti e infrastrutture fragili - Domus.” Accessed: Oct. 16, 2024. [Online]. Available: https://www.domusweb.it/it/architettura/2019/11/28/oltre-linfrastruttura-alcune-considerazioni-sullo-stato-del-territorio-italiano.html

[20] T. L. Ripa Alonso, N. Corral Moraleda, M. García Alberti, R. M. Pavón, and J. C. Gálvez, “The Use of De-Icing Salts in Post-Tensioned Concrete Slabs and Their Effects on the Life of the Structure,” *Applied Sciences*, vol. 13, no. 12, pp. 6961–6961, Jun. 2023, doi: 10.3390/APP13126961.

[21] I. Carpintero and J. Rueda, “Structural assessment of an historical steel railway bridge in the north of Spain,” *ce/papers*, vol. 6, no. 5, pp. 440–447, Sep. 2023, doi: 10.1002/CEPA.2000.

[22] A. Kasprzak and A. Berger, “Strengthening and Widening of Steel Single Box Girder Bridge in Warsaw,” *Structural Engineering International*, vol. 29, no. 4, pp. 533–536, Oct. 2019, doi: 10.1080/10168664.2019.1625296.

[23] T. Siwowski, “Fatigue assessment of existing riveted truss bridges: Case study,” *Bulletin of the Polish Academy of Sciences: Technical Sciences*, vol. 63, no. 1, pp. 125–133, 2015, doi: 10.1515/BPASTS-2015-0014.

[24] F. Melakessou, T. Derrmann, and T. Engel, “Asymmetry analysis of inbound/outbound car traffic load distribution in Luxembourg,” *MobiWac 2015 - Proceedings of the 13th ACM International Symposium on Mobility Management and Wireless Access*, pp. 5–12, Nov. 2015, doi: 10.1145/2810362.2810374.

[25] G. M. Hadjidemetriou, M. Herrera, and A. K. Parlikad, “Condition and criticality-based predictive maintenance prioritisation for networks of bridges,” *Structure and Infrastructure Engineering*, vol. 18, no. 8, pp. 1207–1221, 2022, doi: 10.1080/15732479.2021.1897146.

[26] “Structurally Deficient Bridges | 2021 Infrastructure Report.” Accessed: Nov. 20, 2024. [Online]. Available: https://infrastructurereportcard.org/cat-item/bridges-infrastructure/

[27] B. Westcott and D. Thomson, “Deferred cost savings for an inventory of bridges using SHM,” *Structural Health Monitoring 2015: System Reliability for Verification and Implementation - Proceedings of the 10th International Workshop on Structural Health Monitoring, IWSHM 2015*, vol. 2, pp. 294–301, 2015, doi: 10.12783/SHM2015/39.

[28] A. Zulfiqar, M. Cabieses, A. Mikhail, and N. Khan, “Design of a bridge vibration monitoring system (BVMS),” *2015 Systems and Information Engineering Design Symposium, SIEDS 2015*, pp. 342–347, Jun. 2015, doi: 10.1109/SIEDS.2015.7117001.

[29] Y. J. Kim and L. B. Queiroz, “Big Data for condition evaluation of constructed bridges,” *Eng Struct*, vol. 141, pp. 217–227, Jun. 2017, doi: 10.1016/J.ENGSTRUCT.2017.03.028.

[30] H. M. Salem and H. M. Helmy, “Numerical investigation of collapse of the Minnesota I-35W bridge,” *Eng Struct*, vol. 59, pp. 635–645, Feb. 2014, doi: 10.1016/J.ENGSTRUCT.2013.11.022.

[31] T. Minami, M. Fujiu, J. Takayama, S. Suda, and S. Okumura, “A Study on Image Diagnostic Technology for Bridge Inspection Using Ultra High Resolution Camera,” *5th International Conference on Road and Rail Infrastructure*, vol. 5, pp. 79–85, Mar. 2019, doi: 10.5592/CO/CETRA.2018.828.

[32] K. Ozasa, “NEXCO西日本の橋梁の長期保全に向けた取り組み,” *Zairyo-to-Kankyo*, vol. 64, no. 10, pp. 429–437, Oct. 2015, doi: 10.3323/JCORR.64.429.

[33] H. Ito and T. Mizobuchi, “Effective bridge maintenance based on load-bearing performance simple evaluation,” *Sustainable Construction Materials and Technologies*, vol. 2, 2019, doi: 10.18552/2019/IDSCMT5065.

[34] T. Kawanaka, M. Matsumaru, S. Rokugawa, and H. Suzuki, "Employing a bridge triage method in municipalities with decreasing populations: An empirical analysis of the characteristics of road networks," *IEEE International Conference on Industrial Engineering and Engineering Management*, vol. 2016-January, pp. 475–479, Jan. 2016, doi: 10.1109/IEEM.2015.7385692.

[35] X. Zhang, G. Liu, J. Ma, H. Wu, B. Fu, and Y. Gao, "Status and prospect of technical development for bridges in China," *Chinese Science Bulletin*, vol. 61, no. 4–5, pp. 415–425, Oct. 2015, doi: 10.1360/N972015-00912.

[36] M. Feng, "Modern bridges in China," *Structure and Infrastructure Engineering*, vol. 10, no. 4, pp. 429–442, Apr. 2014, doi: 10.1080/15732479.2013.769608.

[37] M. Yang and J. Gong, "Survey and investigation of performance of superstructure of long span bridges in China," *International Conference on Performance-based and Life-cycle Structural Engineering*, pp. 1210–1219, Jan. 2015, doi: 10.14264/UQL.2016.626.

[38] S. A. Hassan and A. H. Mhebs, "Behavior of High Strength Hybrid Reinforced Concrete Deep Beams under Monotonic and Repeated Loading," *The Open Civil Engineering Journal*, vol. 12, no. 1, pp. 263–282, Aug. 2018, doi: 10.2174/1874149501812010263.

[39] H.-B. Xie, Y.-F. Wang, H.-L. Wu, and Z. Li, "Condition Assessment of Existing RC Highway Bridges in China Based on SIE2011," *Journal of Bridge Engineering*, vol. 19, no. 12, p. 04014053, Apr. 2014, doi: 10.1061/(ASCE)BE.1943-5592.0000633.

[40] M. Ma, M. Liu, and Z. Li, "Quantifying the Environmental Impact of Vehicle Emissions Due to Traffic Diversion Plans for Road Infrastructure Construction Projects: A Case Study in China," *Sustainability 2023, Vol. 15, Page 7825*, vol. 15, no. 10, p. 7825, May 2023, doi: 10.3390/SU15107825.

[41] B. Pang, P. Yang, Y. Wang, A. Kendall, H. Xie, and Y. Zhang, "Life cycle environmental impact assessment of a bridge with different strengthening schemes," *International Journal of Life Cycle Assessment*, vol. 20, no. 9, pp. 1300–1311, Sep. 2015, doi: 10.1007/S11367-015-0936-1/FIGURES/8.

[42] I. Gokasar, M. Deveci, and O. Kalan, "CO2 Emission based prioritization of bridge maintenance projects using neutrosophic fuzzy sets based decision making approach," *Research in Transportation Economics*, vol. 91, p. 101029, Mar. 2022, doi: 10.1016/J.RETREC.2021.101029.

[43] D. Y. Yang and D. M. Frangopol, "Life-cycle management of deteriorating bridge networks with network-level risk bounds and system reliability analysis," *Structural Safety*, vol. 83, p. 101911, Mar. 2020, doi: 10.1016/J.STRUSAFE.2019.101911.

[44] W. Hou, S. Liang, T. Zhang, T. Ma, and Y. Han, "Low-Carbon Emission Demolition of an Existing Urban Bridge Based on SPMT Technology and Full Procedure Monitoring,"

Buildings 2023, Vol. 13, Page 1379, vol. 13, no. 6, p. 1379, May 2023, doi: 10.3390/BUILDINGS13061379.

[45] A. E. Aktan *et al.*, "Condition Assessment for Bridge Management," *Journal of Infrastructure Systems*, vol. 2, no. 3, pp. 108–117, Sep. 1996, doi: 10.1061/(ASCE)1076-0342(1996)2:3(108).

[46] "BMDV - Bundesverkehrswegeplan 2030 - Gesamtplan." Accessed: Sep. 08, 2024. [Online]. Available: https://bmdv.bund.de/SharedDocs/DE/Publikationen/G/bundesverkehrswegeplan-2030-gesamtplan.html

[47] S. Li, S. Zhu, Y. L. Xu, Z. W. Chen, and H. Li, "Long-term condition assessment of suspenders under traffic loads based on structural monitoring system: Application to the Tsing Ma Bridge," *Struct Control Health Monit*, vol. 19, no. 1, pp. 82–101, Feb. 2012, doi: 10.1002/STC.427.

[48] S. Ye, X. Lai, I. Bartoli, and A. E. Aktan, "Technology for condition and performance evaluation of highway bridges," *J Civ Struct Health Monit*, vol. 10, no. 4, pp. 573–594, Sep. 2020, doi: 10.1007/S13349-020-00403-6/TABLES/9.

[49] W. Zhang and C. S. Cai, "Fatigue Reliability Assessment for Existing Bridges Considering Vehicle Speed and Road Surface Conditions," *Journal of Bridge Engineering*, vol. 17, no. 3, pp. 443–453, May 2011, doi: 10.1061/(ASCE)BE.1943-5592.0000272.

[50] Y. Q. Ni, X. G. Hua, and J. M. Ko, "Reliability-Based Assessment of Bridges Using Long-Term Monitoring Data," *Key Eng Mater*, vol. 321–323, pp. 217–222, Oct. 2006, doi: 10.4028/WWW.SCIENTIFIC.NET/KEM.321-323.217.

[51] A. Geβler, B. Hoffmeister, and T. Geers, "Digital Life-Cycle and Asset-Management for Steel Bridges," *ce/papers*, vol. 6, no. 5, pp. 1127–1131, Sep. 2023, doi: 10.1002/CEPA.2185.

[52] S. Abu Dabous, S. Yaghi, S. Alkass, and O. Moselhi, "Concrete bridge deck condition assessment using IR Thermography and Ground Penetrating Radar technologies," *Autom Constr*, vol. 81, pp. 340–354, Sep. 2017, doi: 10.1016/J.AUTCON.2017.04.006.

[53] S. Lee and N. Kalos, "Bridge inspection practices using non-destructive testing methods," *Journal of Civil Engineering and Management*, vol. 21, no. 5, pp. 654–665, May 2015, doi: 10.3846/13923730.2014.890665.

[54] S. Abdelkhalek and T. Zayed, "Performance assessment model of non-destructive technologies in inspecting concrete bridge decks," *Structure and Infrastructure Engineering*, vol. 19, no. 2, pp. 216–237, 2023, doi: 10.1080/15732479.2021.1937234.

[55] D. J. Clem, T. Schumacher, and J. P. Deshon, "A consistent approach for processing and interpretation of data from concrete bridge members collected with a hand-held GPR

device," *Constr Build Mater*, vol. 86, pp. 140–148, Jul. 2015, doi: 10.1016/J.CONBUILDMAT.2015.03.105.

[56] S. Rahmatalla, K. Hudson, Y. Liu, and H. C. Eun, "Finite element modal analysis and vibration-waveforms in health inspection of old bridges," *Finite Elements in Analysis and Design*, vol. 78, pp. 40–46, Jan. 2014, doi: 10.1016/J.FINEL.2013.09.006.

[57] S. Gonen and E. Erduran, "A Hybrid Method for Vibration-Based Bridge Damage Detection," *Remote Sensing 2022, Vol. 14, Page 6054*, vol. 14, no. 23, p. 6054, Nov. 2022, doi: 10.3390/RS14236054.

[58] D. H. Nguyen, Q. B. Nguyen, T. Bui-Tien, G. De Roeck, and M. Abdel Wahab, "Damage detection in girder bridges using modal curvatures gapped smoothing method and Convolutional Neural Network: Application to Bo Nghi bridge," *Theoretical and Applied Fracture Mechanics*, vol. 109, p. 102728, Oct. 2020, doi: 10.1016/J.TAFMEC.2020.102728.

[59] S. Das, P. Saha, and S. K. Patro, "Vibration-based damage detection techniques used for health monitoring of structures: a review," *J Civ Struct Health Monit*, vol. 6, no. 3, pp. 477–507, Jul. 2016, doi: 10.1007/S13349-016-0168-5/FIGURES/28.

[60] F. L. Zhang, C. W. Kim, and Y. Goi, "Efficient Bayesian FFT method for damage detection using ambient vibration data with consideration of uncertainty," *Struct Control Health Monit*, vol. 28, no. 2, p. e2659, Feb. 2021, doi: 10.1002/STC.2659.

[61] J. Liu, S. Xu, M. Berges, J. Bielak, J. H. Garrett, and H. Y. Noh, "An Expectation-maximization Algorithm-based Framework for Vehicle-vibration-based Indirect Structural Health Monitoring of Bridges," *Structural Health Monitoring 2019*, vol. 0, no. 0, pp. 333–340, 2019, doi: 10.12783/SHM2019/32132.

[62] E. OBrien, C. Carey, and J. Keenahan, "Bridge damage detection using ambient traffic and moving force identification," *Struct Control Health Monit*, vol. 22, no. 12, pp. 1396–1407, Dec. 2015, doi: 10.1002/STC.1749.

[63] B. Zhang, Y. Qian, Y. Wu, and Y. B. Yang, "An effective means for damage detection of bridges using the contact-point response of a moving test vehicle," *J Sound Vib*, vol. 419, pp. 158–172, Apr. 2018, doi: 10.1016/J.JSV.2018.01.015.

[64] M. Mousavi, D. Holloway, J. C. Olivier, and A. H. Gandomi, "A baseline-free damage detection method using VBI incomplete measurement data," *Measurement*, vol. 174, p. 108957, Apr. 2021, doi: 10.1016/J.MEASUREMENT.2020.108957.

[65] A. Sabamehr, C. Lim, and A. Bagchi, "System identification and model updating of highway bridges using ambient vibration tests," *J Civ Struct Health Monit*, vol. 8, no. 5, pp. 755–771, Nov. 2018, doi: 10.1007/S13349-018-0304-5/FIGURES/31.

[66] B. Heitner, F. Schoefs, E. J. OBrien, A. Žnidarič, and T. Yalamas, "Using the unit influence line of a bridge to track changes in its condition," *J Civ Struct Health Monit*, vol. 10, no. 4, pp. 667–678, Sep. 2020, doi: 10.1007/S13349-020-00410-7/FIGURES/17.

[67] Z. Sun, T. Nagayama, D. Su, and Y. Fujino, "A Damage Detection Algorithm Utilizing Dynamic Displacement of Bridge under Moving Vehicle," *Shock and Vibration*, vol. 2016, 2016, doi: 10.1155/2016/8454567.

[68] N. B. Wang, L. X. He, W. X. Ren, and T. L. Huang, "Extraction of influence line through a fitting method from bridge dynamic response induced by a passing vehicle," *Eng Struct*, vol. 151, pp. 648–664, Nov. 2017, doi: 10.1016/J.ENGSTRUCT.2017.06.067.

[69] A. P. Adewuyi, Z. Wu, and N. H. M. Kammrujaman Serker, "Assessment of Vibration-based Damage Identification Methods Using Displacement and Distributed Strain Measurements," *http://dx.doi.org/10.1177/1475921709340964*, vol. 8, no. 6, pp. 443–461, Aug. 2009, doi: 10.1177/1475921709340964.

[70] B. Wu, G. Wu, H. Lu, and D. C. Feng, "Stiffness monitoring and damage assessment of bridges under moving vehicular loads using spatially-distributed optical fiber sensors," *Smart Mater Struct*, vol. 26, no. 3, p. 035058, Feb. 2017, doi: 10.1088/1361-665X/AA5C6F.

[71] J. W. Lee, K. H. Choi, and Y. C. Huh, "Damage detection method for large structures using static and dynamic strain data from distributed fiber optic sensor," *International Journal of Steel Structures*, vol. 10, no. 1, pp. 91–97, 2010, doi: 10.1007/BF03249515/METRICS.

[72] A. Entezami, H. Sarmadi, B. Behkamal, and S. Mariani, "Big Data Analytics and Structural Health Monitoring: A Statistical Pattern Recognition-Based Approach," *Sensors 2020, Vol. 20, Page 2328*, vol. 20, no. 8, p. 2328, Apr. 2020, doi: 10.3390/S20082328.

[73] D. Tonelli, M. Luchetta, F. Rossi, P. Migliorino, and D. Zonta, "Structural Health Monitoring Based on Acoustic Emissions: Validation on a Prestressed Concrete Bridge Tested to Failure," *Sensors 2020, Vol. 20, Page 7272*, vol. 20, no. 24, p. 7272, Dec. 2020, doi: 10.3390/S20247272.

[74] L. Cheng, H. Xin, R. M. Groves, and M. Veljkovic, "Acoustic emission source location using Lamb wave propagation simulation and artificial neural network for I-shaped steel girder," *Constr Build Mater*, vol. 273, p. 121706, Mar. 2021, doi: 10.1016/J.CONBUILDMAT.2020.121706.

[75] K. M. Holford, A. W. Davies, R. Pullin, and D. C. Carter, "Damage Location in Steel Bridges by Acoustic Emission," *http://dx.doi.org/10.1177/1045389O122145311*, vol. 12, no. 8, pp. 567–576, Aug. 2001, doi: 10.1177/10453890122145311.

[76] A. Behnia, H. K. Chai, and T. Shiotani, "Advanced structural health monitoring of concrete structures with the aid of acoustic emission," *Constr Build Mater*, vol. 65, pp. 282–302, Aug. 2014, doi: 10.1016/J.CONBUILDMAT.2014.04.103.

[77] D. G. Aggelis, T. Shiotani, S. Momoki, and A. Hirama, "Acoustic Emission and Ultrasound for Damage Characterization of Concrete Elements," *Materials Journal*, vol. 106, no. 6, pp. 509–514, Nov. 2009, doi: 10.14359/51663333.

[78] M. Ohtsu, M. Uchida, T. Okamoto, and S. Yuyama, "Damage Assessment of Reinforced Concrete Beams Qualified by Acoustic Emission," *Structural Journal*, vol. 99, no. 4, pp. 411–417, Jul. 2002, doi: 10.14359/12109.

[79] S. Mahmoudkhani, B. Algohi, J. Zhao, H. Ling, A. Mufti, and D. Thomson, "Acoustic Emissions Sensor and Fuzzy C-mean Clustering Based Break Detection in Post-Tensioning Tendons," *Proceedings of IEEE Sensors*, vol. 2019-October, Oct. 2019, doi: 10.1109/SENSORS43011.2019.8956661.

[80] V. H. Nguyen, S. Schommer, S. Maas, and A. Zürbes, "Static load testing with temperature compensation for structural health monitoring of bridges," *Eng Struct*, vol. 127, pp. 700–718, Nov. 2016, doi: 10.1016/J.ENGSTRUCT.2016.09.018.

[81] J. Kwiatkowski, W. Anigacz, and D. Beben, "Comparison of Non-Destructive Techniques for Technological Bridge Deflection Testing," *Materials 2020, Vol. 13, Page 1908*, vol. 13, no. 8, p. 1908, Apr. 2020, doi: 10.3390/MA13081908.

[82] N. Boumechra, "Damage detection in beam and truss structures by the inverse analysis of the static response due to moving loads," *Struct Control Health Monit*, vol. 24, no. 10, p. e1972, Oct. 2017, doi: 10.1002/STC.1972.

[83] Y. Tian, J. Zhang, Q. Xia, and P. Li, "Flexibility identification and deflection prediction of a three-span concrete box girder bridge using impacting test data," *Eng Struct*, vol. 146, pp. 158–169, Sep. 2017, doi: 10.1016/J.ENGSTRUCT.2017.05.039.

[84] X. Meng, F. Xiao, Y. Yan, G. S. Chen, and Y. Ma, "Non-Destructive Damage Evaluation Based on Static Response for Beam-like Structures Considering Shear Deformation," *Applied Sciences 2023, Vol. 13, Page 8219*, vol. 13, no. 14, p. 8219, Jul. 2023, doi: 10.3390/APP13148219.

[85] F. Xiao, H. Sun, Y. Mao, and G. S. Chen, "Damage identification of large-scale space truss structures based on stiffness separation method," *Structures*, vol. 53, pp. 109–118, Jul. 2023, doi: 10.1016/J.ISTRUC.2023.04.027.

[86] B. Wu, H. Lu, B. Chen, and Z. Gao, "Study on Finite Element Model Updating in Highway Bridge Static Loading Test Using Spatially-Distributed Optical Fiber Sensors," *Sensors 2017, Vol. 17, Page 1657*, vol. 17, no. 7, p. 1657, Jul. 2017, doi: 10.3390/S17071657.

[87] H. Abdel-Jaber and B. Glisic, "Monitoring of long-term prestress losses in prestressed concrete structures using fiber optic sensors," *Struct Health Monit*, vol. 18, no. 1, pp. 254–269, Jan. 2019, doi: 10.1177/1475921717751870/ASSET/IMAGES/LARGE/10.1177_1475921717751870-FIG17.JPEG.

[88] E. A. Oskoui, T. Taylor, and F. Ansari, “Method and monitoring approach for distributed detection of damage in multi-span continuous bridges,” *Eng Struct*, vol. 189, pp. 385–395, Jun. 2019, doi: 10.1016/J.ENGSTRUCT.2019.02.037.

[89] Y. Ren, E. J. Obrien, D. Cantero, and J. Keenahan, “Railway Bridge Condition Monitoring Using Numerically Calculated Responses from Batches of Trains,” *Applied Sciences 2022, Vol. 12, Page 4972*, vol. 12, no. 10, p. 4972, May 2022, doi: 10.3390/APP12104972.

[90] Z. Yunkai, G. Jianjun, L. Guohua, and F. Yuchen, “Damage Identification of Simply-Supported Beam Bridge Based on Deflection Influence Line,” *IOP Conf Ser Earth Environ Sci*, vol. 643, no. 1, p. 012049, Jan. 2021, doi: 10.1088/1755-1315/643/1/012049.

[91] Z. W. Chen, Q. L. Cai, and S. Zhu, “Damage quantification of beam structures using deflection influence lines,” *Struct Control Health Monit*, vol. 25, no. 11, p. e2242, Nov. 2018, doi: 10.1002/STC.2242.

[92] G. Marasco, G. Piana, B. Chiaia, and G. Ventura, “Genetic Algorithm Supported by Influence Lines and a Neural Network for Bridge Health Monitoring,” *Journal of Structural Engineering*, vol. 148, no. 9, p. 04022123, Jun. 2022, doi: 10.1061/(ASCE)ST.1943-541X.0003345.

[93] D. Erdenebat and D. Waldmann, “Application of the DAD method for damage localisation on an existing bridge structure using close-range UAV photogrammetry,” *Eng Struct*, vol. 218, p. 110727, Sep. 2020, doi: 10.1016/j.engstruct.2020.110727.

[94] D. Erdenebat, D. Waldmann, F. Scherbaum, and N. Teferle, “The Deformation Area Difference (DAD) method for condition assessment of reinforced structures,” *Eng Struct*, vol. 155, pp. 315–329, Jan. 2018, doi: 10.1016/j.engstruct.2017.11.034.

[95] D. Erdenebat, D. Waldmann, and N. Teferle, “Curvature based DAD-method for damage localisation under consideration of measurement noise minimisation,” *Eng Struct*, vol. 181, pp. 293–309, Feb. 2019, doi: 10.1016/j.engstruct.2018.12.017.

[96] D. Martinez, A. Malekjafarian, and E. OBrien, “Bridge health monitoring using deflection measurements under random traffic,” *Struct Control Health Monit*, vol. 27, no. 9, p. e2593, Sep. 2020, doi: 10.1002/STC.2593.

[97] A. Rytter, “Vibrational Based Inspection of Civil Engineering Structures,” 1993. Accessed: Nov. 23, 2023. [Online]. Available: https://vbn.aau.dk/en/publications/vibrational-based-inspection-of-civil-engineering-structures

[98] J. S. Owen and N. Haritos, “Damage Detection in Large-Scale Laboratory Bridge Models,” *Key Eng Mater*, vol. 245–246, pp. 35–42, 2003, doi: 10.4028/WWW.SCIENTIFIC.NET/KEM.245-246.35.

[99] M. Ghrib, M. Rébillat, G. Vermot des Roches, and N. Mechbal, “Automatic damage type classification and severity quantification using signal based and nonlinear model based

damage sensitive features," *J Process Control*, vol. 83, pp. 136–146, Nov. 2019, doi: 10.1016/J.JPROCONT.2018.08.002.

[100] L. A. Bull, T. J. Rogers, C. Wickramarachchi, E. J. Cross, K. Worden, and N. Dervilis, "Probabilistic active learning: An online framework for structural health monitoring," *Mech Syst Signal Process*, vol. 134, p. 106294, Dec. 2019, doi: 10.1016/J.YMSSP.2019.106294.

[101] L. A. Bull, K. Worden, and N. Dervilis, "Towards semi-supervised and probabilistic classification in structural health monitoring," *Mech Syst Signal Process*, vol. 140, p. 106653, Jun. 2020, doi: 10.1016/J.YMSSP.2020.106653.

[102] M. I. Friswell and J. E. Mottershead, "Finite Element Model Updating in Structural Dynamics," vol. 38, 1995, doi: 10.1007/978-94-015-8508-8.

[103] Z. Zong, X. Lin, and J. Niu, "Finite element model validation of bridge based on structural health monitoring—Part I: Response surface-based finite element model updating," *Journal of Traffic and Transportation Engineering (English Edition)*, vol. 2, no. 4, pp. 258–278, Aug. 2015, doi: 10.1016/J.JTTE.2015.06.001.

[104] A. Teughels and G. De Roeck, "Structural damage identification of the highway bridge Z24 by FE model updating," *J Sound Vib*, vol. 278, no. 3, pp. 589–610, Dec. 2004, doi: 10.1016/J.JSV.2003.10.041.

[105] M. Sanayei, A. Khaloo, M. Gul, and F. Necati Catbas, "Automated finite element model updating of a scale bridge model using measured static and modal test data," *Eng Struct*, vol. 102, pp. 66–79, Nov. 2015, doi: 10.1016/J.ENGSTRUCT.2015.07.029.

[106] A. J. Garcia-Palencia, E. Santini-Bell, J. D. Sipple, and M. Sanayei, "Structural model updating of an in-service bridge using dynamic data," *Struct Control Health Monit*, vol. 22, no. 10, pp. 1265–1281, Oct. 2015, doi: 10.1002/STC.1742.

[107] Y. Zhao, J. Zhang, D. Li, D. Zhou, and D. Xin, "Finite Element Model Updating of Bridge Structures Based on Improved Response Surface Methods," *Struct Control Health Monit*, vol. 2023, no. 1, p. 2488951, Jan. 2023, doi: 10.1155/2023/2488951.

[108] D. Reagan, A. Sabato, and C. Niezrecki, "Feasibility of using digital image correlation for unmanned aerial vehicle structural health monitoring of bridges," *https://doi.org/10.1177/1475921717735326*, vol. 17, no. 5, pp. 1056–1072, Oct. 2017, doi: 10.1177/1475921717735326.

[109] F. Ioli, A. Pinto, and L. Pinto, "UAV PHOTOGRAMMETRY FOR METRIC EVALUATION OF CONCRETE BRIDGE CRACKS," *The International Archives of the Photogrammetry, Remote Sensing and Spatial Information Sciences*, vol. XLIII-B2-2022, no. B2-2022, pp. 1025–1032, May 2022, doi: 10.5194/ISPRS-ARCHIVES-XLIII-B2-2022-1025-2022.

[110] J. Valença, E. N. B. S. Júlio, and H. J. Araújo, "Applications of photogrammetry to structural assessment," *Exp Tech*, vol. 36, no. 5, pp. 71–81, Sep. 2012, doi: 10.1111/J.1747-1567.2011.00731.X/METRICS.

[111] A. Mirzazade, C. Popescu, T. Blanksvärd, and B. Täljsten, "Application of close range photogrammetry in structural health monitoring by processing generated point cloud datasets," *IABSE Congress, Ghent 2021: Structural Engineering for Future Societal Needs*, pp. 450–458, 2021, doi: 10.2749/GHENT.2021.0450.

[112] J. Hu, E. Liu, and J. Yu, "Application of Structural Deformation Monitoring Based on Close-Range Photogrammetry Technology," 2021, doi: 10.1155/2021/6621440.

[113] Y. Xu, "Photogrammetry-based structural damage detection by tracking a visible laser line," *Struct Health Monit*, vol. 19, no. 1, pp. 322–336, Jan. 2020, doi: 10.1177/1475921719840354/ASSET/IMAGES/LARGE/10.1177_1475921719840354-FIG9.JPEG.

[114] B. Riveiro, H. González-Jorge, M. Varela, and D. V. Jauregui, "Validation of terrestrial laser scanning and photogrammetry techniques for the measurement of vertical underclearance and beam geometry in structural inspection of bridges," *Measurement*, vol. 46, no. 1, pp. 784–794, Jan. 2013, doi: 10.1016/J.MEASUREMENT.2012.09.018.

[115] H. Yang and X. Xu, "Structure monitoring and deformation analysis of tunnel structure," *Compos Struct*, vol. 276, p. 114565, Nov. 2021, doi: 10.1016/J.COMPSTRUCT.2021.114565.

[116] S. Zollini, M. Alicandro, D. Dominici, R. Quaresima, and M. Giallonardo, "UAV Photogrammetry for Concrete Bridge Inspection Using Object-Based Image Analysis (OBIA)," *Remote Sensing 2020, Vol. 12, Page 3180*, vol. 12, no. 19, p. 3180, Sep. 2020, doi: 10.3390/RS12193180.

[117] S. Feroz and S. A. Dabous, "UAV-Based Remote Sensing Applications for Bridge Condition Assessment," *Remote Sensing 2021, Vol. 13, Page 1809*, vol. 13, no. 9, p. 1809, May 2021, doi: 10.3390/RS13091809.

[118] S. Zhuge *et al.*, "Noncontact deflection measurement for bridge through a multi-UAVs system," *Computer-Aided Civil and Infrastructure Engineering*, vol. 37, no. 6, pp. 746–761, May 2022, doi: 10.1111/MICE.12771.

[119] Z. Xu, Y. Wang, X. Hao, and J. Fan, "Crack Detection of Bridge Concrete Components Based on Large-Scene Images Using an Unmanned Aerial Vehicle," *Sensors 2023, Vol. 23, Page 6271*, vol. 23, no. 14, p. 6271, Jul. 2023, doi: 10.3390/S23146271.

[120] B. J. Perry, Y. Guo, R. Atadero, and J. W. van de Lindt, "Streamlined bridge inspection system utilizing unmanned aerial vehicles (UAVs) and machine learning," *Measurement*, vol. 164, p. 108048, Nov. 2020, doi: 10.1016/J.MEASUREMENT.2020.108048.

[121] X. Peng, X. Zhong, C. Zhao, A. Chen, and T. Zhang, "A UAV-based machine vision method for bridge crack recognition and width quantification through hybrid feature learning," *Constr Build Mater*, vol. 299, p. 123896, Sep. 2021, doi: 10.1016/J.CONBUILDMAT.2021.123896.

[122] S. Yoon, B. F. Spencer, S. Lee, H. J. Jung, and I. H. Kim, "A novel approach to assess the seismic performance of deteriorated bridge structures by employing UAV-based damage detection," *Struct Control Health Monit*, vol. 29, no. 7, p. e2964, Jul. 2022, doi: 10.1002/STC.2964.

[123] L. Deng, W. Wang, and Y. Yu, "State-of-the-Art Review on the Causes and Mechanisms of Bridge Collapse," *Journal of Performance of Constructed Facilities*, vol. 30, no. 2, p. 04015005, Jan. 2015, doi: 10.1061/(ASCE)CF.1943-5509.0000731.

[124] "2021 Fern Hollow Bridge Inspection | PDF | Concrete | Reinforced Concrete." Accessed: Jul. 10, 2022. [Online]. Available: https://www.scribd.com/document/575091953/2021-Fern-Hollow-Bridge-Inspection#download&from_embed

[125] S. Narayanan, "COLLAPSE OF THE MEXICO CITY METRO OVERPASS," *Indian Association of Structural Engineers*, no. July, 2021.

[126] N. Scattarreggia, R. Salomone, M. Moratti, D. Malomo, R. Pinho, and G. M. Calvi, "Collapse analysis of the multi-span reinforced concrete arch bridge of Caprigliola, Italy," *Eng Struct*, vol. 251, no. PA, p. 113375, 2022, doi: 10.1016/j.engstruct.2021.113375.

[127] C. Z. Dong, S. Bas, and F. N. Catbas, "A portable monitoring approach using cameras and computer vision for bridge load rating in smart cities," *J Civ Struct Health Monit*, vol. 10, no. 5, pp. 1001–1021, 2020, doi: 10.1007/s13349-020-00431-2.

[128] "Tables of Frequently Requested NBI Information - National Bridge Inventory - Bridge Inspection - Safety - Bridges & Structures - Federal Highway Administration." Accessed: Apr. 07, 2022. [Online]. Available: https://www.fhwa.dot.gov/bridge/britab.cfm

[129] BMVBS, "Bauwerksprüfung nach DIN 1076 Bedeutung, Organisation, Kosten," *Bauwerksprüfung nach DIN 1076 Bedeutung, Organisation, Kosten*, p. 78, 2013.

[130] K. Gkoumas *et al.*, "Research and innovation in bridge maintenance, inspection and monitoring - A European perspective based on the Transport Research and Innovation Monitoring and Information System (TRIMIS)," 2019, doi: 10.2760/719505.

[131] W. A. Megid, M. A. Chainey, P. Lebrun, and D. Robert Hay, "Monitoring fatigue cracks on eyebars of steel bridges using acoustic emission: A case study," *Eng Fract Mech*, vol. 211, no. February, pp. 198–208, 2019, doi: 10.1016/j.engfracmech.2019.02.022.

[132] K. Y. Koo, J. J. Lee, C. B. Yun, and J. T. Kim, "Damage detection in beam-like structures using deflections obtained by modal flexibility matrices," *Smart Struct Syst*, vol. 4, no. 5, pp. 605–628, 2008, doi: 10.12989/SSS.2008.4.5.605.

[133] V. U. of L. > F. of S. T. and C. (FSTC) > E. R. U. Bungard, "Condition assessment of concrete structures and bridges using vibration monitoring in comparison to changes in their static properties," Nov. 2010, Accessed: Feb. 02, 2024. [Online]. Available: https://orbilu.uni.lu/handle/10993/15605

[134] F. N. Catbas, M. Gul, and J. L. Burkett, "Damage assessment using flexibility and flexibility-based curvature for structural health monitoring," *Smart Mater Struct*, vol. 17, no. 1, p. 015024, Dec. 2007, doi: 10.1088/0964-1726/17/01/015024.

[135] G. Bernagozzi, L. Landi, and P. P. Diotallevi, "Truncation error analysis on modal flexibility-based deflections: application to mass regular and irregular structures," *Eng Struct*, vol. 142, pp. 192–210, Jul. 2017, doi: 10.1016/J.ENGSTRUCT.2017.03.057.

[136] S. H. Sung, H. J. Jung, and H. Y. Jung, "Damage detection for beam-like structures using the normalized curvature of a uniform load surface," *J Sound Vib*, vol. 332, no. 6, pp. 1501–1519, Mar. 2013, doi: 10.1016/J.JSV.2012.11.016.

[137] E. J. OBrien, J. M. W. Brownjohn, D. Hester, F. Huseynov, and M. Casero, "Identifying damage on a bridge using rotation-based Bridge Weigh-In-Motion," *J Civ Struct Health Monit*, vol. 11, no. 1, pp. 175–188, Feb. 2020, doi: 10.1007/s13349-020-00445-w.

[138] F. Moses, "Weigh-in-Motion System Using Instrumented Bridges," *Transportation Engineering Journal of ASCE*, vol. 105, no. 3, pp. 233–249, May 1979, doi: 10.1061/TPEJAN.0000783.

[139] Michael QUILLIGAN, "Development and Testing of a 2-Dimensional Multi-Vehicle Bridge-WIM Algorithm." Accessed: Nov. 20, 2021. [Online]. Available: https://www.researchgate.net/publication/281031263_Development_and_Testing_of_a_2-Dimensional_Multi-Vehicle_Bridge-WIM_Algorithm

[140] B. Heitner, F. Schoefs, E. J. OBrien, A. Žnidarič, and T. Yalamas, "Using the unit influence line of a bridge to track changes in its condition," *J Civ Struct Health Monit*, vol. 10, no. 4, pp. 667–678, 2020, doi: 10.1007/s13349-020-00410-7.

[141] D. Martinez, A. Malekjafarian, and E. OBrien, "Bridge flexural rigidity calculation using measured drive-by deflections," *J Civ Struct Health Monit*, vol. 10, no. 5, pp. 833–844, Nov. 2020, doi: 10.1007/s13349-020-00419-y.

[142] W.-Y. He, W.-X. Ren, and S. Zhu, "Damage detection of beam structures using quasi-static moving load induced displacement response," 2017, doi: 10.1016/j.engstruct.2017.05.009.

[143] T. M. Ha and S. Fukada, "Nondestructive damage detection in deteriorated girders using changes in nodal displacement," *J Civ Struct Health Monit*, vol. 7, no. 3, pp. 385–403, Jul. 2017, doi: 10.1007/s13349-017-0231-x.

[144] R. Ono, T. M. Ha, and S. Fukada, "Analytical study on damage detection method using displacement influence lines of road bridge slab," *J Civ Struct Health Monit*, vol. 9, no. 4, pp. 565–577, 2019, doi: 10.1007/s13349-019-00352-9.

[145] D. Erdenebat, D. Waldmann, and F. N. Teferle, “Static load deflection experiment on a beam for damage detection using the deformation area difference method,” Life Cycle Analysis and Assessment in Civil Engineering: Towards an Integrated Vision.

[146] “Numerical studies on vibration propagation and damping test V1 - pdf.” Accessed: Jul. 10, 2022. [Online]. Available: https://rakenteidenmekaniikka.journal.fi/article/view/68954/35911

[147] “The box plot: a simple visual method to interpret data.: EBSCOhost.” Accessed: Apr. 26, 2022. [Online]. Available: https://web-s-ebscohost-com.proxy.bnl.lu/ehost/pdfviewer/pdfviewer?vid=1&sid=f2e25db4-9bc8-45e4-a4a1-35d2a7304e3c%40redis

[148] A. Castel, D. Coronelli, R. François, and D. Cleland, “Modelling the stiffness reduction of corroded reinforced concrete beams after cracking,” *RILEM Bookseries*, vol. 5, pp. 219–230, 2011, doi: 10.1007/978-94-007-0677-4_15/COVER.

[149] G. Malumbela, P. Moyo, and M. Alexander, “Longitudinal strains and stiffness of RC beams under load as measures of corrosion levels,” *Eng Struct*, vol. 35, pp. 215–227, Feb. 2012, doi: 10.1016/J.ENGSTRUCT.2011.11.021.

[150] Z. Sun, T. Nagayama, and Y. Fujino, “Minimizing noise effect in curvature-based damage detection,” *J Civ Struct Health Monit*, vol. 6, no. 2, pp. 255–264, 2016, doi: 10.1007/s13349-016-0163-x.

[151] K. Geißler, “Handbuch Brückenbau Entwurf, kontruktion,Berchnung, Bewertung und Ertüchtigung,” p. 1355, 2014.

[152] “EN 1992-2: Eurocode 2: Design of concrete structures - Part 2: Concrete bridges - Design and detailing rules,” 1992.

[153] N. Europeenne and E. Norm, “EUROPEAN STANDARD Eurocode 3-Design of steel structures-Part 2: Steel Bridges,” 2006.

[154] N. Europeenne and E. Norm, “EUROPEAN STANDARD English Version Eurocode 4-Design of composite steen and concrete structures-Part 2: General rules and rules for bridges,” 2005.

[155] C. J. Amante, “Uncertain seas: probabilistic modeling of future coastal flood zones,” *International Journal of Geographical Information Science*, vol. 33, no. 11, pp. 2188–2217, 2019, doi: 10.1080/13658816.2019.1635253.

[156] W. Soo Lon Wah, Y. T. Chen, and J. S. Owen, “A regression-based damage detection method for structures subjected to changing environmental and operational conditions,” *Eng Struct*, vol. 228, p. 111462, Feb. 2021, doi: 10.1016/J.ENGSTRUCT.2020.111462.

[157] R. M. Delgadillo and J. R. Casas, “Non-modal vibration-based methods for bridge damage identification,” *Structure and Infrastructure Engineering*, vol. 16, no. 4, pp. 676–697, Apr. 2020, doi: 10.1080/15732479.2019.1650080.

[158] Z. Yunkai, G. Jianjun, L. Guohua, C. Tingrui, and L. Yongqi, "Research on Single Damage Identification of Multi-span Bridge Based on Influence Line," *IOP Conf Ser Earth Environ Sci*, vol. 760, no. 1, p. 012001, Apr. 2021, doi: 10.1088/1755-1315/760/1/012001.

[159] Y. Zhang, Q. Xie, G. Li, and Y. Liu, "Multi-Damage Identification of Multi-Span Bridges Based on Influence Lines," *Coatings 2021, Vol. 11, Page 905*, vol. 11, no. 8, p. 905, Jul. 2021, doi: 10.3390/COATINGS11080905.

[160] Q. Ma and M. Solís, "Multiple Damage Identification in Beams from Full-Field Digital Photogrammetry," *J Eng Mech*, vol. 145, no. 8, p. 04019054, May 2019, doi: 10.1061/(ASCE)EM.1943-7889.0001629.

[161] N. T. Le, D. P. Thambiratnam, A. Nguyen, and T. H. T. Chan, "A new method for locating and quantifying damage in beams from static deflection changes," *Eng Struct*, vol. 180, pp. 779–792, Feb. 2019, doi: 10.1016/j.engstruct.2018.11.071.

[162] A. Mohammed, B. Nadir, and H. Karim, "Damage identification in RC bridges by confronting two approaches: visual inspection and numerical analysis," *Frattura ed Integrità Strutturale*, vol. 17, no. 64, pp. 77–92, Mar. 2023, doi: 10.3221/IGF-ESIS.64.05.

[163] A. Rageh, D. G. Linzell, and S. Eftekhar Azam, "Automated, strain-based, output-only bridge damage detection," *J Civ Struct Health Monit*, vol. 8, no. 5, pp. 833–846, Nov. 2018, doi: 10.1007/S13349-018-0311-6/FIGURES/19.

[164] F. Ioli, A. Pinto, and L. Pinto, "UAV PHOTOGRAMMETRY FOR METRIC EVALUATION OF CONCRETE BRIDGE CRACKS," *The International Archives of the Photogrammetry, Remote Sensing and Spatial Information Sciences*, vol. XLIII-B2-2022, no. B2-2022, pp. 1025–1032, May 2022, doi: 10.5194/ISPRS-ARCHIVES-XLIII-B2-2022-1025-2022.

[165] A. Khaloo and D. Lattanzi, "Automatic Detection of Structural Deficiencies Using 4D Hue-Assisted Analysis of Color Point Clouds," *Conference Proceedings of the Society for Experimental Mechanics Series*, pp. 197–205, 2019, doi: 10.1007/978-3-319-74421-6_26.

[166] T. Čamo and D. Waldmann, "Potential and limits using the DAD method for condition assessment of bridge structures," *Eng Struct*, vol. 308, p. 117972, Jun. 2024, doi: 10.1016/J.ENGSTRUCT.2024.117972.

[167] C. Andrade *et al.*, "Condition Assessment," pp. 39–59, Oct. 2023, doi: 10.35789/FIB.BULL.0109.CH03.

[168] F. Leonhardt, "Vorlesungen über Massivbau," *Vorlesungen über Massivbau*, 1978, doi: 10.1007/978-3-642-61884-0.

[169] H. F. Brinson and L. C. Brinson, "Differential Constitutive Equations," *Polymer Engineering Science and Viscoelasticity*, pp. 169–209, 2015, doi: 10.1007/978-1-4899-7485-3_5.

[170] M. Marčiš, M. Fraštia, and T. Augustín, "Measurement of Flat Slab Deformations by the Multi-Image Photogrammetry Method," *Slovak Journal of Civil Engineering*, vol. 25, no. 4, pp. 19–25, Dec. 2017, doi: 10.1515/SJCE-2017-0019.

[171] C. Lee, W. A. Take, and N. A. Hoult, "Optimum Accuracy of Two-Dimensional Strain Measurements Using Digital Image Correlation," *Journal of Computing in Civil Engineering*, vol. 26, no. 6, pp. 795–803, Dec. 2011, doi: 10.1061/(ASCE)CP.1943-5487.0000182.

[172] E.-M. Eichinger-Vill, J. Kollegger, F. Aigner, and G. Ramberger, "Überwachung, Prüfung, Bewertung und Beurteilung von Brücken," *Handbuch Brücken*, pp. 1009–1068, 2010, doi: 10.1007/978-3-642-04423-6_11.

[173] C. J. Amante, "Uncertain seas: probabilistic modeling of future coastal flood zones," *International Journal of Geographical Information Science*, vol. 33, no. 11, pp. 2188–2217, 2019, doi: 10.1080/13658816.2019.1635253.

[174] "The box plot: a simple visual method to interpret data.: EBSCOhost." Accessed: Apr. 26, 2022. [Online]. Available: https://web-s-ebscohost-com.proxy.bnl.lu/ehost/pdfviewer/pdfviewer?vid=1&sid=f2e25db4-9bc8-45e4-a4a1-35d2a7304e3c%40redis

[175] J. Valença, E. N. B. S. Júlio, and H. J. Araújo, "Applications of photogrammetry to structural assessment," *Exp Tech*, vol. 36, no. 5, pp. 71–81, Sep. 2012, doi: 10.1111/J.1747-1567.2011.00731.X.

[176] N. J. Bertola and E. Brühwiler, "Framework to evaluate the value of monitoring-technique information for structural performance monitoring," *Structure and Infrastructure Engineering*, 2023, doi: 10.1080/15732479.2023.2280727.

[177] T. Rakha and A. Gorodetsky, "Review of Unmanned Aerial System (UAS) applications in the built environment: Towards automated building inspection procedures using drones," *Autom Constr*, vol. 93, pp. 252–264, Sep. 2018, doi: 10.1016/J.AUTCON.2018.05.002.

[178] P. Nooralishahi *et al.*, "Drone-Based Non-Destructive Inspection of Industrial Sites: A Review and Case Studies," *Drones 2021, Vol. 5, Page 106*, vol. 5, no. 4, p. 106, Sep. 2021, doi: 10.3390/DRONES5040106.

[179] H. Lv *et al.*, "Practical issues on the use of drones for construction inspections," *J Phys Conf Ser*, vol. 1249, no. 1, p. 012016, May 2019, doi: 10.1088/1742-6596/1249/1/012016.

[180] A. Karami, F. Menna, and F. Remondino, "Combining Photogrammetry and Photometric Stereo to Achieve Precise and Complete 3D Reconstruction," *Sensors 2022, Vol. 22, Page 8172*, vol. 22, no. 21, p. 8172, Oct. 2022, doi: 10.3390/S22218172.

[181] S. Malihi, M. J. V. Zoej, and M. Hahn, "Large-Scale Accurate Reconstruction of Buildings Employing Point Clouds Generated from UAV Imagery," *Remote Sensing 2018, Vol. 10, Page 1148*, vol. 10, no. 7, p. 1148, Jul. 2018, doi: 10.3390/RS10071148.

[182] P. Miao, H. Yokota, and Y. Zhang, “Extracting procedures of key data from a structural maintenance database,” *Structure and Infrastructure Engineering*, vol. 18, no. 2, pp. 219–229, 2022, doi: 10.1080/15732479.2020.1838561.

[183] K. G. Papakonstantinou, C. P. Andriotis, and M. Shinozuka, “POMDP and MOMDP solutions for structural life-cycle cost minimization under partial and mixed observability,” *Structure and Infrastructure Engineering*, vol. 14, no. 7, pp. 869–882, Jul. 2018, doi: 10.1080/15732479.2018.1439973.

[184] L. J. Butler, W. Lin, J. Xu, N. Gibbons, M. Z. E. B. Elshafie, and C. R. Middleton, “Monitoring, Modeling, and Assessment of a Self-Sensing Railway Bridge during Construction,” *Journal of Bridge Engineering*, vol. 23, no. 10, p. 04018076, Oct. 2018, doi: 10.1061/(ASCE)BE.1943-5592.0001288.

[185] C. Gheorghiu, P. Labossière, and J. Proulx, “Fiber Optic Sensors for Strain Measurement of CFRP-strengthened RC Beams,” *http://dx.doi.org/10.1177/1475921705049754*, vol. 4, no. 1, pp. 67–80, Mar. 2005, doi: 10.1177/1475921705049754.

[186] American Society of Civil Engineers, “A COMPREHENSIVE ASSESSMENT OF AMERICA’S INFRASTRUCTURE,” *The 2021 Report Card for America´s Infrastructure*, 2021, Accessed: Sep. 06, 2024. [Online]. Available: www.infrastructurereportcard.org

[187] EUROPEAN COMMISSION, “State of infrastructure maintenance,” Directorate-General for Internal Market, Industry, Entrepreneurship and SMEs, Industrial Transformation and Advanced Value Chains. Accessed: Sep. 06, 2024. [Online]. Available: https://ec.europa.eu/docsroom/documents/34561

[188] S. Teng, G. Chen, Z. Yan, L. Cheng, and D. Bassir, “Vibration-based structural damage detection using 1-D convolutional neural network and transfer learning,” *https://doi.org/10.1177/14759217221137931*, vol. 22, no. 4, pp. 2888–2909, Dec. 2022, doi: 10.1177/14759217221137931.

[189] S. Umar, M. Vafaei, and S. C. Alih, “Sensor clustering-based approach for structural damage identification under ambient vibration,” *Autom Constr*, vol. 121, p. 103433, Jan. 2021, doi: 10.1016/J.AUTCON.2020.103433.

[190] A. Soleymani, H. Jahangir, M. Rashidi, F. F. Mojtahedi, M. Bahrami, and A. Javanmardi, “Damage Identification in Reinforced Concrete Beams Using Wavelet Transform of Modal Excitation Responses,” *Buildings*, vol. 13, no. 8, Aug. 2023, doi: 10.3390/BUILDINGS13081955.

[191] B. Miao, M. Wang, S. Yang, Y. Luo, and C. Yang, “An Optimized Damage Identification Method of Beam Using Wavelet and Neural Network,” *Engineering*, vol. 12, no. 10, pp. 748–765, 2020, doi: 10.4236/ENG.2020.1210053.

[192] J. Zhan, F. Zhang, M. Siahkouhi, X. Kong, and H. Xia, “A damage identification method for connections of adjacent box-beam bridges using vehicle–bridge interaction analysis and

model updating," *Eng Struct*, vol. 228, p. 111551, Feb. 2021, doi: 10.1016/J.ENGSTRUCT.2020.111551.

[193] J. Zhou, Z. Zhou, Z. Jin, S. Liu, and Z. Lu, "Comparative study of damage modeling techniques for beam-like structures and their application in vehicle-bridge-interaction-based structural health monitoring," *https://doi.org/10.1177/10775463231209357*, Oct. 2023, doi: 10.1177/10775463231209357.

[194] J. P. McCrory, M. R. Pearson, R. Pullin, and K. M. Holford, "Optimisation of acoustic emission wavestreaming for structural health monitoring," *Struct Health Monit*, vol. 19, no. 6, pp. 2007–2022, Nov. 2020, doi: 10.1177/1475921720912174.

[195] A. Boniface, J. Saliba, Z. M. Sbartaï, N. Ranaivomanana, and J. P. Balayssac, "Evaluation of the acoustic emission 3D localisation accuracy for the mechanical damage monitoring in concrete," *Eng Fract Mech*, vol. 223, p. 106742, Jan. 2020, doi: 10.1016/J.ENGFRACMECH.2019.106742.

[196] Z. Peng, J. Li, H. Hao, and Y. Zhong, "Smart structural health monitoring using computer vision and edge computing," *Eng Struct*, vol. 319, p. 118809, Nov. 2024, doi: 10.1016/J.ENGSTRUCT.2024.118809.

[197] D. Feng and M. Q. Feng, "Computer vision for SHM of civil infrastructure: From dynamic response measurement to damage detection – A review," *Eng Struct*, vol. 156, pp. 105–117, Feb. 2018, doi: 10.1016/J.ENGSTRUCT.2017.11.018.

[198] W.-J. Yan and K.-V. Yuen, "A new probabilistic frequency-domain approach for influence line extraction from static transmissibility measurements under unknown moving loads," 2020, doi: 10.1016/j.engstruct.2020.110625.

[199] B. Ghahremani, A. Enshaeian, and P. Rizzo, "Bridge Health Monitoring Using Strain Data and High-Fidelity Finite Element Analysis," *Italian National Conference on Sensors*, vol. 22, no. 14, Jul. 2022, doi: 10.3390/S22145172.

[200] Z. R. Lu, J. Zhou, L. Wang, and J. Liu, "Damage identification from static tests by eigenparameter decomposition and sparse regularization," *Struct Health Monit*, vol. 19, no. 5, pp. 1351–1374, Sep. 2020, doi: 10.1177/1475921719880980/FORMAT/EPUB.

[201] Z. Wu, B. Huang, K. F. Tee, and W. Zhang, "A Novel Stochastic Approach for Static Damage Identification of Beam Structures Using Homotopy Analysis Algorithm," *Italian National Conference on Sensors*, vol. 21, no. 7, Apr. 2021, doi: 10.3390/S21072366.

[202] T. Čamo, D. Waldmann, and E. Apostolidi, "Enhancing Structural Health Monitoring with the extension of the Deformation Area Difference (DAD) Method into the Strain Area Difference (SAD) Method: A Comparative Study of Photogrammetry and Strain Measurement Techniques," *unpublished*, 2024.

[203] F. Falcetelli, N. Yue, R. Di Sante, and D. Zarouchas, “Probability of detection, localization, and sizing: The evolution of reliability metrics in Structural Health Monitoring,” *Struct Health Monit*, vol. 21, no. 6, pp. 2990–3017, Nov. 2021, doi: 10.1177/14759217211060780.

[204] S. Greś, M. Döhler, and L. Mevel, “Statistical model-based optimization for damage extent quantification”, doi: 10.1016/j.ymssp.2021.107894.

[205] M. A. Bud, M. Nedelcu, I. Moldovan, and E. Figueiredo, “Hybrid Approach for Supervised Machine Learning Algorithms to Identify Damage in Bridges,” *Journal of Bridge Engineering*, vol. 29, no. 8, p. 04024056, Aug. 2024, doi: 10.1061/JBENF2.BEENG-6537.

[206] D. C. Nguyen, M. Salamak, A. Katunin, and M. Gerges, “Finite Element Model Updating of RC Bridge Structure with Static Load Testing: A Case Study of Vietnamese ThiThac Bridge in Coastal and Marine Environment,” *Sensors*, vol. 22, no. 22, Nov. 2022, doi: 10.3390/S22228884.

[207] C. Ye, S. C. Kuok, L. J. Butler, and C. R. Middleton, “Implementing bridge model updating for operation and maintenance purposes: examination based on UK practitioners’ views,” *Structure and Infrastructure Engineering*, vol. 18, no. 12, pp. 1638–1657, 2022, doi: 10.1080/15732479.2021.1914115.

[208] G. Zhang and T. Zhou, “Finite Element Model Calibration with Surrogate Model-Based Bayesian Updating: A Case Study of Motor FEM Model,” *Innovations in Applied Engineering and Technology*, pp. 1–13, Sep. 2024, doi: 10.62836/IAET.V3I1.232.

[209] F. Tu, “Application of Sliding Smoothing Method Denoising in Model Updating Damage Identification,” *J Phys Conf Ser*, vol. 2185, no. 1, p. 012014, Jan. 2022, doi: 10.1088/1742-6596/2185/1/012014.

[210] K. Zilch and G. Zehetmaier, “Bemessung im konstruktiven Betonbau,” *Bemessung im konstruktiven Betonbau*, 2010, doi: 10.1007/978-3-540-70638-0.

[211] “Rhino - Rhinoceros 3D.” Accessed: Mar. 19, 2025. [Online]. Available: https://www.rhino3d.com/de/

[212] “Grasshopper - algorithmic modeling for Rhino.” Accessed: Mar. 19, 2025. [Online]. Available: https://www.grasshopper3d.com/

[213] “SOFiSTiK FEM, BIM and CAD Software for Structural Engineers.” Accessed: Mar. 19, 2025. [Online]. Available: https://www.sofistik.com/en/

[214] “Karamba3D.” Accessed: Mar. 19, 2025. [Online]. Available: https://karamba3d.com/

[215] P. Di Re, I. Vangelisti, and E. Lofrano, “Influence of the Objective Function in the Dynamic Model Updating of Girder Bridge Structures,” *Buildings 2025, Vol. 15, Page 341*, vol. 15, no. 3, p. 341, Jan. 2025, doi: 10.3390/BUILDINGS15030341.

[216] D. Rutten, “Galapagos: On the logic and limitations of generic solvers,” *Architectural Design*, vol. 83, no. 2, pp. 132–135, Mar. 2013, doi: 10.1002/AD.1568.

[217] Y. An, E. Chatzi, S. H. Sim, S. Laflamme, B. Blachowski, and J. Ou, "Recent progress and future trends on damage identification methods for bridge structures," *Struct Control Health Monit*, vol. 26, no. 10, p. e2416, Oct. 2019, doi: 10.1002/STC.2416.

[218] B. T. Svendsen, O. Øiseth, G. T. Frøseth, and A. Rønnquist, "A hybrid structural health monitoring approach for damage detection in steel bridges under simulated environmental conditions using numerical and experimental data," *Struct Health Monit*, vol. 22, no. 1, pp. 540–561, Jan. 2023, doi: 10.1177/14759217221098998/ASSET/C7F1B44F-36AF-4838-AAF2-1F93CAB599CE/ASSETS/IMAGES/LARGE/10.1177_14759217221098998-FIG20.JPG.

[219] E. Sotoudehnia, F. Shahabian, and A. Aftabi Sani, "Damage detection of cylindrical shells based on Sander's theory and model updating using incomplete modal data considering random noises," *European Journal of Mechanics - A/Solids*, vol. 85, p. 104110, Jan. 2021, doi: 10.1016/J.EUROMECHSOL.2020.104110.

[220] "ELCOVISION 10 3D Photogrammetrie und Vermessungsoftware." Accessed: Mar. 19, 2025. [Online]. Available: https://de.elcovision.com/

[221] A. Zilian, I. S. Marx, I. M. Gutermann, and H. Bremen, "Condition assessment of bridge structures by damage localisation based on the DAD-method and close-range UAV photogrammetry," Mar. 2020, Accessed: Mar. 19, 2025. [Online]. Available: https://orbilu.uni.lu/handle/10993/43231

[222] Z. Zhou, L. D. Wegner, and B. F. Sparling, "Vibration-Based Detection of Small-Scale Damage on a Bridge Deck," *Journal of Structural Engineering*, vol. 133, no. 9, pp. 1257–1267, Sep. 2007, doi: 10.1061/(ASCE)0733-9445(2007)133:9(1257).

[223] Q. L. Cai, Z. W. Chen, S. Zhu, and L. Y. Mo, "On damage detection of beam structures using multiple types of influence lines," *Structures*, vol. 42, pp. 449–465, Aug. 2022, doi: 10.1016/J.ISTRUC.2022.06.022.